Department of Chemical Engineering
University of Newcastle, Australia.

MATHEMATICAL MODELLING OF ENTRAINED FLOW COAL GASIFICATION

A thesis submitted in partial fulfilment of the
requirements for the Doctor of Philosophy
by

Andrew Charles Beath
B.Eng. (Chem.) Hons.

March, 1996.

I hereby certify that the work embodied in this thesis is the results of original research and has not been submitted for a higher degree to any other University or Institution.

(Signed) _____

A. C. Beath

NOTE FOR THIS ELECTRONIC VERSION:

This electronic version is not identical to the original published work. Due to software version changes and incompatibility issues, it was not possible to reconstruct the document as originally published and some pages have been scanned for insertion. Paging of the document has changed significantly and the figures are typically inserted at the end of the relevant section, rather than through the text as originally arranged. The Errata section addressing reviewers concerns has been included (note that the original page numbers are used in this section). For comparison purposes, the original table of contents is included.

NEW TABLE OF CONTENTS

ERRATA

a) Typographical Errors.

Page	Location	Statement	Replacement
xxi	Paragraph 2, Line 6	*accuracy*	*accurate*
1	Paragraph 2, Line 4	*theoretical*	*theoretically*
4	Paragraph 2, Line 10	*initial*	*initially*
22	Paragraph 3, Line 10	*of*	-
66	Paragraph 2, Line 7	*gasifierss*	*gasifiers*
93	Table 4.2	*Eq 39*	*Equation 2.8*
181	Paragraph 2, Line 7/8	*The range of experimental results considered allows for*	-

b) The following text and equations should be included directly following page 102.

algorithm was developed for the model and is described below. The expressions were obtained by 'inverting' the model and calculating the length of time per step of conversion, rather than the conversion per length of time. Due to the difficulties in calculations for this model a number of simplifications had to be made, namely to the kinetics and heat transfer models employed and in that only one particle size can be used. From results predicted with this model an adaptable algorithm for estimating the trend in conversion with time was construction, a version of which is given in equations 4.25 to 4.27 in terms of step time predictions and illustrated in figure 4.6. Two adjustable parameters are used in the algorithm with the first, $\Delta X_{i,specified}$, giving a suggested value for the size of the slice in terms of change in conversion and the second, *f*(Coal), is given in table 4.3 and allows for variation in size of slice dependent on the degree of conversion in the previous slice and the coal used. This requires input of a factor dependant on the coal used, g(Coal), which accounts for variations due to coal properties in the early stages of gasification, mostly affected by the quantity of volatile released from the coal, and generally ranges from 0.5 for a low volatile coal to 2.5 for a very high volatile coal.

$$\Delta t_i = \frac{\Delta t_{i-1}}{\Delta X_{i-1}} . \Delta X_{i,specified} \cdot \frac{\alpha}{f(X, Coal)} . \log_{10}(\beta X) \qquad \text{Equation (4.25)}$$

$$\alpha = 0.5208 . \log_{10}\left(6.232 \Delta X_{i,specified}\right) . \frac{P_{total}}{30} \qquad \text{Equation (4.26)}$$

$$\beta = 10^{\left(\frac{8.671}{\Delta X_{i,specified}^{0.8277}} - \frac{7.641}{\Delta X_{i,specified}^{0.5078}}\right)}$$ Equation (4.27)

c) The following references should be included in section 10. REFERENCES.

Bautista, J. R., Russel, W. B., Saville, D. A., 1986, "Time-Resolved Pyrolysis Product Distributions Softening Coals", Ind. Eng. Chem. Fund., V25, pp536-544.

Gibbins, J. R., Kandiyoti, R., 1989, "The Effect Of Variations In Time-Temperature History On Product Distribution From Coal Pyrolysis", FUEL, V68, pp895-903.

Hastaoglu, M. A., Karmann, M., 1987, "Modelling Of Catalytic Carbon Gasification", Chem. Eng. Sci., V42, pp1121-1130

Reid, R. C., Prausnitz, J. M., Poling, B. E., 1987, "The Properties of Gases and Liquids", McGraw-Hill, New York.

Schoen, P., 1992, "Mathematical Model Of A Slagging Pulverised Coal Gasifier", Int. Power Eng. Conf., Hangzhou, China, May 17-21.

Sharma, D. K., Sulimma, A., van Heek, K. H., 1986, "Comparative Studies Of Pyrolysis Of Coal In Inert Gas, Steam And Hydrogen Under Pressure", Erdol Und Kohle - Erdgas – Petrochemie Vereinigt Mit Brennstoff-Chemie, V39, pp173-176.

Strimbeck, G. R., Cordiner, J. B. Jr., Taylor, H. G., Plants, K. D., Schmidt, L. D., 1953, *See USBM (1953).*

Suuberg, E. M., 1977, *See Howard, J. B. in Chemistry of Coal Utilization, 2nd Suppl. Vol. (1981).*

Wagner, R., Wanzl, W., van Heek, K. H., 1985, "Influence Of Transport Effects On Pyrolysis Reaction Of Coal At High Heating Rates", Fuel, V64, pp571-573.

CLARIFICATIONS

Page	Additional Comments
3	The higher efficiency referred to as occurring in gasifiers relative to pulverised coal boilers refers to the use of gasifiers in integrated gasification combined cycle (IGCC) power generation compared to conventional pulverised coal-fired boiler power plant. This is due to the higher thermodynamic efficiency achieved in IGCC plant.
21	In relation to the use of equations (2.1) and (2.2) to prediction of devolatilisation rates at high pressures, it is necessary to input some measure of the expected ultimate volatile yields at the desired pressure, V^* in equation (2.1) or a_1 and a_2 in equation (2.2). These yields must either be experimentally obtained or estimated by another model, as equations (2.1) and (2.2) do not compensate for variations in pressure. If the yields are input to either expression a devolatilisation rate can be estimated, although the accuracy of the estimate at pressures differing from atmospheric is unknown.
29	The identification of reaction steps in sequence from Step 1 to Step 17 should not suggest that the steps should progress in this order. Therefore it is not necessary for oxygen gasification to precede carbon dioxide gasification, or carbon dioxide gasification to precede steam gasification, etcetera, during gasification.
37	The reaction order 'n' defined by equation (2.8) is for the oxygen gasification reaction and is used in the estimation of reaction rate according to equation (2.7).
53	In assuming that all nitrogen in the product gases from a gasifier is in the form of molecular nitrogen reference is made to *Strimbeck et al. (1953).* (This reference is listed in the references as *USBM (1953).*) The gasifier used in that study was a pilot scale entrained flow, high pressure and oxygen blown unit. The dominance of production of molecular nitrogen compared to other nitrogen containing gases in gasifiers was also reported in Watkinson *et al.* (1991) for a range of gasifiers, including entrained flow, fluidised bed and fixed bed designs, using either oxygen or air and variously operating at high and atmospheric pressures. This does not mean that other nitrogen containing species will not exist in gasifiers but suggests that they will be in only minor concentrations. By

	neglecting these other nitrogen containing species it becomes possible to analytically solve some of the equations concerning gas phase equilibria and therefore this approximation is seen as justifiable for use in the model.
86	In the work of Neoh and Gannon (1984) a set of 13 coals of North American origin with rank ranging from lignite to anthracite was studied. The majority of these, nine of the 13, were in the range sub-bituminous to low volatile bituminous that would typically be considered applicable for use in entrained flow gasification.
92	The magnitudes of the reactivity correlation coefficients listed in Table 4.1 do not indicate the relative magnitudes of the different reactions but are solely used to represent the influence of coal rank (based on carbon content) on reaction rate for the individual gasification reactions. For example, from the figures in the table it is possible to state that rank appears to have greatest influence on the reaction rate of steam with carbon and the least influence on the reaction rate of hydrogen with carbon. The magnitude of the rates is estimated from the value of the pre-exponential rate constant calculated from the reactivity coefficient and other terms using Equation (4.8), as well as the activation energy for the reaction and other diffusional interferences that are independent of the calculated reactivity coefficient.
96	In the chemical reaction rate limited regime mass loss will occur both from the external particle surface and the internal pore surface, however as internal pore area is typically much greater than external particle area, reaction will effectively lead to increasing particle porosity with negligible particle shrinkage. For the pore diffusion hindered regime the rates of change in porosity and particle size will vary depending on the particle effectiveness factors for the heterogeneous reactions. At low effectiveness factor the particle will mostly shrink with reaction with little change in porosity, and at high effectiveness factor the particle porosity will increase with little reduction in particle size.
101	The gas properties of significance to modelling in an entrained flow coal gasifier are density, emissivity, diffusivity, specific heat and thermal conductivity. In general only the gases present in significant concentrations in the gasifier, carbon monoxide, carbon dioxide, steam, hydrogen, oxygen and nitrogen, are considered in the sub-models for gas properties. Density is calculated using the Ideal Gas Law, which involves the assumptions of non-

	interaction between gas molecules and therefore is subject to minor error at high pressures. The gas emissivity is assumed to be uniform for the entire spectrum of relevance to heat transfer, termed 'grey' gas modelling, and the calculation of emissivity is considered in section 2.6.2 (pp61-63), with inclusion of pressure dependent terms. Calculation of diffusivity for use in determination of boundary layer and pore diffusion effects is discussed in section 2.3.7.2 (pp48-52), with the expressions defined incorporating the effects of pressure on the calculated variables. Calculation of the specific heats and thermal conductivities of gas mixtures at high temperatures and pressures are not discussed in the thesis as relatively common methods were used. Specific heats were calculated from the average values for the individual gases (averaged on a molar basis), which in turn were estimated using quadratic polynomials of best fit to available experimental data with respect to changing temperature. The thermal conductivities of gas mixtures were estimated using the Brokaw Method (Reid, Prausnitz and Poling (1987)), with individual values estimated from linear regression of the available experimental data with respect to changing temperature. This method compensates for the anomalous influence of significant quantities of hydrogen on the overall thermal conductivity of the gas mixture. For both the estimation of specific heat and thermal conductivity of the gas mixtures no correction for high pressures was deemed necessary as the available experimental data indicated insignificant variation in property with pressure when compared to the uncertainties involved in the estimation of the property at atmospheric pressure.

ORIGINAL TABLE OF CONTENTS

ORIGINAL TABLE OF TABLES

ORIGINAL TABLE OF FIGURES

ABSTRACT

A mathematical model for entrained flow coal gasification was developed with the objective of predicting the influence of coal properties and gasification conditions on the performance of entrained flow gasifiers operating at pressures up to 21 atmospheres (2.1MPa). The model represents gasifiers as plug flow reactors and therefore neglects any mixing or turbulence effects. Coal properties were predicted through use of correlations from a variety of literature sources and others that were developed from experimental data in the literature. A sensitivity analysis of the model indicated that errors in the calculated values of coal volatile yield, carbon dioxide gasification reactivity and steam gasification may significantly affect the model predictions. Similarly errors in the input values for gasifier wall temperatures and gasifier diameter, when affected by slagging, can cause model prediction errors. Model predictions were compared with experimental gasification results for a range of atmospheric and high pressure gasifiers, the majority of the results being obtained by CSIRO at atmospheric pressure for a range of coals. Predictions were accurate for the majority of atmospheric pressure results over a large range of gas feed mixtures. Due to the limited range of experimental data available for high pressure gasification the capability of the model is somewhat uncertain, although the model provided accurate predictions for the majority of the available results. The model was also used to predict the trends in particle reactions with gasification and the influence of pressure, gasifier diameter and feed coal on gasifier performance. Further research on coal volatile yields, gasification reactivities and gas properties at high temperatures and pressures was recommended to improve the accuracy of model inputs. Additional predictions and model accuracy improvements could be made by extending the model to include fluid dynamics and slag layer modelling.

ACKNOWLEDGMENTS

A significant proportion of the work performed in this study was associated with a project performed under an ACARP/NERDDP grant.

My thanks go to Prof. Terry Wall for his assistance and valuable insights, Dr. David Harris and colleagues at CSIRO for extensive data from their experiments, Dr. Allen Lowe and Dr. Rod Boyd of Pacific Power for their support, and my wife Helen for keeping me going.

SUMMARY

1. INTRODUCTION

The aim of this study is to develop a mathematical model of entrained flow coal gasification. Emphasis in the model will be on the ability to distinguish differences in gasification performance caused by changes in coal and gasification conditions, and for this reason accurate modelling of the coal gasification reactions is required rather than the fluid flow aspects. In order to allow general use of the model it is also desirable that coal related inputs can be estimated from basic coal analysis results, such as proximate and ultimate analyses.

Gasification of coal or other forms of carbon has been used for generation of combustible gases since the late 1700s. Important reactions identified in the gasification of coal are given in reactions 1 to 14. Reactions 1 to 5 are actually involved in gasifying the coal while reactions 6 to 14 are responsible for determining the gas composition.

Devolatilisation

$$Coal \rightarrow Char + Volatiles \qquad \text{Reaction (1)}$$

Heterogeneous Gasification

$$C + \tfrac{1}{Z} O_2 \rightarrow \left(2 - \tfrac{2}{Z}\right) CO + \left(\tfrac{2}{Z} - 1\right) CO_2 \qquad \text{Reaction (2)}$$

$$C + CO_2 \rightarrow 2CO \qquad \text{Reaction (3)}$$

$$C + H_2O \rightarrow H_2 + CO \qquad \text{Reaction (4)}$$

$$C + 2H_2 \rightarrow CH_4 \qquad \text{Reaction (5)}$$

Homogeneous Combustion

$$CO + \tfrac{1}{2} O_2 \longrightarrow CO_2 \qquad \text{Reaction (6)}$$

$$H_2 + \tfrac{1}{2} O_2 \longrightarrow H_2O \qquad \text{Reaction (7)}$$

$$CH_4 + 2O_2 \longrightarrow CO_2 + 2H_2O \qquad \text{Reaction (8)}$$

$$H_2S + \tfrac{3}{2} O_2 \longrightarrow SO_2 + H_2O \qquad \text{Reaction (9)}$$

$$COS + \tfrac{3}{2} O_2 \longrightarrow CO_2 + SO_2 \qquad \text{Reaction (10)}$$

Homogeneous Equilibrium

$$H_2O + CO \longleftrightarrow H_2 + CO_2 \qquad \text{Reaction (11)}$$

$$CO + 3H_2 \longleftrightarrow CH_4 + H_2O \qquad \text{Reaction (12)}$$

$$SO_2 + 3H_2 \longleftrightarrow 2H_2O + H_2S \qquad \text{Reaction (13)}$$

$$COS + H_2O \longleftrightarrow CO_2 + H_2S \qquad \text{Reaction (14)}$$

More recently the concept of coupling a gasifier with a gas turbine and steam generation plant to produce electricity has led to further development of gasification, these plants are termed integrated gasification combined cycle (IGCC). The form of gasifier used in IGCC can vary with the most common types being fixed bed, fluidised bed and entrained flow. In this study entrained flow gasification is considered and this involves the addition of pulverised coal with oxygen, or air, and steam into the gasifier. For IGCC use the gasifier will commonly be operated in the range of 20 to 30 atmospheres pressure.

2. LITERATURE REVIEW

The quantity of literature available for gasification is vast due to the large number of reactions involved, however only a small proportion of the literature is relevant to the high pressure and high temperatures experienced in large entrained flow gasifiers. Key areas of interest are the yield of volatiles from coal heated rapidly at both atmospheric and high pressures, rates of heterogeneous gasification reactions at high temperatures and pressures and the modelling of coal particle structure. Other topics of lesser significance are methods for modelling the homogeneous reactions and heat transfer during gasification.

3. EVALUATION OF LITERATURE

From detailed analysis of the available literature it was determined that sufficient information is available to produce a mathematical model of entrained flow gasification. The major limitation of the literature is the scant experimental experience with high pressure and high temperature heterogeneous gasification rates. This leads to difficulty in determining the best modelling method for these reactions and two alternate methods where identified, Langmuir-Hinshelwood and pressure order expressions.

4. DESCRIPTION OF MATHEMATICAL MODEL

A plug flow model for entrained flow coal gasification was developed from a combination of literature correlations, correlations developed from literature data and some experimental data. The model considers a number of discrete size fractions of coal particles flowing along the gasifier in parallel to the longitudinal axis of the gasifier. All reactions previously mentioned are considered to occur in the gasifier. The devolatilisation yield for a given coal is estimated from a published correlation that bases the yield on the

coal ultimate analysis, with another correlation changing this estimate depending on the pressure. This corresponds to literature results that indicate that volatile yield decreases with increasing pressure. Reactivities and coal particle structures are determined from general correlations obtained from the literature, although experimentally determined reactivities for a char that was formed under similar conditions are required. Heterogeneous reaction rates are calculated using a complex particle effectiveness factor dependant on particle pore structure, reactant gas diffusivity and coal reactivity. A comparison of model predictions using either Langmuir-Hinshelwood or pressure order expressions led to adopting the pressure order expressions as being more representative of gasification performance. The homogeneous combustion reactions listed previously are considered to occur instantaneously if oxygen is present and if it is not the homogeneous equilibrium reactions are assumed to be at equilibrium in the gasifier. Heat transfer in the gasifier is considered to occur by both convection and radiation, with convective transfer being approximated using established literature correlations and radiative transfer being modelled using the Long Furnace Model. This model assumes that no radiative transfer occurs along the gasifier and transfer is only within hypothetical thin slices of the gasifier. Coupled to this model is the assumption that the gas in the gasifier has significant emissivity and can be considered as a grey gas. The grey gas emissivity is calculated using a published algorithm. The model is not capable of calculating the temperature of the gasifier wall as generally insufficient data is available on the thermal properties of materials in the gasifier, so the temperature of the wall at different distances along the gasifier must be input from experimental data or estimated by other means. An empirical solution algorithm was produced to assist in the selection of step times in the model.

5. SENSITIVITY ANALYSIS

A study of the sensitivity of the developed mathematical model to changes in the values of inputs indicated significant sensitivity to a wide range of variables. Further analysis indicated that expected error ranges in the input values for coal volatile yield, carbon dioxide and steam reactivities, total coal surface area, gasifier wall temperatures and the internal diameter of the gasifier, if coated with slag, are sufficiently large to produce significant errors in the model predictions. These errors can be minimised by performing more accurate experimental measurements or developing more accurate correlations than are presently available.

6. COMPARISON OF MODEL PREDICTIONS WITH AVAILABLE EXPERIMENTAL MEASUREMENTS

Predictions were made using the mathematical model for comparison with experimental results from a selection of experimental gasifiers. The majority of the results considered were for the atmospheric pressure CSIRO gasifier, in which eight different coals were gasified using a wide range of conditions. Other atmospheric pressure results were for an United States Bureau of Mines gasifier with five different coals and a Brigham Young University gasifier with four different coals. At high pressures some results were available from an Institute of Gas Technology gasifier with four coals at pressures between 1.7 and 6.1 atmospheres and a different United States Bureau of Mines gasifier with one coal at pressures between 7.8 and 21.4 atmospheres.

In general, predictions made for the atmospheric pressure gasifiers were accurate, although less accuracy was evident for some particular coals. A general trend of increasing gasification performance with decreasing coal rank, as indicated by coal carbon content, was identified in experimental results and model predictions for all three atmospheric pressure gasifiers. The limited number of results available at high pressures led to inconclusive findings, with the majority of predictions being accuracy but those for some coals being extremely unreliable. More detailed analysis of the performance of some individual model components suggested that the volatile yield and reactivity estimates were more accurate than predicted in the sensitivity analysis.

7. USE OF MODEL PREDICTIONS TO DETERMINE REACTION MECHANICS AND OPTIMUM GASIFIER FEED MIXTURES

Additional model predictions were performed to predict trends in reaction behaviour and the variations in optimum feed mixtures with changing pressure, gasifier size and coal.

Detailed analysis of the progress of reactions at a single particle in the gasifier suggested a sequence of reactions commencing with devolatilisation then oxygen gasification, and continuing with simultaneous carbon dioxide and steam gasification. Some overlap between these reactions occurs but while the volatiles are being released it is predicted that it is not possible for reactant gases to diffuse to the particle. When devolatilisation has ceased the rate of oxygen gasification is much higher than the other reactions and dominates carbon conversion until the oxygen is depleted. Carbon dioxide

and steam gasification continue until the endothermic nature of the reactions lowers temperatures and the rates become insignificant.

In the study of optimum gas mixtures fed to the gasifier when pressure, gasifier diameter and coal are varied it was indicated that the optimum mixture can be affected by the changes. Predictions suggest that lower oxygen input is required at low gasification pressures than at high pressures. It is expected that this is due to the lower volatile yield at high pressures leaving more char to be consumed by heterogeneous reactions. Increasing gasifier diameter did not indicate changes in the optimum feed mixture but better gasifier performance was indicated at large gasifier diameters, excepting the largest diameter tested for which the predictions may have been affected by the use of some model components outside the limits of the correlations. The increase in gasifier performance with diameter is expected because of lower heat losses to the gasifier walls at higher diameters. The variations in gasification performance and optimum feed mixtures for different coals suggests that performance is linked to the reactivity and volatile yield of the coal and the optimum mixture is dependant on the moisture content and reactivity of the coal.

8. CONCLUSIONS

The mathematical model described and used in this study is the result of a combination of literature methods, correlations developed from literature data and experimental results. Errors associated with the methods used in the model were defined through a detailed sensitivity analysis. Key areas of possible inaccuracy are in the estimation of coal volatile yield, heterogeneous reactivities, particle structural properties, gasifier temperatures and gasifier diameter. Regardless of these possible inaccuracies the model predictions compared well with experimental results from atmospheric pressure gasifiers. Less conclusive comparison was possible for high pressure gasification, mostly due to the limited availability of high pressure experimental results. Predictions from the model suggested a sequencing of reactions occurring at a given particle commencing with devolatilisation then oxygen gasification followed by simultaneous carbon dioxide and steam gasification, with some overlap between the reactions. Optimum feed conditions and maximum gasifier performance were predicted to vary with changing gasifier pressure, gasifier diameter and feed coal. Various of the predictions suggested that errors in the model could arise at high pressures and large gasifier diameters due to extrapolation of gas physical property correlations outside the range of experimental data.

9. RECOMMENDATIONS FOR FURTHER WORK

It is suggested that further work be performed on the following topics to improve the accuracy of model predictions in future models.

(a) High Temperature and Pressure Heterogeneous Reaction Kinetics

(b) High Pressure Devolatilisation Yields

(c) Gas Physical Properties

(d) Slag Layer Modelling

(e) Fluid Dynamics Modelling

GLOSSARY OF SPECIALISED TERMINOLOGY AND ABBREVIATIONS

Term	Definition
ad	Coal analysis figures on an ‘air dried’ basis.
ar	Coal analysis figures on an ‘as recieved’ basis.
Atmosphere	Pressure measurement taken as equal to 101.325kPa in this study.
Boundary layer	Gas close to a particle which has composition or other properties that are significantly different from those of the bulk gas.
Carbon conversion	Gasified carbon relative to initial total coal carbon, usually expressed as a percentage.
Cold gas efficiency	Calcorific value of product gas at 25°C relative to calorific value of coal feed, usually expressed as a percentage.
daf	Coal analysis figures on a ‘dry, ash free’ basis.
Effectiveness factor	Ratio of actual heterogeneous reaction rate to that possible without diffusion resistances, usually approximated by an estimated proportion of total particle surface area available for reaction.
External reactivity	Reactivity calculated from experimental results on the basis that all reaction occurs on the external surface of the particle.
Fuel ratio	Ratio of volatile matter to fixed carbon in a coal used as an indicator of coal performance.
IGCC	Integrated gasification combined cycle electricity generation plant.
Intrinsic reactivity	Reactivity calculated from experimental results on the basis that reaction occurs at a proportion of the total particle surface area that is given by the particle effectiveness factor.
Vitrinite reflectance	Measure of coal rank based upon the degree of structure in vitrinite macerals of the coal.

NOMENCLATURE

Symbol	Units	Definition
α	-	Proportion of volatile type.
α	-	Ratio of Knudsen to bulk diffusivities of reactant
α	-	Absorptivity of gas to radiation from source
σ	-	Standard deviation in distribution.
σ_a	kg/m^3	Particle density
ϕ	-	Thiele Modulus
η	-	Effectiveness factor
ε	-	Particle porosity
$\varepsilon_{substance}$	-	Emissivity of substance
ρ_{gas}	kg/m^3	Gas density
μ_{gas}	Pa.s	Gas viscosity
ζ	-	Ratio of steam to steam and carbon dioxide
a	-	Stoichiometry of reactant gas to carbon
$A_{external}$	m^2	External area of particle
A_g	m^2/kg	Internal area of particle
$A_{p,j}$	m^2	Transfer area of particle j
A_{total}	m^2	Total particle area
b	-	Stoichiometry of combined product gases to reactant
C_{base}	% daf basis	Carbon content of base coal
$C_{p,gas}$	J/kg/K	Specific heat of gas
d	m	Particle size
D	m	Gasifier internal diameter
$D_{eff,A}$	m^2/s	Effective diffusivity of compound A
$D_{A,K}$	m^2/s	Knudsen diffusivity of compound A
$D_{A,B}$	m^2/s	Binary diffusivity of compound A through compound B
$D_{A,mixture}$	m^2/s	Diffusivity of compound A through gas mixture
d_{pore}	m	Pore diameter
E	MJ/kmol	Activation energy of reaction.

h	$J/s/m^2$	Convective heat transfer between substances
k	s^{-1}	Frequency factor of reaction.
k	$kg/m^2/s/atm^n$	Reaction rate
k_0	$kg/m^2/s/atm^n$	Pre-exponential term of reaction rate
$k_{0,base}$	$kg/m^2/s/atm^n$	k_0 for base coal
$K_{chemical}$	$kg/m^2/s$	Chemical rate
K_{diff}	$kg/m^2/s/atm$	Diffusion rate
k_g	J/K/m	Convective heat transfer coefficient
k_{gas}	J/m	Thermal conductivity of gas
l_{pore}	m	Pore length
m_C	kg	Mass of coal
M_c	kg/kmol	Atomic mass of carbon
n	-	Pressure or Reaction order
n_{pores}	-	Number of pores
Nu	-	Nusselt number
$P_{Compound}$	atm	Partial pressure of Compound
Q	-	Ratio of volatile yield to Proximate Volatile Matter
q	$J/s/m^2$	Radiative transfer between substances
R	MJ/kmol.K	Gas constant
R_g	m^3.atm/kmol/K	Gas constant
r	-	Reactivity coefficient
RF	-	Roughness factor
T	K	Temperature
$T_{gas\ or\ g}$	K	Gas temperature
$T_{particle\ or\ p}$	K	Particle temperature
$T_{wall\ or\ w}$	K	Gasifier wall temperature
V	kg	Mass of volatiles released
V	% daf basis	Volatile yield at any time
V^*	kg or %daf	Ultimate volatile yield
V_{gas}	m/s	Gas Velocity
VM	kg	Proximate volatile yield
VM_C	kg	Adjustment for volatile condensation

V_{nr}^*	kg	Non-reactive volatiles (Yield at high pressure)
V_P^*	% daf basis	Ultimate volatile yield at pressure P
V_r^*	kg	Reactive volatiles (Yield at low pressure-V_{nr}^*)
$X_{Compound}$	-	Mole fraction of Compound
z	-	Unadjusted ratio of combustion products
Z	-	Size corrected ratio of combustion products

1. INTRODUCTION

1.1 Definition of Entrained Flow Coal Gasification

Entrained flow coal gasification describes a specific type of process in which coal is converted into gases. Variations in design may occur between different plants, such as feeding fuel into the top or the bottom of the gasifier, but in all cases the coal is considered to be entrained in the feed gases so that the velocities of both solids and gases are approximately equal (Littlewood (1977), Mangold *et al.* (1982), Merrick (1984)). This generally means that coal particle sizes are small and the gas velocities are relatively high. Coal gasification can refer to a variety of processes, all of which convert coal to gases, but is most notably comprised of devolatilisation, and gasification of carbon by reaction with any of oxygen, carbon dioxide, steam and hydrogen (Hoy and Wilkins (1958), Ergun and Menter (1966)). The products of gasification depend on the coal, the ratio of feed gases, the temperature and the pressure, with the object of gasification being to produce a combustible gas mixture comprising of high proportions of carbon monoxide and hydrogen. This is effectively a partial oxidation of coal, as is distinct from the complete oxidation of coal desired in combustion of coal.

1.2 Reactions in Gasification

The reactions involved in gasification of coal can be divided into three major types, thermal decomposition reactions, heterogeneous gas-solid reactions and homogeneous gas-gas reactions (Hoy and Wilkins (1958), Watkinson *et al.* (1991)). While a large number of reactions are theoretical possible in a gasifier those that are typically regarded as of major importance are given below in reactions 1 to 14. Thermal decomposition of coal is termed devolatilisation and is represented in a simple in reaction 1 as the breakdown of coal on heating into char and volatiles. Obviously more complex representation must be used in order to define the quantities and compositions of the products for modelling purposes but this will be discussed in later sections. Reactions 2 to 5 describe the heterogeneous reactions between carbon in coal or char with various gases. In reaction 2, commonly called combustion, oxygen reacts with carbon to produce carbon dioxide and carbon monoxide in varying ratios. The other heterogeneous reactions are typically called the gasification reactions, although technically both devolatilisation and combustion are also gasification reactions. Reactions 6 to 10 are gas phase combustion

reactions which result in the complete oxidation of any gases if oxygen is present. These reactions are strictly reversible reactions so that small quantities of oxygen and unoxidised gases will exist at all times, however the quantities are so minor that representation as irreversible reactions appears more appropriate. In the absence of oxygen a series of homogeneous gas phase equilibrium reactions determines the gas composition in the gasifier, as represented by reactions 11 to 14.

Devolatilisation

$$Coal \rightarrow Char + Volatiles$$ Reaction (1)

Heterogeneous Gasification

$$C + \tfrac{1}{Z} O_2 \rightarrow \left(2 - \tfrac{2}{Z}\right) CO + \left(\tfrac{2}{Z} - 1\right) CO_2$$ Reaction (2)

$$C + CO_2 \rightarrow 2CO$$ Reaction (3)

$$C + H_2O \rightarrow H_2 + CO$$ Reaction (4)

$$C + 2H_2 \rightarrow CH_4$$ Reaction (5)

Homogeneous Combustion

$$CO + \tfrac{1}{2} O_2 \longrightarrow CO_2$$ Reaction (6)

$$H_2 + \tfrac{1}{2} O_2 \longrightarrow H_2O$$ Reaction (7)

$$CH_4 + 2O_2 \longrightarrow CO_2 + 2H_2O$$ Reaction (8)

$$H_2S + \tfrac{3}{2} O_2 \longrightarrow SO_2 + H_2O$$ Reaction (9)

$$COS + \tfrac{3}{2} O_2 \longrightarrow CO_2 + SO_2$$ Reaction (10)

Homogeneous Equilibrium

$$H_2O + CO \longleftrightarrow H_2 + CO_2$$ Reaction (11)

$$CO + 3H_2 \longleftrightarrow CH_4 + H_2O$$ Reaction (12)

$$SO_2 + 3H_2 \longleftrightarrow 2H_2O + H_2S$$ Reaction (13)

$$COS + H_2O \longleftrightarrow CO_2 + H_2S$$ Reaction (14)

1.3 Historical Use of Gasification

Gasification of carbon has a long history initially founded on the production of fuel gas from coal for domestic lighting in 1792 (Littlewood (1977)) and later generation of hydrogen from charcoal for use in hot air balloons in the 1800s (van Heek (1990)). Gasification of coal was at one stage widely used in the production of "town gas" using coke oven style fixed-bed gasifiers with the product gas used for street-lighting and domestic consumption. High pressure gasification is used commercially for the production of gases for synthesising chemicals, such as ammonia, although the feed material is commonly heavy oil residues rather than coal. More recently gasification has been proposed to generate fuel gas for electricity production from gas turbines. The advantages in gasification over the more common pulverised coal combustion boilers arise from both the higher thermodynamic efficiency of, and lower emissions of pollutant gases by, the gasification process.

1.4 Gasification Technologies

Three distinct variations in designs of gasifiers have been commonly used in industry, namely fixed bed, fluidised bed and entrained flow. Due to the differences in designs each of the gasifier types has different characteristics in operating conditions and performance. A detailed analysis of the different gasifier types is found in Littlewood (1977) and a brief summary from this is given below with additional references for more recent gasifier designs.

Early gasifiers were almost exclusively fixed bed, utilising lump coal and operating at low temperatures to avoid slagging of the ash. This had noticeable production, safety and environmental problems due to the presence of tars in the product gas and slow conversion of the coal. Numerous arrangements are possible for fixed bed gasifiers by varying the direction of gas flow and coal feeding methods. Modern fixed bed gasifiers have slag handling equipment to allow high temperature operation to avoid tar formation and operate at high pressures in order to supply higher gas flowrates (Evans *et al.* (1985)). Limitations on the properties of coal used in fixed-bed gasifiers are fairly self-evident, as extensive swelling of the coal with devolatilisation or high ash content could lead to blocking of gas flows in the gasifier. Also excessive break-up of coal lumps would hinder the operational efficiency of the gasifier.

Another type of gasifier to be developed is the fluidised bed, which maintains a dense suspension of large coal particles in a reactor. This style of gasifier

requires that only moderate temperatures be attained as agglomeration of particles, caused by the ash melting, cannot be handled. The temperatures attained in the gasifiers lead to a restriction of coals to those which are highly reactive, typically low rank coals such as lignite or sub-bituminous, or excessively long residence times are required for conversion. For coals with high ash fusion temperatures an advantage can be gained in this type of gasifier by raising the operating temperature of the gasifier without causing slagging. Typically fluidised bed gasifiers are now operated at high pressures to give better reaction rates and improve the usefulness of the product gas in gas turbines or synthesis (Schwartz (1982)).

Entrained flow gasifiers are the only other major gasification technology in use. The layout of an entrained flow coal gasifier is shown in figure 1.1, however significant differences between different proprietary designs exist (Schafer *et al.* (1988), EPRI (1993), EPRI (1978)). These gasifiers utilise finely ground coal and operate at conditions of high temperature and pressure to produce gas with only a brief particle residence time in the gasifier. Due to this short residence time it is expected that the gasifier can be made very responsive to changes in requirements for gas, ideally suiting it for electricity generation plant. Entrained flow gasifiers have been extensively utilised in synthesis gas production for the last 50 years and interest in their suitability for electricity generation plant has been evident from the 1970's onward. The intense reaction conditions in these gasifiers initial led to materials problems caused by liquid coal ash slag destroying refractory linings but these problems have been largely controlled by introduction of water-wall cooling of the gasifier, producing a protective layer of solidified slag on the refractory membrane. Due to the intense operating conditions a wide range of coal can be used for gas production within an acceptable range of performance, however limitations have been experienced with some designs when the temperature is not sufficiently high to keep the slag fluid at the tapping point. Most plant designs allow for addition of a flux, such as limestone, to lower ash viscosity when problems are experienced.

1.5 Current Interest in Gasification

Recently interest in coal gasification has resurfaced due in most part to environmental concerns about existed pulverised coal fired power plants. The advantages in using an entrained flow coal gasifier plant in power generation have several bases. Firstly, the sulfur content of the coal can be recovered from the exit gases from the gasifier, due to its form as the acidic gas hydrogen sulfide, and therefore prevent emission of sulfur oxides from the plant. Secondly, the integration of a gasifier in a combined cycle plant incorporating a gas turbine, heat recovery boiler and a steam turbine leads to greater thermal efficiency than existing coal fired plant with associated reductions in coal usage and greenhouse gas emissions.

1.6 Process Description of Entrained Flow IGCC

An integrated gasification combined cycle (IGCC) plant is based on a number of major plant items which can be arranged in a number of configurations (Brown (1982)). In figure 1.2 a generic IGCC plan is shown based on those given in Anon. (1990) and Brown (1982). The gasifier is supplied with pulverised coal and high pressure feed gas. Feed gas is generally a combination of oxygen and steam, where oxygen is produced in an air separation plant and compressed using compressors powered by a shaft from the turbines and steam is bled from the heat recovery boiler. Heat is recovered from the gasifier through water-wall cooling and steam generated from this water using a heat recovery boiler using the flue gas. Actual power generation is therefore via two turbines, a gas turbine fuelled by the product gas and a steam turbine for steam from the heat recovery boiler. A gas clean-up facility is included between the gasifier and the gas turbine to remove particulates and sulfur species from the gas. Depending on the plant design gas may be cooled before treatment and nitrogen from the air separation plant, or steam, may be added as a diluent before the gas is combusted. The addition of a diluent reduces the temperature reached during gas combustion, a limitation imposed by the materials in the gas turbine and also resulting in reduced nitrogen oxide formation during combustion.

1.7 Current and Future Gasification Plant

A summary of existing and proposed IGCC plants worldwide is given in table 1.1, including plants with fixed bed, fluidised bed and entrained flow gasifiers. Data that is unreliable or unavailable is indicated by '?' in the table. Some of the plants indicated are intended for commercial applications, such as waste disposal or co-generation of electricity and steam. However, many of the plants are intended only to demonstrate the reliability of the technologies before implementation on a full commercial scale. It is uncertain whether construction will proceed for a number of the proposed plants, and completion of a number of plants has been delayed. It is evident from the relative numbers of each type of plant that entrained flow gasifiers are expected to provide better performance than the other types of gasifiers in this application. This is largely due to the short residence time in entrained flow gasifiers allowing more rapid changes in gas production, and therefore power generation. The operating pressure for most of the designs is in the range of 20 to 30 atmospheres, indicating some convergence of design and performance factors in this range.

Fuels used by the various gasifiers can vary markedly, with various of the fluidised bed gasification processes using biomass, pulp mill sludge, peat, lignite, black coal, oil and natural gas, the fixed bed gasifier operating on either petroleum coke and black coal, and the entrained flow gasifiers utilising on sewage sludge, lignite, petroleum coke, sludge, natural gas, distillate and black coal. The use of natural gas and distillate in the gasifiers is to increase gasification temperatures when using lower grade fuels. As demonstration plant the variety of fuels used is intended to show the flexibility of the plant and it is not expected that use of all fuels would be economically viable.

Details for the operation of the various gasifier designs can differ greatly between designs, for example the feeds can be fed into the top or bottom of the gasifier, or can be staged so that part of the fuel enters at the bottom and the remainder at a higher level. The feed method can also vary so that either slurried or dry fuel is added. Similarly the oxidant gases used in gasification can be either compressed air or compressed oxygen, with the nature of the design being determined by the economics of a larger gasifier versus those of an air separation plant.

The list of gasifiers considered is not detailed, as it is limited to IGCC usage while a large number of gasifiers have been installed for the purposes of gas synthesis, rather than power generation. Synthesis gas producing gasifiers can vary in design from those used for IGCC as lower temperatures and different feed mixtures are used to promote

formation of the desired gas product, typically hydrogen. Pressures utilised in these gasifiers are also commonly higher than for IGCC gasifiers, usually being greater than 50 atmospheres.

Table 1.1: Existing and proposed IGCC plant (Anon. (1992)).

Gasifier Type	Startup Year	Country	Fuel Feed Rate (t/day)	Pressure (atm)
Fixed Bed				
British Gas/Lurgi	1984	UK	500	28
Fluidised Bed				
U-Gas/Tampella	1991	Finland	-	<30
Uhde/Lurgi	1996	Germany	6408	28
U-Gas/Tampella	1996	Sweden	1440	26
KRW	1996	USA	800	120 (?)
U-Gas/Tampella	1998	USA	390	24
Entrained Flow				
Texaco	1984	USA	907	42
Destec Energy	1987	USA	2400	29
Mitsubishi	1991	Japan	200	26
Shell/Steinmüller	1994	Netherlands	2000	29
ABB	1995 (?)	USA	566	19
Destec Energy	1995 (?)	USA	2640	29
Texaco/Deutsche Babcock	1996	USA	2076	33
Texaco	1996	USA	2000	28 (?)
Texaco	1996	USA	1900	-
Deutsche Babcock	1996	Germany	120	21
Deutsche Babcock	1996	Germany	48	6
Deutsche Babcock	1997	Spain	2580	26
Krupp Koppers	?	Germany	2400	27
Krupp Koppers	?	Spain	2590	27
Mitsubishi	?	Japan	2500	20-30

1.8 Mathematical Modelling of Gasification

The design of most industrial plant has traditionally been performed by using a "rule of thumb" approach that uses knowledge acquired from previous plants. This approach has been widely used in the design of power generation plant in the past and has resulted in poorly designed plant that operates at far below the maximum attainable efficiency (Babcock and Willcox Company (1978)). Pulverised coal boilers, the most commonly used power generation technology worldwide, are an example of how not to develop technology as at the time of construction of the first plants (circa 1920) there was little understanding of the basic mechanisms of pulverised coal combustion. This resulted in power plants with as little as 10% overall efficiency, compared to the current efficiencies approaching the thermodynamic cycle maximum of approximately 38%. The current trends in gasification technology development appear to be paralleling this in the building of plant prior to understanding the fundamental processes involved in gasification. This is illustrated in the experiences with the 203.2 tonne per day Shell pilot plant gasifier at Deer Park, USA, reported in EPRI (1993). The results of tests show that the gasifier was greatly overdesigned, to the extent that capacity exceeded 144% of design and could not be found due to limitations of ancillary plant. This indicates that the reaction mechanisms in the gasifier were poorly understood by the designers and this has led to the overdesign. While an overdesigned plant is generally preferable to one that is underdesigned, in this case at maximum coal feed rate the gasifier efficiency was still increasing with increasing coal feed. The results from the Deer Park gasifier were used in the design of a 2000 tonne per day gasifier (currently in operation at Buggenum in the Netherlands), presumably including a degree of overdesign as the capacity of the Deer Park gasifier was not determined. In Australia little experimental research on gasification has been performed due to the high cost of equipment and, therefore, reliance on the experience gained in overseas research will be required. In this the development of models that account for the differences in gasification performance between different coals and operating conditions will be crucial for the proper design of gasifiers for Australian coals.

1.9 Requirements of Model

The major requirements for the present study mathematical modelling are to identify the key factors involved in coal selection, gasifier design and gasification conditions for entrained flow coal gasification. Determination of these factors enables prediction of optimum coal and gas feeds for given gasification conditions or, conversely, prediction of optimum gasification conditions for given coal and gas feeds. In order for a model to satisfy these requirements a number of criteria must be met. The major criteria for a gasification model would be based upon the ability of the model to distinguish between different coals and operating conditions and provide predictions that accurately rank the performance of a gasifier relative to some base index. To extend the usefulness of a model it should be able to perform these predictions without requiring excessive specialised testing of the coal, such as volatile yield and reactivities measured at high pressures. The emphasis of modelling in this study will be to implement methods to estimate coal properties from minimal experimental data using standard analysis results, such as the coal proximate and ultimate analysis.

1.10 Simplified Model Description

The model that will be developed and tested in the following sections is based upon a plug flow reactor. In this form of reactor flow is assumed to be uni-dimensional parallel to the longitudinal axis of the reactor, with perfect mixing radially. This is a simplification on reality in a reactor, where complex turbulent motion can cause radial flows and longitudinal mixing, but can be justified for small diameter reactors such as are used in laboratory scale testing. Plug flow modelling was chosen in preference to more complex turbulent flow modelling techniques as the simplicity of the flow arrangements allows for detailed analysis of coal particle structure and reaction mechanisms during gasification. In this regard the model is most suitable for prediction of differences in coal performance under given conditions rather than for differences between the performance of different gasifiers.

The reactions involved in gasification of coal can be divided into two major types, heterogeneous gas-solid reactions and homogeneous gas-gas reactions. The concentration of individual gases and the temperature in the gasifier determine the importance of the reactions, however in approximate order of reaction rate the major heterogeneous reactions are shown in Reactions (1) to (5). Reactions (6) to (13) are gas phase equilibrium reactions that affect the gas composition throughout the gasifier and

have varying importance depending on the gasification conditions and the quantities of gaseous components present.

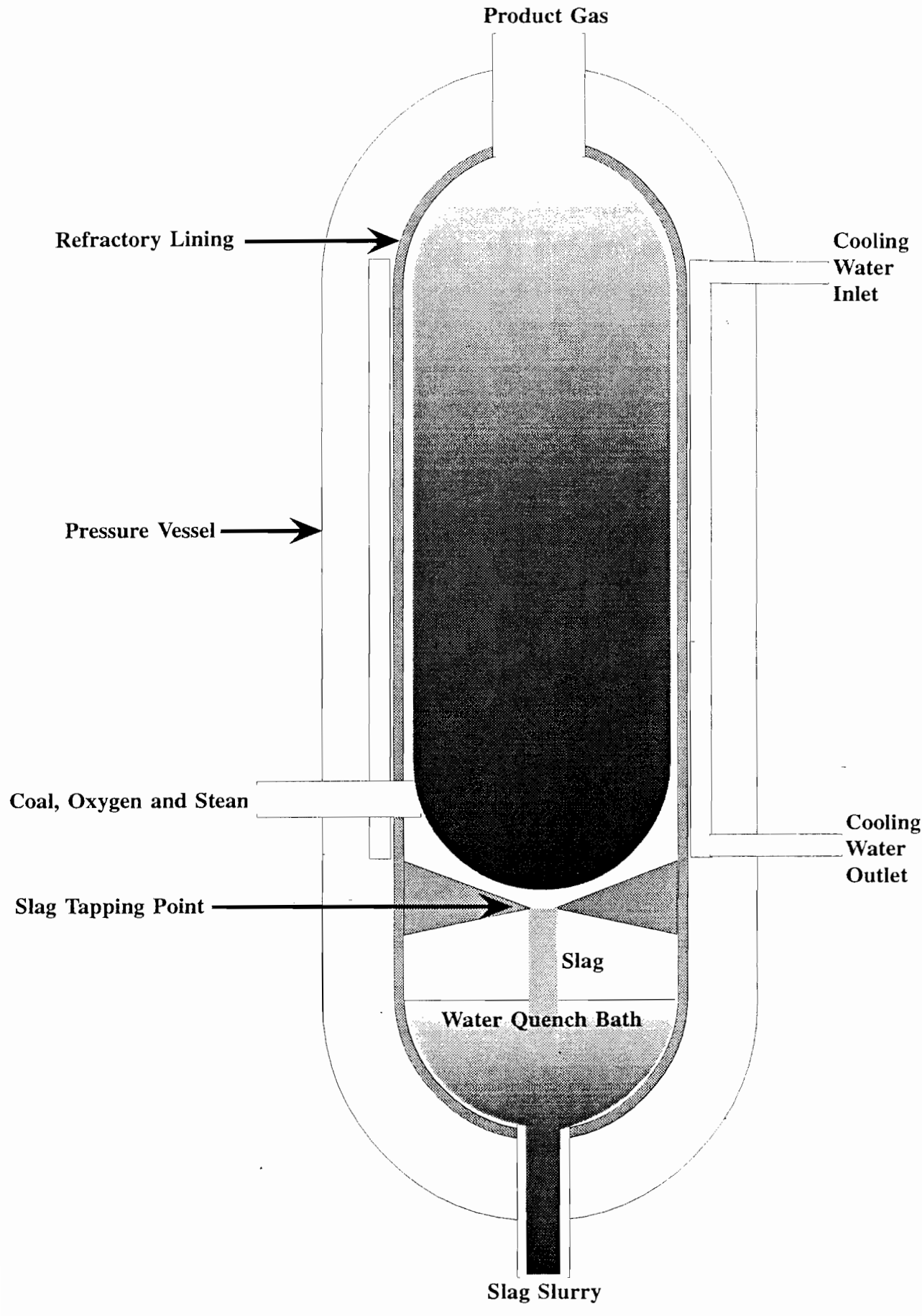

Figure 1.1: Layout of a typical entrained flow gasifier.

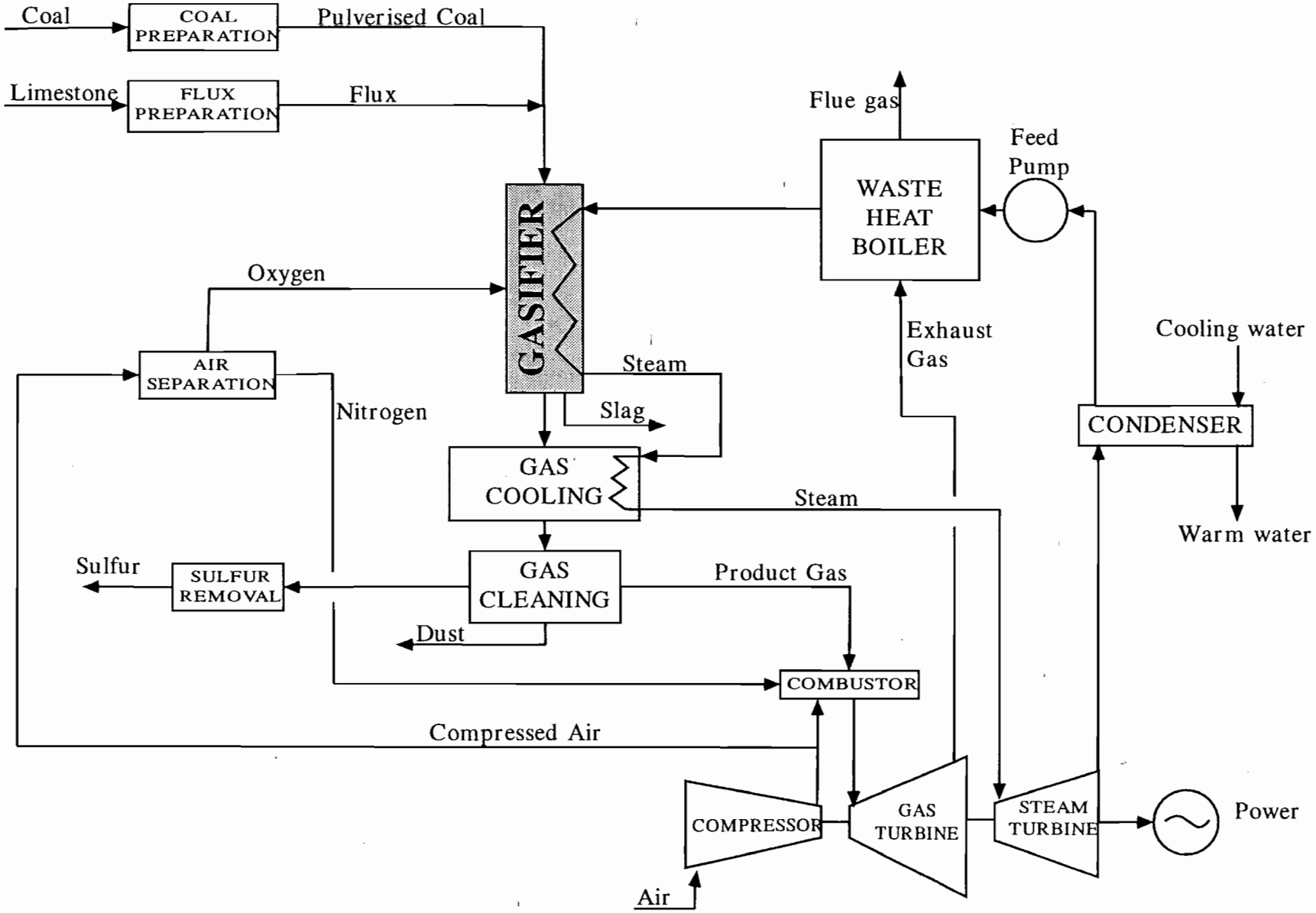

Figure 1.2 : Schematic of a typical integrated combined cycle coal gasification power plant with gasifier highlighted

2. LITERATURE REVIEW

2.1 The Components of a Coal Gasification Model

One of the major problems involved in modelling any process is the acquisition of reliable data on the sub-processes occurring. In entrained flow gasification this problem is complicated by the number of feasible reactions that can occur and the extremes of temperature and pressure experienced in a gasifier. A selection of reactions that are considered the most important in gasification were discussed in a previous section but a large number of other reactions are possible, due in part to the chemical complexity of coal. Processes occurring during gasification can be summarised as given in figure 2.1, with the addition of homogeneous gas reactions which are not shown as a simplification. This figure is an indication of the expected progress of gasification and the dominant processes are not expected to be occuring exclusively in the periods indicated. The expected progress of gasification in an entrained flow gasifier can be summarised as rapid heating of gas and particles accompanied by devolatilisation of the coal with resultant combustion of volatiles. When the flux of volatiles from the particles is sufficiently low to allow diffusion of reactant gases to the particles the heterogeneous reactions will proceed. As oxygen gasification is far more rapid than the other gasification reactions it will dominate while oxygen is present and after all oxygen is consumed carbon dioxide and steam gasification will become dominant owing to the high concentrations present as products of combustion. Owing to the homogeneous equilibrium reactions it is unlikely that all carbon dioxide and steam will be consumed but as the reactions proceed further the quantity of hydrogen present may cause hydrogen gasification to occur. As hydrogen gasification is a slow reaction this will only occur in large, high pressure gasifiers with high carbon conversion. This summary neglects the complicating features of the associated heat transfer processes, the changing gas composition and the diffusional processes to simplify the overall process. In modelling such a process it is theoretically possible to consider all the mechanisms of all relevant processes by monitioring them under conditions applicable to entrained flow gasification, however this is rarely feasible due to the difficulties involved in making measurements under these conditions. In practice literature results for a range of conditions must be extrapolated to higher temperatures and pressures, with the extrapolation being subject to possibly considerable error in some cases. The purpose of this literature survey is therefore to isolate suitable

data and methods from a considerable base of scientific literature, and in some cases translate raw data into suitable sub-models, preferably in equation form.

In order to simplify the arrangement of models it is common to break a model into a number of components which are considered independently. While there can be inter-relation between components a degree of independence must be allowed in order that solution of the modelling problem can be achieved. For example, in the components to be discussed, the total yield of volatiles will be dependant on the maximum temperature achieved by the coal particles, a variable that is influenced by a complex heat and mass balance. It is probably not possible to solve for this maximum temperature without assuming a volatile yield, and the problem is complicated by other reactions possibly occurring simultaneous to devolatilisation. Thus an approximation of the maximum particle temperature is used in determining the volatile yield expected and this is then independent of the actual temperature calculated in the heat and energy balance. This example is typical of the difficulties in modelling complex systems and, in some cases, leads to an iterative process in the modelling when original estimates are found to be suspect when the model reaches a more advanced stage. For this reason the literature survey is condensed from earlier stages of the study by omission of data that has proven to be superfluous to the model.

In table 2.1 the major sub-models of an entrained flow gasification model are defined, along with components that are usually associated with these models and the inputs that are needed in order to prepare a suitable model of the process. In some cases previous work has established well known expressions that enable simplistic modelling of the process, while in other cases no reasonable approach to modelling has previously been suggested for the process. In the following sections suitable modelling techniques based on published experimental or theoretical work will be discussed for some of the components defined in the table. The subject of gas mixing and particle dispersion will not be discussed at length as if is not relevant to plug flow models and topics of a general nature, such as calculation of basic gas properties will be neglected.

Table 2.1: Gasification modelling components:

Sub-models	**Typical Components**	**Required Inputs**
Particle Heating	a. Convection	i. General Correlations
	b. Radiation	i. Particle Emissivity ii. Gas Emissivity iii. Wall Emissivity
Drying	a. Instantaneous Rate	i. Moisture Content
	b. Rate	i. Experimental Expression
Devolatilisation	a. Instantaneous Rate	i. Volatile Yield (see below)
	b. Rate	i. Experimental Expression
	c. Yield	i. Coal Properties ii. Temperature Effects iii. Pressure Effects
Char Reactions	a. Boundary Layer Diffusion	i. Gas Properties
	b. Chemical Kinetics	i. Rate Expression ii. Pressure Effects iii. Experimental Rates
	c. Pore Diffusion Hindrance	i. Particle Structure ii. Pore Effectiveness Factor
Gas Reactions	a. Rate	i. Experimental Data
	b. Equilibrium	i. Equilibrium Expression
Gas Mixing and Particle Dispersion	a. Turbulence Model	i. Gas Properties ii. Correction for Particles
Wall Heat Balance	a. Conductive Transfer	i. Slag Properties ii. Refractory Properties iii. Metal/Water Conditions

2.2 Devolatilisation

Coal is a complex non-homogeneous organic material containing inclusions of inorganic matter incorporated in the structure. Heating a coal above approximately 400°C results in breakdown of some parts of the organic and inorganic structures with the net effect of devolatilisation given in its simplest form by reaction 1.

$$Coal \rightarrow Char + Volatiles \qquad \text{Reaction (1)}$$

The process can be considered in more depth to understand the degree of disruption, in both a physical and chemical sense, to the coal while it becomes char. Functional groups and some smaller organic chains will be separated from the main carbon matrix of the coal and attempt to vapourise. The smaller compounds are likely to escape from the particles into the gas phase but some of the larger chains can act as solvents for the carbon matrix and result in softening of the remaining solid. With increasing temperature the quantity of material separating from the char matrix will increase and the formation of gases in the particle will cause swelling and radical changes in the pore structure of the char. As the solvents in the coal particles either vapourise and escape or recombine with the solid the particles will resolidify. Char from high temperature devolatilisation will have been stripped of the majority of the non-carbon atoms and may contain low reactivity graphite-like structures formed during resolidification. A range of changes in the structure of the particles may have occurred, typically large pores may have formed due to the escape of gases from the particles, bubbles may be trapped in the solid and the particles will probably be rounded, rather than the angular shapes of coal.

It is difficult to study devolatilisation experimentally as the process is extremely rapid at temperatures resembling combustion conditions and, in a reactive environment, changes in the coal due to devolatilisation are difficult to distinguish from those due to heterogeneous reactions. For these reasons most researchers have preferred to study pyrolysis of coal under inert or reducing atmosphere conditions. This means that an overlying assumption that behaviour of coal in devolatilisation under combustion or gasification conditions is similar to that measured experimentally with a less reactive environment. To some extent this cannot be true as it is difficult, if not impossible, to replicate the heating conditions of a particle igniting, possibly with heterogeneous ignition if oxygen concentrations are high, in an inert atmosphere. In the following discussion it is largely assumed that the changes occurring during pyrolysis, with respect to volatile release, accurately reflect those occurring in a gasifier. Variations from this assumption

will be identified where it is obvious that pyrolysis results cannot realistically approximate devolatilisation in a gasifier.

2.2.1 Description of Devolatilisation

Devolatilisation can be viewed from either of two perspectives, as a chemical process or as a physical process. The chemical basis of devolatilisation is that, upon heating, functional groups and some fragments of the coal structure are separated from the coal by the breaking of bonds. Some of the smaller units thus formed will exist as gases, or volatiles, at the ambient temperature and pressure, and will therefore attempt to diffuse out of the coal to the bulk phase. Other fragments will either remain as solids or liquid tars which can either remain on the coal surface or vaporise later at higher temperatures. Secondary reactions can occur between volatiles and the coal structure or with other volatiles and the products of these reactions may condense or solidify in the coal structure (Solomon *et al.* (1992)). The coal that remains after devolatilisation has been stripped of many of the non-carbon atoms, with removal of the functional groups, and is now termed char. Besides this carbon enrichment the release of volatiles has a profound effect on the physical structure of the coal, with the enlargement and increase in numbers of pores and changes in the shape of the particle (Simons 1984). This occurs because some of the products of devolatilisation are trapped in the particles and act as solvents, liquefying or softening the coal. Internal pressure changes in the particles due to the creation of gases inside the particle can lead to bubbling and resultant distortion of the particles. In this regard two types of coal are defined as softening and non-softening coals. Softening coals are those that have marked deformation during devolatilisation while non-softening, due to more rigid internal structuring, do not deform significantly. In modelling devolatilisation factors that should be considered are the rate, the yield of volatiles, the composition of the volatiles, the resultant particle structure and composition. Devolatilisation rate is expected to have only minor significance in the modelling of gasification as the high temperatures lead to devolatilisation proceeding at a rapid rate and therefore the devolatilisation time is negligible compared to the overall gasification time. Conversely, the total yield of volatiles is significant as this determines the quantity of char that remains to be gasified, and the structure of the char will have an impact on the heterogeneous reaction rates. The composition of the volatiles released has a minor impact as gas species will change rapidly due to gas phase combustion or equilibrium shifts, and therefore the volatile elemental composition is more significant than the species released.

2.2.2 Devolatilisation Kinetics

The kinetics of devolatilisation are a very complex area of research due to the varied chemical structures of different coals, and in fact variations within the same coal. While recent kinetic models have concentrated on analytical approach dealing with the types and frequency of different chemical bonds in a particular coal (eg. Solomon (1988)) or have even treated the release of volatiles as a complex fractional distillation (Niksa (1988)), more traditional approaches are based mostly upon experimentally measured rates. The literature for devolatilisation is extensive due to the similarity between combustion and gasification in its preliminary stages. Early experimental studies on devolatilisation under conditions similar to combustion were performed by Badzioch and Hawksley (1970), who found that the experimental rate of devolatilisation could be modelled by a rate expression that was first order with respect to the volatile content remaining in the coal at any given time, as shown in equation 2.1, with V^* being the ultimate volatile yield and V the instantaneous yield. Under varying

$$Rate_{Devolatilisation} = k.e^{\frac{-E}{RT}}.\left(V^* - V\right) \qquad \text{Equation (2.1)}$$

conditions other authors have reported that a first order expression does not correctly represent the profile of volatile emissions. Notable amongst these authors is Ubhayakar (1977) who defined two types of volatiles, ethylene and benzene, which are released at different rates. This leads to a twin reaction rate expression, as shown in equation 2.2, where a_1 and a_2 are the possible yields of the two volatile types and m_c is the mass of

$$Rate_{Devolatilisation} = (a_1 k_1 e^{\frac{-E_1}{RT}} + a_2 k_2 e^{\frac{-E_2}{RT}}).m_c.e^{-\int (k_1 e^{\frac{-E_1}{RT}} + k_2 e^{\frac{-E_2}{RT}})dt} \qquad \text{Equation (2.2)}$$

undevolatilised coal. Increasing the complexity of the kinetic model can provide a better analysis of the time-temperature profile of volatile release however it also makes for more complex modelling techniques. From only considering volatiles as one or then two compounds an obvious extension is to consider a normal distribution of compounds, such a model was defined by Anthony (1976). Further to this are the more recent models which statistically determine the rates of devolatilisation of individual gases from the breakdown of specific bond types (Solomon (1988), van Heek (1990), Niksa (1988)). However the more complex models do not seem to be required for very rapid devolatilisation processes as greater resolution on a process that is expected to take only tens of milliseconds, compared to total gasifier residence times in the order of seconds, appears unnecessary.

Some advantages can be seen in calculating the generation rates of individual gas species to increase the accuracy of mass balances but a penalty is imposed in the extensive analysis of coals required.

While the previously discussed kinetic models have defined the rate of volatile release only in terms of the quantity of volatiles in the coal and the temperature, it is significant to note that other variables can also affect the rate. Significant amongst these are diffusion of the volatiles out of the coal particles to the bulk gas and the influence of total pressure on both diffusion rate and the reactions either releasing or recombining the volatile compounds. There are many difficulties in studying diffusion in a devolatilising particle due to the rapidity of the reaction and the changing porous structure of the particles. While published experimental work has neglected diffusion a modelling study by Simons (1984) considered its influence and suggested that, in the particle size range of pulverised fuel, diffusion should have no major impact on the rate. Similarly the effect of pressure on rate has been neglected, although the change in yield has been studied and this will have an effect through the rate expression. A modelling study by Oh *et al.* (1989) implicitly expects high pressures to slow devolatilisation in softening coals by requiring an increase in internal pressure of volatiles in bubbles attempting to escape from the softened coal. To achieve a greater pressure in the bubbles a longer heating period is required before volatiles can escape from the coal particles, but this would be expected to be significant only in larger coal particles. In the only relevant published experimental data, Lee *et al.* (1991) found that the rate of devolatilisation of coal in an entrained flow reactor was slowed with increasing pressure for the initial stages of devolatilisation. This change in rate was attributed to a decrease in volatile yield at higher pressures and the rates for different pressures converged at later stages of devolatilisation. The simple kinetic models defined in equations 2.1 and 2.2 support these changes with pressure if the input parameters for ultimate volatile are adjusted for pressures greater than atmospheric.

2.2.3 Volatile Yield

The yield of volatiles in gasification is more significant than in a combustion system as the remaining char must be converted by slow gasification reactions. A number of researchers have studied the influence of variables on the total yield of volatiles from particular coals. General conclusions have been that the maximum temperature achieved and the length of time the particles spend at this temperature are the major influences on volatile yield. Also, in some cases, the species of gas present at the

time of devolatilisation will affect yield. It is certain that volatile yield under high temperature conditions will be different to the proximate volatile matter analysis for the coal, mostly due to the different temperatures involved.

Badzioch and Hawksley (1970) probably published the first work applicable to combustion processes and identified difference between proximate volatile matter and high temperature volatile yield for a number of coals. They defined a factor relating the two quantities, commonly known as the Q factor and defined in equation 2.3, but did not determine reasons for the variations in behaviour of different coals.

$$Q = \frac{V^*}{VM\left(1 - VM_C\right)} \qquad \text{Equation (2.3)}$$

The Q factor of Badzioch and Hawksley (1970) corrects for residual volatile matter in the char, VM_C, which was considered by the authors to be the result of condensation of some volatiles. However later works have redefined the Q factor as simply the ratio of volatile release to proximate volatile yield, and this simpler definition is use in this work. The Q factor tends to be highest for low volatile coals and decreases to close to unity for high volatile coals. Anthony (1976(a)) considered heating rate separately to temperature and concluded that the final temperature was significant in determining total volatile yield while heating rate had only a minor influence. More recent experimental work by Gibbins (1989) disputed this, showing that a slight increase in yield with heating rate occurs.

Another factor in the total yield from devolatilisation is the pressure at which the reaction occurs. Several researchers have shown that a substantial decrease in volatile release occurs at higher pressures, a selection of experimental results is shown in figure 2.2 (Anthony (1976), Suuberg (1977), Bautista (1986), van Heek (1990), Lee (1991), Sharma (1986)). The reasons for this decrease in volatile yield at high pressures remains uncertain, with traditional theory claiming an increase in the impact of secondary reactions on the volatiles, particularly at high pressures, (Anthony (1976)) and more recent models claiming that the increase in boiling point of liquid hydrocarbons at high pressures leads to reduced vapour pressures of the volatiles (Niksa (1991)). Anthony (1976) and Sharma (1986) also showed that the composition of the gas surrounding the particle can change the volatile yield, in particular steam was shown to slightly increase, and hydrogen greatly increase, volatile yields at high pressures. The effect of steam and hydrogen in gas mixtures under the extremely rapid heating conditions in an entrained flow gasifier is

expected to be minimal due to the rate of devolatilisation being great enough to prevent diffusion of gases to the coal particles.

Particle size also has a noticeable effect on yield but Wagner (1985) showed that this is only significant for particles approaching 1 mm in diameter, much larger than is normal for the pulverised coal feed for entrained flow gasifiers. Also, the effect of pore structure on diffusional resistance for the volatiles escaping from the coal is discussed by Simons (1984), but as the structure is hard to define it is difficult to determine the change in yield from coal to coal.

The work of Neoh and Gannon (1984) is significant in estimating the volatile yield of a wide range of coals as it correlates volatile yield with commonly measured coal properties. This work covered a wide range of coals at a high temperature (2400K), similar to the peak temperature experienced in a gasifier, and the authors proposed a simple expression for volatile yield based on the mole fractions of some elements in the coal analysis, as shown in equation 2.4. The experiments performed by Neoh and Gannon (1984) involved ignition of a stoichiometric hydrogen-oxygen mixture containing a suspension of coal particles. As the reaction vessel was sealed pressure fluctuations were produced, peaking at approximately 10 atmospheres. Also a correction was applied to the results to counter the loss of carbon due to heterogeneous reaction with steam. In figure 2.3 the errors in predicted of volatile yields from the correlation of Neoh and Gannon (1984) are indicated for their experimental results and also a variety of other literature results for volatile yield, limited to experimental temperatures greater than 1700K. The comparison shows that the correlation predicts well for the results of Neoh and Gannon (1984) but has lower accuracy for other literature results. This low accuracy is most probably due to variations in experimental methods causing significant variations in volatile yield for different researchers and in this case it is unlikely that any correlation not considering reaction conditions could accurately predict the volatile yield for all experimental results.

$$V^* = 52.6\left(\frac{X_{Hydrogen} + 2.X_{Oxygen}}{X_{Carbon} + X_{Sulfur}}\right) + 6.89 \qquad \text{Equation (2.4)}$$

2.2.4 Volatile Composition

The composition of volatiles released from coal has been studied extensively and a variety of gases have been found in the volatiles, with the proportions of

different gases dependant on coal chemistry and the conditions of devolatilisation. Published research of Suuberg (1977) for a single coal under a wide range of devolatilisation conditions shows trends of more complex hydrocarbons in the volatiles at higher temperatures and simpler volatiles at higher pressures. These findings are logical as at high temperatures it is expected that a larger number of chemical bounds would be broken and the resultant tars would become vapours while at high pressures it is possible that some of the compounds would not vapourise or could possibly undergo secondary reactions during diffusion out of the particles.

As it is difficult to measure the volatile composition for a particular coal under any set of conditions that may be required to be modelled, Brown *et al.* (1988) used a technique of estimating the elemental yields in devolatilisation and adding these to the existing gas, using the assumption that gas phase equilibrium is reached. While this approach simplifies estimation of volatile composition it has a limiting feature that the energy balance of devolatilisation cannot be accurately calculated as the form of the gases leaving the particle is not known. The approach of Solomon (1988) or van Heek (1990), which consider the formation rates of individual gases from the breakage of specific bond types, avoids this problem as the amount of energy required to break a particular bond type is known and the amount of a gas being released at a particular time is given. This approach allows for estimation of individual gas yields if information on the concentration of active groups in the coal structure is available. However Hobbs *et al.* (1992) found that the Functional Group Devolatilisation (FGD) model of Solomon (1988) was not suitable for predicting the yields of large organic molecules for devolatilisation in practical systems.

2.2.5 Structural Changes during Devolatilisation

It has long been noted that devolatilisation can have a marked effect on coal structure, as is indicated by various indices used to describe coal swelling (eg. crucible swell number (CSN), free swell index (FSI), British Swell Number (BSN) and Gray-King coke type). Obviously the magnitude of coal swelling will vary from coal to coal, influenced largely but not exclusively by the volatile content of the coal. Also the degree of swell will be influenced by the heating rate, temperature and gas composition to which the particles are exposed. In this regard it has been found (Field (1970)) that combustion conditions of high heating rate, high temperature and oxidising atmosphere hinder particle swelling compared to the pyrolysis conditions of laboratory analysis.

Figure 2.4 shows the predicted swell, based on the swelling number, and experimentally measured swell for the range of coals studied by Field (1970) and for three char samples generated in the CSIRO experimental gasifier under different stoichiometric conditions (CSIRO (1995)). In more recent work Khan and Jenkins (1986) found that the volumetric swell for a set of 12 coals heated in an entrained flow reactor with nitrogen was unpredictable and showed considerable variation with pressure up to 28 atmospheres. The range of swell in this study was from zero to 400% on a volumetric basis, with the majority of results between 50 and 150%. As a particle swells with devolatilisation it has been recognised that the shape changes from typically rectangular prisms of coal to near spherical particles of char (Smoot and Smith (1985), Khan and Jenkins (1986)). The approach to spherical shape is dependant on the degree of softening of individual particles, which is largely based upon the maceral components of the particles (Unsworth *et al.* (1991)). It is commonly assumed in modelling that all particles of both coal and char are perfectly spherical, as a simplification for mass transfer and particle dynamics calculations, however this has an inherent error, particularly in the early stages of the gasifier when particle heating occurs with definitely non-spherical coal particles. A discussion of the errors associated with this simplification is given by Maloney *et al.* (1993), who estimates possible errors of 25 to 50% in heating rates when spherical particles are assumed.

2.3 Heterogeneous Reactions

2.3.1 General Characteristics

A total of four major heterogeneous reactions are considered to occur in coal gasification. These are the reactions of oxygen, carbon dioxide, steam and hydrogen with carbon, as shown below in reactions 2 to 5. The oxygen-carbon reaction is considered to have two alternate products in carbon monoxide and carbon dioxide, the ratio of these being determined by the conditions under which the reaction occurs. The reactions of oxygen and hydrogen with carbon are exothermic and therefore elevate the particle temperature, while the reactions of carbon dioxide and steam with carbon are endothermic, resulting in a lowered particle temperature.

$$C + \tfrac{1}{Z} O_2 \rightarrow \left(2 - \tfrac{2}{Z}\right) CO + \left(\tfrac{2}{Z} - 1\right) CO_2 \qquad \text{Reaction (2)}$$

$$C + CO_2 \rightarrow 2CO \qquad \text{Reaction (3)}$$

$$C + H_2O \rightarrow H_2 + CO \qquad \text{Reaction (4)}$$

$$C + 2H_2 \rightarrow CH_4 \qquad \text{Reaction (5)}$$

All of the heterogeneous reactions have been experimentally studied with extensive quantities of published literature on the oxygen reaction at atmospheric pressure due to its importance in conventional coal combustion. Less has been published on the other reactions, in particular the steam reaction due to the experimental difficulties arising from the handling of steam. At the high pressures relevant to commercial entrained flow gasification only a limited number of studies have been published, notably Muhlen *et al.* (1985), Blackwood and co-authors (1958, 1959, 1960, 1962), Monson *et al.* (1995) and Ranish and Walker (1993), due to the expensive equipment required. Due to the limited nature of the studies it will emerge that some doubts as to the kinetics and interactions of these reactions exists.

2.3.2 Fundamental Reaction Mechanisms

The mechanisms of heterogeneous reactions of carbon have been discussed widely in the literature for many years. Most proposed mechanisms have centred on adsorption/desorption of various complexes onto active sites of the carbon surface, sometimes also considering the effects of equilibrium reactions in the vicinity of the surface. One of the more recent studies of reactions with carbon was published by Chen *et al.* (1993) and mechanisms based on those identified by their study are given below, where C_f is a free carbon site and (O) is an adsorbed oxygen atom. While the reactions of oxygen, carbon dioxide and steam are similar, hydrogen gasification differs by not involving oxygen and oxygen can also bond to carbon via a more rapid, one step process.

(a) Oxygen Gasification

$$O_2 + 2C_f \Leftrightarrow 2C_fO \qquad \text{Step (1)}$$
$$2C_fO + O_2 \Leftrightarrow 2C(O)C_fO \qquad \text{Step (2)}$$
$$O_2 + C_f \Leftrightarrow C(O)C_fO \qquad \text{Step (3)}$$
$$C(O)C_fO \rightarrow CO + C_{f,new}O \qquad \text{Step (4)}$$
$$C_fO \rightarrow CO + C_{f,new} \qquad \text{Step (5)}$$

(b) Carbon Dioxide Gasification

$$CO_2 + C_f \Leftrightarrow C_fO + CO \qquad \text{Step (6)}$$
$$CO_2 + C_fO \Leftrightarrow C(O)C_fO + CO \qquad \text{Step (7)}$$
$$C(O)C_fO \rightarrow CO + C_{f,new}O \qquad \text{Step (8)}$$
$$C_fO \rightarrow CO + C_{f,new} \qquad \text{Step (9)}$$

(c) Steam Gasification

$$H_2O + C_f \Leftrightarrow C_fO + H_2 \quad \text{Step (10)}$$
$$H_2O + C_fO \Leftrightarrow C(O)C_fO + H_2 \quad \text{Step (11)}$$
$$C(O)C_fO \rightarrow CO + C_{f,new}O \quad \text{Step (12)}$$
$$C_fO \rightarrow CO + C_{f,new} \quad \text{Step (13)}$$

(d) Hydrogen Gasification

$$H_2 + 2C_f \Leftrightarrow 2C_fH \quad \text{Step (14)}$$
$$H_2 + 2C_fH \Leftrightarrow 2C_fH_2 \quad \text{Step (15)}$$
$$H_2 + 2C_fH_2 \Leftrightarrow 2C_fH_3 \quad \text{Step (16)}$$
$$H_2 + 2C_fH_3 \rightarrow 2CH_4 \quad \text{Step (17)}$$

The process followed in the oxygen, carbon dioxide and steam reactions involves bonding of an oxygen atom dissociated from the gas to a free carbon site (Steps 1, 6 or 10), and then another oxygen atom can adsorb on a nearby carbon to form a large adsorbed complex (Steps 3, 7 or 11). This complex can then release a carbon monoxide molecule to remove the free carbon and create another free carbon with a bonded oxygen atom (Steps 4, 8 or 12). It is also possible for a single oxygen atom bound to a free carbon site to form carbon monoxide (Steps 5, 9 or 13), but the path involving a second oxygen adsorbing was favoured by Chen *et al.* (1993) as it produces a less stable complex which will rapidly deteriorate to produce carbon monoxide. The reaction of hydrogen is more simplistic, with hydrogen bonding to and eventually saturating two adjacent free carbon sites to yield methane (Steps 14 to 17). The reaction schemes given above are represented diagrammatically in figures 2.6 to 2.7, with figure 2.5 identifying the location of sites on the edges of a graphite structure. As can be seen from the figures it is expected that oxygen, carbon dioxide and steam will react at zig-zag sites while hydrogen reacts at armchair sites. The mechanisms proposed show that any of three gases can supply an equivalent oxygen to a site and therefore it would expected that all three gases would have similar reaction rates, dependant possibly on dissociation rates. However, oxygen has faster modes of reaction, as shown in step 3, where oxygen directly forms an unstable complex, and Chen *et al.* (1993) also suggests that oxygen may be capable of forming bonds with carbon atoms in the plane of graphite as well as with the edge atoms. When considering a mixture of gases reacting it can be seen that the equilibrium of steps 6 and 7 will be affected by carbon monoxide and that of steps 10 and 11 will be affected by hydrogen. These gases have been noted by earlier researchers as inhibiting the reactions of steam and carbon dioxide with carbon, although controversy existed as to the method of this inhibition, various authors suggesting the inhibition being due to either adsorption of

gases on the carbon or due to variation of the equilibrium of reactions. Some of this controversy is no longer valid as it has been shown that large gas molecules cannot be adsorbed on carbon, so carbon monoxide cannot inhibit in this way (Essenhigh (1981)). However, hydrogen can adsorb on carbon directly due to the small size of the molecules, and this explains the greater inhibition of reactions by hydrogen compared to other gases, in fact Biederman *et al.* (1976) showed that it was essentially impossible to measure a reaction rate of carbon without hydrogen inhibition due to small quantities of hydrogen being present on the carbon.

In addition to the processes for gases reacting with carbon in graphite-like structures it should be noted that other reaction mechanisms will be possible in disordered and heterogeneous char. Notably, the presence of non-carbon atoms in the char structure will create reaction sites other than at the edges of the graphite-like structures and mineral inclusions can catalyse the heterogeneous reactions.
Traditional reaction kinetics methods assume that all gases will react at the same sites and the rates of the different reactions are related to the proportion of active sites occupied by the individual gases. This is largely refuted by the findings of more recent years but the traditional methods are possibly as relevant as any others due to the complex nature of char, the catalytic activity of inorganic inclusions and variability of active sites for different gases.

2.3.3 Oxygen Gasification

Oxygen gasification refers to the same process as combustion, about which much research has been performed. While the mechanism discussed previously from the work of Chen *et al.* (1993) produces only carbon monoxide, other researchers have found that carbon dioxide can also be produced (Du *et al.* (1991), Tognotti *et al.* (1990)). The mechanism of formation of carbon dioxide is uncertain but may be via catalytic reactions or combustion of carbon monoxide very close to the carbon surface. In either case the reaction should be considered as occurring at the particle in order to ensure proper analysis of heat generation at the particle. The ratio of carbon monoxide to carbon dioxide formed during combustion was reported by both Du *et al.* (1991) and Tognotti *et al.* (1990) as varying markedly with the temperature of reaction, with carbon monoxide formation being favoured at high temperatures and carbon dioxide at low temperatures. The expression of Tognotti *et al.* (1990), given by equation 2.5, also considers the effect of oxygen pressure on the ratio of products. While the work of

Tognotti *et al.* (1990) was performed at low pressures the expression developed relates well to the results of Ranish and Walker (1993) for oxygen reacting with a purified carbon at pressures up to 70 atmospheres. Only limited work has been published for coal char reacting at high pressures and the findings of Monson *et al.* (1995) were that pressure has no obvious effect on the product gas ratio, however their results are greatly scattered and an unspecified number were ignored as inconsistent. Interestingly Monson *et al.* (1995) find a temperature effect on product gas ratio having an 'activation energy' approximately an order of magnitude greater than that of Tognotti *et al.* (1990), with both authors citing supporting literature and ignoring conflicting literature. This discrepancy could either be due to differences between purified carbon and coal char or differences in the experimental techniques, as Tognotti *et al.* (1990) monitored the gas composition near the carbon and Monson *et al.* (1995) determined the ratio from an energy balance relying on the different heats of reaction. In addition a particle size correction expression from Wen and Dutta (1979) can be applied to the product gas ratio to correct for near particle combustion of carbon monoxide, the correction being given by equations 2.6a and 2.6b.

$$z = \frac{X_{CarbonMonoxide}}{X_{CarbonDioxide}} = 50.P_{Oxygen}^{-0.21}.e^{\frac{-3000}{T}} \qquad \text{Equation (2.5)}$$

$$Z = \frac{2.z+2}{z+2} \quad \text{when d} < 50\mu\text{m} \qquad \text{Equation (2.6a)}$$

$$Z = \frac{1}{z+2}\left((2z+2) - \frac{z(d-50\times10^{-6}}{950\times10^{-6}}\right) \quad \text{when d} > 50\mu\text{m} \qquad \text{Equation (2.6b)}$$

The reaction of oxygen with carbon can be inhibited by interaction of other gases with the carbon or the oxygen before reaction. It has previously been mentioned that Biederman *et al.* (1976) found that it is virtually impossible to prevent hydrogen from adsorbing on carbon and therefore inhibiting reactions from occurring. This is not a major concern in practice as the rate of reaction which was measured experimentally will also have been inhibited by residual hydrogen on the char, as long as no attempt was made to remove it. Therefore, in a practical system the initial rate of reaction of the char should be similar to that found experimentally if the char formation methods are similar. As any oxygen present in the reactor will be rapidly consumed by either reaction with carbon or other gases, including hydrogen, it is unlikely that any free hydrogen could cause inhibition of the carbon-oxygen reaction before the oxygen is consumed. Steam has also been considered to cause inhibition of oxygen reacting with carbon and several studies have attempted to quantify the extent of inhibition and the

mechanisms responsible. Matsui *et al.* (1983) determined that the steam had an effect on the carbon-oxygen reaction and hypothesised that it was most likely to be due to steam catalysing the oxidation of carbon monoxide close to the carbon surface, and therefore decreasing the quantity of oxygen reaching the carbon. In a more detailed study Matsui *et al.* (1986) showed that the earlier hypothesis was correct and found a maximum reduction in rate of the oxygen reaction of approximately 5% at low steam concentrations. At high steam concentrations they found that the rate of reaction was increased, probably due to the carbon-steam reaction. In all experiments in the study the carbon-oxygen reaction was probably diffusion limited and therefore removal of oxygen due to oxidation of carbon monoxide in the boundary layer would affect the reaction rate, however it is unlikely to have a significant under non-diffusion limited conditions.

The carbon-oxygen reaction is generally modelled using simple Arrhenius rate expression, as given by equation 2.7 where k_0 is a pre-exponential constant, E_A is the activation energy and n is the reaction, or pressure, order. Another expression, the Strickland-Constable expression, has been used for high temperature reactions of very small carbon particles but has not been applied to char combustion. This expression form accounts for adsorption of oxygen atoms to carbon and is characterised by a reduction in reaction rate at very high temperatures (Essenhigh (1981)). While this expression form may be more realistic than equation 2.7, an absence of published data for coal chars makes evaluation impossible.

$$Rate = k_0 \exp\left(\frac{-E_A}{RT}\right) P_{O_2}^n \qquad \text{Equation (2.7)}$$

A large range of experimentally determined values of pre-exponential constants, activation energies and pressure orders have been published for the carbon-oxygen reaction, however the definition of reactivity has varied for many of these. Reactivity in this work will be defined as the intrinsic chemical reactivity of the char with a basis of mass of carbon removed per unit of effective surface area per some function of reactant gas pressure. A number of other definitions are used in the literature and include reactivities with a basis of the mass of char (either initial or instantaneous), volume of reactant gas (from techniques used for catalytic gas reactions) and external surface area (shrinking sphere models). Care must be used in converting from one basis to another, with attention given to the assumptions used in determining the reactivity, as many researchers ignore the effects of pore diffusion on their experimental results. In particular many of the published char combustion results are based upon the shrinking sphere model

with the reactivities stated on an external area basis. This will give excessively high reaction rates if the rate expression is mistaken for an intrinsic reactivity expression. Smith (1978) converted a range of experimental results to an intrinsic basis for comparison and found that similarities in intrinsic reactivity exist but a variation of two or more orders of magnitude between chars can be expected. It is evident from examination of a variety of experimental results that the variability in methods of char formation and reactivity measurement, and data analysis, have lead considerable confusion in the field of combustion kinetics. For example, the pressure order for similar chars can be reported anywhere in the range of zero to unity depending on technique, and similarly the activation energy can be reported as 70 to 200 MJ/kmol. Figure 2.8 shows the reactivities of a selection of Australian coal chars from literature, as referenced on the figure. The large temperature range indicated for some sets of experimental results means that more than one type of apparatus was used to determine the reactivity, for example fixed bed reactor at low temperatures and entrained flow reactor at high temperatures. Use of a large temperature range produces more predictable curves, with low rank coals being more reactivity at low temperatures and all coals converging in reactivity at high temperatures. For results determined over a small temperature range the activation energy, which determines the slope of the lines in the figure, is less predictable and extrapolation of the data can lead to considerable error, for example consider the results for Yallourn coal from Smith (1982) and Wall *et al.* (1988). It is difficult to determine whether the activation energy determined over a small temperature range is incorrect or if it simply represents a different reaction, such as a specific catalytic reaction, which is dominant in that temperature range only. Diffusion processes also affect the observed reaction rate in experiments and the intrinsic rate determined should have been corrected for these at high temperatures. External area based rate expressions tend to only consider boundary layer diffusion and not pore diffusion, so this may explain the approach of intrinsic to external reaction rates at high temperatures in the figure. The 'General' curve of Smith (1978) represents the average of intrinsic reactivities for a multitude of different carbons, which were calculated from literature results.

Reaction order with respect to oxygen pressure is still a matter of some conjecture, with varying results being published for experiments using different chars and experimental techniques. A large degree of this uncertainty is undoubtably due to diffusional effects interfering with some experimental results and the small ranges of pressure used for most experiments. As previously mentioned, only a limited range of

experimental results for the carbon-oxygen reaction at high pressures has been published, and, owing to the errors involved in extrapolating experimental results at low pressures to high pressures with an incorrect pressure order, a detailed analysis of these results is required. The results of Monson *et al.* (1995) appear most applicable to this study as they deal with char combusting at total pressures of up to 15 atmospheres, partial pressures of oxygen up to 3.1 atmospheres and particle temperatures up to 2100K in an entrained flow reactor. On close examination however the study does not provide conclusive results, mostly due to the analysis of reaction rates neglecting the effects of diffusion to and into the particles and also due to significant experimental scatter in the results. Difficulties were also experienced in interpreting the experimental results due to significantly lower temperatures being experienced at high pressures, a factor which masks the effects of pressure. In summary, Monson *et al.* (1995) found a negative reaction order above 5 atmospheres total pressure and a positive reaction order from 1 to 5 atmospheres total pressure, but the accuracy of their findings is suspect due to the methods of analysis used. In comparison the results of Ranish and Walker (1993) for oxygen pressures from 1 to 64 atmospheres over a temperature range of 733 to 844K indicate reaction orders that vary in a predictable manner with temperature and are constant with oxygen pressure (neglecting the highest temperature result which may have been affected by diffusion). The consistency of these results, compared to those of Monson *et al.* (1995), is most likely due to the use of lower temperatures reducing the interference of diffusional effects and conditions in the apparatus used being more readily controlled. A representation of the pressure order as a function of temperature is given in equation 2.8, based on the results of Ranish and Walker (1993).

$$n = 4.544 \times 10^{-0.001T} \qquad \text{Equation (2.8)}$$

2.3.4 Gasification by Other Gases

It has been shown clearly from experimental work by a number of researchers that gasification by any of carbon dioxide, steam or hydrogen is affected by the presence of any of the other gases and also by carbon monoxide (Long and Sykes (1948), Gadsby *et al.* (1948), Blackwood and colleagues (1958, 1959, 1960, 1962)). For this reason it is suitable to discuss gasification by these gases as a single topic. From earlier discussion of mechanisms of gasification it appears most likely that hydrogen inhibits reactions by adsorption onto active carbon sites and therefore prevents reaction of other gases at these sites. Other oxygen containing gases are expected to dissociate at the carbon

surface to result in bonding of oxygen atoms to active carbon sites. Sites for reaction of oxygen containing species appear to be limited and, owing to molecular limitations, carbon dioxide and steam cannot react as rapidly as oxygen. Of significance to this study are functions describing the rate of reaction of the different gases individually and in any combinations.

A number of studies have dealt with the reaction rates of pure gases with various forms of carbon at atmospheric pressure, although studies of hydrogen reacting typically use high pressure due to the slow reaction rate at low pressure. Other studies have looked at the reaction rate with mixtures of two gases, usually one a reactant and the other an inhibitant, at both high and low pressures. Two common approaches to modelling the reaction rate have been used, that of a simple Arrhenius expression with a pressure order term or Langmuir-Hinshelwood expressions with varying degrees of complexity. In general, low pressure studies without an inhibitant have used simple Arrhenius expressions while those at high pressures and those with inhibitants have used Langmuir-Hinshelwood. An often cited work that tried to fit an Arrhenius expression to the reaction rate of carbon dioxide with coal char over a large pressure range is Dutta (1977), which states that the pressure order must drop from unity at atmospheric pressure to zero at 15 atmospheres pressure for the expression to represent the reaction rate correctly. This finding has influenced later research on the carbon dioxide and other reactions so that Langmuir-Hinshelwood expressions are now more likely to be used for both low and high pressure reaction rates so that pressure order difficulties are avoided (Bliek *et al.* (1986), Matsui *et al.* (1987)). A multiple reactant Langmuir-Hinshelwood expression has been suggested by Muhlen *et al.* (1985) and is given by equation 2.9, where each k term is an exponential expression with an experimentally determined pre-exponential constant and activation energy. The form of this expression is based largely upon experimental work of Blackwood and co-authors (1958, 1959, 1960, 1962) and theoretical work of Shaw (1977), with the constants being determined experimentally by Muhlen *et al.* (1985) from reaction rates of gas pairs with a bituminous coal char at high pressures. The expression implicitly assumes that all reactants utilise the same reaction sites, an assumption refuted by Bliek (1984) who found that steam and carbon dioxide neither react entirely at the same sites nor entirely at different sites. Experimental work by Bliek (1984) was at atmospheric pressure, neglected the reactions involving hydrogen and ignored all but the first order expressions for steam and carbon dioxide, and therefore it is difficult to assess the accuracy of the findings.

$$Rate = \frac{k_1 P_{CO_2} + k_4 P_{H_2}^2 + k_8 P_{CO_2}^2 + k_9 P_{H_2O} + k_{11} P_{H_2O}^2 + k_{12} P_{H_2O} P_{H_2}}{1 + k_2 P_{CO_2} + k_3 P_{CO} + k_5 P_{H_2} + k_6 P_{H_2}^2 + k_7 P_{H_2}^{\frac{1}{2}} + k_{10} P_{H_2O}} \qquad \text{Equation (2.9)}$$

A survey of published Langmuir-Hinshelwood expressions for carbon dioxide, steam and hydrogen reactions with carbon found an excessive degree of variability in the experimental values for the k terms in equation 2.9. A summary of these findings is presented in figure 2.9 as the activation energies found for the different terms by a number of authors. Most authors referenced in figure 2.9 considered only gas pairs reacting, usually carbon dioxide-carbon monoxide and steam-hydrogen, and therefore did not calculate values for many of the terms. Values for the terms were calculated for Goyal *et al.* (1989) from the raw experimental data presented in the paper, as a different form of rate expression was defined in the paper. The calculated values are of extremely low magnitudes owing to the low rates and small variations in rate with differing conditions measured experimentally. Of the research reported in figure 2.9 only that of Muhlen *et al.* (1985), Blackwood and co-authors (1958, 1959, 1960, 1962) and Goyal *et al.* (1989) was performed at high pressures, and only that of Goyal *et al.* (1989) considered the reaction rate in gas mixtures containing all species in equation 2.9 simultaneously. Variation between activation energies reported for the different terms are large for different authors, in some case even being of opposite sign, and this suggests that in some cases an improper selection of constants from experimental data has occurred. The large number of experimentally determined constants in equation 2.9, a total of 24 with the most used in the published results being 20, means that is possible to fit entirely erroneous values to constants in order to make the expression fit minor experimental errors. These erroneous values may not be evident when comparing the fit of the expression with the experimental results but could become inaccurate if used to extrapolate results to different conditions than those experienced in the experiments. For this reason a large number of experimental results should be obtained over a wide range of conditions to ensure suitability of the expression constants.

Some recent work has been published using pressure order expressions to fit experimental results obtained at high pressures. The results of Shufen and Ruizheng (1994) indicated pressure orders of 0.34, 0.26 and 0.50 for carbon dioxide, steam and hydrogen gasification reacting with a lignite char at 19.6 atmospheres pressure. It is unclear how these orders were obtained and the order for hydrogen gasification is much below the figure of unity found by Tomita *et al.* (1977) in a more detailed study.

The result for steam gasification is supported by the work of Zhi-hua *et al.* (1992) which suggests an order of approximately 0.2 for anthracite char over a pressure range of 1 to 14.2 atmospheres. Experimental work of Frederick *et al.* (1993) for gasification of black liquor char in carbon dioxide up to 25 atmospheres pressure was more complex and produces best fit reaction orders of 0.03, 0.14 and 0.30 for char at either 20, 40 or 60% conversion. This variation was considered to be due to catalysis by calcium in the char, with the catalyst sites being lost at higher conversion. Pressure orders can also be approximated from published Langmuir-Hinshelwood expressions in the absence of experimental data. The published expression of Muhlen *et al.* (1985) suggest best fit pressure orders of 0.25, 0.2 and 1.0 for carbon dioxide, steam and hydrogen gasification reactions in the pressure range 1 to 15 atmospheres of pure gas.

2.3.5 Chemical Rate Forms

While the previous section has considered the possible rate expression used to determine the chemical reaction rate is also relevant to consider the bases upon which the chemical rate is founded. A number of different forms of chemical rate have been used in the literature based upon either the mass of solid reactant, the level of conversion of the solid, various representation of the area of the reactant solid or the volume of reactant gas. Selection of the type of reaction rate to use can be influenced by the type of reactor being modelled and the trend of experimentally determined results. For example, it is commonly found that the rate of reaction is a function of the level of carbon conversion for a particular char and therefore the may be given as a function of conversion. However it may also be possible to correlate the reaction rate with changes in the accessible internal surface area of the char with reaction and therefore relates the rate in terms this area, which defines an intrinsic rate. Some forms of chemical rate have been shown to be fundamentally incorrect outside a narrow range in which they were determined, for instance a rate on a basis of mass of char is unlikely to be correct for particles of different size to those used experimentally. This also applies to rates determined on a basis of external surface area, a method commonly used in early char combustion modelling but which ignores the affect of char structure on the reaction rate. The method of intrinsic rate, where the proportion of internal area of the char particles accessed by reactant gases is used, has been shown by Smith and Tyler (1972, 1974) to be applicable over a wide range of reaction conditions for coal chars. Improvement of this method has been suggested by considering only the active surface area (ASA) or reactive

surface area (RSA) of the char but this involves detailed analysis of the coal char while intrinsic reactivity can be calculated relatively simply (Radovic *et al.* (1991)).

2.3.6 Variability of Char Reactivities

Chemical reactivities for coal chars are distinct for individual chars, with a wide variation in reactivities reported in the literature. This has been indicated previously for oxygen gasification in figure 2.8, and is shown in figures 2.10, 2.11 and 2.12 for carbon dioxide, steam and hydrogen gasification respectively. In these figures a wide range of experimental gasification rates are evident for a variety of chars, mostly coal derived. The reactivities are also shown to vary in magnitude at the same temperature and also the response to changes in temperature, indicated by the slope. In a pressure order reactivity expression this corresponds to changes in both pre-exponential constant and activation energy. Several researchers have attempted to find correlations between the reactivity of different chars and other properties of the coal. In general it has been found that the rank of the coal is an indicator of the resultant char reactivity, with low rank coals having greater reactivity than high rank coals. Fung and Kim (1984) determined a correlation for gasification of char by oxygen based solely on the carbon content of the coal, as given in equation 2.10 where the reactivity of a char is calculated from the known reactivity of another char. Figure 2.13 shows how correlations of this form fit the experimental data from a number of authors for oxygen, carbon dioxide, steam and hydrogen gasification of coal char, with variations in the location of the correlation lines being in part due to the different char preparation and reactivity measurement conditions for different researchers. It is clear from the figure that the correlations defined are not accurate for all chars, with the correlation for hydrogen gasification showing a high level of inaccuracy. Note that due to the logarithmic axis of the figures variation between the correlation and a data point where the data point lies below the correlation line is less significant than when a point is above the correlation line.

$$k_0 = k_{0,base}.e^{\left(r\left(C_{base}-C\right)\right)} \qquad \text{Equation (2.10)}$$

Correlations of a similar type but more complex in form have been defined by other authors and a review of some of these is given by Miura *et al.* (1989). The major conclusion of this review was that existing methods for reactivity correlation of chars were not reliable, although methods using coal carbon content or coal reflectance can be suitable for approximate indications of reactivity. Since this review other published

work has added little to understanding of char reactivity. Raghunathan and Yang (1989) have shown that the time for conversion of 50% of the carbon in a char under constant reaction conditions is directly proportional to the reactivity of the char, and therefore the reactivity of different chars can be easily compared. This method requires experimental analysis of any char for which the reactivity is required and reactivity measurement for at least one char formed under similar conditions. The method proposed by Charpenay *et al.* (1992) similarly requires analysis of char samples, in this case for hydrogen content, and uses this with the oxygen content of the coal to predict oxygen gasification rate. Hampartsoumian *et al.* (1993) uses a more complex equation considering char density, surface area, carbon and hydrogen contents for estimation of the oxygen gasification rate. In contrast, the findings of Lee *et al.* (1992) for chars produced under conditions of varying temperature and pressure from the same coal have reactivities in proportion to the residual volatile matter of the char. Unfortunately this finding has not been verified for other coals.

2.3.7 Interaction with Diffusion Processes

2.3.7.1 Boundary Layer Diffusion

At high temperatures the heterogeneous reaction rates can become sufficiently rapid that the reactant gas may be exhausted within the particles and be of negligible concentration at the particle surface. In this case the reaction rate is determined by the rate of diffusion of reactant gas to the particle from the bulk gas. The most common method for calculating the reaction rate due to diffusion to the particle assumes the existence of a boundary layer about the particle in which the concentration changes from zero to the bulk gas concentration, as used by Field (1969). The expression derived by Field (1969) for this rate is give by equation 2.11, where Φ is the molar ratio of gaseous products to gaseous reactants and T_m is the average of the particle and gas temperatures.

$$Rate = K_{diff} . A_{external} . P_{Reactant} = \frac{24 \Phi D_{Reactant,mix}}{dRT_m} . A_{external} . P_{Reactant} \qquad \text{Equation (2.11)}$$

2.3.7.2 Pore Diffusion

Pore diffusion can be interpreted as a resistance which acts to reduce the rate of reaction. Due to the constriction to gas diffusion imposed by fine pores and the reaction of gas with the pore surface a decrease in concentration with distance into the pore occurs, as indicated in figure 2.14a and b. This decrease results in a reduction in

the reaction rate and is commonly envisaged as reducing the pore area accessed by the gas at the surface concentration, as indicated in figure 2.14c, and denoted as the effective pore area. The effective pore area varies depending on the relative values of the pore diffusion rate and the chemical reaction rate, so will vary for different reactant gases. Pore diffusion is expected to significantly slow the reaction rates of the steam and carbon dioxide gasification reactions. Pore diffusion rates are dependant largely on the structure of the char particles and therefore, from a modelling viewpoint, the selection of a pore structural model will be important in determining the difficulty and methods of calculation. In most cases the effects of pore diffusion are represented by a particle effectiveness factor that defines the fraction of internal area accessed by the reactant gas. An exception to the use of effectiveness factor is the use of percolation theory (Miccio and Salatino (1992)) that calculates the probability of gas molecules reaching and reacting individual finite elements of area inside a particle, which will not be considered here for reasons discussed in the later section on pore models. The formulation of effectiveness factors for simple reactions in well-defined porous media has been considered at length in literature on catalysis. The basic expressions for a simple first order reaction have been defined for a cylindrical pore in a planar surface by equations 2.12 and 2.13, with ϕ referred to as the Thiele modulus and η the effectiveness factor.

$$\phi = L\sqrt{k_{chemical} / D_{eff}} \qquad \text{Equation (2.12)}$$

$$h = \frac{\tanh(\phi)}{\phi} \qquad \text{Equation (2.13)}$$

The definition of the Thiele modulus becomes much more complex with any difference in the reaction from a simple first order, such as a different order, a change in gas volume with reaction or a stoichiometry of reaction other than unity. As all of these differences are expected for the gasification reactions analysis of the available methods for correcting the Thiele modulus is required. Smith and Tyler (1972, 1974) considered the partial order reaction of oxygen with carbon and used a simplification of $\phi\tanh(\phi)\rightarrow\phi^2$, which is valid only for $\eta\rightarrow 1$, in order to calculate intrinsic reactivities. For more general solutions complex calculation techniques must be used, as detailed by Kehoe and Aris (1973). This is based on the finding that a spherical particle effectiveness factor will be approximately given by equation 2.14 for any reaction if the Thiele modulus is correctly defined (Aris (1957), Kehoe and Aris (1973)).

$$\eta = \frac{3}{\phi}\left(\frac{1}{\tanh(\phi)} - \frac{1}{\phi}\right) \qquad \text{Equation (2.14)}$$

Methods for defining a generalised Thiele modulus for use in equation 2.14 are discussed by Kehoe and Aris (1973), with a combined expression from simplification of their work given in equation 2.15. The simplifications involved include approximation of the integral term F(1) in Kehoe and Aris (1973) as given in equation 2.16, which involves an error of approximately 5%. It should be noted that additional terms included in equation 2.15 compared to most published effectiveness factor expressions are due to conversion from a basis of gas reacting with catalyst to one of carbon removal from char (Laurendeau (1978)).

$$\phi = \frac{d_{particle}}{6}\sqrt{\frac{A_g \sigma_a a k_{chemicl} P_A^{n-1} R_{gas} T_{particle} (n+1)(1+\alpha\sqrt{b})}{2\alpha M_c D_{eff,A}}} \qquad \text{Equation (2.15)}$$

$$F(1) \approx \frac{\sqrt{b}}{n+1} \qquad \text{Equation (2.16)}$$

An additional difficulty arising from pore diffusion calculations with fractional orders is that analytical solution for a reaction rate is not possible due to the partial pressure of reactant gas (P_A in equation 2.15) being dependant on the rate. This means that iterative procedures must be used in order to accurately predict the effectiveness factor and thereby the reaction rate.

A component of the Thiele modulus calculation that must be determined mathematically is the effective diffusivity, which is considered to be dependant on both the bulk diffusivity and the Knudsen diffusivity, and therefore also the pore structure. Knudsen diffusion becomes significant only as the pores become small and the gas concentration becomes low, so at high pressures the Knudsen diffusivity will only be significant in the smallest of the micropores. Methods for calculating both Knudsen and bulk diffusivity are well established, although errors are inevitable in calculations for gas mixtures at high temperatures and pressures, however there are a number of variations in calculation methods the effective diffusivity. The most common approaches approach appears to be that of Wheeler (1951) which is given by equation 2.17, however it should be noted that this has no foundation in theory and was selected by the author on the basis of appearing to give reasonable values for various pore sizes. The standard approaches for calculation of diffusivity of a gas in a gas mixture (Wilke equation), Knudsen diffusivity and binary diffusivity (Chapman-Enskog equation) are given in equations 2.18 to 2.20, respectively.

$$D_{eff} = \tfrac{1}{2}\varepsilon D_{A,mixture}\left(1 - e^{-\frac{D_{A,K}}{D_{A,mixture}}}\right) \qquad \text{Equation (2.17)}$$

$$D_{A,mixture} = \frac{1 - X_A}{\sum_{\substack{B=1 \\ B \neq A}}^{n} \frac{X_B}{D_{A,B}}} \qquad \text{Equation (2.18)}$$

$$D_{A,K} = \tfrac{2}{3} a \sqrt{\frac{8RT}{\pi M_A}} \qquad \text{Equation (2.19)}$$

$$D_{A,B} = \frac{0.000000266.T^{\frac{3}{2}}}{P\sigma_{AB}^2 \Omega_{A,B} \sqrt{1/M_A + 1/M_B}} \qquad \text{Equation (2.20)}$$

2.4 Homogeneous Reactions

A number of gas phase reactions are significant in coal gasification as, in some cases, they will be significant in determining the usefulness of the product gas from a gasifier. Initially in a gasifier the presence of oxygen will dominate the gas phase reactions due to the rapidity of reaction with unoxidised gases. A summary of the major gas phase combustion reactions considered in a gasifier is given by reactions 6 to 10. It should be noted that the reactions are considered as irreversible when in reality gas phase reactions exhibit equilibria, this is a simplification as the equilibrium of these reactions lies far to the right and in modelling terms it is difficult to predict the composition of a gas when considering many equilibrium reactions.

$$CO + \tfrac{1}{2}O_2 \longrightarrow CO_2 \qquad \text{Reaction (6)}$$

$$H_2 + \tfrac{1}{2}O_2 \longrightarrow H_2O \qquad \text{Reaction (7)}$$

$$CH_4 + 2O_2 \longrightarrow CO_2 + 2H_2O \qquad \text{Reaction (8)}$$

$$H_2S + \tfrac{3}{2}O_2 \longrightarrow SO_2 + H_2O \qquad \text{Reaction (9)}$$

$$COS + \tfrac{3}{2}O_2 \longrightarrow CO_2 + SO_2 \qquad \text{Reaction (10)}$$

Another set of reactions are considered in gasification and are perhaps more significant as they dominate determination of gas composition at the gasifier outlet. These reactions all involve exchange of oxygen between different gas species and are considered to be at equilibrium, as indicated in reactions 11 to 14. Reaction 11, the water-gas shift reaction, is regarded as the most important of the equilibrium reactions as it largely determines the ratio of carbon monoxide to hydrogen in the gas, which has significance for later gas use, and also the relative proportions of reactant species carbon dioxide, steam

and hydrogen. At high pressures reaction 12, the methanation reaction, tends to produce methane which is a desired product in hydrogasifiers. The other equilibrium reactions considered are of lower significance due to the generally low sulfur content of coal, but are considered for completeness as the ratio of sulfur species may be significant for gas cleanup analysis.

$$H_2O + CO \longleftrightarrow H_2 + CO_2 \qquad \text{Reaction (11)}$$

$$CO + 3H_2 \longleftrightarrow CH_4 + H_2O \qquad \text{Reaction (12)}$$

$$SO_2 + 3H_2 \longleftrightarrow 2H_2O + H_2S \qquad \text{Reaction (13)}$$

$$COS + H_2O \longleftrightarrow CO_2 + H_2S \qquad \text{Reaction (14)}$$

While the reactions above consider a wide range of gas species and many other reactions can be considered by combination of these reactions, it is significant to consider reactions that have been neglected. The only major set of gases expected in a gasifier that have been neglected are nitrogen, its oxides and ammonia. This neglection follows that of most literature gasification models mentioned in a later section, however no reason for this omission was identified in those publications. It is evident that reactions of nitrogen will occur in gasification as the initial devolatilisation occurs in an oxygen rich environment at high temperature, indicating high rates of nitrogen oxide formation according to combustion literature. However, results from the United States Bureau of Mines pilot plant pressurised gasifier (Strimbeck *et al.* (1953)) indicate that at the gasifier exit in excess of 99% of the nitrogen is in the form of nitrogen gas. Results from commercial gasifiers (Watkinson *et al.* (1991)) typically indicate nitrogen gas as the only nitrogen species in the product gas. Therefore it is clear that while nitrogen oxides will exist in the early stages of gasification they must rapidly be reduced to nitrogen gas in the absence of oxygen but are not expected to be further reduced to ammonia in significant quantities. It is unlikely from this that considering nitrogen gas as the only form of nitrogen in a gasifier will have significant effects on model predictions.

Another consideration for gas phase reactions is whether equilibrium can be reached in the time available. Ergun and Menter (1966) found that the water-gas shift reaction could not have been at equilibrium at the exit of the experimental gasifier. It is possible that this finding was inaccurate or due to low temperatures as the rate of the water-gas shift reaction was found to be extremely rapid by Tingey (1966) and Singh and Saraf (1977) found that the reaction was accelerated by catalysts common in coal ash.

2.5 Particle Structure

In gasification processes coal particles are initially only slightly porous but with devolatilisation of the coal on heating, and later with heterogeneous reaction, the particles can undergo dramatic changes in structure. With the generation of volatiles, as discussed earlier, the particle material can become softened and swell with resultant increase in porosity. High temperatures can also decrease the porosity of the particles by consolidating material into graphite-like structures and therefore causing destruction of very small pores. Heterogeneous reactions in the pores will increase the porosity by removal of carbon from the particle interior. The structure of coal and char particles can have important ramifications in determining the rate of heterogeneous reactions by influencing the available reaction area.

2.5.1 Pore Structure Modelling

A number of approaches have been made in modelling the pore structure and how it develops with devolatilisation and reaction but all are limited by being only simplifications of structures that are both complex and can vary markedly between particles. A number of pore structure models that have been found to fit experimental data for expected reactions rates based on intrinsic reactivities are given in table 2.2, with diagrammatic representation of the models mentioned given in figure 2.15. The exact formulation of a pore model for a given char is performed by measuring characteristics of a char structure, such as porosity, surface area, pore size distribution and changes in these with reaction, and then calculating the parameters to fit a particular model to the char. For example the characteristics of the average pore size model are calculated according to rules defined by Wheeler (1951) based upon the porosity and surface area of the char. The length, diameter and number of pores defined by Wheeler (1951) are given in equations 2.21 to 2.23 respectively, with ε the char porosity, RF a roughness factor and A_{pores} the internal surface area of the particle.

$$l_{pore} = \frac{\sqrt{2}.d_{particle}}{6} \qquad \text{Equation (2.21)}$$

$$d_{pore} = \frac{2.\varepsilon(1-\varepsilon)\pi.RF.d_{particle}^{3}}{3.A_{pores}} \qquad \text{Equation (2.22)}$$

$$n_{pores} = \frac{4.\varepsilon.d_{particle}^{2}}{\sqrt{2}.d_{pore}^{2}} \qquad \text{Equation (2.23)}$$

Each of the models indicated in figure 2.15 has different characteristics, although some have obvious similarities. The simplest is the average pore size model which allows for only identical cylindrical pores with no intersections. This allows straightforward calculation of pore efficiencies for pore diffusion hindered reactions, as shown by Smith and Tyler (1972, 1974). Extension of this model can be made by considering a number different pore sizes, as used by the random pore model, and even allowing for random variation in the diameter of pores between pore intersections, as used by the stochastic pore network. A conceptual difficulty with these model extensions is involved in the random distribution of pores in the particle, as the porous structure of char is largely the result of physical processes involved in the release of volatiles and therefore a truly random structure cannot be formed. This is largely the base of the dendritic pore distribution and vesicle pore structure models. The dendritic pore distribution model assumes that volatiles generated in the interior of particles create fine pores which combine closer to the surface to form larger pores. This model can be constructed from data on the pore size distribution of char to determine a number of characteristic pore sizes, for example micro-, meso- and macro-pores, and determining the number of small pores which should combine to form a larger pore. Both Smith and Tyler (1972) and Bliek (1984) used dendritic models to model pore diffusion and reaction in porous char, both using only two different pore sizes. Smith and Tyler (1972) showed that as most internal area and highest diffusion resistance was in the smallest pores the other pore sizes were not significant in the modelling of reaction rate. The vesicle pore structure model is an attempt at modelling bubbling of softening coal with volatile release. A number of spherical bubbles of equivalent or different sizes are linked by pores, with the majority of the particle surface area being in micropores connected to the vesicles. A limitation of this model is the difficulty in determining realistic sizes for the vesicles and pores, and then in determining the diffusion into the same. The remaining two models that are shown in figure 2.15, the grain and discrete pore models, appear similar except for the size of the non-porous particles comprising the char particle. The major difference is in the formulation of the models, with sizes in the grain model being determined by experimental rate measurements a various levels of char conversion and the discrete pore model being generated entirely randomly. Use of the grain model appears to be limited to the chemical reaction rate regime due to the difficulty involved in calculating diffusion rates through the unevenly sized pores. The discrete pore model is generated by division of the char particle into numerous small blocks and then removing a random selection of blocks to account for

particle porosity. Modelling reaction of the particle then requires determination of percolation rates of reactant gases into the pores and removal of more blocks based on determined reaction probabilities. This method involves an excessive number of calculations for an individual particle and Sandmann and Zygourakis (1986) showed that predictions have significant differences depending on whether a 1024x1024, 2048x2048 or 4096x4096 grid of blocks was used with the model.

As has been indicated a large number of markedly different models can be made to represent the pore structure of char particles, however not all models will fit a particular char and many of the papers referred to discuss the shortcomings of different models with reference to a specific set of experimental data. The discrepancies are related to the definition of pore models based upon macroscopic properties of a char sample, such as porosity and pore size distribution, when the properties of individual particles can be markedly different and therefore affect the reaction rates measured. From this it can be seen that none of the pore models discussed can be taken as accurate for all coal chars and it is unlikely that an accurate general model can be formulated.

Table 2.2: Experimental correlations for pore structure.

Model Type	Researcher	Gases	Solids
Average	Balci *et al.* (1987)	CO_2	Char from coal 71%C
	Smith & Tyler (1974)	O_2	Brown coal char
	Smith & Tyler (1972)	O_2	Semi-Anthracite char
Grain	Adschiri *et al.* (1987)	H_2O	Chars from coals ~70%C
	Fuertes *et al.* (1989)	CO_2	Coke from coal 80% C
	Charpenay *et al.* (1992)	O_2	Low Rank Char
	Haga & Nishiyama (1988)	H_2O	Chars from coals 66-88%C
Random	Gavalas (1980)	General	Chars from literature
	Chin *et al.* (1983)	H_2O	Brown & Bituminous Chars
	Su & Perlmutter (1984)	General	
	Su & Perlmutter (1985)	Air	Chars from coals 78-82%C
	Bliek *et al.* (1986)	CO_2;H_2O	Lignite & Bituminous chars
	Ballal & Zygourakis (1987)	CO_2;H_2O	Lignite & Bituminous chars
	Chi & Perlmutter (1989)	H_2O	Bituminous char
	Charpenay *et al.* (1992)	O_2	High Rank char
Dendritic	Bliek (1984)	CO_2;H_2O	Lignite & Bituminous chars
	Simons & Finson (1987)	General	Chars from literature
	Tseng & Edgar (1989)	Air	Bituminous & Lignite chars
Vesicle	Foster & Jensen (1990)	CO_2	Anthracite coal and chars
Stochastic	Mann *et al.* (1986)	None	Oil-bearing rock
	Reyes & Jensen (1986)	O_2;CO_2	Chars from literature
	Shah & Ottino (1987)	CO_2	Chars from literature
Discrete	Sandmann & Zygourakis (1986)	CO_2	Chars from literature
	Miccio & Salatino (1992)	O_2	Carbon

2.5.2 Coal Particle Properties

The modelling of particle structure relies upon knowledge of basic particle properties in order to fit the parameters of the various models accurately. Foremost amongst these properties is the total porosity of the coal but some of the models require more detailed information on the size ranges of the pores in which the porosity occurs. An extensive analysis of coal porosity was performed by Gan *et al.* (1972) which

identified that porosity was a function of coal rank for. This study gives the total porosity of a number of coals and also categorises the porosity as occuring in either micro-, meso- or macro-pores. The data of this study is summarised in figure 2.16 and approximate correlations, of simple quadratic form, for each type of porosity are indicated. The pore size classifications used by Gan *et al.* (1972) were based on pore diameters of $25x10^{-9}$m for micropores, $100x10^{-9}$m for mesopores and $250x10^{-9}$m for macropores. It is also possible to correlate internal surface from this data as the surface area for each pore size can be calculated using the methods of Wheeler (1951) that were previously discussed and the total internal surface area calculated by summation.

2.6 Heat Transfer

In entrained flow coal gasification the processes of heat transfer will determine the distribution of heat between gas, particles and gasifier wall. In this regard individual particles, wall and gas will have distinctive temperatures, and transfer between any two items can occur by the applicable processes. At different stages along the gasifier the major heat transfer processes occuring can vary. Specifically, heating of gas and particles on entry to a hot gasifier and the later loss of heat from hot gas and particles to wall are expected to be important to the progress of gasification. For all physical processes heat is transferred by conduction, convection and radiation. However, in gasification the high temperatures suggest that conduction will be of little significance and convection is likely to have significance only in cooler sections of the gasifier. While there is some cross-influence between the different heat transfer processes it is far simpler, and more common, to neglect this and consider the processes to be wholly independent. Due to the physical properties of the system it is considered that the gas will act as an intermediate to transfer between particles and the gasifier wall, and also between different particles. This limits the heat transfer processes considered to radiative and convective transfer gas-particles and gas-wall, although in practice it is easier to consider radiative transfer as wall-particles, wall-wall, particles-particles with the gas as a subtractive influence, via adsorption, to each of these processes.

2.6.1 Convective Transfer

Convection refers to the transfer of heat through a boundary layer between a solid or liquid and a gas due to movement of the gas caused by turbulence or induced by buoyancy differences in hot and cold gases. While it is a difficult process to

model analytically due to the complexity of transfer patterns a number of empirical correlations have been found to approximately represent the process when standard shapes are involved. In a gasifier convection will apply to heat transfer between the gas and both approximately spherical particles and the inner wall of a cylinder. In both these cases correlations exist and commonly used expressions from combustion modelling are given by equations 2.24 and 2.25 in terms of transfer from gas to particle and gas to wall respectively (Babcock and Wilcox Co. (1978)). Numerous other correlations are available for the same processes however those given below appear to be the most widely accepted.

$$h_{g\to p} = Nu.\frac{k_g.\left(T_g - T_p\right)}{d} \qquad \text{Equation (2.24)}$$

$$h_{g\to w} = \left(0.023\frac{\left(\rho_{gas}V_{gas}\right)^{0.8}}{D^{0.2}}\right)\left(\frac{C_{p,gas}^{0.4}k_{gas}^{0.6}}{\mu_{gas}^{0.4}}\right)\left(\frac{T_{gas}}{T_{wall}}\right)^{0.8} \qquad \text{Equation (2.25)}$$

2.6.2 Radiative Transfer

Treatment of radiative transfer is complicated in gasification by the high concentrations of carbon dioxide and steam present in some stages of the process. These gases are known to be radiatively emissive and absorbant, and therefore interfere with radiative exchange between solid surfaces, namely the gasifier walls and the particles. Methods for calculating heat transfer involving an emissive gas are complex as they can involve numerous cases of transmittance, absorbance and reflectance between any of the materials in the gasifier and, to be entirely correct, the gas will only absorb and emit radiation in specific wavelengths.

A number of methods for simplifying and solving heat transfer problems are discussed by Hottel and Sarofim (1967) with the most applicable methods appearing to be the Zonal method and the Long Furnace model. The Zonal method involves division of the entire gasifier into a number of zones, within any of which the physical properties of the material and its conditions are regarded as constant. In the case of a gasifier this would mean dividing the gasifier walls into small sections, generating numerous categories of particles divided on the bases of size and temperature, and dividing the gas into small volumes of similar composition and temperature. A solution for a particular set of circumstances in the gasifier is determined by iterative solution of the heat transfer between each of the zones, including effects from the gas between these zones. As the characteristics of the particle-gas mixture in a particular region in the gasifier are

influenced by reactions in regions through which the mixture has previously passed, the temperatures cannot be independently varied relative to the mixture characteristics. This means that a larger iterative loop must be performed to allow correct calculation of all particle-gas characteristics simultaneous throughout the gasifier, rather than just temperatures. The Long Furnace model allows simplification of the Zonal method through some strategic assumptions that are acceptable only in the case of a reactor which is long in the direction of flow relative to all other dimensions. Major assumptions are that no heat transfer occurs along the reactor, that is all transfer is perpendicular to the flow, and that variation in conditions occurs only in the direction of flow. The net effect is that the gasifier would be divided into thin slices with all radiant energy emitted in the slice being absorbed within the same slice by assuming perfect refractory prevents transmittance into adjacent slices. For this assumption to be analytically correct it would be required that all slices had identical characteristics, so that the energy received by a slice is exactly equal to the amount transmitted by it. In reality the model can be only approximately correct when the changes from slice to slice are very small and only slight gradients in temperature along the gasifier occur. It is not possible for the model to be exact in practical situations as heat will always flow along the gasifier from a hotter to a cooler region, which is not allowed for.

In consideration of any modelling technique employed it is required that certain characteristics of the gas and particles must be calculated for accurate radiative heat transfer calculations. The radiative properties of both solids and liquids are well defined in literature, notably for char in Hottel and Sarofim (1967) and for slags in Mills and Rhine (1989). It is evident that the properties of these substances either vary predictably or are constant with changing temperature and are not significantly affected by changing pressure. In the case of gas, as previously noted, variability of emissive properties are marked for changing composition, temperature and pressure. The early work in this field of Hottel and Sarofim (1967) presents changes in emissivity and absorptivity of gases in graphical form and does not extend to the high pressures of gasification. This work focussed on gray gas properties which average the properties over the entire wavelength range of interest, rather than identifying the emissivity in specific wavelength ranges. The favoured method of more recent researchers is to quantify the emissive properties due to specific bond types in the gas molecules, allowing for more accurate determination of the emissive properties of gas mixtures when the overall properties of the mixture are the result of interference and overlap of different gas

characteristics (Edwards and Matavosian (1984)). However this method involves a large number of calculations in determining heat transfer through an emissive gas and therefore the results of Leckner (1972) also included a method for calculating a gray gas emissivity. This method involves separate calculation of steam and carbon dioxide emissivities from arrays of coefficients then combining these emissivities to give an overall gas mixture emissivity, as given by equations 2.26 to 2.30 with additional data in table 2.3.

$$\varepsilon = \varepsilon_s + \varepsilon_c - \Delta\varepsilon \qquad \text{Equation (2.26)}$$

$$\varepsilon_{(P_aL,P,T)a} = \varepsilon_{0(P_aL,1bar,T)a}\left(1 - \frac{(a-1)(1-P_E)}{a+b-1+P_E} e^{-c\left[\log_{10}\left(\frac{(P_aL)_m}{P_aL}\right)\right]^2}\right) \qquad \text{Equation (2.27)}$$

$$\varepsilon_{0(P_aL,1bar,T)a} = e^{\left[\sum_{i=0}^{M}\sum_{j=0}^{N} c_{ji}\left(\frac{T}{T_0}\right)^j \left(\log_{10}\left(\frac{P_aL}{(P_aL)_0}\right)\right)^i\right]} \qquad \text{Equation (2.28)}$$

$$\Delta\varepsilon = \left[\frac{\zeta}{10.7+101\zeta} - 0.0089\zeta^{10.4}\right]\left(\log_{10}\left(\frac{\left(P_{H_2O}+P_{CO_2}\right)L}{\left(P_aL\right)_0}\right)\right)^{2.76} \qquad \text{Equation (2.29)}$$

$$\zeta = \frac{P_{H_2O}}{P_{H_2O}+P_{CO_2}} \qquad \text{Equation (2.30)}$$

Table 2.3: Values of coefficients in Equations 2.27 and 2.28 (Leckner (1972)).

Values for a=s (ie. Steam)					
C_{00}	-2.2118	C_{01}	-1.1987	C_{02}	0.035596
C_{10}	0.85667	C_{11}	0.93048	C_{12}	-0.14391
C_{20}	-0.10838	C_{21}	-0.17156	C_{22}	0.045915
P_E			$\frac{\left(P+2.56\frac{P_a}{\sqrt{t}}\right)}{P_0}$		
$\frac{(P_aL)_m}{(P_aL)_0}$			$13.2t^2$		
a for t<0.75			2.479		
a for t>0.75			$1.888-2.053\log_{10}(t)$		
b			$\frac{1.10}{t^{1.4}}$		
c			0.5		

Values for a=c (ie. Carbon Dioxide)							
C_{00}	-3.9893	C_{01}	2.7669	C_{02}	-2.1081	C_{03}	0.39163
C_{10}	1.2710	C_{11}	-1.1090	C_{12}	1.0195	C_{13}	-0.21897
C_{20}	-0.23678	C_{21}	0.19731	C_{22}	-0.19544	C_{23}	0.04464
P_E				$\frac{(P+0.28P_a)}{P_0}$			
$\frac{(P_aL)_m}{(P_aL)_0}$ for t<0.7				$\frac{0.054}{t^2}$			
$\frac{(P_aL)_m}{(P_aL)_0}$ for t>0.7				$0.225t^2$			
a				$1+\frac{0.1}{t^{1.45}}$			
b				0.23			
c				1.47			
Where : T_0=1000K, P_0=1 bar, t=T/T_0, $(P_aL)_0$=1 bar.cm							

2.7 Gasification Modelling

2.7.1 Model Types

Modelling of complex physical systems is largely a process of simplification into mathematical equations as a balance between computational simplicity and accuracy of prediction is sought. As previously given the process of entrained flow gasification can be broken into a number of components which may be used in production of a model. Depending on the components included, or excluded, the model can be

classified into various categories of model. The most complex model will incorporate all known data on reactions, heat transfer and fluid dynamics in the gasifier to provide predictions on all aspects of the process. The least complex model will provide simple predictions for a limited range of variables based upon known output for a given gasifier. In essence, this translates into two types of model which have been published for gasifiers. The first type relies on a 'black box' model of a gasifier and gives predictions on the composition of exit gases from this gasifier based upon a mass and energy balances over the gasifier under equilibrium conditions. This type of model will be referred to as equilibrium models and do not utilise any knowledge of conditions, processes or reactions in the gasifier. The second type of model can have a wide range of complexity and uses knowledge of the gasifier dimensions and conditions to calculate the nature of changes that occur in the gasifier to produce predictions of the outputs. As these models rely on knowledge of reaction rates they will be termed kinetic models, the most complex form of this model type also incorporates fluid dynamics

Thermodynamic models require an initial knowledge of the gasifier performance to work, as they cannot predict the level of carbon conversion in a given gasifier. The use of this form of model is usually limited to systems where carbon conversion is maintained as a constant by use of char recycle and then the model can predict the exit gas composition and efficiency of the process, if heat losses are known. This essentially allows only a small range of usefullness as a large quantity of experimental data on the gasifier must already be available.

Kinetic models require information on the gasifier design, as well as flowrates into the gasifier and temperatures, but do not require knowledge of the exit conditions. In the simplest form a kinetic model can be formulated that considers reaction of a single particle of coal only. While this form of model allows for testing of hypotheses about reaction mechanisms, it is not suitable for the modelling of gasifiers as it neglects the effects of radiant transfer to the particle from other surfaces and is generally used for predictions with constant conditions. Kinetic models can be greatly complicated by considering flow patterns inside the gasifier and detailed analysis of the structure of, and reactions occurring at, individual coal particles. In order to reduce the complexity of these models a number of standard simplifications have been used. The most complex form of kinetic model considers flow in a three-dimensional grid but commonly ignores changes in particle structure and size with conversion and uses simple reaction mechanisms, such as considering the particles as non-porous spheres. A simplification of this can occur by

considering motion only in two dimensions, usually performed by considering a plane through an axis of symmetry in the gasifier so that only two dimensions are significant. By only considering flow in one direction, directly along the axis, a model that essentially ignores flow considerations and the corresponding fluid mechanics problems can be produced. This form of model is termed plug flow and allows for more complex analysis of particle structure and reactions. While ignoring flow patterns in a model is inaccurate in large furnaces, plug flow models can be applicable in small diameter reactors where complex flow patterns do not exist.

2.7.2 Published Models

Numerous models have been published for gasification, mostly considering gasification of single char particles and often with only a single reactant gas. A number of models have also been constructed to predict the performance of gasifiers based on the equilibrium composition of the product gas, ignoring reaction kinetics completely or having minimal use of simplified kinetics. Of more significance is the large number of published reactor models for gasification, although the majority have been for variations of fixed-bed gasifiers and the models are typically applied to low pressure gasifierss only. In the following sections the methods used in previously published models to model the reactions, particles, reaction regime calculations and heat transfer will be examined and discussed. It should be noted that differences in modelling techniques for different gasifier types can occur due to physical differences in design and operating conditions, for example in some fixed bed gasifiers gas flow is counter-current to coal feed so that oxygen is consumed during contact with char and devolatilisation occurs at relatively low temperatures in a reducing atmosphere. This form of gasifier should have different modelling treatment for devolatilisation than entrained flow gasifiers where devolatilisation will generally occur at high temperatures in an oxygen rich environment. Similarly heat transfer in the solid bed of a fixed bed gasifier could be considerably influenced by conduction when in an entrained flow gasifier radiation may dominate.

2.7.2.1 Reaction Modelling

A number of published coal gasification models are listed in table 2.4 in categories dependant on the format of the model or the type of reactor modelled, and with indication of the reactions considered in the model. It can be seen from the table that a large number of different reactions can be considered in gasification and a

large range of complexity of model can be identified on the basis of the number of reactions considered. It is also suggested that in some cases the models will not produce sensible predictions if they consider only the reactions stated in the publication. For example the model of Lim (1991) fails, in published form, to consider any gas phase reactions so could not predict realistic gas compositions. In other cases it may not have been stated in the publication the means used to model a particular reaction which appears essential to operation of the model.

Single particle models are generally concerned with the heterogeneous reaction kinetics of char only, so do not consider devolatilisation and tend to use only a simplified range of homogeneous gas phase reactions. The usual concern of these models are the reactions of gases at the particle and in the boundary layer. In contrast the equilibrium models are concerned with the bulk gas composition and neglect the heterogeneous reactions, except for calculation of heat balances. As a large number of homogeneous reactions are possible each model considers only as many as is required to link the gas species that the researchers wish to include in the model. For example, three sulfur containing species are considered by Watkinson *et al.* (1991) but only two are considered by Dave and Duffy (1992) and Ni and Williams (1995), and therefore Watkinson *et al.* (1991) use an additional reaction (Reaction 14) which is not required in the other models. The gasifier models are more complicated with consideration of devolatilisation, heterogeneous kinetics and homogeneous reactions. Models for variants of fixed-bed gasifiers are most common, perhaps due to the high numbers of these gasifiers in operation worldwide, and a number of differing approaches to modelling are evident. In gasifier modelling it is possible to simplify the model by assuming that some reactions are rate determining and therefore faster reactions can be assumed to occur instantaneously if the reactants are present. This approach is evident in the models of Denn (1979), Kosky (1980), Ruprecht (1988) and Schoen (1992) where most reactions are assumed to occur instantaneously, resulting in what are essentially equilibrium models but with specific application to a particular gasifier. The models of Adanez (1990) and Saffer (1988) use less drastic simplifications to produce models which may produce relevant predictions with more rapid computation than rigorous models. The model of Brown *et al.* (1988) is the only model to consider the influence of turbulent gas mixing on the reactions, being two-dimensional while the other models are either non-dimensional or plug flow. Of the gasifier reaction modelling those of Hobbs *et al.* (1992), Wen and Chaung (1979), and Govind and Shah (1984) are the most comprehensive, considering the widest range of

reactions, and were all also used to model high pressure gasification. Treatment of high pressure gasification is generally poor however, with extension of rate expressions determined at atmospheric pressure to high pressures without experimental analysis of pressure order, in fact all authors using Arrhenius pressure order expressions assume pressure orders of unity for all reactions as a simplification. The model of Bliek (1984) is significant in its use of Langmuir-Hinshelwood reaction rate expressions for both carbon dioxide and steam gasification reactions. These rate expressions were experimentally determined by the author and the resultant model has the most complex published heterogeneous reaction model, however due to the nature of the gasifier studied a full range of reactions was not considered and only atmospheric pressure was considered. The model of Vamvuka *et al.* (1995) does not consider devolatilisation and the heterogeneous reactions are taken to occur with coal, rather than char, due to an assumption that the release of volatiles is slow compared to the rate of diffusion of reactant gases to the particles. This assumption is based on experimental results from thermogravimetric apparatus experiments and therefore may not be applicable in an entrained flow reactor. The consideration of several homogeneous combustion reactions as equilibrium reactions by Vamvuka *et al.* (1995) was found to be unneccessary, as the reactions were found to proceed effectively to completion.

Table 2.4: Comparison of reactions considered in various models.

Model Author	Year	Reaction Number														
		1	2	3	4	5	6	7	8	9	10	11	12	13	14	15
Single Particle Models																
Arri *et al.*	1978	-	-	-	A	G	G	G	E	-	E	E	-	-	-	-
Srinivas *et al.*	1980	-	-	-	-	A	H	A	E	-	-	-	-	-	-	-
Zygourakis *et al.*	1982	-	-	-	-	A	-	-	-	-	-	-	-	-	-	-
Haynes	1982	-	-	-	-	A	H	A	E	-	-	-	-	-	-	-
Sotirchos *et al.*	1984	-	-	-	A	A	-	-	-	-	-	A	-	-	-	-
Hastaoglu	1987	-	-	-	-	H	-	-	-	-	-	-	-	-	-	-
Chang	1988	-	-	-	-	A	H	A	A	-	-	-	-	-	-	-
Doraiswamy	1988	-	-	-	-	H	-	-	-	-	-	-	-	-	-	-
Ballal *et al.*	1989	-	-	-	?	A	H	A	E	-	I	I	I	-	-	-
Morell *et al.*	1990	-	-	-	A	A	H	A	A	-	A	A	-	-	-	-
Equilibrium Models																
Batchelder	1950	I	I	-	-	-	I	-	E	-	-	I	-	-	-	-
Watkinson *et al.*	1991	-	-	-	-	-	-	-	E	E	-	-	-	-	E	E
Dave and Duffy	1992	-	-	-	-	-	Z	Z	Z	-	-	Z	Z	-	-	Z
Ni and Williams	1995	-	-	-	-	-	-	-	E	E	-	-	-	-	-	E
Fixed Bed Reactors																
Yoon *et al.*	1978	S	L	A	A	-	A	A	E	-	-	-	-	-	-	-
Denn *et al.*	1979	I	?	I	I	-	I	-	E	-	-	-	-	-	-	-
Stillman	1979	N	N	M A	M A	M A	M A	M A	E	E	-	-	-	-	-	-
Kosky and Floess	1980	I	C	I	I	I	I	I	E	-	I	E	-	-	-	-
Caram *et al.*	1982	-	-	-	A	-	A	-	-	-	I	I	-	-	-	-
Bliek	1984	T	T	A	A	H	H	-	E	-	-	-	-	-	-	-
Adanez *et al.*	1990	I	C	A	-	A	A	-	E	-	A	A	I	I	-	-
Monazam *et al.*	1992	-	-	A	A	A	A	A	E	-	-	-	-	-	-	-
Hobbs *et al.*	1992	V	V	A	A	A	A	-	Z	Z	Z	Z	Z	-	Z	-
Fluidised Bed Reactors																
Kojima *et al.*	1986	-	-	-	-	H	-	-	-	-	-	-	-	-	-	-
Saffer *et al.*	1988	I	L	I	-	-	M A	-	E	-	-	I	-	-	-	-
Lim *et al.*	1991	C	Y	A	-	A	A	-	-	-	-	-	-	-	-	-
Entrained Flow Reactors																
Batchelder *et al.*	1953-54	-	-	-	D	H	*	-	*	-	E	E	-	-	-	-
Ubhayakar *et al.*	1977	T	T	-	-	-	-	-	-	-	-	-	-	-	-	-
Wen and Chaung	1979	S	L	A	A	A	A	A	A E	A E	I	I	-	-	-	-
Govind and Shah	1984	S	L	A	A	A	A	A	A E	A E	I	I	-	-	-	-
Brown *et al.*	1988	T	E	-	F	A	A	-	E	-	-	-	-	-	-	-
Ruprecht *et al.*	1988	-	-	-	I	I	I	I	E	E	-	E	-	-	-	-
Schoen	1992	I	C	-	I	I	I	-	E	-	-	-	-	-	-	-
Vamvuka *et al.*	1995	-	-	A	A	A	A	A	E	-	E	E	E	-	-	-

Reaction:

1	Devolatilisation Rate
2	Volatile Composition
3	$C + O_2 \Rightarrow CO_2$
4	$C + 0.5\ O_2 \Rightarrow CO$
5	Carbon Dioxide-Carbon Reactions
6	Steam-Carbon Reactions
7	Hydrogen-Carbon Reaction
8	$CO + H_2O \Leftrightarrow CO_2 + H_2$
9	$CH_4 + H_2O \Leftrightarrow CO + 3\ H_2$
10	$2\ H_2 + O_2 \Leftrightarrow 2\ H_2O$
11	$2\ CO + O_2 \Leftrightarrow 2\ CO_2$
12	$CH_4 + 2\ O_2 \Leftrightarrow CO_2 + 2\ H_2O$
13	$2\ C_6H_6 + 15\ O_2 \Leftrightarrow 12\ CO_2 + 6\ H_2O$
14	$3\ H_2 + SO_2 \Leftrightarrow H_2S + 2\ H_2O$
15	$H_2S + CO \Leftrightarrow COS + H_2$

Nomenclature for Table:

- **A** Arrhenius rate expression
- **C** Constant
- **D** Diffusion limited
- **E** Equilibrium
- **F** Field (1969) rate correlation
- **G** IGT Kinetics expressions
- **H** Langmuir-Hinschelwood rate expression
- **I** Infinite rate
- **L** Loison-Chauvin (1964) distribution
- **M** Modified
- **N** 'n' independent first order reactions
- **S** Single first order reaction
- **T** Twin parallel reaction scheme
- **V** Functional Group Devolatilisation
- **Y** Gas Yield equations
- **Z** Gibbs free energy minimization
- ***** Combined reactions (of form M H)
- **?** Not stated in reference

2.7.2.2 Particle Structure and Reaction Regimes

It is simplest to consider the modelling treatment of particle structure and reaction regimes in combination due to the links between pore structure and determination of particle efficiency. A summary of modelling techniques used for particle structure and the reaction regimes considered by various models is given in table 2.5. Some methods are common to many of the models, in particular the shrinking core model with a porous ash layer and no consideration of pore diffusion is often used, because of well defined modelling techniques being available. In some cases the particle and reaction models have been acquired from models designed for other purposes, particularly combustion or catalytic reactions, and may not accurately reflect the processes involved in gasification. Most significant in incorrect modelling techniques is the shrinking sphere with porous ash layer as not only does it fail to recognise the importance of pore diffusion in determining rate but the reported results of these models generally indicate that particle temperatures exceed the ash melting point, so that a porous ash layer cannot remain. While these limitations have sometimes been acknowlegded by users of this model type, they have chosen this method because of the simplicity of calculations and the common representation of chemical reaction rate expressions in terms of particle external surface area. Predictions made using these models are generally corrected by inclusion of a semi-empirical diffusion resistance for the porous ash layer which acts as a substitute for pore diffusion in the absence of a pore structure model. This provides a pseudo regime II, which is neglected in the table so that the model type is reported as only considering the chemical and diffusion limited regimes.

Single particle modelling allows more complex particle structures to be considered and a number of the models in this section of the table use complex methods for determining the extent of diffusion of reactant gases into the particle pores and thereby the reaction rate, rather than using particle effectiveness factors as was described in a previous section. As the computational requirements of these models is excessive for a reactor model the methods used will not be discussed.

Of the reactor models only the model of Bliek (1984) uses a realistic particle and pore structure model. This model is based on the work of Simons *et al.* (1979) which defines the pore structure of a particle as a tree-like or dendritic structure. In

this work large pores were assumed to join to the exterior of the particles then branch into smaller pores, which in turn branch into even smaller pores. In the variation used by Bliek (1984) only two distinct pore sizes are used, macropores and micropores, and diffusion of each reactant gas into the pores is calculated independently. From the calculations effectiveness factors for the different reactions are found and used independently. The modelling approach of Stillman (1979) also requires explanation as it uses a combination of a shrinking sphere model and a surface area correlation. It appears that the model modifies the effective external surface area of the particles used for reactions by estimating an effectiveness factor from the change in total effective surface area. The total effective surface area is calculated from a correlation proposed by Dutta (1977) to represent the change in reaction rate with particle conversion. Combination of these methods in the same model is peculiar and appears to complicate the model without introducing greater accuracy.

Table 2.5: Particle structures and reaction regimes considered in various models.

Model Author	Year	Particle or Pore Model	Porous Ash Layer	Oxygen Regimes	Carbon Dioxide Regimes	Steam Regimes	Hydrogen Regimes
Single Particle Models							
Arri *et al.*	1978	Shrinking	Yes	I, III	I, III	I, III	I, III
Srinivas *et al.*	1980	Correlation	Yes	-	I, II, III	I, II, III	I, II, III
Zygourakis *et al.*	1982	Vesicle	No	-	I	-	-
Haynes	1982	Correlation	Yes	-	I, II, III	I, II, III	I, II, III
Sotirchos *et al.*	1984	Bimodal & Shrinking	Yes	I, II, III	I, II, III	-	-
Hastaoglu	1987	Grain	No	-	I	-	-
Chang	1988	Shrinking	Yes	-	I, III	I, III	I, III
Doraiswamy	1988	Expanding	No	-	I	-	-
Ballal *et al.*	1989	Shrinking	No	I, II, III	I, II, III	I, II, III	I, II, III
Morell *et al.*	1990	Bimodal	No	I, II, III	I, II, III	I, II, III	I, II, III
Equilibrium Models							
Batchelder	1950	N/A	-	-	-	-	-
Watkinson *et al.*	1991	N/A	-	-	-	-	-
Dave and Duffy	1992	N/A	-	-	-	-	-
Ni and Williams	1995	N/A	-	-	-	-	-
Fixed Bed Reactors							
Yoon *et al.*	1978	Shrinking	Yes	I, III	I, III	-	I, III
Denn *et al.*	1979	N/A	-	-	-	-	-
Stillman	1979	Shrinking /Correlation	Yes	I, II, III	I, II, III	I, II, III	I, II, III
Kosky and Floess	1980	N/A	-	-	-	-	-
Caram *et al.*	1982	Shrinking	No	I	-	I	I
Bliek	1984	Dendritic	No	I, II, III	I, II, III	I, II, III	-
Adanez *et al.*	1990	Shrinking	Yes	I, III	I, III	I, III	-
Monazam *et al.*	1992	Shrinking	Yes	I, III	I, III	I, III	I, III
Hobbs *et al.*	1992	Shrinking	Yes	I, III	I, III	I, III	-
Fluidised Bed Reactors							
Kojima *et al.*	1986	Correlation	No	-	I	-	-
Saffer *et al.*	1988	Grain	No	-	-	I	-
Lim *et al.*	1991	N/A	No	I	I	I	I
Entrained Flow Reactors							
Batchelder *et al.*	1953-54	Shrinking	No	III	I, III	I, III	-
Ubhayakar *et al.*	1977	Non-spherical	-	-	-	-	-
Wen and Chaung	1979	Shrinking	Yes	I, III	I, III	I, III	I, III
Govind and Shah	1984	Shrinking	Yes	I, III	I, III	I, III	I, III
Brown *et al.*	1988	Shrinking	No	I, III	I, III	I, III	-
Ruprecht *et al.*	1988	N/A	-	-	-	-	-
Schoen	1992	N/A	-	-	-	-	-
Vamvuka *et al.*	1995	Shrinking	No	I, III	I, III	I, III	I, III

Nomenclature for Table:
Bimodal Two sizes of pores in particle.
Correlation Uses surface area correlation to estimate particle effectiveness factor.
Dendritic Pore branching model, in this case only two pore sizes are used.
Expanding Considers expansion of the particle core with reaction.
Grain Particle composed of numerous non-porous grains.
Non-spherical Corrections in model for non-spherical particles but no pore model used.
Shrinking Shrinking sphere model with or without inert porous ash layer (as indicated).
Vesicle Particle contains macropores and vesicles with micropores opening off the vesicles.
Regime I Chemical reaction rate control considered.
Regime II Considers influence of pore diffusion on reaction rate.
Regime III Diffusion rate to particle considered.

2.7.2.3 Heat Transfer

A summary of the forms of heat transfer and the methods used for any consideration of radiative transfer is given in table 2.6 for a selection of published models. The additional consideration radiative transfer is given arises from its importance in entrained flow gasification as the high temperatures should mean that it is the dominant heat transfer process. It should be recognised in examining the methods listed below that the emissivity of gas is neither zero nor unity but will vary with the concentration of emissive gases, mainly carbon dioxide and steam. As gasification progresses these will change and the emisivity of the gas will be dependant on location in the gasifier.

Heat transfer in single particle modelling is dominated by conductive transfer as other objects are not defined. An exception is the model of Ballal *et al.* (1989) which considers radiative exchange between bulk gas and the particle as being the most significant influence. Little information is given in the published models on the details of the heat transfer methods used, so it is possible that convective transfer may have been considered without mention in the publication.

Heat transfer modelling in gasifier models is influenced strongly by the type of gasifier considered. In fixed bed gasifiers the role of conductive transfer is greater, due to the close spacing of solids, while in all the models for fluidised bed gasifiers considered no heat transfer model is used, presumably due to an assumption of thermal equilibrium. The model of Hobbs *et al.* (1992) is the most comprehensive in its treatment of heat transfer in a fixed bed gasifier with inclusion of all three heat transfer mechanisms. Of the entrained flow gasifier models the methods used in the model of Brown *et al.* (1988) are the most complex, with use of a six flux model to predict radiative transfer from each boundary of a volume but neglecting the emissive properties of the gas. This method is essentially a simplification of the Zonal method of Hottel and Sarofim (1967) discussed in a previous section. A heat loss term is also included in the model of Brown *et al.* (1988) to correct for energy loss from a gasifier operating under practical conditions, this term is similar to that used by Batchelder *et al.* (1953-54) in place of radiative transfer to the reactor walls. The methods used by Wen and Chaung (1979), and Govind and Shah (1984), consider the gas to have a constant emissivity of 0.9 throughout the reactor but as a simplification assume that all objects in the gasifier have an unobstructed view of each other, which may not be

applicable in high pressure applications. In all other models simplistic heat transfer methods are used, usually neglecting that the gas may be significantly emissive and absorptive.

Table 2.6: Aspects of heat transfer between solids considered in various models.

Model Author	Year	Conduction	Convection	Radiation	Gas Emissivity	Additional Comments
Single Particle Models						
Arri *et al.*	1978	Yes	-	-	-	-
Srinivas *et al.*	1980	Yes	-	-	-	-
Zygourakis *et al.*	1982	Yes	-	-	-	-
Haynes	1982	Yes	-	-	-	-
Sotirchos *et al.*	1984	Yes	-	-	-	-
Hastaoglu	1987	Yes	-	-	-	-
Chang	1988	Yes	-	-	-	-
Doraiswamy	1988	Yes	-	-	-	-
Ballal *et al.*	1989	-	-	Yes	Constant	-
Morell *et al.*	1990	Yes	-	-	-	-
Equilibrium Models						
Batchelder	1950	-	-	-	-	-
Watkinson *et al.*	1991	-	-	-	-	-
Dave and Duffy	1992	-	-	-	-	-
Ni and Williams	1995	-	-	-	-	-
Fixed Bed Reactors						
Yoon *et al.*	1978	Yes	-	-	-	-
Denn *et al.*	1979	-	-	-	-	-
Stillman	1979	-	Yes	-	-	-
Kosky and Floess	1980	-	-	-	-	-
Caram *et al.*	1982	-	-	-	-	-
Bliek	1984	Yes	Yes	-	-	-
Adanez *et al.*	1990	-	Yes	Yes	0	-
Monazam *et al.*	1992	Yes	Yes	-	-	-
Hobbs *et al.*	1992	Yes	Yes	Yes	0	-
Fluidised Bed Reactors						
Kojima *et al.*	1986	-	-	-	-	-
Saffer *et al.*	1988	-	-	-	-	-
Lim *et al.*	1991	-	-	-	-	-
Entrained Flow Reactors						
Batchelder *et al.*	1953-54	Yes	-	-	-	Heat Loss
Ubhayakar *et al.*	1977	Yes	Yes	-	-	-
Wen and Chaung	1979	-	Yes	Yes	0.9	View Factor 1
Govind and Shah	1984	-	Yes	Yes	0.9	View Factor 1
Brown *et al.*	1988	-	Yes	Yes	0	Six Flux
Ruprecht *et al.*	1988	-	-	-	-	-
Schoen	1992	-	-	Yes	1	-
Vamvuka *et al.*	1995	Yes	-	Yes	0	-

Nomenclature for Table:
Heat Loss This method allows for a constant heat loss through the gasifier wall in place of radiation.
View Factor 1 Assumes that all particles have a complete view of the gasifier wall.
Six Flux Takes radiation as occurring in six directions only for a given volume of the gasifier.

2.7.2.4 Summary of Published Models

The published models discussed all have limitations, however the range of methods used allows for selection of preferred techniques for modelling reactions, particle structure and heat transfer. In all aspects of the modelling it is important to avoid the inconsistencies present in many of the published models.

An example of inconsistencies in modelling is the unrealistic modelling of particle structure and reaction rates represented by the shrinking core model with porous ash layer. This model allows a simplification in reaction rate determination by considering only the external surface of non-porous spheres as a reaction site, which may be acceptable if the reaction rate is correctly calculated, but the porous ash layer cannot exist at temperatures greater than the ash melting point. Preferred methods for modelling of particle structure would be the bimodal distribution method, used in several single particle models, or the dendritic method, used by Bliek (1984). However, these required experimental analysis of the char in order to set parameter values so the Wheeler method of single pore size is easier to implement but was not used by any of the published models reviewed.

The modelling of the heterogeneous reactions in most models does not match current understanding of the reactions as most recent experimental work has found fractional reaction orders for the oxygen, carbon dioxide and steam gasification reactions but the majority of the models use unity reaction orders, presumably to simplify calculations. An exception is the work of Bliek (1984) which uses Langmuir-Hinshelwood expressions determined at atmospheric pressure, however methods are also available for using fractional pressure order expressions for reaction rate calculations.

Care should be taken with the selection of the homogeneous reactions considered to avoid anomalies, as evidenced in the work of Vamvuka *et al.* (1995) where it was found that hydrogen, carbon monoxide and methane do not coexist with oxygen, leaving no means for methane formed during hydrogen gasification to react, as the methanation equilibrium reaction is not considered. This leads to high predictions of methane which would not have been present if a more complete set of equilibrium reactions was considered in the reaction scheme. For this reason the equilibrium reactions modelled should include all gases of interest such as is performed in the model of Watkinson *et al.* (1991), for example.

Treatment of heat transfer processes is neglected in many of the published models by lack of consideration of a partial emissive gas. As high temperatures are expected in entrained flow gasifiers, radiative heat transfer will be of considerable influence and it should be noted that the high concentrations of carbon dioxide and steam present in regions of the gasifier will lead to a gas with significant and variable emissivity. In this regard none of the published models are considered satisfactory, although data is available in the literature to calculate the emissivity of gases containing carbon dioxide and steam.

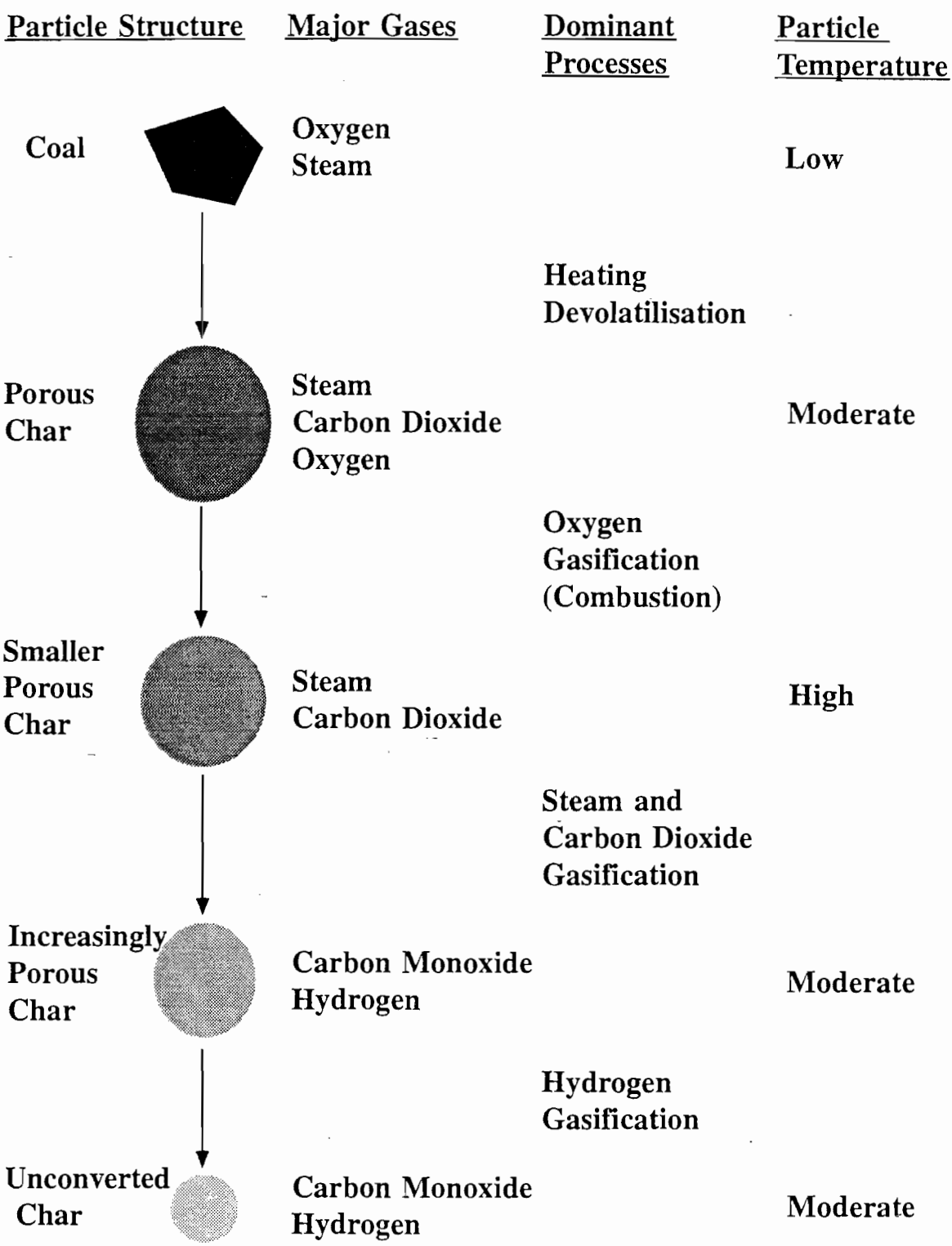

Figure 2.1: Schematic of processes in entrained flow coal gasification

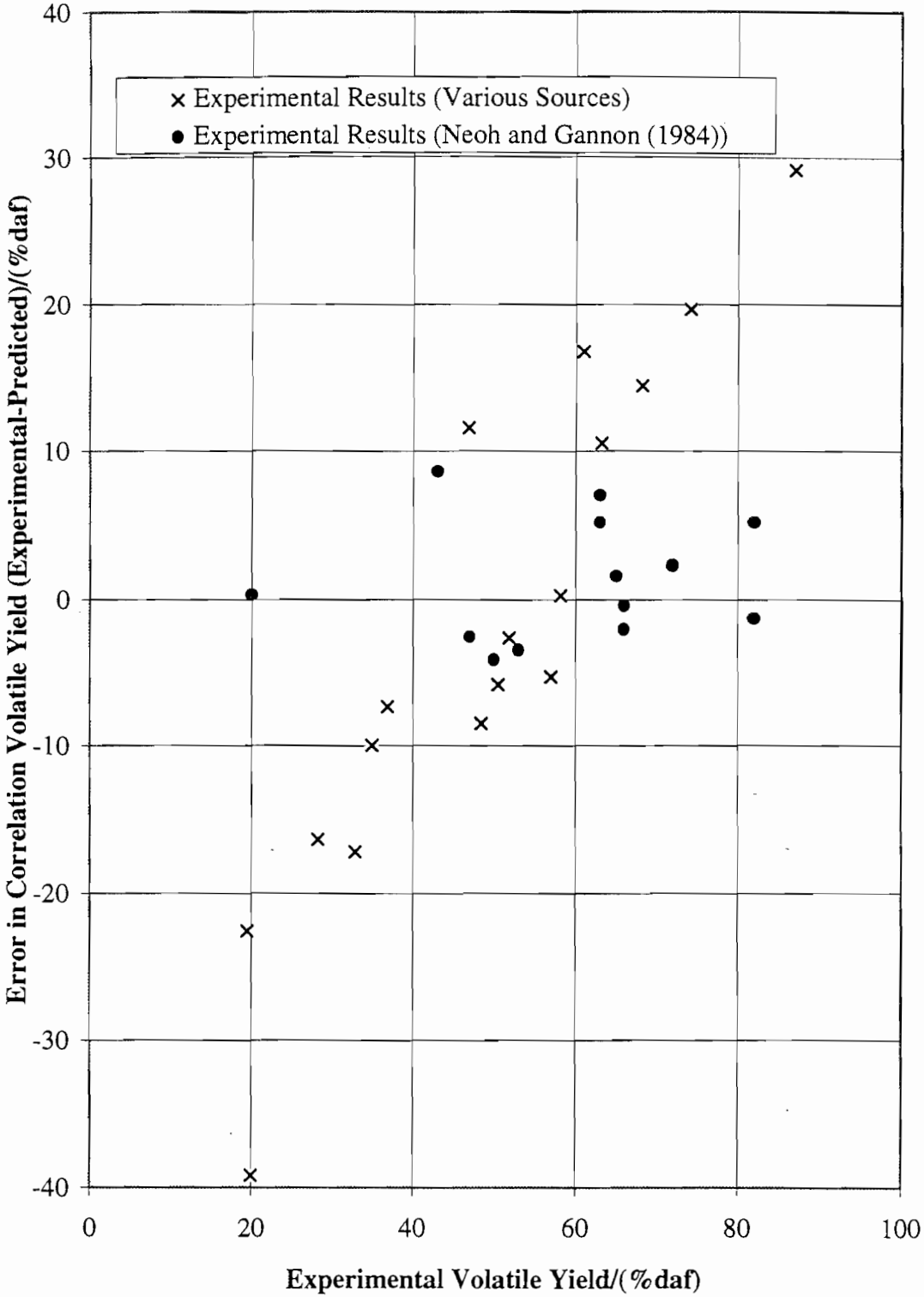

Figure 2.3: Errors in predicted volatile yield from the correlation of Neoh and Gannon (1984) when compared to experimental results.

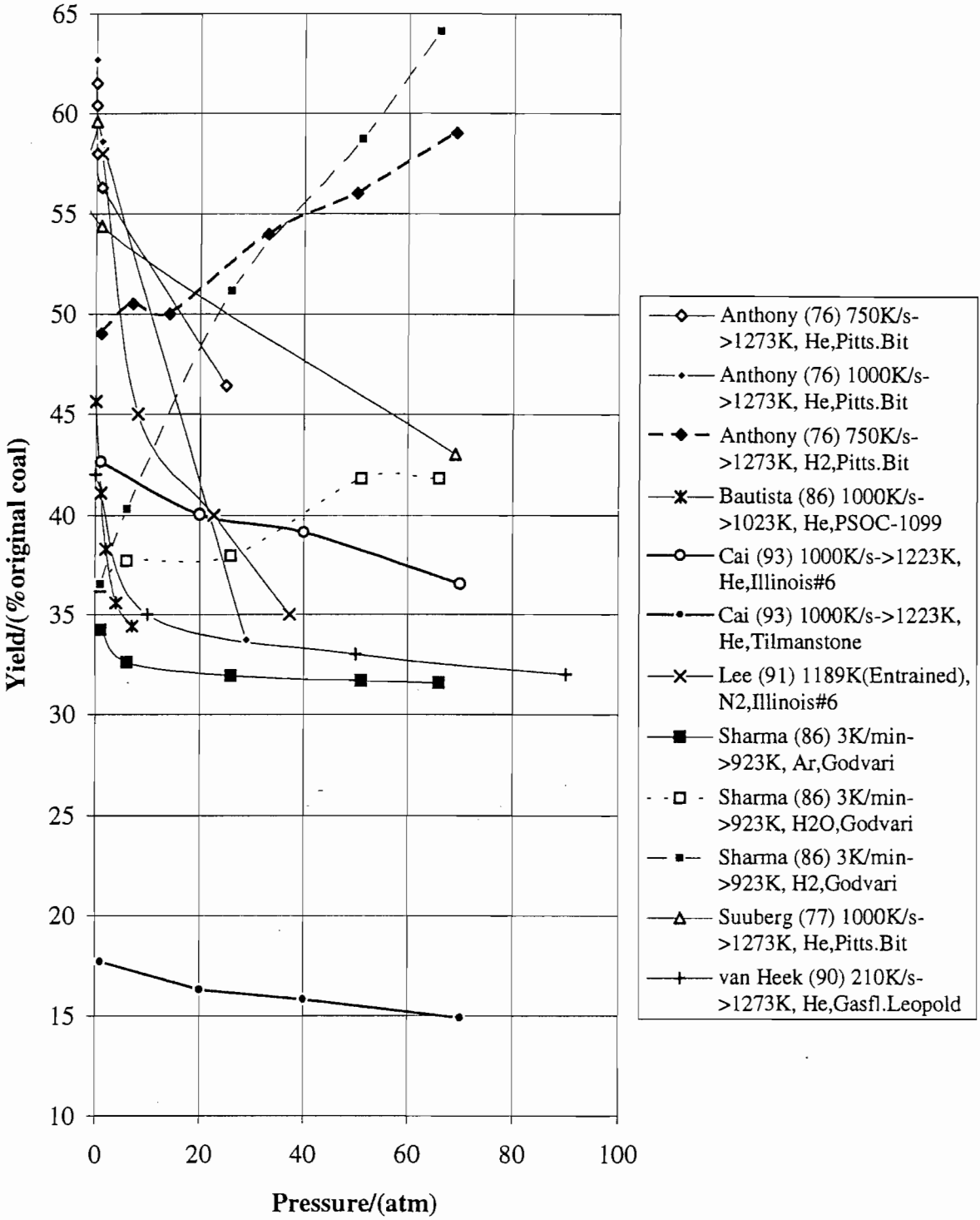

Figure 2.2: Comparison of published results for volatile yield varying with pressure in different atmospheres.

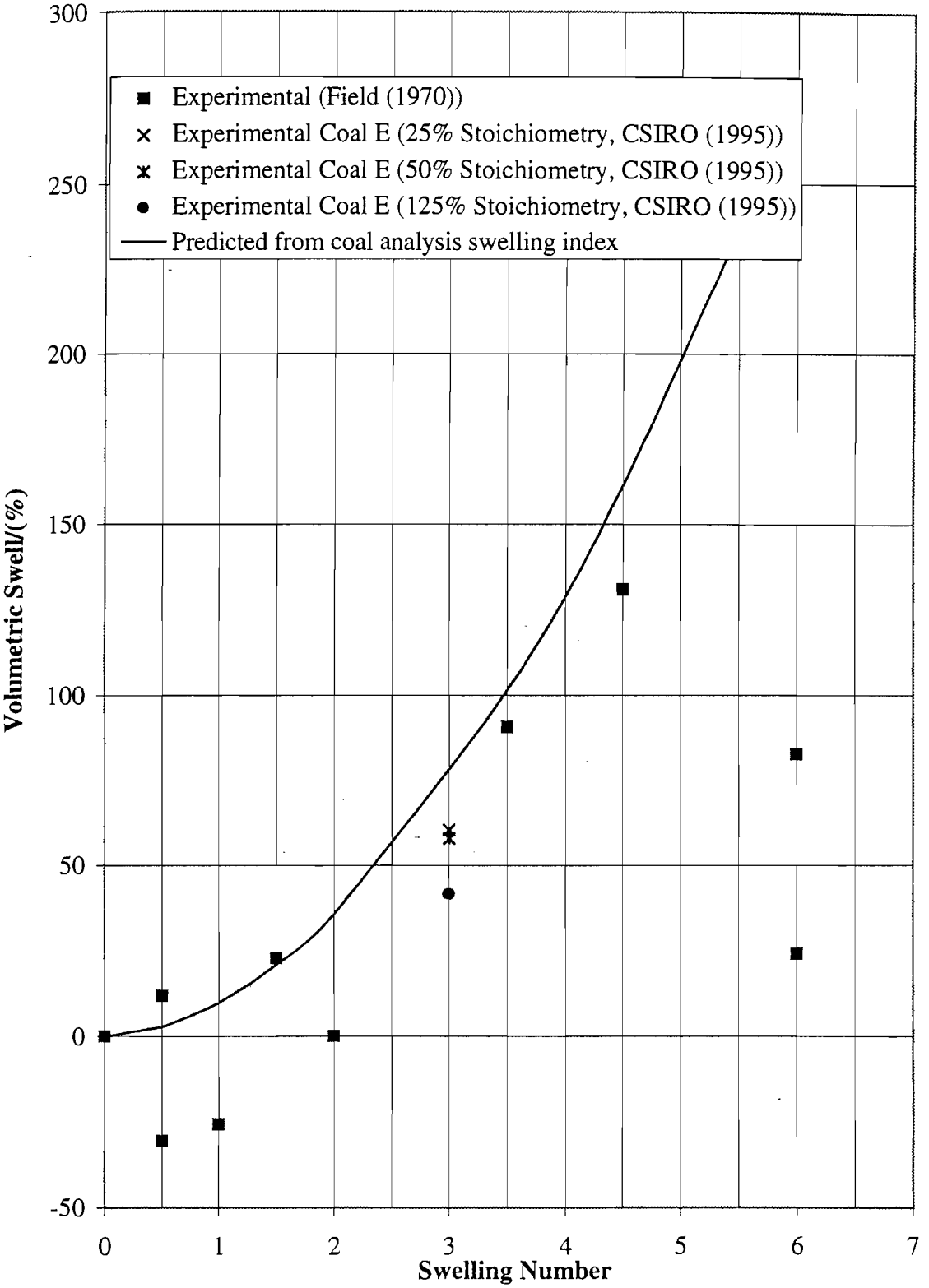

Figure 2.4: Comparison of measured swell from analysis with that under combustion and gasification conditions.

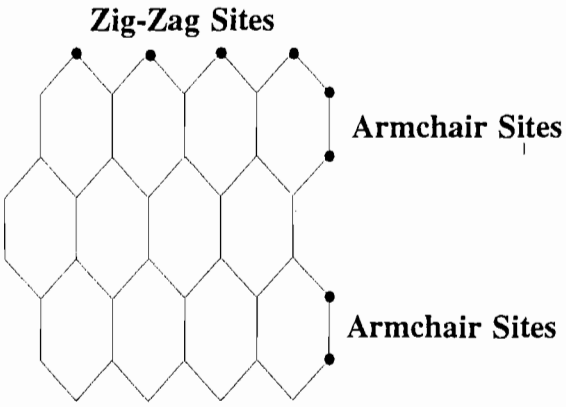

Figure 2.5: Graphite structure showing reaction sites.

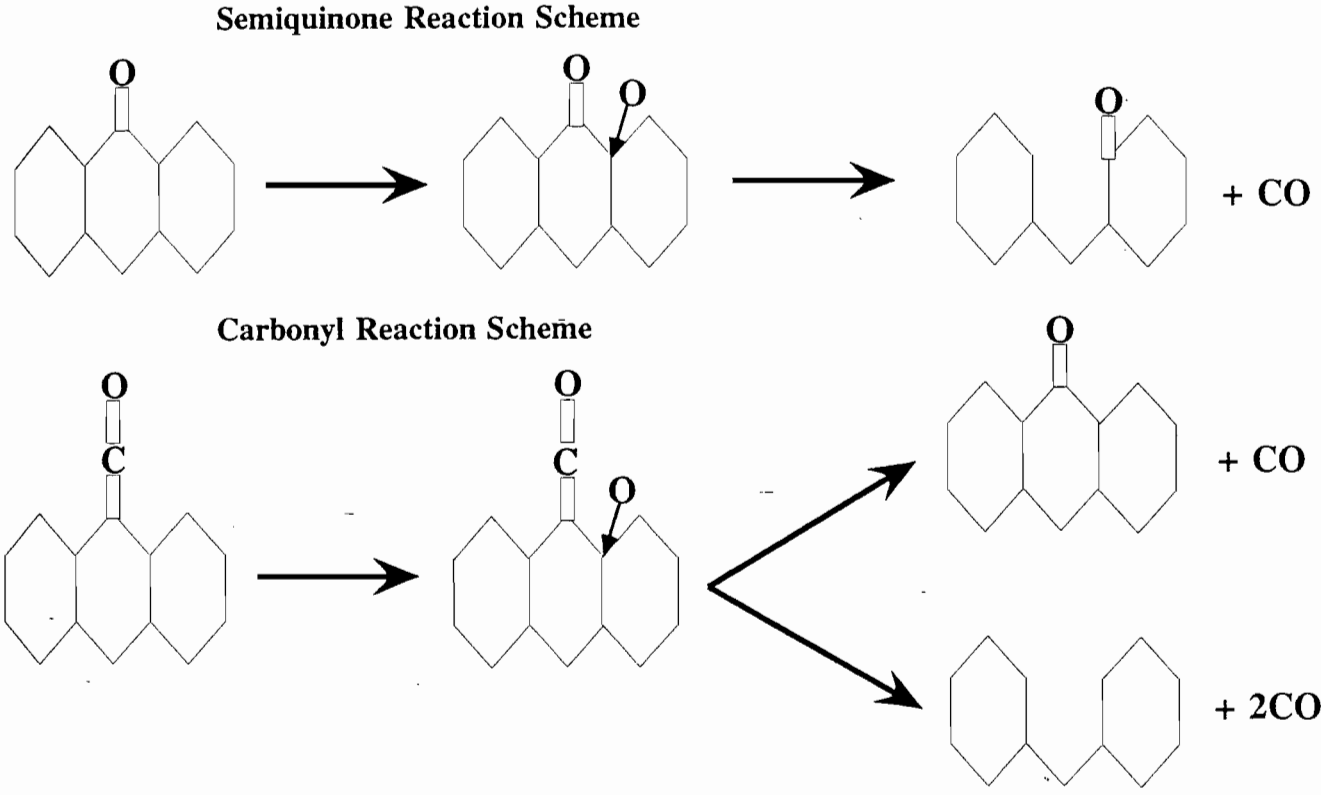

Figure 2.6: Proposed reaction schemes for carbon removal by oxygen (Chen et al. (1993))

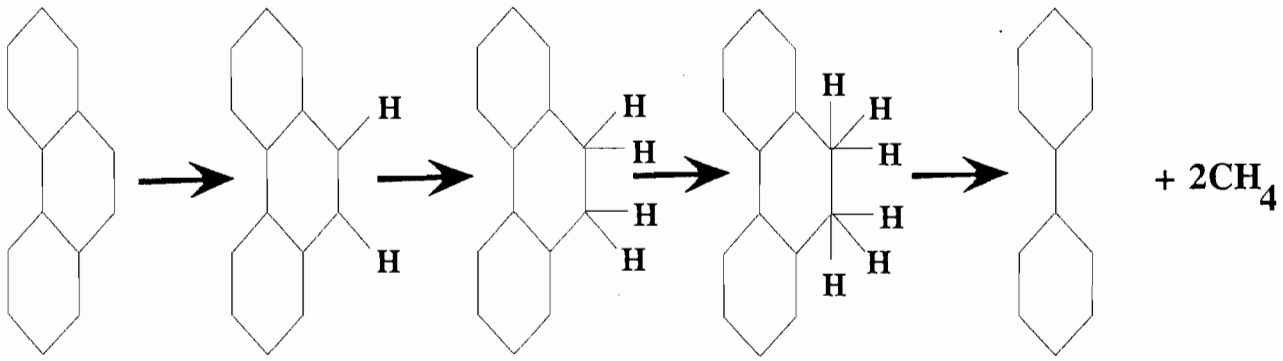

Figure 2.7: Proposed reaction scheme for carbon removal by hydrogen (Walker (1959))

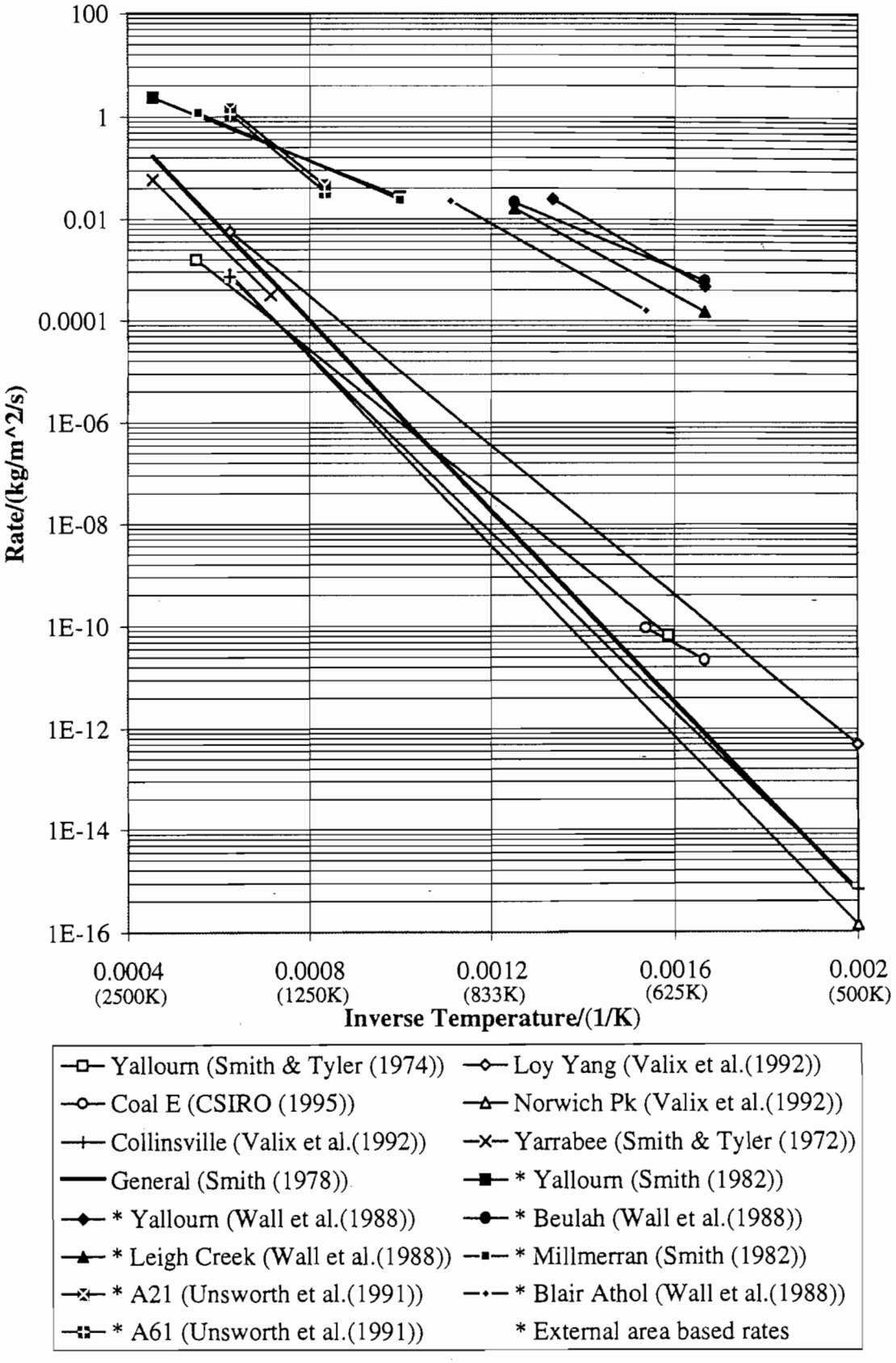

Figure 2.8: Comparison of a selection of intrinsic and external reactivities of Australian coal chars to 1 atmosphere of oxygen.

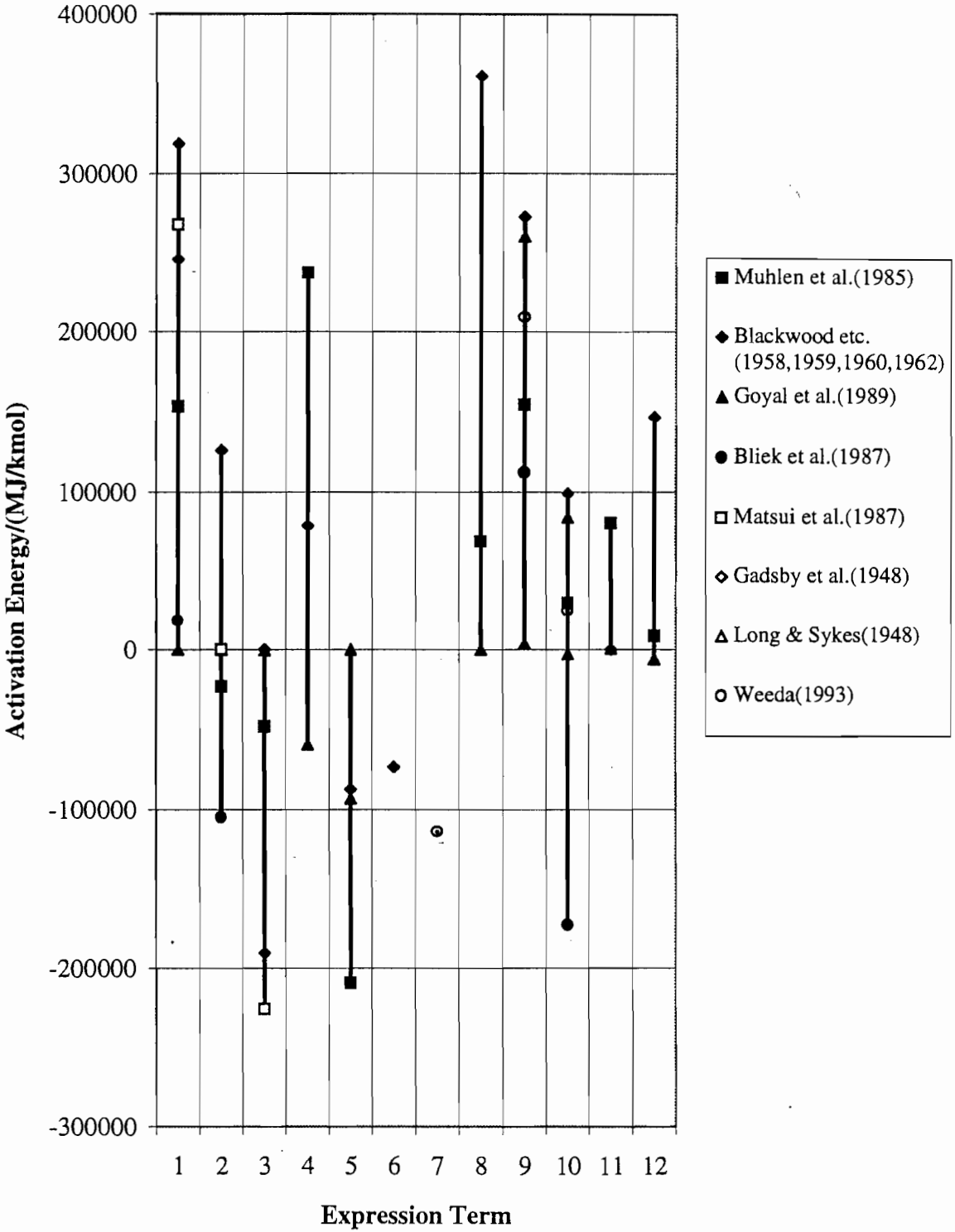

Figure 2.9: Comparison of published activation energies for terms in complex Langmuir-Hinshelwood expression.

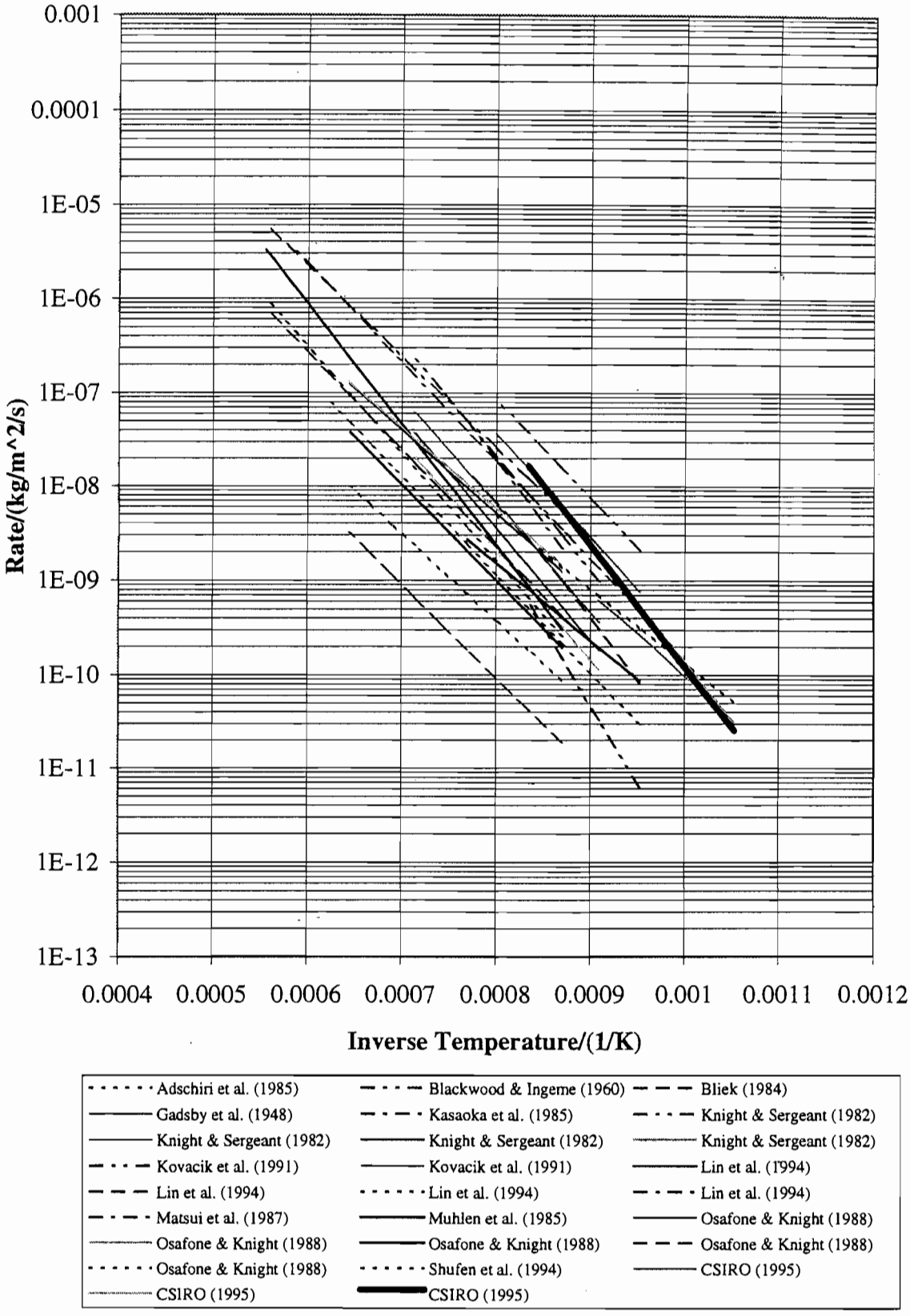

Figure 2.10: Comparison of a selection of published intrinsic reactivities of chars to 1 atmosphere of carbon dioxide.

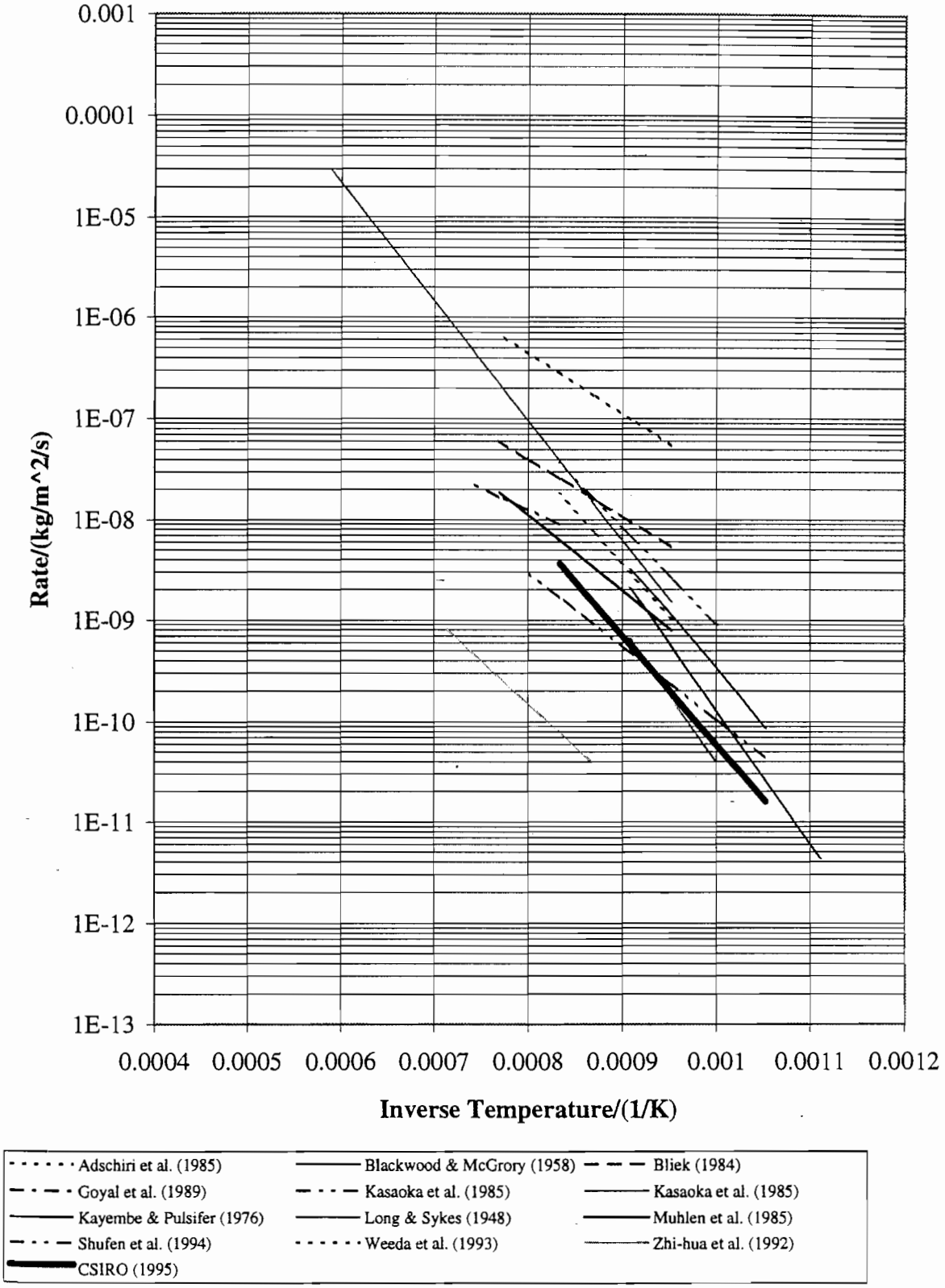

Figure 2.11: Comparison of a selection of published intrinsic reactivities of chars to 1 atmosphere of steam.

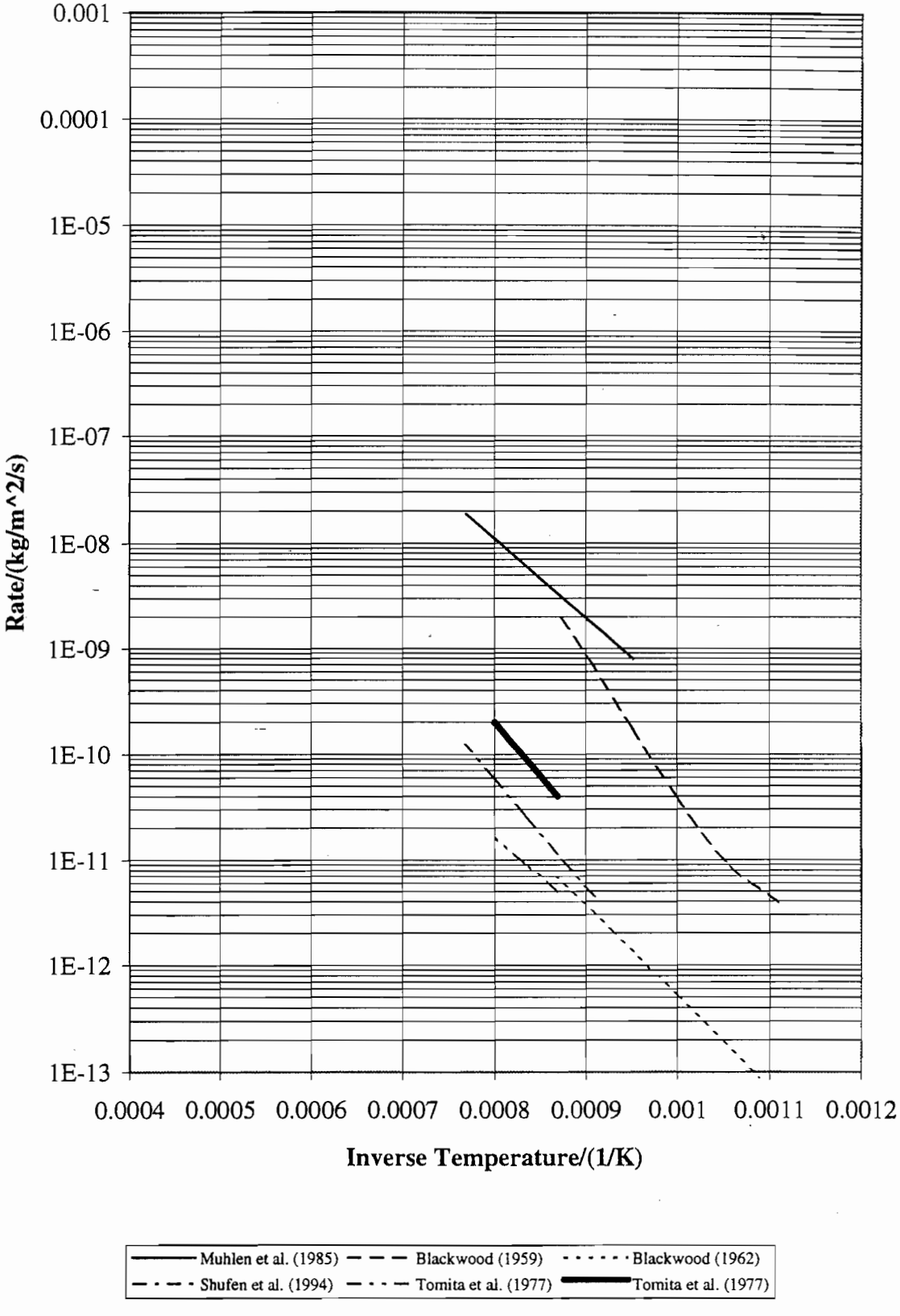

Figure 2.12: Comparison of a selection of published intrinsic reactivities of chars to 1 atmosphere of hydrogen.

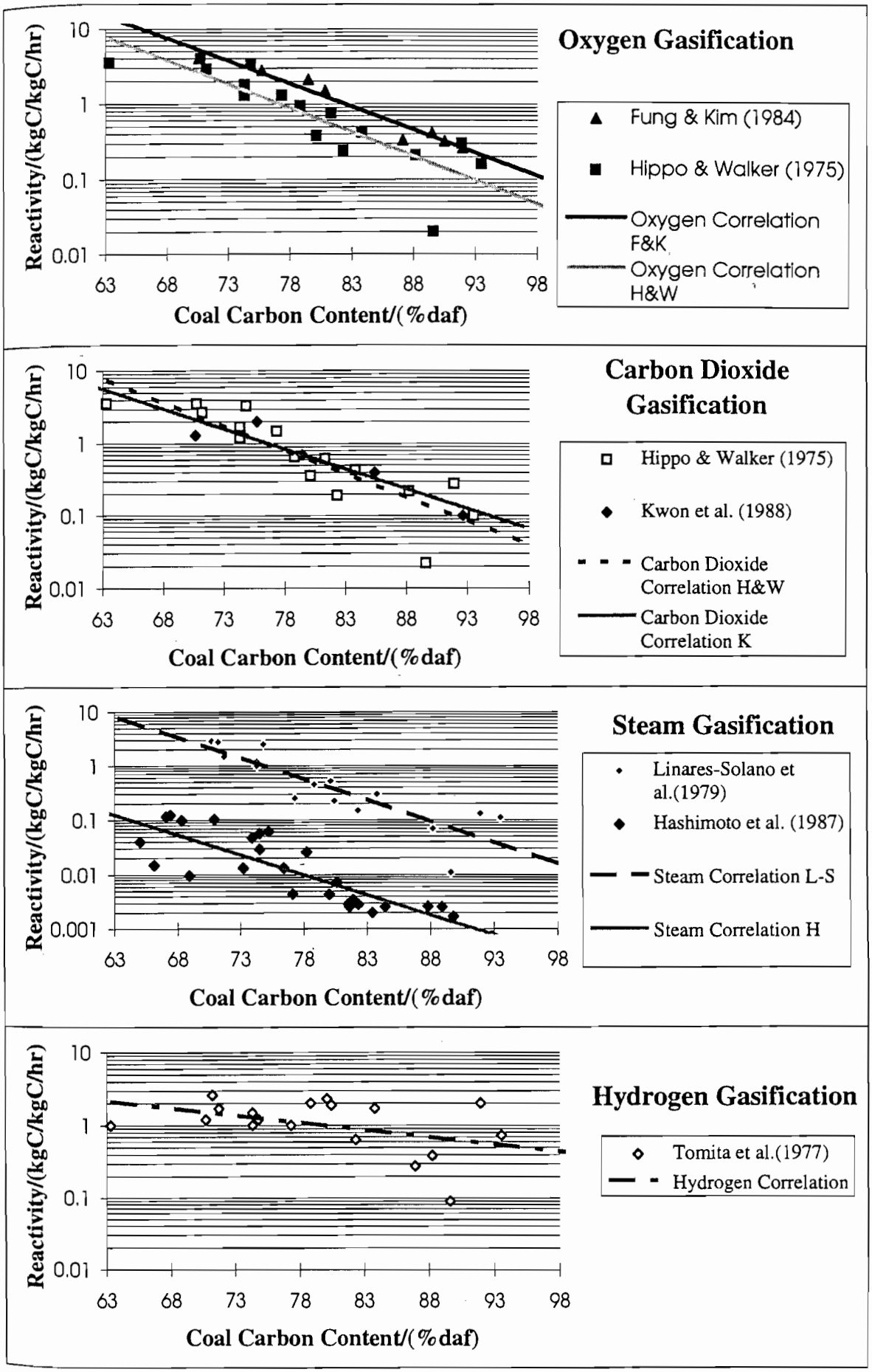

Figure 2.13: Correlations of reactivity with respect to coal carbon content for gasification reactions as per Fung and Kim (1984).

(a) Pore Diffusion Processes Schematic

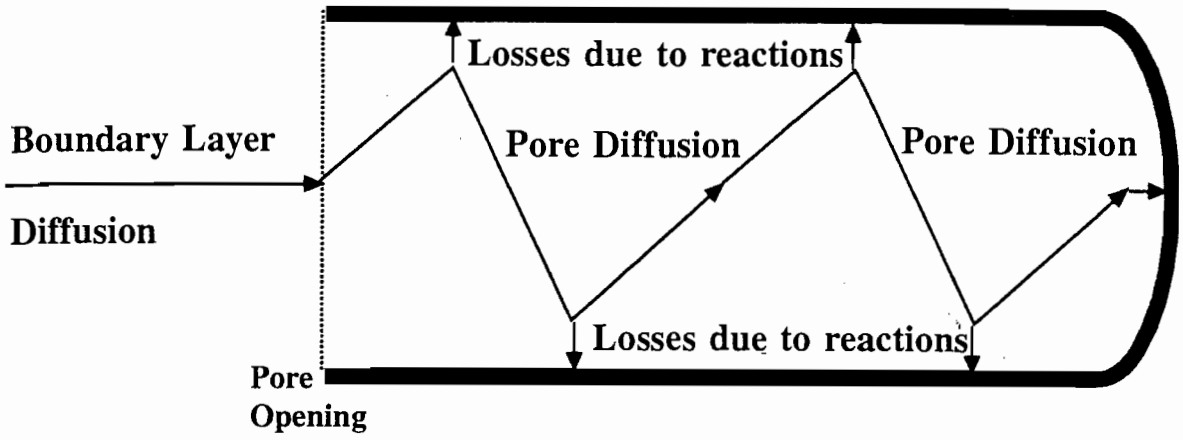

(b) Typical Reactant Concentration Profile in Pore

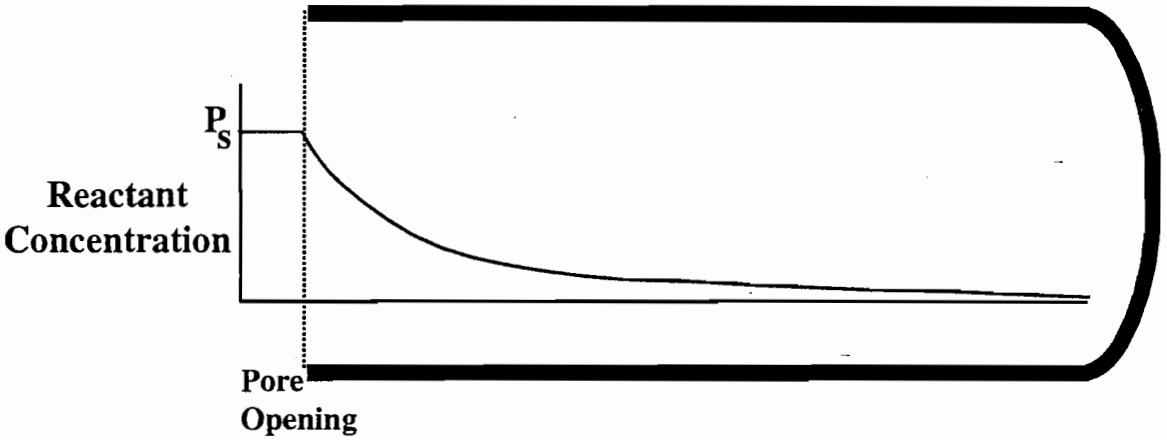

(c) Effectiveness Factor Pore Model

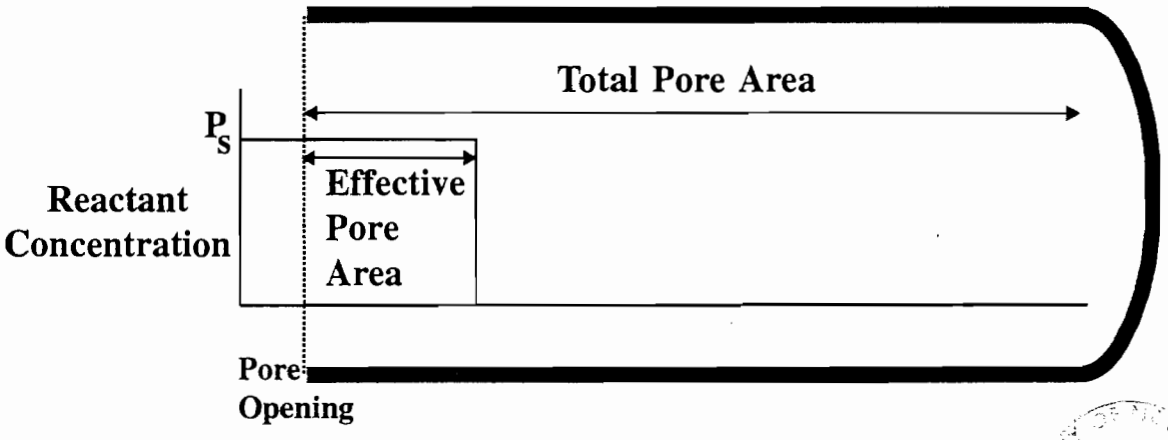

Effectiveness Factor=(Effective Pore Area)/(Total Pore Area)

Figure 2.14: Schematic representation of diffusion of reactant gas into a pore

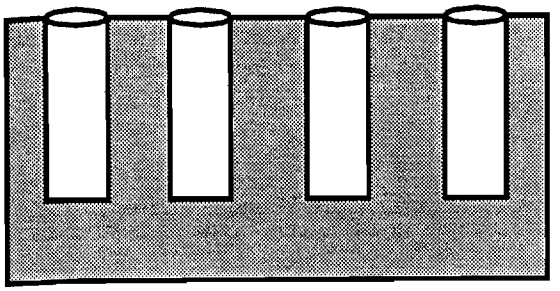

Average Pore Size Model
-All pores same diameter and length
-No pore intersections
(Wheeler (1951))

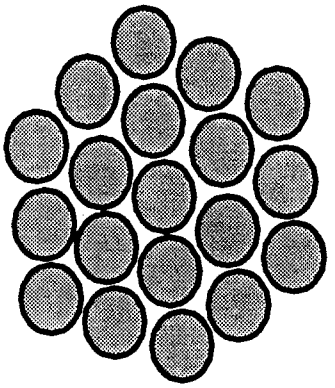

Grain Model
-Particles composed of non-porous grains
-Each grain reacts as a shrinking sphere
-May have variable grain sizes
(Szekely, Evans and Sohn (1976))

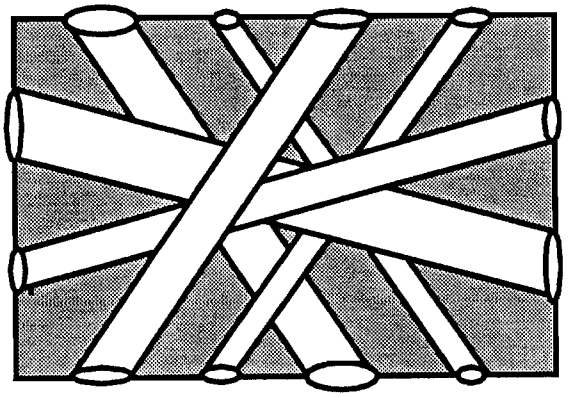

Random Pore Model
-Pores of random size and orientation
-May adjust for intersections
(Gavalas (1980))

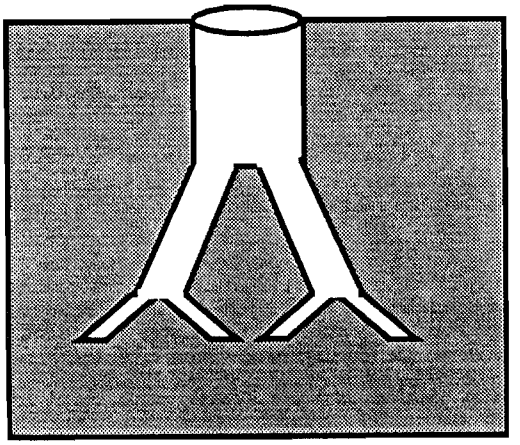

Dendritic Pore Distribution Model
-Pores sized according to distribution
-Smaller pores branch from larger pores
(Simons and Finson (1979))

Figure 2.15: Diagrammatic representation of literature pore models

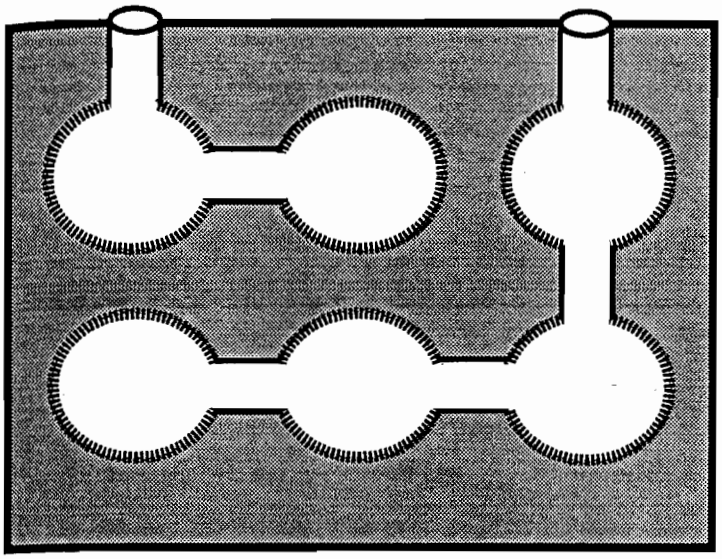

Vesicle Pore Structure Model
-Spherical vesicles linked by pores
(Foster and Jensen (1990))

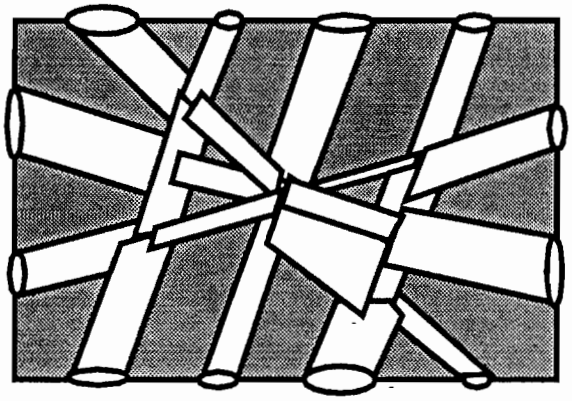

Stochastic Pore Network Model
-Random orientation of pores
-Each section of pore different size
(Mann *et al.* (1986))

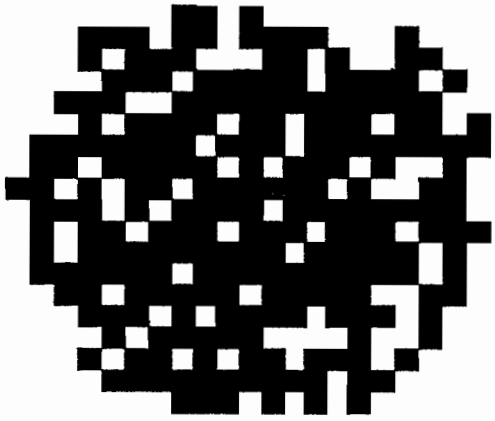

Discrete Pore Model
-Particle comprised of small blocks
-Random vacancies in particle
(Sandmann and Zygourakis (1986))

Figure 2.15(cont) : Diagrammatic representation of literature pore models

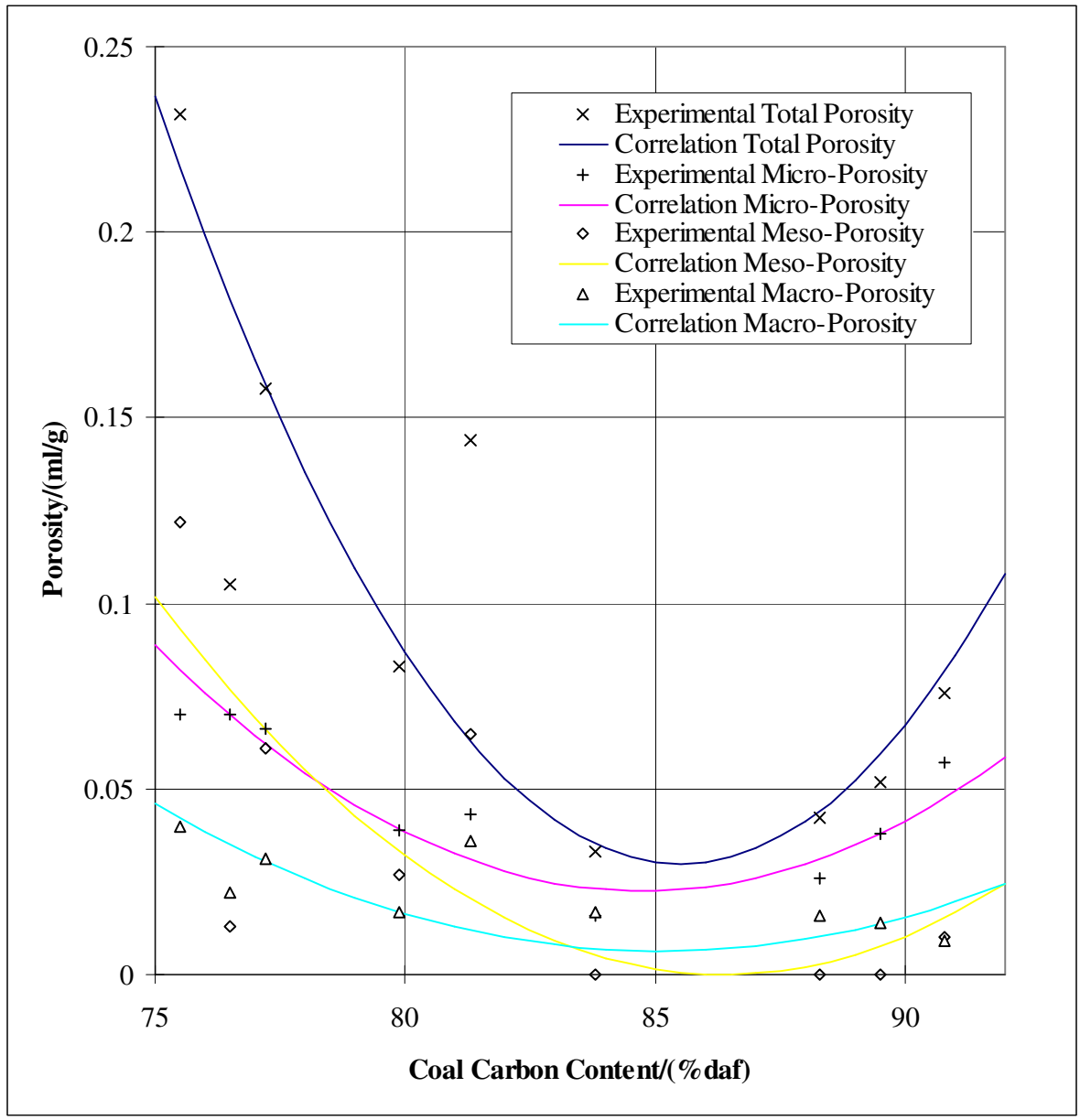

Figure 2.16: Variation in coal porosity (total and in various pore size ranges) with coal carbon content (Gan et al. (1972))

3. EVALUATION OF LITERATURE

3.1 Devolatilisation

The quantity of volatiles released from a specific coal under the conditions of entrained flow gasification conditions was identified as the major requirement from data on devolatilisation literature. The elemental composition of the volatiles is also required, but is of lesser significance. Data on devolatilisation occurring under conditions similar to those experienced in entrained flow gasifiers is extremely rare and no comprehensive work has been published. Despite this, results from a number of studies utilising either high temperatures, high heating rates, high pressures and a variety of gas atmospheres, for a varied range of coals, can be combined to allow correlation of the volatile yield with changes in conditions and coal properties. This relies upon assumptions relating to similarities in the behaviour of devolatilising coal regardless of conditions. Notable amongst these is the assumption that the quantity of volatiles released under low pressure conditions in an inert atmosphere can be related to the yield at high pressure in an oxidising atmosphere. Using this assumption it is possible to extrapolate the correlation of volatile yield with coal composition at atmospheric pressure (Neoh and Gannon (1984)) to predict the yield of any coal devolatilising at high pressures by incorporating the results of another study of only one coal devolatilising at a variety of pressures (Lee *et al.* (1991)).

3.2 Particle Structure

There is considerable uncertainty surrounding the changes in particle structure during rapid devolatilisation and reaction. Research has been published applicable to atmospheric combustion showing that large variations in the shapes of particles can occur within the same coal and between coals. It is typically assumed in models that all particles are spherical as an approximation, although this can introduce significant errors in heating rates of the particles. Swelling during devolatilisation has been studied under combustion conditions at atmospheric pressure and in an inert atmosphere at high pressures, but correlations have not been developed. Numerous models of varying complexity have been proposed for the porous structure of particles but no model has been shown to be universally applicable. However the

simplest model, the single pore size model, has shown adequate reliability in interpretation of experimental results for coal char combustion at atmospheric pressure.

3.3 Heterogeneous Reactions

The heterogeneous reactions of oxygen, carbon dioxide, steam and hydrogen with carbon are considered the most significant heterogeneous reactions in coal gasification. Varying levels of research have been performed for each of the reactions. For all reactions the major considerations are involved in determination of the rate at high pressures, as high temperature rates at atmospheric pressure have been well studied, and the variations in rate between different coals. The variation in rate with pressure can be modelled using either Langmuir-Hinshelwood expressions or using a pressure order term in the Arrhenius type expression commonly utilised for combustion modelling. The limitations of each expression are defined by the range of experimental results for each, namely the Langmuir-Hinshelwood expressions have been applied at high pressure, but not high temperature, and pressure order terms have been applied over a large temperature range, but not high pressures. For the oxygen gasification reaction some experimental results have shown relatively constant pressure order over a wide range of pressure with slight variation with temperature. For the other reactions the selection of a reaction rate model is not clear simply from the literature and the subject is considered by comparison of model predictions using the different model forms in a subsequent section.

The actual rate of a heterogeneous reaction is also dependant on diffusion rates to and into the particles, as well as the chemical reaction rate. Diffusion to a spherical particle is readily calculated using methods in the literature but the influence of diffusion into pores on the reaction rate is more complex and is typically determined by calculation of an effectiveness factor. To use available methods of calculating effectiveness factors it must be assumed that the pores are straight cylinders of known size, reactions are first order, and the molar flowrates of product and reactant gases in the pores are identical. For reactions that are not first order and have non unity stoichiometry approximations can be used to adapt more complex literature methods into a simpler form, some error is involved in these approximations but it is considered acceptable.

3.4 Homogeneous Reactions

A large range of reactions between different gases in a gasifier is possible but previous experimental and modelling experience can be used to limit this range to a suitable selection. An assumption has been made in the treatment of homogeneous reactions by considering that all gaseous combustion reactions are extremely rapid and proceed to completion. This assumption is supported by the model of Vamvuka *et al.* (1995) who considered these reactions to be at equilibrium but found that negligible oxygen remained at equilibrium. In addition a number of reactions not involving combustion are considered to be at equilibrium. Experimental data on the reaction rates of the most significant reaction of these reactions, the water-gas shift, suggests that temperatures in the gasifier are sufficiently high to consider the reaction is always at equilibrium. Calculation of gas composition based on this finding can be readily performed using literature expressions for the equilibrium constants.

3.5 Heat Transfer

Most aspects of heat transfer in gasification are similar to those involved in atmospheric pressure combustion and for these modelling techniques are well established in the literature. A significant variation is the presence of large quantities of the radiatively emissive gases carbon dioxide and steam. The impact of these is to make radiative heat transfer more complex as the gas is significantly emissive, particularly at high pressures, during most stages of gasification and with varying emissivity. Literature is available to allow approximate calculation of a grey gas emissivity in a gasifier, although with large gasifiers at high pressures it may not be sufficient. Modification of existing literature heat transfer models can be used to provide approximate rates of transfer when the gasifier being modelled is long compared to its diameter.

3.6 Previous Models

A number of previously published models are available for evaluation and some techniques used in these are applicable to modelling in this study, but in some aspects the models appear to have been unrealistically simplified. The most useful results of these models may be the identification of reactions significant to gasification rates and determining gas composition, as previously listed in table 2.4. In general the methods used for heterogeneous reaction modelling in models ignore the influence of pore diffusion, although as an exception Bliek (1984) used a dendritic pore model and a complex diffusion rate calculation (Table 2.5). Also the treatment of heat transfer in entrained flow models neglects the influence of the presence of an emissive gas mixture (Table 2.6). This leads to a requirement to extract new techniques from the general literature to provide better modelling techniques for these components.

3.7 Conclusions

From the analysis of available literature it appears that sufficient data is available to produce an entrained flow gasification model. A lack of heterogeneous reactivity data at high temperatures and pressures is the major limitation and two alternate methods for modelling will be trialed in a later section to identify the more realistic method for extrapolating data to these conditions. While previous models have neglected the influence of pore diffusion on reaction rates it is possible to generate expressions from the literature to predict its influence on gasification rates. Similarly, the influence of emissive gases on heat transfer has been neglected in previous models but can be approximated using available techniques and expressions. A lack of data for devolatilisation of coal under entrained flow conditions can be overcome by combining data from a number of sources to produce correlations to predict the quantity of volatiles released and provide indications of the particle structure. Gas composition may be determined by categorising gas phase reactions as either instantaneous or equilibrium.

The levels of uncertainty involved in using literature correlations to provide input values for mathematically modelling can be quantified by the accuracy of the correlation in fitting available experimental data. This allows determination of the sensitivity of model predictions to the approximations made in using the correlations.

4. DESCRIPTION OF MATHEMATICAL MODEL

4.1 Model Description

The objective of this study is to develop a mathematical model to predict the level of carbon conversion in a gasifier under known reaction conditions and identify the sensitivity of gasifier performance to changes in conditions and the coals used. Validation of the model against experimental results and testing of the sensitivity of the model predictions will be treated in later sections. The focus of this section is on the modelling methods required to achieve this, foremost among these is the requirement that the model incorporates reaction kinetics, as models relying on reaction equilibrium require pre-knowledge of the gasifier performance. Kinetic models can have varying levels of complexity dependant on the number of dimensions in which flow is considered to occur and the accuracy of particle reaction modelling. As was discussed in a previous section, the previously published entrained flow gasification models have used inaccurate methods for modelling particle structure and heterogeneous reaction rates. Therefore the focus of this work will be to model the reaction aspects of gasification, with less emphasis on fluid dynamics in a gasifier. For this reason the relatively simple, one dimensional, flow pattern of a plug flow gasifier are used in the model to allow for more complex analysis of particle reactions. While ignoring flow patterns in a model is inaccurate in large furnaces, plug flow models can be applicable in small diameter reactors where complex flow patterns do not exist, and for this reason the model is more applicable to analysis of results from small experimental gasifiers than for modelling commercial gasifiers. The division of a gasifier into compartments, also called slices or disks, used in plug flow modelling is shown in figure 4.1. The sizing of the slices is dependant on the rate of change in the section of gasifier so initial slices, during rapid devolatilisation, are thin compared to the later slices, where gasification is occuring. Additional information on the figure will be discussed in a later sub-section.

The proposed model will consider all of the reactions defined in reactions 1 to 14, where the volatiles defined in reaction 1 are composed entirely of simple gases and the entire set of gases considered includes only nitrogen, oxygen, steam, carbon monoxide, carbon dioxide, hydrogen, methane, hydrogen sulfide, carbon oxide sulfide and sulfur dioxide. While other gases have been considered in published models it is considered that more complex

organic molecules released during devolatilisation will either rapidly react or thermally decompose at the high temperatures of entrained flow gasification to form simple compounds. The presence of ammonia has been detected in gasifier product gas, however experimental results have shown that over 99% of nitrogen is in the form of molecular nitrogen at the exit of a high pressure gasifier (Mahagaokar and Krewinghaus (1990)). Formation of nitrogen oxides would be expected in the initial stages of gasification but would rapidly revert to molecular nitrogen or ammonia on depletion of oxygen and with the reducing conditions in the later stages of gasification. Inclusion of the sulfur containing species is not essential to the model as the species will have low concentrations for most coals but the ratios of the different sulfur species may be of importance for indications as to the gas cleaning requirements to prepare the product gas for later use. Restriction of the total number of gas species considered is advantageous in modelling the homogeneous equilibrium reactions, as the number considered allows for simpler techniques to be applied to finding the gas equilibrium concentrations.

Devolatilisation

$$Coal \rightarrow Char + Volatiles$$ Reaction (1)

Heterogeneous Gasification

$$C + \tfrac{1}{Z} O_2 \rightarrow \left(2 - \tfrac{2}{Z}\right) CO + \left(\tfrac{2}{Z} - 1\right) CO_2$$ Reaction (2)

$$C + CO_2 \rightarrow 2CO$$ Reaction (3)

$$C + H_2O \rightarrow H_2 + CO$$ Reaction (4)

$$C + 2H_2 \rightarrow CH_4$$ Reaction (5)

Homogeneous Combustion

$$CO + \tfrac{1}{2} O_2 \longrightarrow CO_2$$ Reaction (6)

$$H_2 + \tfrac{1}{2} O_2 \longrightarrow H_2O$$ Reaction (7)

$$CH_4 + 2O_2 \longrightarrow CO_2 + 2H_2O$$ Reaction (8)

$$H_2S + \tfrac{3}{2} O_2 \longrightarrow SO_2 + H_2O$$ Reaction (9)

$$COS + \tfrac{3}{2} O_2 \longrightarrow CO_2 + SO_2$$ Reaction (10)

Homogeneous Equilibrium

$$H_2O + CO \longleftrightarrow H_2 + CO_2$$ Reaction (11)

$$CO + 3H_2 \longleftrightarrow CH_4 + H_2O$$ Reaction (12)

$$SO_2 + 3H_2 \longleftrightarrow 2H_2O + H_2S \qquad \text{Reaction (13)}$$

$$COS + H_2O \longleftrightarrow CO_2 + H_2S \qquad \text{Reaction (14)}$$

The techniques used for modelling the heterogeneous gasification reactions 2 to 5 will be discussed in detail below, but are similar to the intrinsic reactivity methods used by Smith and Tyler (1972) but with a more general calculation method for the particle effectiveness factor to allow for fractional reaction orders over the full range of possible effectiveness factors for all of the heterogeneous reactions. Due to the uncertainty associated with reaction kinetics at high pressures and temperatures two variants of the model were produced, one utilisizing pressure order expressions and the other a complex Langmuir-Hinshelwood expression for carbon dioxide, steam and hydrogen gasification rates.

In essence a plug flow model assumes that all properties, such as temperatures and gas composition, are evenly dispersed across the reactor (radially) and therefore changes occur only with distance along the reactor (axially). The result of this is that the differential equations of mass and energy transfer in the gasifier can be approximated by slicing the gasifier into numerous small disks, each representing an infinitesimally small change in any given characteristic from the previous disk. The contents of each disk are considered well mixed so that no quality varies from centre to outside of the disk. Considering a particular disk, the model can approximate solution of the numerous differential equations involved if the time scale is sufficiently small that any changes in critical properties, such as temperatures, gas composition and particle structures, within the disk are small. The properties of a given disk are found by the altering the values for the previous disk, so that a gradual change in properties occurs along the gasifier in approximation of differential changes.

4.2 Model Components

A number of sub-models, or components, are required to replicate actual physical processes in the gasifier. The following sections describe the techniques used by each of these components and where relevant justify the selection of these methods in preference to other possible techniques.

4.2.1 Devolatilisation

Devolatilisation is a rapid process that results in a chemical simplification of coal to form char. As this commences at lower temperatures than the heterogeneous reactions it is regarded that the heterogeneous reactions will occur with char, rather than coal. In devolatilisation most of the non-carbon atoms are released from the coal, along with some carbon, in the form of light gases, hydrocarbons and some complex tars. This process has been described by various different researchers according to different models, ranging from single reaction rate expressions to a series of expressions to account for the many possible types of chemical bonds present in coal. The critical features of devolatilisation for modelling are the rate that volatiles are released, the quantity of volatiles released and the composition of the volatiles.

In entrained flow gasification temperatures are high and therefore devolatilisation will occur very rapidly relative to the other processes occurring. For this reason the form of model used for the rate is relatively unimportant and the simplest model form, a single rate expression, was used. The model is described by equation 4.1, where T is the particle temperature.

$$Rate_{Devolatilisation} = k.e^{\frac{-E}{RT}}.(V^* - V) \qquad \text{Equation (4.1)}$$

The quantity of volatiles released is more significant as it determines the amount of char that remains for the slower heterogeneous reactions to consume. Unfortunately the volatile release can differ greatly from the proximate analysis volatile matter due to the extreme conditions in a flame. Numerous results have been presented in the literature for the actual volatile release of particular coals under combustion conditions or in an inert atmosphere. However, the work of Neoh and Gannon (1984) is significant as it correlates volatile yield with commonly measured coal properties, although only at nominal atmospheric pressure as previously discussed. This work covered a wide range of coals at a high temperature (2400K), similar to the peak temperature experienced in a gasifier, and they proposed a simple expression based on the mole fractions of some elements in the coal analysis, as shown in equation 4.2, which is used in the model.

$$V^*_{1atm} = 52.6\left(\frac{X_{Hydrogen} + 2.X_{Oxygen}}{X_{Carbon} + X_{Sulfur}}\right) + 6.89 \qquad \text{Equation (4.2)}$$

Devolatilisation modelling must be modified for high pressure gasification owing to the marked change in volatile yield with pressure changes. Based upon the published work of a number of researchers discussed in the literature review it is clear that volatile yield would be expected to drop at high pressures. The results of Lee *et al.* (1991) for devolatilisation of a single coal in an entrained flow reactor over a range of pressures were used to predict the effect of pressure on volatile yield, as given in equation 4.3 which was derived from the results of the study. Figure 4.2 shows the experimental results of Lee *et al.* (1991) and the correlation described by equation 4.3. The atmospheric volatile yield predicted from equation 4.2 is extrapolated to other pressures using this equation. The work of Lee *et al.* (1991) was selected as the basis for volatile yield predictions owing to similarities between the experimental apparatus used and the experimental gasifier, however the trend described by the equation is similar to that in other published works which used experimental results from other forms of apparatus. Results from other studies are shown in the literature review.

$$V_P^* = \frac{V_{1atm}^*}{P^{0.13}} \qquad \text{Equation (4.3)}$$

The gases released during devolatilisation vary with the conditions under which devolatilisation occurs, with a tendency towards simpler gases at higher temperatures and lower pressures. Experimental results at high pressures and temperatures, as experienced in entrained flow gasifier, suggest that simple gases are more likely to be produced. As the composition of the gases will change when mixed into the reactive bulk gases, where oxygen and steam will react with the volatiles, the only major consideration is in the ratios of the various elements in the volatiles. A simple method is used that assumes all non-carbon elements are removed from the organic portion of coal, with carbon making up the remainder of the volatiles according to a mass balance. For convenience the elements are grouped into simple gases, namely carbon monoxide, carbon dioxide, steam, hydrogen, nitrogen, methane and hydrogen sulfide, which then react in the bulk gas phase according to the homogeneous reaction mechanisms.

4.2.2 Heterogeneous Reactions

Four heterogeneous reactions are taken to be possible in the gasifier, namely combustion, carbon dioxide gasification, steam gasification and hydrogasification of carbon. There are two common methods of modelling the reaction rates of heterogeneous

reactions, pressure order and Langmuir-Hinshelwood expressions, as discussed in the literature review. Langmuir-Hinshelwood expressions are rarely used for oxygen gasification modelling and, as was established in the literature review, pressure order expressions appear to provide an accurate fit to experimental data over a wide range of temperature and pressure (Ranish and Walker (1993), Smith and Tyler (1972, 1974)). The other gasification reactions can be considered together in a complex Langmuir-Hinshelwood expression as given in equation 4.4, however large disparities in the values of terms in this expression from different researchers (Blackwood and co-authors (1958, 1959, 1960,1962), Muhlen *et al.* (1985) and Goyal *et al.* (1989)) lead to uncertainity in the application of this type of rate expression. The variations between different rate expressions are shown in figures 4.3 and 4.4 for a gas mixture of 40% carbon dioxide, 27% carbon monoxide, 13% hydrogen and 20% steam. Also included on the figures are curves showing the sums of the rates of individual pressure order expression based on either unity or "best-fit" pressure orders. The rates for the pressure order expressions were chosen to be identical to those predicted by the expression of Muhlen *et al.* (1985) for 1 atmosphere of pure reactant gas at 1000K and the "best-fit" orders were chosen to fit rates from the same expression over a pressure range of 1 to 15 atmospheres of pure reactant gas. From the figures it is evident that the extrapolation of the Langmuir-Hinshelwood expression using terms from Blackwood and co-authors (1958, 1959, 1960, 1962) or Goyal *et al.* (1989) to high temperatures produces unlikely trends, and the unity pressure order expression has an exaggerated rate at high pressure. The best-fit pressure order expression and that of Muhlen *et al.* (1985) follow similar trends with both temperature and pressure, albiet with a difference of approximately two orders of magnitude in rate. As this difference is relatively constant over the range indicated in the figures it suggests that if the correct reactivity for a char is known under one set of conditions then it can be extrapolated to high temperature and pressure if either of these expressions is used. As the terms, other than the pressure order, for the pressure order expressions can be obtained readily at atmospheric pressure, while those of the Langmuir-Hinshelwood expression are subject to large errors when measured at low pressures as discussed in the literature review, the pressure order expressions were selected for use in the model. The pressure orders will be assumed to be the same as those determined as best-fit to the Muhlen *et al.* (1985) expression for all coals. These were 0.25 for carbon dioxide, 0.2 for steam and 1.0 for hydrogen gasification.

$$Rate = \frac{k_1 P_{CO_2} + k_8 P_{CO_2}^2 + k_9 P_{H_2O} + k_{11} P_{H_2O}^2 + k_{12} P_{H_2O} P_{H_2} + k_4 P_{H_2}^2}{1 + k_2 P_{CO_2} + k_3 P_{CO} + k_{10} P_{H_2O} + k_5 P_{H_2}} \qquad \text{Equation (4.4)}$$

By using pressure order expressions for all reactions it means that all of the heterogeneous reactions are modelled using essentially the same techniques, with the exception that in combustion the reaction product can be any ratio of carbon monoxide to carbon dioxide. This can be estimated using the expression of Tognotti *et al.* (1990), given in equation 4.5, with a particle size correction expression from Wen and Dutta (1979) given in equations 4.6a and 4.6b, as discussed in the literature review. A minor additional calculation is also used for the oxygen gasification reaction as the pressure order is assumed to vary with temperature according to equation 4.7, as derived from the work of Ranish and Walker (1993), while for the other gasification reactions the order is assumed to be constant.

$$z = \frac{X_{CarbonMonoxide}}{X_{CarbonDioxide}} = 50.\, P_{Oxygen}^{-0.21}.e^{\frac{-3000}{T}} \qquad \text{Equation (4.5)}$$

$$Z = \frac{2.z+2}{z+2} \quad \text{when d} < 50\,\mu\text{m} \qquad \text{Equation (4.6a)}$$

$$Z = \frac{(2.z+2) - z\left(d - 50\times10^{-6}\right)}{950\times10^{-6}(z+2)} \quad \text{when d} > 50\,\mu\text{m} \qquad \text{Equation (4.6b)}$$

$$n = 4.544\times10^{-0.001T} \qquad \text{Equation (4.7)}$$

The reaction rates are determined according to methods established for combustion with definition of three different reaction regimes, boundary layer diffusion regime, chemical reactivity regime and pore diffusion hindered regime. While the techniques for different reactions are the same the regime is dependant on the partial pressure, diffusion rate and chemical reaction rate of the particular gas, so regimes can vary for different reactions at any given time. The regime is determined on the basis of particle effectiveness factor, a complex iterative calculation that determines the proportion of the internal pore area of the particle that is being used for reaction. Calculation of this is described in the pore diffusion hindered regime section below.

Chemical reactivities for coal chars are distinct for individual chars, with a wide variation in reactivities reported in the literature. For most coals little is known about the gasification reactivities and therefore a correlation method was developed based on

that used by Fung and Kim (1984). The data of these authors was extended by using data from Hippo and Walker (1975), Linares-Solano *et al.* (1979) and Tomita *et al.* (1977). This method is based upon an observed trend in char reactivity with the carbon content of the raw coal, as defined in equation 4.8. Using this correlation method the reactivity of a given coal char can be estimated if the reactivity of a char formed under similar conditions from a different coal is known. The reactivity coefficient, r, used in the equation has varying value dependant on the heterogeneous reaction under consideration and values determined from the data of the aforementioned authors are given in table 4.1. In equation 4.8 the variables subscripted 'base' refer to a coal of known reactivity. This method only affects the pre-exponential terms of rate expressions with the activation energy considered as equal for all coals.

$$k_0 = k_{0,base}.e^{\left(r\left(C_{base}-C\right)\right)} \qquad \text{Equation (4.8)}$$

Table 4.1 : Reactivity correlation coefficients for gasification reactions

Reactant Gas	**Dimensionless Reactivity Coefficient, r**
Oxygen	0.13560
Carbon Dioxide	0.15077
Steam	0.17872
Hydrogen	0.07378

The base values for reactivities used in the model were determined using char samples from experimental gasification runs in the CSIRO gasifier described in a later section. A full description of the methods used for determining the reactivities is given in appendix A along with a summary of the experimental data. Samples of char for three runs under different conditions for coal E were used to determine reactivities of the chars to oxygen, carbon dioxide and steam under atmospheric pressure conditions. A small fixed bed reactor was used for reaction rate determination at low temperatures, 400 to 900°C, in the chemically limited regime. Intrinsic reactivities were then calculated by measuring the total surface area of the char with respect to nitrogen adsorption. The intrinsic reactivities of the three char samples to the same gas were found to be approximately equal. On examination of the reactivities it was decided that the oxygen reactivity values found for char E, while being

consistent in the experimental determination, were not suitable for extrapolation to high temperatures due to the activation energy being significantly lower than commonly found in the literature. The general correlation of oxygen reactivities for numerous chars determined by Smith (1978) was used in its place. Also, as hydrogen reactivity was not determined experimentally, the reactivity of a similar rank coal char determined by Tomita *et al.* (1977) was used for the hydrogen reactivity. The experimentally and literature reactivities are given in table 4.2, along with the assumed pressure orders discussed previously.

Table 4.2: Intrinsic reactivity data for coal E char and other literature values

Reactant Gas	**Pre-exponential Constant, k_0 ($kg.m^{-2}.s^{-1}.atm^{-n}$)**	**Pressure Order 'n'**	**Activation Energy, E (kJ/kmol)**
Oxygen (Coal E char)	0.002852	Eq. 39	93.2
Oxygen (Smith (1978))	300.0	Eq. 39	179.4
Carbon Dioxide (Coal E char)	689.0	0.25	243.3
Steam (Coal E char)	2.745	0.2	205.8
Hydrogen (Tomita *et al.* (1977))	0.00002848	1.0	150.0

(i) Boundary Layer Diffusion Regime

The boundary layer diffusion regime is applicable at high temperatures where the rate of diffusion of reactant gas to the particle is less than the rate of chemical reaction on the external surface of the particles. This leads to complete consumption of reactant at the surface, so that the overall reaction rate is equivalent to the diffusion rate from the bulk gas to the particle. In this case the reaction rate for a specific gas is given by equation 4.9, based on Field (1969), where Φ is the molar ratio of gaseous products to gaseous reactants and T_m is the average of the particle and gas temperatures.

$$Rate = K_{diff} . A_{external} . P_{Reactant} = \frac{24 \Phi D_{Reactant,mix}}{dRT_m} . A_{external} . P_{Reactant} \qquad \text{Equation (4.9)}$$

(ii) Chemical Reactivity Regime

The chemical reactivity regime defines the opposite of the boundary layer diffusion regime as it refers to the situation where diffusion is rapid compared to the chemical reaction rate, usually occurring at lower temperatures. Effectively this allows diffusion of reactant gas completely into the pores of the particle and reaction is at the chemical reaction rate for the bulk partial pressure of reactant gas over the total particle area. The expression used for this calculation is given in equation 4.10, where n is the reaction order with respect to the reactant gas and the terms k_0 and E define the chemical reactivity of a particular char.

$$Rate = K_{chem}.A_{total} = k_0.\exp(\frac{-E}{RT}).P^n_{Reactant}.A_{total} \qquad \text{Equation (4.10)}$$

(iii) Pore Diffusion Hindered Regime

The pore diffusion hindered regime is probably the most important regime in gasification as it describes the condition where only a fraction of the pore area of a particle is effectively used for reaction, common for the carbon dioxide and steam gasification reactions. Critical to the determination of reaction rate in these circumstances is the particle effectiveness factor, η, which is the reaction rate as a fraction of the rate that would be found if the reaction was in the chemical reactivity regime. Calculation of the effectiveness factor is complex and requires an iterative procedure as an analytical solution to the equations for mass transfer into the pores does not exist. An equation for a generalised Thiele modulus, ϕ, equation 4.11, was derived from published work to allow for calculation of the modulus for reactions with any reaction order, a change in gas volume with reaction and the a non-unity molar ratio of reactant to carbon removed. This is largely based on the results of Kehoe and Aris (1973), although rearranged into a suitable form for carbon gasification reactions. A full description of the equation development and the literature sources is given in the literature review. This generalised Thiele modulus is used directly to obtain the particle effectiveness factor and rate, according to equations 4.12 and 4.13, but the procedure should be iterated as the surface pressure of reactant gas is affected by the determined rate. The rate determined is approximate due to simplifications made in the calculations, however the error

is relatively minor compared with those caused by a limited knowledge of structural changes in char particles during gasification.

$$\phi = \frac{d}{6}\sqrt{\frac{A_{total}\sigma_a a k_{chem} P_{Reactant,s}^{n-1} R_{gas} T_p (n+1)(1+\alpha\sqrt{b})}{2\alpha M_c \Phi_e}} \qquad \text{Equation (4.11)}$$

$$\eta = \frac{3}{\phi}\left(\frac{1}{\tanh(\phi)} - \frac{1}{\phi}\right) \qquad \text{Equation (4.12)}$$

$$Rate = \eta . A_{total} . k_{chem} . P_{Reactant,s}^{n} \qquad \text{Equation (4.13)}$$

4.2.3 Particle Structure

The structure of char particles is important in determining the reaction area for the various heterogeneous reactions. Conceptually the particle structure will vary markedly from that of the coal when devolatilisation occurs. It has been observed that devolatilisation can cause swelling of the particles and produce large increases in the porosity and surface area of the particles. Particle structure is difficult to model accurately as numerous different structural variations can occur and it is known that even particles from the same coal can exhibit massive variations in char morphology. Numerous models have been proposed for char particle structure, ranging from simple single pore size models to complex random tree network models. The modelling method used does not attempt to model the particles accurately, as that is probably impossible, but uses the standard single average pore size technique of Wheeler (1951). This method has been used by numerous previous researchers and work by Smith and Tyler (1972) has shown that that the model results are relevant and approximately the same as those of a more complex bimodal pore size distribution model. To use the Wheeler model the total surface area and porosity of the particle must be known and these were estimated using correlations for the variation of coal porosity in different pore size regimes with the carbon content of the coal, sourced from data in van Krevelan (1993). From the initial values for raw coal particles the single average pore diameter, length and number of pores are calculated using equations 4.14 to 4.16. After the initial calculation of these characteristics they are then modified with reaction according to the effects that those reactions have on the particles. As the coal particle devolatilises swelling occurs to a degree dependant upon the crucible swell number for the coal, and this results in increases in the pore diameter and length to compensate for the increase in particle porosity.

Also the loss of volatiles increases the particle porosity and this is taken to lead to generation of new pores so that the number of pores increases rather than the pore dimensions.

$$d_{pore} = \frac{2.\pi.d^2.\varepsilon.(1-\varepsilon).RF}{3.A_{total}} \qquad \text{Equation (4.14)}$$

$$l_{pore} = \frac{d.\sqrt{2}}{6} \qquad \text{Equation (4.15)}$$

$$n_{pores} = \frac{4.\varepsilon.d^2}{\sqrt{2}.d_{pore}^2} \qquad \text{Equation (4.16)}$$

The heterogeneous reactions affect particle structure differently in different regimes. For reactions occurring in the diffusion limited regime mass loss will be exclusively from the outer particle surface, so will result in particle size reduction. In either the chemically limited or pore diffusion hindered regimes mass loss will be both from the internal pore surface and the external particle surface so that the particle pores will increase in diameter and the particle will shrink.

4.2.4 Homogeneous Reactions

A number of homogeneous, or gas phase reactions, are possible in gasifiers and two series of reactions have been defined earlier as combustion or equilibrium reactions. The combustion reactions can only occur in the presence of oxygen and as a simplification have been considered in the model to occur instantaneous due to their rapid rate. In the absence of oxygen a more complex process occurs with a multiple reaction equilibrium existing in the gas phase. Reactions that appear to be most significant in this equilibrium have been previously defined and an iterative procedure is used to solve for the most likely equilibrium composition. The gas phase equilibrium composition is important in determining the efficiency of the gasifier, as the calorific value of the product gas can be used as a performance indicator. Calculation of gas equilibrium composition and temperature are performed by solution of gas equilibrium, at a given temperature, then correction of the temperature, caused by changes in gas enthalpy when composition changes, with iteration until a stable solution is found. While this method would normally be unwieldy due excessive calculation it is extremely rapid and simple when starting estimates of gas composition and temperature are accurate which, as previously described, is the case when using small

incremental slices with little change between slices. Solution for equilibrium can be performed by two major methods, either minimisation of the Gibbs free energy of the gas mixture or solution on the basis of independant equilibrium expressions for each method. Both of these methods resulted in complex solution algorithms with associated lengthy computations and risk of instability arising during solution. For these reasons a simplified method was designed to specifically fit reactions 11 to 14 for the conditions expected in entrained flow gasification. To this end a number of assumptions were made, namely that the concentrations of methane, sulfur dioxide, hyrogen sulfide and carbon oxide sulfide are low relative to steam, carbon monoxide, carbon dioxide and hydrogen, and that the equilibrium of reaction 11 is dominant, and more important than, the equilbria of the other reactions. By assuming that the concentrations of some species are low it can be taken that changes in these concentrations with adjustment of equilibrium will not affect concentrations of the high concentration species. The method of solution for equilibrium commences with definition of the equilibrium constants for the temperature and, in some cases, pressure conditions of the gas. Equilibrium concentrations for reaction 11 are calculated analytically with the assumption of independence from the other reactions and then the concentration of methane is adjusted to give equilibrium for reaction 12, with associated changes in other gas concentrations as required. Solution for equilibrium in reactions 13 and 14 is carried out simultaneously by determining the required ratios of hydrogen sulfide to sulfur dioxide and hydrogen sulfide to carbon oxide sulfide from the equilibrium constants for the reactions. As an accuracy test the gas composition is checked against each equilbrium constant and, if errors are significant, the process will be iterated. Due to the small changes in concentrations and temperatures between model slices iteration is generally not required. The gas temperature is then adjusted to account for compositional changes, if the temperature change is significant the equilibrium calculations are repeated until negligible change occurs. This method was found to markedly enhance model speed, compared to using a complex method that solved the set of non-linear expressions simultaneously, with no identifiable loss of accuracy of predicted gas composition.

4.2.5 Heat Transfer

Heat transfer is one of the more complex elements of modelling in gasifiers. Modelling of heat transfer involves simultaneous determination of the temperatures of numerous particles, the gas and the gasifier wall at the gas-wall interface. Two forms of heat transfer are considered in the model, convective and radiative (conductive is neglected as insignificant) and these are considered to be independent. Convective transfer is treated in a relatively simple manner by using established correlations for heat transfer flux from gas to solid spheres, equation 4.17, and from gas to a cylindrical shell, equation 4.18, both from Babcock and Wilcox Company (1978). In figure 4.1 a digrammatic representation of the gasifier divided into slices is shown with the radiative heat transfer processes indicated for a single slice of the gasifier. As shown and commented in the figure it is considered that radiative transfer occurs between all particles and the wall of the gasifier with the gas acting as an emitter and absorber of radiation and the upper and lower boundaries of the slice, which are hypothetical, acting as refractory. The effect of refactory surfaces is to neither emit or absorb but to perfectly reflect any incident radiative energy.

$$h_{g\to p} = Nu.\frac{k_g.\left(T_g - T_p\right)}{d} \qquad \text{Equation (4.17)}$$

$$h_{g\to w} = \left(0.023\frac{\left(\rho_{gas}V_{gas}\right)^{0.8}}{D^{0.2}}\right)\left(\frac{C_{p,gas}^{0.4}k_{gas}^{0.6}}{\mu_{gas}^{0.4}}\right)\left(\frac{T_{gas}}{T_{wall}}\right)^{0.8} \qquad \text{Equation (4.18)}$$

Treatment of radiative transfer is complicated by the high concentrations of carbon dioxide and steam present in some stages of gasification. These gases are known to be radiatively emissive and absorbant, and therefore interfere with radiative exchange between solid surfaces, namely the gasifier walls and the particles. In general methods for calculating heat transfer involving an emissive gas are complex as they can involve numerous cases of transmittance, absorbance and reflectance between any of the materials in the gasifier and, to be entirely correct, the gas will only absorb and emit radiation in specific wavelengths. As a first simplification the gas will be considered 'grey' so that a single emissivity will be taken to apply across all wavelengths. The grey gas emissivity and absorbtivities are calculated using arrays of coefficients for both carbon dioxide and steam and a series of algorithms as described in Modest (1993), or other texts as the Leckner method.

Net radiative transfer between any combination of particles, wall and gas is calculated according to the Long Furnace Model of Hottel and Sarofim (1967). This model assumes that the furnace length is far greater than its diameter and therefore net radiative flux along the furnace is negligible, and also that there is no temperature gradient across the furnace. Although this is an approximation (energy will always flow from a hot region to a cooler region along the furnace) the effect is a dramatic reduction in the complexity of the heat transfer problem. The error in this approximation was found to be minimal by forcing more realistic smoothed gas temperature profiles on the model and comparing overall carbon conversion predictions. Using the Long Furnace Model it can be taken that each disk of the gasifier modelled is bounded above and below by a perfectly reflective refractory so that all radiation emitted inside the disk must be absorbed by either particles, wall or gas that is also inside the disk. This is equivalent to, in reality, the disk receiving as much radiant energy from the disks above and below as it emits to them, a reasonable assumption if there is negligible change in properties between disks and one also used in the models of Vamvuka *et al.* (1995), Govind and Shah (1984), and Wen and Chaung (1979). The heat transfer problem now becomes one of division of radiant energy between the different components inside the disk, which can be performed using equations 4.19 to 4.24 where n is the number of different particles and the A terms refer to the external surface area of objects in the disk under consideration. The general meaning of these equations is that a solid will receive a proportion of radiant energy emitted from any surface, including itself, and the gas. This proportion is related to the transfer area of the solid relative to the total transfer area of all solids in the disk, with a correction for absorbance by the gas. For all solids and the gas radiant emissions are calculated according to the standard grey body Stefan-Boltzmann law.

$$q_{w\to p} = \sum_{i=1}^{n}\left[\frac{A_w \sigma \varepsilon_w T_w^4 \left(1-\alpha_{g\leftarrow w}\right) A_{p,i}}{\sum_{j=1}^{n}\left(A_{p,j}\right) + A_w}\right] \qquad \text{Equation (4.19)}$$

$$q_{p\to w} = \sum_{i=1}^{n}\left[\frac{A_{p,i} \varepsilon_{p,i} \sigma T_{p,i}^4 \left(1-\alpha_{g\leftarrow p,i}\right) A_w}{\sum_{j=1}^{n}\left(A_{p,j}\right) + A_w}\right] \qquad \text{Equation (4.20)}$$

$$q_{g\to p,i} = \varepsilon_g \sigma T_g^4 A_{p,i} \qquad \text{Equation (4.21)}$$

$$q_{\Sigma p \to p_i} = \sum_{i=1}^{n}\sum_{j=1}^{n}\left[\frac{A_{p,i}\varepsilon_{p,i}\sigma T_{p,i}^4\left(1-\alpha_{g\leftarrow p_i}\right)A_{p,j}}{\sum_{k=1}^{n}\left(A_{p,k}\right)+A_w}\right] \qquad \text{Equation (4.22)}$$

$$q_{g\to w} = \varepsilon_q \sigma T_g^4 A_w \qquad \text{Equation (4.23)}$$

$$q_{w\to w} = \frac{A_w^2\varepsilon_w\sigma\left(1-\alpha_{g\leftarrow w}\right)T_w^4}{\sum_{i=1}^{n}\left(A_{p,i}\right)+A_w} \qquad \text{Equation (4.24)}$$

Theoretically the wall temperature at the wall-gas interface in a gasifier can be calculated by performing a heat balance through the wall to some body of known temperature, such as the water in a waterwall cooling system, and utilising the methods described above for the heat flux to the wall. However, in practice the available data on gasifiers does not extend to accurate measurements of refractory thickness and thermal transfer properties. In this case the wall temperature must be input using either measured values, an estimated value or a calculated value from slag properties, assuming slagging of the wall occurs. In appendix B a model for calculating the thickness of the slag layer and surface slag temperature in the case of slag coated gasifier walls is discussed and tested. This method requires input of slag viscosity and other properties and is only applicable when the gasifier walls are fully coated with fluid slag. In the gasifiers used for the comparison of model predictions with experimental results little data is available on slag properties and, in the case of the CSIRO gasifier in particular, slagging of the walls was not always noted so other sources of wall temperatures must be found.

4.2.6 Physical Properties

Gasification modelling poses some difficulties in physical property modelling, in particular for gases. It is common in combustion modelling to use constant values for many properties as the gas composition does not have dramatic changes in a furnace, however this is not true for gasification. While data for gases at high temperatures are available, the most common expressions for generating data are limited to temperatures up to 1800 to 2000K and the polynomial expressions used can diverge rapidly outside the range for which they were developed. A number of new expressions were derived for the model and fitted to published experimental data for individual gases. The advantages of these

expressions is that they cover a larger temperature, and in some cases pressure, range and are based upon logarithmic terms, so do not diverge if the range of available data is exceeded.

4.2.7 Modifications for High Pressures

In general the relationships used in the model are capable of modelling at high pressures. For example all gas property data used was reviewed for the effect of pressure and where necessary the expressions used in the model allow for pressures other than atmospheric. This is evident in the gas emissivity calculation, which allows for a partial gas pressure and path length product of up to 10 atm.m with a modification to ensure reasonable estimates above this in large gasifiers.

4.3 Solution Methods and Algorithms

The general method for model calculations is indicated as a flowchart in figure 4.5. After defining the properties of inputs to the gasifier and the gasifier conditions the model performs a loop that provides predictions of gas and particle properties in each of the slices of the gasifier by starting at the inlet end of the gasifier and progressing incrementally along. The basis of the increments is time with distance along the gasifier being determined by volume flowrates. In each loop performed the effects of gasification reactions on particle conversion, structure and temperature for each distinct particle size are performed for a given slice. Resultant changes in gas composition and temperature are calculated and followed by analysis of changes in temperature for the particles and gas due to radiative and convective heat transfer. This completes the calculations for the subject slice and if further slices remain in the gasifier a step time is calculated to determine the size of the next slice and the process repeated. Internal each of the steps mentioned may contain other loops for solution of equations, to check for solution stability or simply to repeat calculations for a number of different particle sizes.

Most model components require only simple iterative solution techniques, such as successive approximation where a new estimate for a variable is back-calculated from the error from the previous estimate with damping of the change in values to reduce the risk of divergence. This method is used successfully for calculation of the heterogeneous reaction rate with complex pore effectiveness factor, and typically only one to two iterations are

required when the reaction rate calculated for the previous slice of the gasifier is used as a starting estimate. Similarly rapid convergence was found for determination of gas temperature and composition when solving for gas phase equilibrium, which is discussed below. In both these cases the critical factor is correct selection of the step time for each slice of the gasifier. If a suitable step time is used the differences in characteristics between two adjacent slices will be small but significant, and predictable. A number of algorithms were trialled in early versions of the model in order to produce an accurate and adaptable method. Traditional methods, such as Newton-Raphson, proved unstable due to the rapid change from initially accelerating reaction rates, with oxidation of volatiles and solid carbon raising gas and solid temperatures, to rapidly deccelerating reaction rates, caused by the high concentrations of steam and carbon dioxide reacting endothermically with solid carbon, and finally very slow reaction rates, due to lower temperatures and low concentrations of reactant gases. As a result a specialised, empirical algorithm was developed for the model and is described below. The expressions were obtained by 'inverting' the model and calculating the length of time per step of conversion, rather than the conversion per length of time. Due to the difficulties in calculations for this model a number of simplifications had to be made, namely to the kinetics and heat transfer models employed and in that only one particle size can be used. From results predicted with this model a adapable algorithm for estimating the trend in conversion with time was construction, a version of which is given in equations 4.25 to 4.27 in terms of step time predictions and illustrated in figure 4.6. Two adjustable parameters are used in the algorithm with the first, $\Delta X_{i,specified}$, giving a suggested value for the size of the slice in terms of change in conversion and the second, *f*(Coal), is given in table 4.3 and allows for variation in size of slice dependent on the degree of conversion in the previous slice and the coal used. This requires input of a factor dependant on the coal used, g(Coal), which accounts for variations due to coal properties in the early stages of gasification, mostly affected by the quantity of volatile released from the coal, and generally ranges from 0.5 for a low volatile coal to 2.5 for a very high volatile coal.

$$\Delta t_i = \frac{\Delta t_{i-1}}{\Delta X_{i-1}} . \Delta X_{i,specified} \cdot \frac{\alpha}{f(X, Coal)} . \log_{10}(\beta X) \qquad \text{Equation (4.25)}$$

$$\alpha = 0.5208 . \log_{10}\left(6.232 \Delta X_{i,specified}\right) . \frac{P_{total}}{30} \qquad \text{Equation (4.26)}$$

$$\beta = 10^{\left(\frac{8.671}{\Delta X_{i,specified}^{0.8277}} - \frac{7.641}{\Delta X_{i,specified}^{0.5078}}\right)}$$ Equation (4.27)

Table 4.3: Values of adjustment factor for step time calculation

X (%Conversion)	*f(X, Coal)* (Adjustment Function)
Less than 0.5	40.*g(Coal)*
0.5 to 2.0	20.*g(Coal)*
2.0 to 5.0	10.*g(Coal)*
5.0 to 10.0	7.*g(Coal)*
10.0 to 20.0	4.*g(Coal)*
20.0 to 30.0	2.*g(Coal)*
30.0 to 40.0	1
Greater than 40.0	0.25

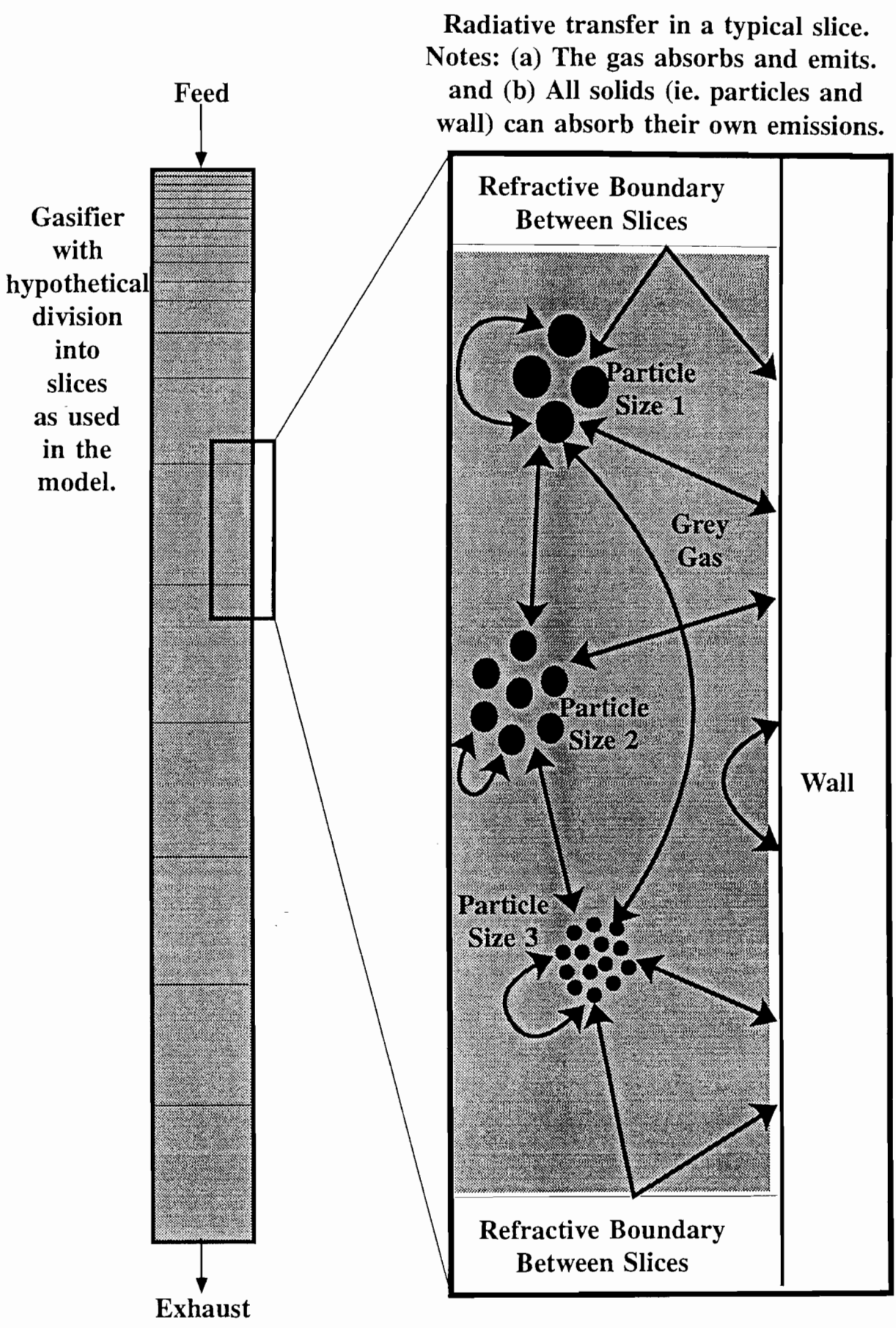

Figure 4.1: Modelled gasifier showing radiative heat transfer model for a typical slice of the gasifier.

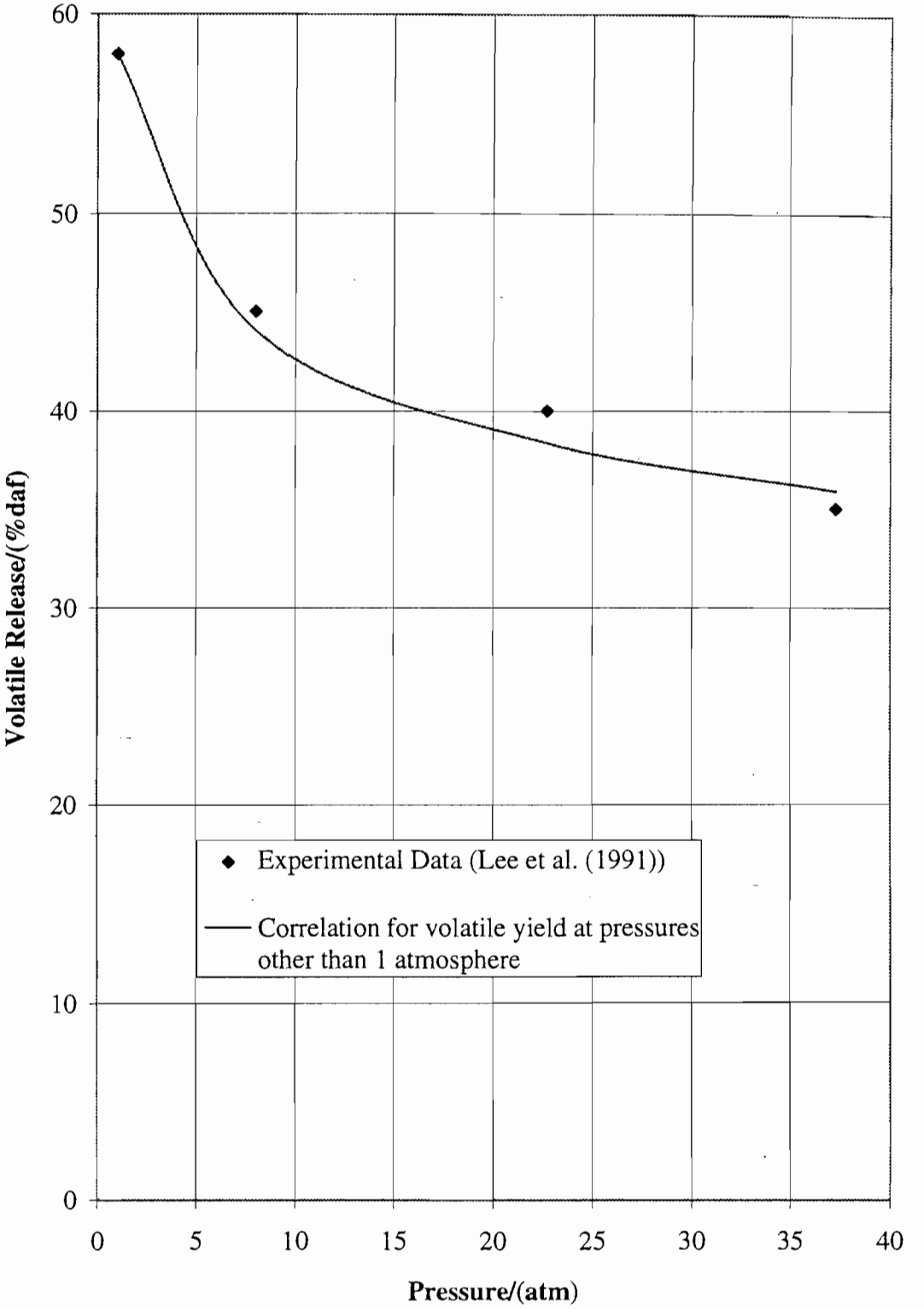

Figure 4.2: Volatile release data for a single coal at various pressures with derived correlation (Lee et al. (1991)).

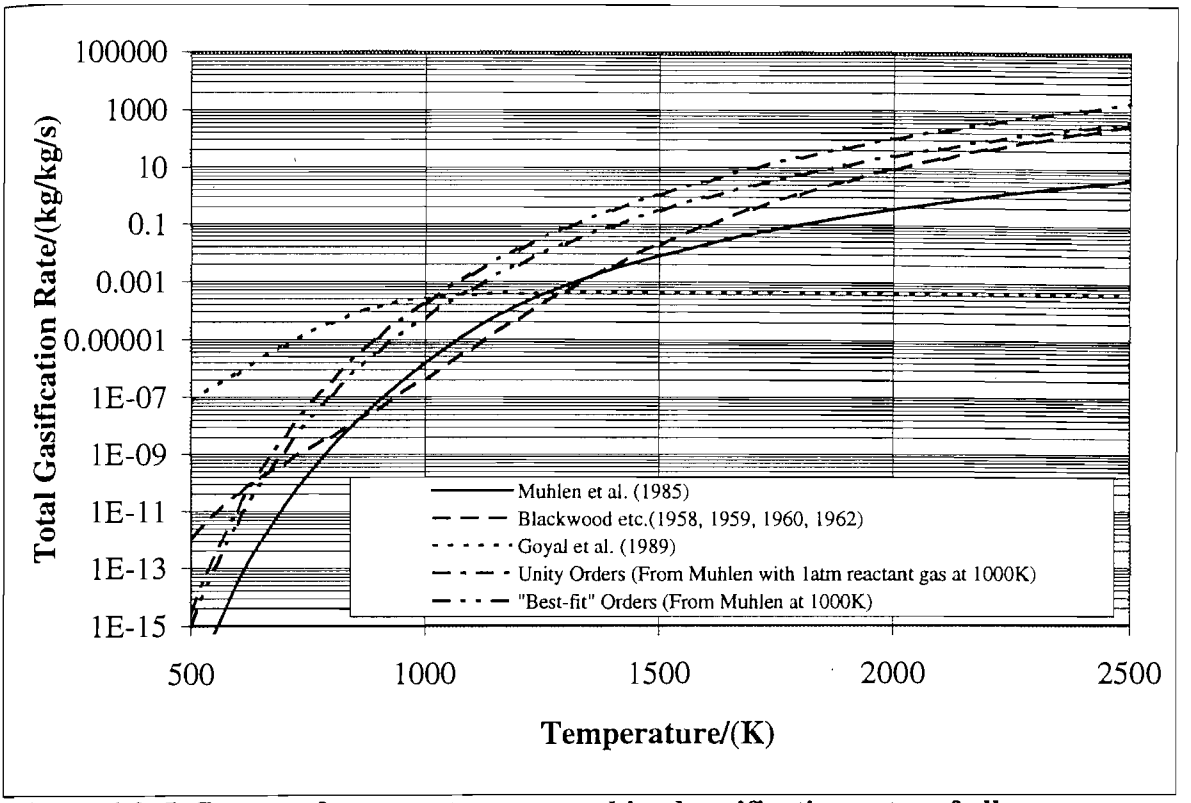

Figure 4.3: Influence of temperature on combined gasification rates of all heterogeneous reactions at 20 atmospheres total pressure (40% carbon dioxide, 27% carbon monoxide, 13% hydrogen, 20% steam)

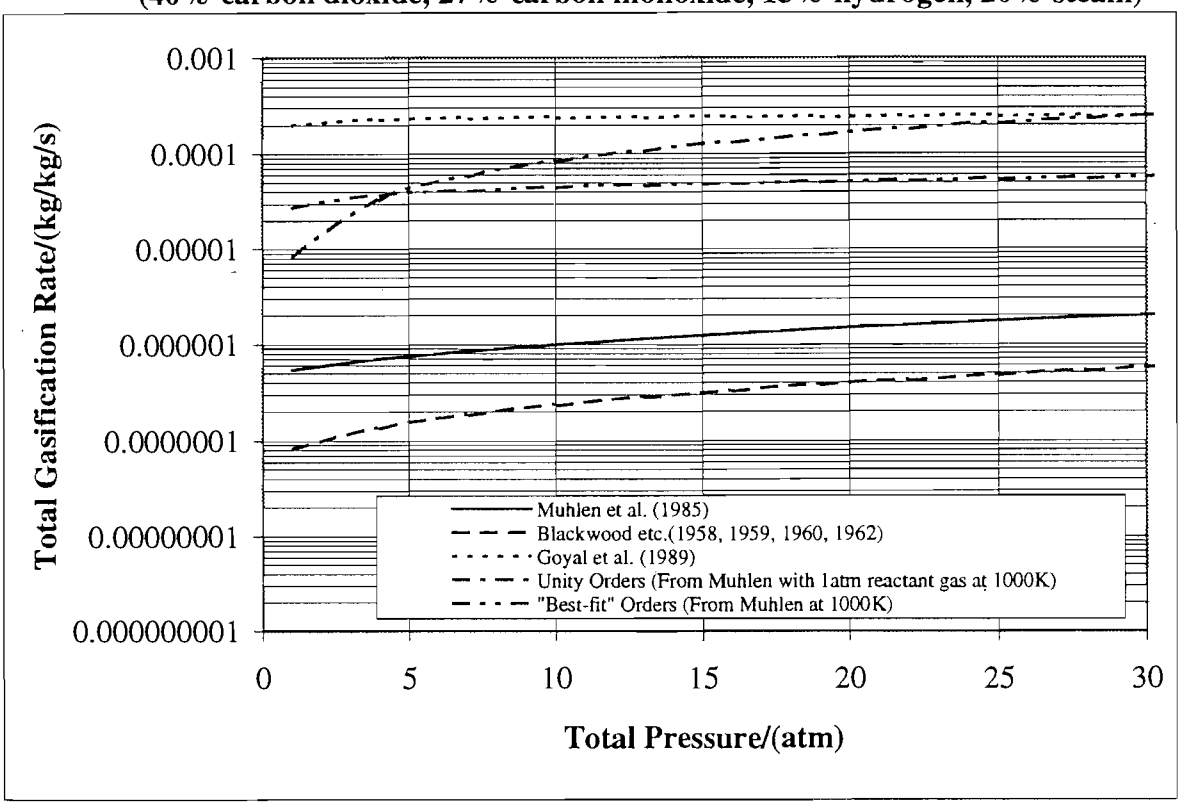

Figure 4.4: Influence of pressure on combined gasification rates of all heterogeneous reactions at 1000K particle temperature (40% carbon dioxide, 27% carbon monoxide, 13% hydrogen, 20% steam)

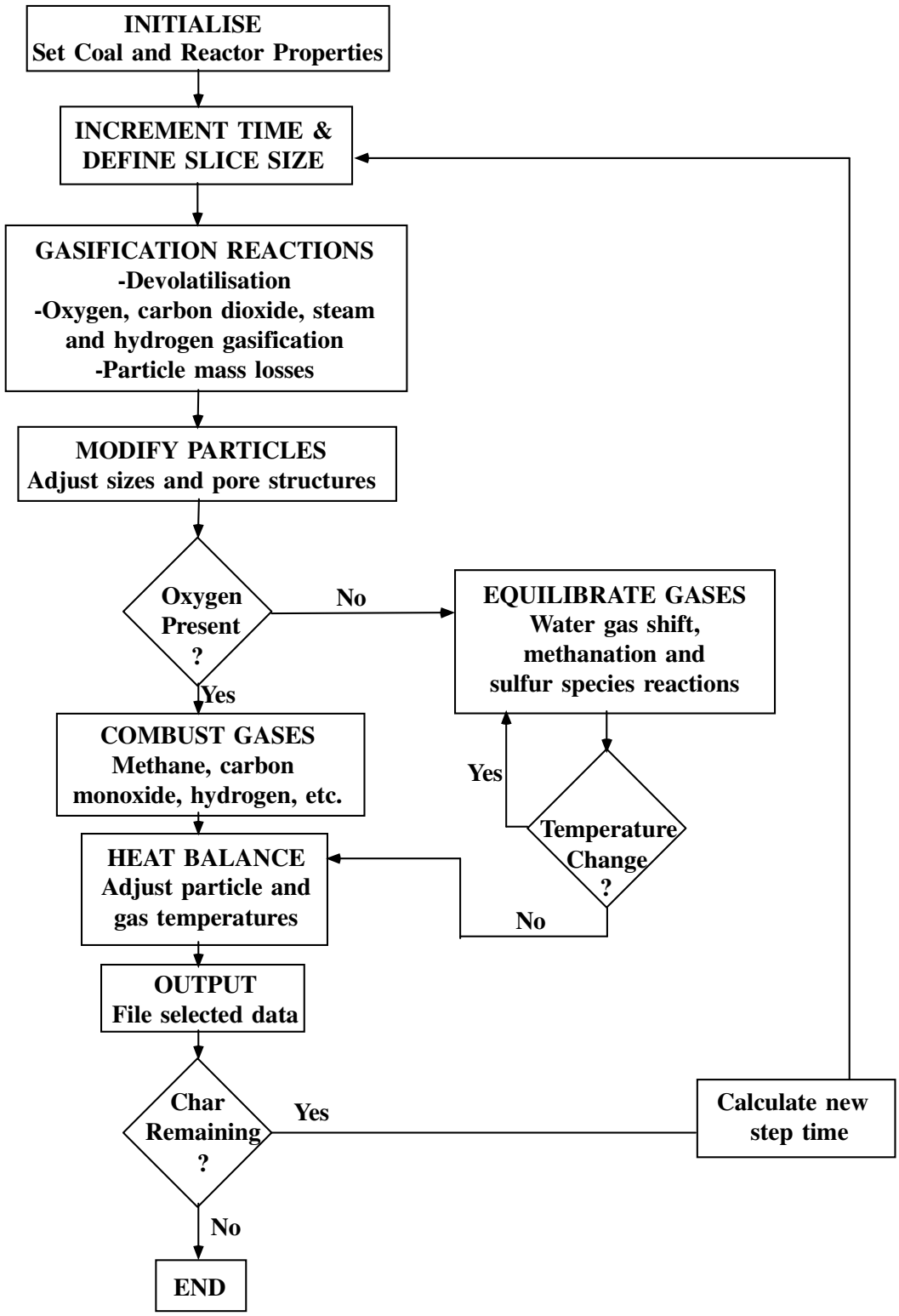

Figure 4.5: Flowchart illustrating model structure

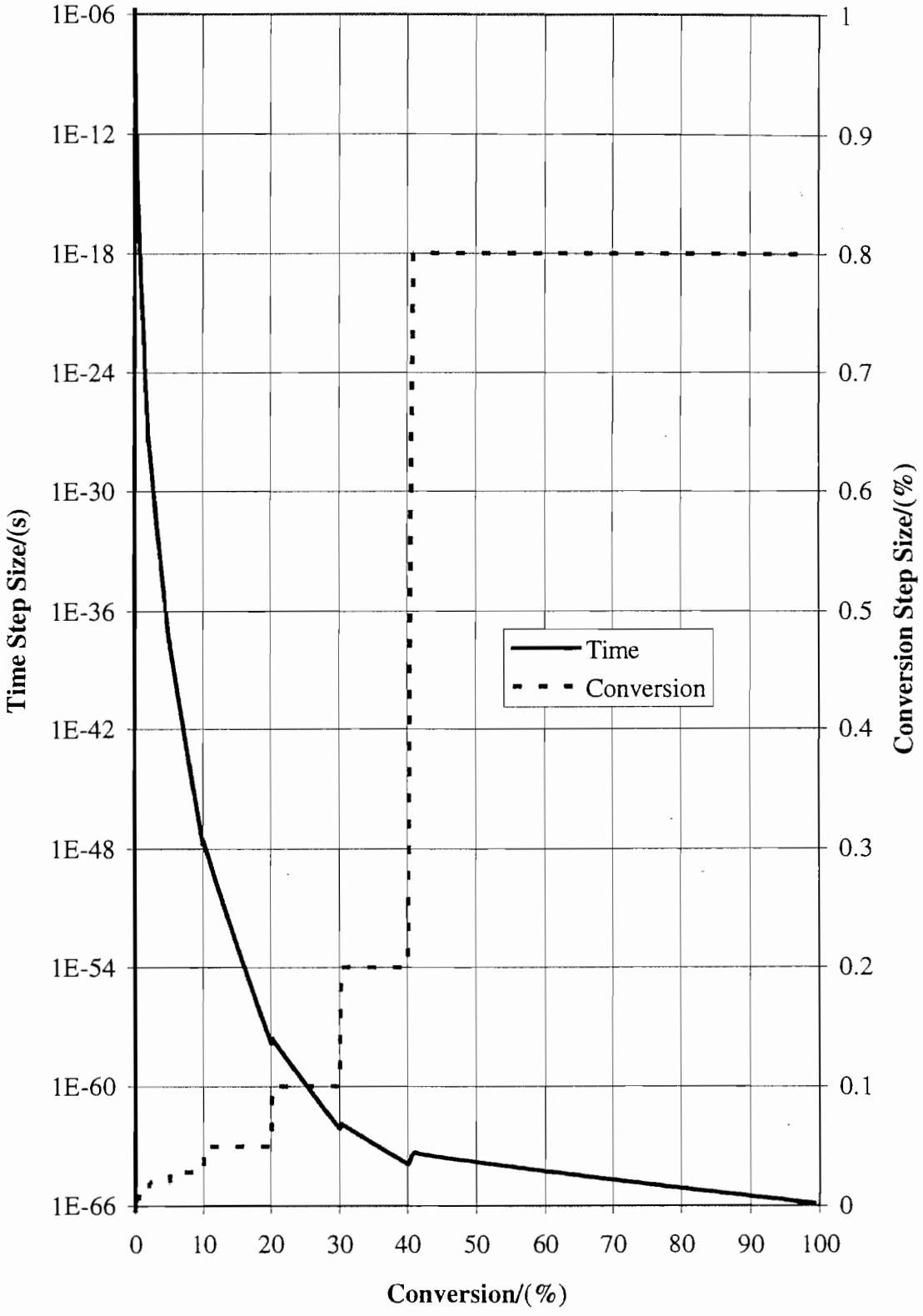

Figure 4.6: Calculated step sizes from solution algorithm for total pressure of 30 atmospheres and coal factor of 1.

5. SENSITIVITY ANALYSIS

5.1 Definition of Sensitivity

The sensitivity of a model refers to the variation in the predictions made by the model when a change occurs to a component of the model or if an input to the model is altered. This can be an indication of possible errors in the model, effects of errors in the values of inputs to the model, or may identify of components of the model that may be simplified with minimal loss of accuracy. In gasification the predictions made by a model can be a number of different variables including carbon converted, cold gas efficiency, gas composition and exit gas temperature. Generally commercial-scale gasifier performance is described by the cold gas efficiency, which is defined as the calorific value of the product gas at 25°C relative to the calorific value of the feed coal, however this can be significantly affected by errors in flow rates and gas composition measurements in smaller gasifiers, as will be discussed in the analysis of experimental results. A more reliable indication of performance for small gasifiers is the carbon conversion, which is determined by either the total carbon in the product gas or in the solid residues relative to the carbon input in the coal. Measurement of this is not affected by temperature effects on gas composition but can still be affected by errors in the feed and exit gas flow rates.

5.2 Variables Considered

Coal gasification performance is influenced by a large number of variables relating to common analyses for coal, estimated coal particle properties, feed rates, temperatures and pressure. In table 5.1 a set of base values is defined for a number of variables with the values relating to a specific experimental run in the CSIRO gasifier (Coal E, Stoichiometry 106%). A sketch of this gasifier is given in the model validation section, along with a full discussion of the experimental method and results. The experimental carbon conversion for this run was 75.7%, calculated from the average product gas composition for the run, compared with a predicted carbon conversion of 79.3%.

Table 5.1: Coal properties and gasifier conditions used for base values.

Variable	Base Value	Units
Bulk Coal Properties		
Coal Moisture	2.6	(% ar)
Coal Ash	9.6	(% ad)
Coal Volatile Matter	31.2	(% ad)
Quantity of Volatiles Released (Estimated)	48.47	(% daf coal)
Coal Carbon Content	84.8	(% daf)
Coal Particle Size 1	48.4 / 5.4 (Diameter/Weight%)	µm / wt%
Coal Particle Size 2	70.5 / 12.9 (Diameter/Weight%)	µm / wt%
Coal Particle Size 3	93.5 / 25.7 (Diameter/Weight%)	µm / wt%
Coal Particle Size 4	123.7 / 29.4 (Diameter/Weight%)	µm / wt%
Coal Particle Size 5	169.4 / 21.0 (Diameter/Weight%)	µm / wt%
Coal Particle Size 6	270.6 / 6.0 (Diameter/Weight%)	µm / wt%
Calculated Particle Properties		
Initial Pore Surface Area	2627.2	m^2/kg
Porosity of Coal	0.0627	m^3/m^3
Volumetric Swell of Coal on Heating	63.677	(%)
Heterogeneous Reaction Rate Terms		
Oxygen Pre-exponential Constant	300.0	$kg/m^2/s/atm^{0.8}$
Carbon Dioxide Pre-exponential Constant	689.0445	$kg/m^2/s/atm^{0.25}$
Steam Pre-exponential Constant	2.7454	$kg/m^2/s/atm^{0.2}$
Hydrogen Pre-exponential Constant	0.00002848	$kg/m^2/s/atm^{1.0}$
Oxygen Activation Energy	179397.6	kJ/kmol
Carbon Dioxide Activation Energy	243299.7	kJ/kmol
Steam Activation Energy	205799.7	kJ/kmol
Hydrogen Activation Energy	150000.0	kJ/kmol
Oxygen Pressure Order	0.8	-
Carbon Dioxide Pressure Order	0.25	-
Steam Pressure Order	0.2	-
Hydrogen Pressure Order	1.0	-
Gasifier Conditions		
Ratio of Oxygen to Feed Coal	1.0539	kg/kg (ar) coal
Ratio of Carbon Dioxide to Feed Coal	1.3919	kg/kg (ar) coal
Ratio of Steam to Feed Coal	0.7565	kg/kg (ar) coal
Ratio of Nitrogen to Feed Coal	1.8334	kg/kg (ar) coal
Coal Feed Rate	0.000528	kg (ar) coal/s
Gas Input Temperature	1754.6	K
Coal-Gas Mixture Input Temperature	1713.1	K
Wall Temperature, T_1(220mm into gasifier)	1541.7	K
Wall Temperature, T_2(400mm into gasifier)	1502.1	K
Wall Temperature, T_3(580mm into gasifier)	1365.2	K
Wall Temperature, T_4(760mm into gasifier)	1185.7	K
Wall Temperature, T_5(940mm into gasifier)	1125.9	K
Wall Temperature, T_6(1120mm into gasifier)	1004.4	K
Wall Temperature, T_7(1620mm into gasifier)	1232.5	K
Wall Temperature, T_8(1820mm into gasifier)	1179.9	K
Wall Temperature, T_9(2020mm into gasifier)	1264.7	K
Wall Temperature, T_{10}(2220mm into gasifier)	1141.0	K
Wall Temperature, T_{11}(2420mm into gasifier)	1004.0	K
Gasification Pressure	1.0	atm
Gasifier Diameter	0.1	m
Gasifier Length (coal feed location to quench sprays)	2.5	m

5.3 Basic Sensitivity Analysis

This section will deal with changes in the values of input data used in the model and the resultant effects on carbon conversion predictions. Variations in the values of variables will generally exceed any reasonable error range for the input and the predictions will identify the importance of each individual variable in determining the predictions. The resultant graphs indicating the changes in predicted carbon conversion for changing variable value will be used in a later section to identify variables which are likely to provide significant errors in the model predictions, but can also be used as a predictive tool to estimate optimum characteristics of the feed coal to produce higher levels of carbon conversion.

5.3.1 Sensitivity to Coal Properties

The effects of varying coal analysis properties independently are show graphically in figure 5.1, where the base value of each property is approximately the value at which the carbon conversion is 80%. The predictions were calculated assuming everything besides the subject variable remains as given in table 5.1. This means that when, for example, the ash content is changed that the total coal feed rate is unchanged, and therefore the coal feed rate on a dry, ash free basis is decreased. As this also changes the quantity of carbon entering the gasifier the carbon conversion predictions shown in the figure have been adjusted to a percentage of the carbon fed to the gasifier in the base case. The ash and moisture contents of the coal have obvious detrimental effects on predicted carbon conversion, partly as less carbon was fed when the ash or moisture occupies more of the coal mass but also a due to the increased energy demand in heating the ash or in vapourising the moisture. This results in lower temperatures in the gasifier and a reduction in reaction rates leading to reduced carbon conversion. An increase in volatile release has an opposite effect, as the increased quantity of volatiles results in higher initial flame temperatures, as well as increasing the quantity of carbon transferred rapidly to the gas phase with the volatiles. The influence of coal carbon content on carbon conversion is less readily explained as it gives a more complex pattern of carbon conversion, with an indicated maximum at approximately 78% carbon content (daf basis). This arises due to conflicting influences of less carbon being

available to be converted at low carbon content and a reduction in char reactivity at high coal carbon content. The curve is influenced by the limit of 100% carbon conversion relative to the amount of carbon in the adjusted model prediction, reached for carbon content less than 60%, as in this case higher coal flow rate could lead to higher quantities of carbon being converted.

As an additional comment for this section it should be noted that the results presented can be affected by the basis assumed for the sensitivity analysis. In this case the coal feed to the gasifier was kept constant using an 'as received' basis however in other cases a basis of 'dry, ash free' may be more applicable. This would allow for adjusting the coal flow to account for a change in the quantity of convertible material when changing the coal feed. The basis of 'as received' coal was used as this is more commonly reported in experimental results as it is a measured variable, while 'dry, ash free' quantities involve calculations that introduce possible error sources from coal analysis figures. It is also more common in the experimental gasification methods discussed in the model validation section for the coal feed rate to be kept constant, on an 'as received' basis, for all coals used in the same experimental gasifier regardless of differences in the coal properties.

5.3.2 Sensitivity to Particle Properties

A range of particle properties was varied independently to show the sensitivity of model predictions with the results presented in figure 5.2. The properties considered were porosity, initial surface area, volumetric swell and the particle sizes and the values were varied over the range of a quarter to four times the base value. All the properties have significant effects on carbon conversion, in the cases of porosity, initial surface area and volumetric swell because of their effects on pore structure and therefore pore diffusion resistances, and for the particle sizes because of changes in the diffusion rate of gases to the particle surface. Of the properties tested increased volumetric swell and initial surface area have positive effects on carbon conversion, while increasing porosity and particle size have detrimental effects. Of these, initial surface area and particle size have predictable effect, as increasing surface area allows for more rapid heterogeneous reactions and increasing particle size results in greater reactant

gas diffusion resistances in the boundary layer and within the particles. The influence of particle porosity is more complex but can be interpreted as a high porosity leading to a slowed rate of increase in pore surface area with particle conversion. This arises as increasing porosity in the particle model without changing the internal surface areas of particles results in large pore diameters. While these allow for easy diffusion of reactant gases into the particles, with resultant high effectiveness factors, the internal surface area increases slowly with conversion compared to small pores and therefore results in generally slower heterogeneous reaction rates. The volumetric swell affects predictions oppositely, although an increase in porosity occurs with increasing volumetric swell. This happens as volumetric swell is taken to occur during devolatilisation of the particle and is considered to affect the number of pores in the particle as well as the porosity. By increasing the number of pores in the particle the pore surface area is also increased and thus increased reaction rates result in higher carbon conversion. The increase in pore numbers during devolatilisation is an assumption used to account for the increase in internal particle surface area commonly noted when coal is devolatilised to char.

5.3.3 Sensitivity to Gas and Coal Feeds

The sensitivity of carbon conversion to the quantity of various gases fed with the coal, and the coal feed itself, is examined in figure 5.3, with the quantity of the gases and coal fed indicated as ratios relative to the base coal feed on a mass basis. Of the gas feed rates, oxygen has the greatest impact with increasing oxygen increasing carbon conversion, excepting at low feed rates where it has negligible effect. Carbon dioxide has the least effect with only slight decrease in carbon conversion with increased input. Increasing steam and nitrogen flows result in almost identical decreases in carbon conversion with increasing input. The obvious correlation is that the exothermic nature of oxygen reacting either with gases or carbon results in higher temperatures and accelerated reaction rates while the other gases have a slightly inhibiting effect due to increasing the mass of gas or through endothermic reactions. A higher oxygen input also results in higher quantities of the other major reactants, carbon dioxide and steam, at later stages in the gasifier. Nitrogen, having no reactions in the model, can only decrease the carbon conversion by acting as a diluent and therefore

reducing temperatures in the gasifier. As a similar effect is noted with steam it appears that the steam has negligible effect on carbon conversion, while the lesser effect of carbon dioxide indicates that it is appreciably involved in carbon conversion but still acts to greater extent as a diluent. The rate of coal feed relative to the base value indicates that reduced carbon conversion is predicted with increasing coal feed. The obvious explanation for this is that the stoichiometry, relative to all reactant gases, in the gasifier increases as the coal feed decreases and this is responsible for a greater proportion of the carbon being converted.

5.3.4 Significance of Reaction Kinetics

The influence of values selected for terms in the pressure order reaction rate equations are shown in figures 5.4 to 5.6. The three variables used in each pressure order expression were a pre-exponential constant, an activation energy and a pressure order. In the ranges of the figures it is indicated that the carbon dioxide gasification reaction is most likely to influence the predicted carbon conversion. Increase in the carbon dioxide gasification pre-exponential constant increases the predicted carbon conversion, as does decreases in either carbon dioxide gasification activation energy or pressure order. An increase of the pre-exponential constant for the steam gasification reaction also increases predicted carbon conversion as does decrease of the activation energy for the steam and hydrogen gasification reactions. Oxygen gasification is more rapid than the other reactions and only a slight increase in carbon conversion is predicted when its activation energy is reduced. The general conclusion from these predictions is that carbon dioxide gasification is the dominant rate determining step of the gasification run considered. This is possibly due only to the high quantities of carbon dioxide introduced with the feed relative to the normal feed ratios of gasification, so steam gasification may also have significant impact under the usual conditions of gasification.

5.3.5 Sensitivity to Gasifier Conditions

Changes in the input values of temperatures of gasifier wall and feeds, gasification pressure and gasifier dimensions can affect the predicted carbon conversion for the gasifier, as indicated in figures 5.7 to 5.10. In figure 5.7 the gasifier

wall temperature is shown to dramatically influence carbon conversion predictions while inlet gas and particle temperatures were less significant. In this case the temperatures at all points along the gasifier were adjusted from their base values simultaneously while in figure 5.8 the temperatures at individual points along the gasifier were varied independently. This figure shows that the wall temperatures in the initial stages of the gasifier were most significant, gradually decreasing to negligible significance from 1000mm onwards. This finding is due to the small internal diameter of the gasifier (0.1m) exaggerating heat transfer between gas-particles and wall relative to a larger gasifier. In the initial stages of the gasifier rapid reaction rates are enhanced by high wall temperatures causing a reduction in heat losses from the gas and particles then, with further progress along the gasifier, the slower endothermic gasification reactions reduce temperatures until reaction rates slow and the wall temperatures become less significant. The influence of pressure on the predicted carbon conversion is shown in figure 5.9, with one curve showing the effect of increasing pressure with no change in coal feed rate and the other that of increasing coal feed proportionally to pressure. The curve with no change in coal feed indicates a rapid increase in carbon conversion with increasing pressure up to 5 atmospheres, followed by a gradual increase at higher pressures until the maximum of 100% carbon conversion is reached. This can be interpreted as due, in large part, to an increase in residence time in the gasifier with increasing pressure. For the curve that shows coal feed increasing with pressure carbon conversion gradually increases with pressure regardless of the particle residence time in the gasifier remaining unchanged, assuming the same gas temperatures occur. In this case it is possible to fit an approximate pressure order, encompassing devolatilisation and all other gasification reactions, of 0.08. This suggests a relatively small pressure influence on gasification performance, resulting from the prediction of decreased volatile yield at high pressures counteracting the predicted increase in heterogeneous reaction rates. Variations in gasifier dimensions and the effects of these on carbon conversion are shown in figure 5.10. The influence of diameter on predictions is far greater than that of length, with a small increase in diameter increasing the carbon conversion significantly while only a dramatic shortening of the gasifier resulting in a decrease in carbon conversion. The effect of diameter can be largely attributed to the change in residence time associated

with the variation in cross sectional area but may also affect heat transfer between the gas-particle mixture and the wall. Length has less significance as the majority of the carbon conversion occurs early in the gasifier, so the gasifier length must be reduced to less than 1m in order to affect carbon conversion significantly.

5.3.6 Conclusions from Basic Sensitivity Analysis

The study of model sensitivity to changes in the values used for input variables identified that numerous variables have significant impact on the predictions made by the model. While some of these variables were expected to cause variations in the predictions, for example coal analysis results and reactivity data, it is surprising that a high degree of sensitivity was found for so many variables. This leads to the conclusion that for accurate modelling of entrained flow coal gasification few assumptions can be made and all of the sub-models considered in this model are required.

Some of the findings of the sensitivity analysis are of a trivial nature but provide some support for casual expectations. Of this nature are the predictions for variations in coal analysis inputs which suggest that low ash, low moisture and high volatile yield coals will give optimum performance in gasifiers. Similarly small particle sizes and high coal surface areas enhance gasification, as do high carbon dioxide and steam gasification reactivities. Less obvious is the relationship of coal carbon content and predicted carbon conversion as it affected by competing influences in varying the amount of carbon available and the char reactivity, via the reactivity correlation. Also the influence of porosity on predictions is variable as initial coal porosity affects the initial pore structure defined for the particles and later porosity changes with particle swelling can have contrasting effects on the predictions. Variations in gas feed rates also indicate the contrast in influences on predictions as increased rates lead to a dilution effect which reduces residence time in the gasifier and therefore predicted carbon conversion drops but, if the gas is reactive, increased reaction rates can partial offset this, or in the case of oxygen overcome the effect entirely. Coal feed rate increases lead to predicted decreases in carbon conversion, in a manner resembling the decrease with decreasing oxygen stoichiometry. Other obviously sensitive variables are those associated with the wall temperatures in the gasifier where an increase in temperature,

particularly near the feed end of the gasifier, results in a noticeable increase in predicted carbon conversion. Similarly, increasing the gasification pressure and gasifier diameter increase the predicted carbon conversion.

A particular finding of the model sensitivity study is worthy of further mention due to a disparity with previously published models. The model was shown to be sensitive to all aspects associated with the internal structure of coal particles that were considered, namely porosity, total surface area and volumetric swelling. This finding suggests that the use of shrinking sphere reaction models for the heterogeneous reactions is unsuitable, as these neglect the internal structure of the particles. In all previously published entrained flow gasification models discussed in the literature review section shrinking sphere reaction models were assumed.

5.4 Determination of Model Reliability

The previous discussion considered the sensitivity of model predictions to changes over wide ranges for many input variables. The figures presented showed that many variables either measured experimentally, assumed from experimental results or collected from literature sources. It is the purpose of this section to quantify the error ranges for these inputs and determine the resultant variations in predictions. This will establish if predictions made by the model are reliable or if the poor quality of particular input data can result in unreliable predictions. To simplify the discussion of model reliability the analysis will be divided into three sections dealing separately with model inputs concerned with coal physical properties, coal reactivity parameters and gasification conditions.

5.4.1 Coal Physical Property Data

Inputs to the model concerning the physical properties of the coal feed can be grouped as either data from the coal analysis or properties estimated from literature. The variations in predictions of carbon conversion for possible errors in the input coal property data of the model are given in Table 5.2 in order of decreasing variation in carbon conversion prediction. Methods used to determine the size of the error ranges and the resultant variations in predictions are discussed below.

Table 5.2: Effect of coal property inputs on carbon conversion predictions

Property Description	**Error Estimate**	**Change in Predicted Carbon Conversion**
Quantity of Volatiles Released	+30% daf coal	+19%
Total Surface Area of coal	÷1.5	-6%
Size of Coal Particles	x1.05	-4%
Volumetric Swell of coal on heating	÷1.5	-4%
Porosity of coal	÷1.5	-3%
Moisture Content of coal	+1.5% ar coal	-0.9%
Carbon Content of coal	+0.6% daf coal	+0.7%
Ash Content of coal	+0.25% ad coal	-0.2%

(a) Coal Analysis Data

Coal analysis data, such as ash, moisture and carbon content, must be determined for each coal that is modelled and therefore the errors in input data are relatively minor. The size of the errors for each of these properties is determined by the analytical technique used and, assuming all analysis is to a similar standard, the error ranges are given by the relevant parts of AS1038 (1986, 1989, 1992). The expected maximum errors given by the Australian standards are given in table 5.2 with the resultant predicted variations in carbon conversion. The moisture content of coal is measured with the least accuracy, due to variations in moisture with atmospheric conditions, and provides the largest change in carbon conversion prediction, 0.9%, arising from the coal analysis inputs. Likely errors in the input values of carbon and ash content of the coal result in changes in predicted carbon conversion of 0.7% and 0.2%, respectively. Considered with the rest of the analysis of error sources these changes are relatively insignificant and suggest that the accuracy of standard coal analysis results is adequate for the model.

(b) Estimated Coal Properties

Error ranges for estimated coal properties are less easily determined but in most cases can be estimated by the accuracy indicated by the various correlations. An exception is in the selection of particle sizes which was performed by using the median particle size for arbitrarily defined weight fractions from experimental particle sizing analysis. This analysis produced approximately 32 size fractions for the coals used in the CSIRO experimental program and the results from this condensed into 6 size fractions for use in the model. (The CSIRO and other experimental gasifier programs will be discussed in detail in a subsequent section but in most cases between 4 and 6 particle size fractions were reported for the feed coals.) To examine the impact of selection of particle sizes on model predictions a modified version of the model was prepared to allow for input of up to 32 particle sizes, the entire size distribution determined experimentally. Carbon conversion predictions when 6, 20 and 32 particle sizes were used in the model are shown in figure 5.11 as functions of distance along the gasifier. Trends in carbon conversion with distance are similar for each set of model predictions with the maximum variation between carbon conversion predictions at the exit being 4%. This equates to an input error in particle size of a factor of 1.05 from figure 5.2. If less than 6 particle sizes are used in the model it is likely that considerable error in the predictions could occur.

The ranges of error for other estimated coal properties are estimated from various figures presented in the literature review to show the fit of correlations to experimental data. Volatile release for the coal was estimated using the correlation of Neoh and Gannon (1984), which was compared with experimental results in figure 2.2. While this correlation fits the experimental results of the authors well, it is less accurate for results from different apparatus and errors in yield of up to 30% (daf coal) are common. As entrained flow gasifiers differ from the experimental apparatus of Neoh and Gannon (1984) significantly, the possible error in the estimated volatile yield will be taken as 30% (daf coal) with a resultant change in predicted carbon conversion of 19%, from figure 5.1. It should be noted that the comparison of model predictions with results from the CSIRO experimental gasifier to be discussed in a later section suggest that the errors in volatile yield predictions for a range of eight Australian coals were

markedly less than this error estimate, indicating that conditions in the gasifier may be comparable to those used in the experimental study of Neoh and Gannon (1984). The possible error in volatile yield previously defined applies to atmospheric pressure predictions but at higher pressures additional error sources arise due to the extrapolation of the correlation using the data of Lee *et al.* (1991). As these results were for only one coal it is not possible to estimate the errors involved in applying these results to other coals. Volumetric swelling of coal particles upon heating was estimated from figure 2.4 and using the laboratory analysis swelling number of the coal (Huleatt (1991)). For coals of swelling number less than 5, an overprediction of up to 25% volumetric swell was common when comparing the correlation curve with the experimental data of Field (1970) obtained under high temperature combustion conditions. This corresponds to a factor of 1.5 change in input value, indicated in figure 5.2 to produce a change in predicted carbon conversion of 4%. Both porosity and total surface area of the feed coal are estimated from figure 2.16, showing the porosity of coals in three pore size ranges as a function of coal carbon content. The maximum variation caused by using simple quadratic correlations for microporosity, mesoporosity and macroporosity as functions of coal carbon content are shown on the figure to be approximately a factor of 1.5 for the total, and each pore size range, porosity. As the pore surface area is calculated from the porosities in each pore size range by assuming that all pores in each range are the average pore size, the possible range of total coal surface area is also taken as a factor of 1.5. The resultant variations in predicted carbon conversion are 6% for the total surface area and 3% for the porosity of the coal.

5.4.2 Coal Reactivity Parameters

In most cases the coal reactivity parameter inputs for the model will be estimated in accordance with correlations determined using the same approach as that of Fung and Kim (1984), excepting the pressure orders that are assumed constant for all coals. This relies upon knowledge of the reactivity of a char formed under similar conditions to those experienced in the gasifier being modelled. In the case of the experimental run used in this study the reactivities used for carbon dioxide and steam gasification were determined experimentally for samples of char from similar

experiments using the same coal, so error sources for these are less than expected typically. The possible errors associated with using reactivities for chars produced under different conditions will be discussed but it is expected that data for at least one similar char will be available for input in most cases. The variations in predicted carbon conversion when values for the reactivity parameters input to the model are varied within the expected error ranges, as determined from the literature, are given in table 5.3 in order of decreasing variation.

Table 5.3: Effect of coal reactivity parameters on carbon conversion predictions

Property Description	**Error Estimate**	**Change in Predicted Carbon Conversion**
Carbon Dioxide Gasification Pressure Order	+0.75	-15%
Carbon Dioxide Gasification Activation Energy	+10MJ/kmol	-13%
Carbon Dioxide Gasification Pre-exponential	÷3	-12%
Steam Gasification Activation Energy	-10MJ/kmol	+7%
Oxygen Gasification Activation Energy	-90MJ/kmol	+4%
Steam Gasification Pre-exponential	x3	+4%
Steam Gasification Pressure Order	+0.8	-1%
Hydrogen Gasification Activation Energy	-10MJ/kmol	+1%
Oxygen Gasification Pre-exponential	x3	~0%
Hydrogen Gasification Pre-exponential	x3	~0%
Oxygen Gasification Pressure Order	-0.3	~0%
Hydrogen Gasification Pressure Order	-0.5	~0%

The variability of char reactivity was indicated in two sets of figures in the literature review. Figures 2.8, 2.10, 2.11 and 2.12 show the range of literature reactivities for chars produced under different conditions for oxygen, carbon dioxide, steam and hydrogen gasification reactions. From these figures the uncertainty in determining reactivity parameters for a given coal char from literature values would be approximately two orders of magnitude for the pre-exponential constant or 10MJ/kmol

(up to 90MJ/kmol for oxygen gasification) for the activation energy. Such large uncertainties for the carbon dioxide and steam gasification rates, in particular, would lead to uncertainty of up to 35% in the carbon conversion prediction (figures 5.4 and 5.5). However, if the uncertainty in reactivity parameters is considered in terms of the error in the reactivity correlations, shown in figure 2.13, a maximum uncertainty of an approximate multiplication factor of three is indicated for the pre-exponential constant. This only applies if reactivity data is available for a char formed under similar conditions to those experienced in the gasifier, which is true in this case. In cases where conditions vary markedly from those which applied to the analysed char the higher errors previously discussed may apply. The reactivity correlation does not consider variations in activation energy between chars so the variability indicated in figures 2.8, 2.10, 2.11 and 2.12 apply to these. The variability of pressure orders was considered previously in the literature review and the range of experimental pressure orders determined indicate likely ranges for each of the gasification reactions. Likely pressure order ranges are 0.5 to 1.0 for oxygen gasification, 0.25 to 1.0 for carbon dioxide gasification, 0.2 to 1.0 for steam gasification and 0.5 to 1.0 for hydrogen gasification. The maximum variations from the orders used in the model can then be estimated.

The variables that provide the most significant error sources in the model predictions are all those associated with the carbon dioxide gasification and the activation energy of the steam gasification reaction. Lesser variations arise from errors in the other parameters used to estimate the steam gasification rate and the activation energies for oxygen and hydrogen gasification. Other parameters in the reaction rate estimation have little significance.

5.4.3 Gasification Conditions

Gasification conditions refer to any factor that affects the conditions experienced by coal in the gasifier. This includes changes in the quantities of gases fed to the gasifier, temperatures of gases and coal particles fed to the gasifier, the pressure in the gasifier, the temperature of the gasifier wall and the dimensions of the gasifier. To a large extent values of these variables will be determined by the accuracy of instruments used to monitor the experimental conditions but, in some cases, values may be affected by unusual experimental conditions such as slag formation on the gasifier wall. Due to the possibility of these types of effects the estimates of possible errors for several of the variables in this section are difficult to justify quantitatively but reasoning for the magnitude of the estimates will be discussed. The variations in carbon conversion predictions for the selected errors in input values are given in table 5.4 for variables associated with gasification conditions.

Table 5.4: Effect of gasification conditions on carbon conversion predictions

Property Description	**Error Estimate**	**Change in Predicted Carbon Conversion**
Overall Gasifier Wall Temperature	-100K	-14%
Wall Temperature At Feed End of Gasifier	-100K	-6%
Gasifier Diameter	-0.01m	-6%
Gasification Pressure	+0.05atm	+1.5%
Ratio of Feed Oxygen to Coal	+0.1kg/kg	+1.3%
Coal Feed Rate Error	+5%	-1.2%
Ratio of Feed Nitrogen to Coal	+0.2kg/kg	-1.2%
Ratio of Feed Steam to Coal	+0.075kg/kg	-0.5%
Ratio of Feed Carbon Dioxide to Coal	+0.14kg/kg	-0.2%
Gasifier Length	+0.25m	+0.1%
Wall Temperature of Second Half of Gasifier	+100K	~0%
Gas Input Temperature	+10K	~0%
Coal-Gas Mixture Input Temperature	+10K	~0%

(a) Gasifier Wall Temperatures

A number of gasifier wall temperatures were used in the model to produce a temperature profile varying with distance along the gasifier. As previously discussed this is required for experimental runs of the type used as the base case in this study as the runs were not sufficiently long to allow the gasifier to reach thermal equilibrium, so wall temperatures cannot be calculated. The temperatures used as wall temperatures were measured using thermocouples buried in the refractory lining the gasifier and the possibility of considerable error between the measured temperature and the actual temperature at the wall surface exists. This is mostly due to the unknown thickness of refractory between the thermocouple and the wall surface, but additional error could exist due to deposition of slag or other fouling of the gasifier wall. Two sets of predictions were made to test the sensitivity of predictions to variations in wall temperature, one where temperatures along the entire length of the gasifier are varied simultaneously and another where individual points along the gasifier, corresponding to thermocouple locations, are varied independently. In both cases the possible errors in wall temperatures input to the model were estimated as up to 100K, although this could not be verified as an accurate estimate. In table 5.4 it is given that an error of this size would lead to a variation in predicted carbon conversion of 14%, if applied along the entire gasifier. Lesser variations are given if the error applies only to certain locations along the gasifier and it is indicated that errors in wall temperature at the feed end of the gasifier are more significant than those further along the gasifier.

(b) Gas and Coal Temperatures

The temperatures of input gases and coal for the gasifier are calculated from experimental temperature measurements. The coal particle temperatures are derived from values measured with thermocouples located in the exhaust from the propane burner used to provide hot gases to the gasifier and also at the point where coal is added to these gases. Using calculated specific heats of the gases and coal, and assuming no reactions have occurred at these points, the coal particle temperatures are calculated from the change in gas temperatures between the two points. This assumes the drop in temperature of the gas is due to heat transfer from gas to particles when mixed

and therefore the coal temperature can be calculated at the entry to the gasifier. This calculation in the model could lead to errors but the input values are directly measured by thermocouples so have been given relatively small possible errors of 10K. Both input temperatures have negligible effect on the predicted carbon conversion.

(c) Gasifier Dimensions

The dimensions of the gasifier itself are subject to a certain degree of error due to various reasons. The diameter of the gasifier is subject to relatively unpredictable changes due to intermittent slagging during gasification runs. An estimate of the possible error in diameter is given as 0.01m, corresponding to an even deposit of 5mm thick slag. Slag pieces of greater than this thickness were recovered from the water quench bath of the CSIRO experimental gasifier, but it is unlikely that this slag deposition uniformly affected the gasifier. In this case the estimate of diameter error is an extreme worst case but further refinement of the error is not possible without more detailed experimental testing to determine the extent of slagging. With this error estimate a significant change of 6% in predicted carbon conversion occurs. The error in gasifier length used in the model has a less significant effect on predicted carbon conversion, although a significant error in input was used. Gasifier length was considered to be from the point of injection of coal into the hot gases to the quenching of gases with water sprays, which is taken to freeze all reactions due to the drop in temperature. Error arises in the imprecise effect of the water sprays which leads to a possible range of the reaction rates freezing. The reason for the small change in carbon conversion predictions within this error range is that the low temperatures and lower reactant gas concentrations in the second half of the gasifier considerable slow reaction rates, so little carbon is converted in this section of the gasifier.

(d) Gas and Coal Feeds

The other variables that can be considered as related to conditions in the gasifier are the inputs of the feed gases and coal. Gas and coal feed rates were determined experimentally as the average flows over the period of the experimental run. Gas flow rates were stable for most runs due to the use of mass flow

controllers and therefore only small errors are expected. The only exception to this is the flow of nitrogen used to convey coal to the gasifier, which was controlled manually using a rotameter indication of flow. Coal flow to the gasifier was less stable with fluctuations of up to 10% in instantaneous flow rate. This effect is common in solid feed systems due to the heterogeneous mixture of gas and solid. Averaging of the coal flow rate over the period of the experimental run reduces the error involved in the model input value. While the coal feed rate is input as this average figure, the gas feed rates are entered in terms of the ratio of feed gas to coal. This method was used to allow variations in feed mixtures to be more readily identified but makes the determination of error estimates more difficult as the error can arise either in the gas or coal feed rate. An error in coal feed rate of 5% (equal to a change of 0.05kg coal per kg base coal in figure 5.3) and errors in ratios of gases to coal of 10% are considered reasonable for the flow rates. These result in changes in carbon conversion predictions of between 0.2 and 1.3% for the various different gases and coal feeds.

(e) Gasifier Pressure

The last of the gasification conditions to be considered is the gasifier pressure. This was not measured experimentally and was taken as a nominal pressure of 1 atmosphere (101.3kPa). It is possible that the pressure in the gasifier varied from atmospheric due to the rapid expansion of gases with reaction but it is assumed that this will involve only minor changes in the pressure. An error of 5% in the assumed pressure results in a change in predicted carbon conversion of 1.5%.

5.4.4 Conclusions of Model Reliability Study

The findings of this section are the most important of the entire study as they define whether it is possible to make meaningful predictions using the model and identifies which input variables should be accurately known to do so. Firstly this requires a definition of ‘meaningful prediction’ and for the purpose of this section it will be assumed that variations in carbon conversion predictions of less than 5% due to error in input values are acceptable. Using this criterion a number of variables have been determined to have sufficient error in their input value to cause unreliability of the model

predictions, these variables are summarised from previous tables in table 5.5. In all cases the errors involved in selection of the variables can be reduced by improving the quality of experimental measurements used to obtain the data, but in some cases modelling techniques could possibly be improved to allow better prediction of the data.

Table 5.5: Summary of variables capable of producing significant variations in predictions

Property Description	**Error Estimate**	**Change in Predicted Carbon Conversion**
Quantity of Volatiles Released	+30% daf coal	+19%
Carbon Dioxide Gasification Pressure Order	+0.75	-15%
Overall Gasifier Wall Temperature	-100K	-14%
Carbon Dioxide Gasification Activation Energy	+10MJ/kmol	-13%
Carbon Dioxide Gasification Pre-exponential	÷3	-12%
Steam Gasification Activation Energy	-10MJ/kmol	+7%
Wall Temperature At Feed End of Gasifier	-100K	-6%
Gasifier Diameter	-0.01m	-6%
Total Surface Area of coal	÷1.5	-6%

Volatile yield estimates used in the model are subject to large possible errors, based on literature results, and can cause large variations in the carbon conversion predictions. It was noted in the discussion that later comparisons of model predictions and experimental results for the CSIRO gasifier at low stoichiometry suggest much smaller errors in the predicted volatile yield and carbon conversion than were identified as possible here. This suggests that the predictive method is accurate for the conditions experienced in entrained flow coal gasification but detailed experimental data is still required to reduce the error estimate.

Various components of the heterogeneous rate expressions are identified in table 5.5 as being potential sources of error in the model predictions. Accuracy in the values of activation energy, pre-exponential constant and pressure order

for the carbon dioxide gasification reaction, and also in the steam gasification activation energy, is required for reliable predictions to be made with the model. The importance of carbon dioxide gasification has been exaggerated in the example used in this sensitivity analysis due to relatively high carbon dioxide concentrations in the feed gas and therefore it is advisable to consider the steam gasification reaction equally significant in general gasification cases. This suggests accurate determination of the terms in the carbon dioxide and steam gasification rate expressions is required to produce accurate model predictions. The error estimates used for these reactions were based on results for chars produced under reproducible conditions, and therefore may actually be smaller than is applicable for entrained flow gasification experiments where conditions of temperature and gas composition are changeable. For this reason it may be necessary to measure the char reactivities of each coal used in the gasification experiments or develop more accurate correlations to estimate these reactivities in order to provide accurate predictions.

It is also indicated in table 5.5 that the values used for wall temperatures in the model can introduce significant errors into the model predictions. As the wall temperatures were measured using thermocouples embedded in the refractory lining of the gasifier errors can vary for different thermocouples depending on the depth into the refractory that the measuring bead is buried to and also the possibility of slag deposition on the wall. Variations in the model were found to be significant if errors in the entered wall temperatures were for the entire gasifier or specifically near the feed end of the gasifier. As these model data were sourced from experimental results the only means of reducing the possible effects of errors on the model is to reduce the errors by more accurate placement of the thermocouples. In cases where it is known that liquid slag coats the gasifier wall it may be possible to make accurate predictions of the wall temperature from knowledge of the slag properties but commonly measured temperatures will be required for accurate model predictions.

Slag deposition on the walls can also be an error source of significance by affecting the actual diameter of the gasifier, and thereby leading to error in the model input value. The error given in table 5.5 for diameter is a worst case value as it affects the entire length of the gasifier, so will considerably reduce the residence

time of gas and particles in the gasifier. The variation in carbon conversion indicated for this error will be reduced for larger diameter gasifiers with the same thickness slag layer as it will have less effect on the residence time of gas and particles in the gasifier. To introduce more accuracy into the model it is possible that the amount of slag deposited on the gasifier wall could be calculated using a fluid dynamics model, and the thickness could be estimated from the fluid properties of the slag, in order to accurately predict the gasifier diameter at all distances along the gasifier. It is also possible that an experimental technique to measure the slag thickness during experiments, but this would be difficult due to the extreme conditions encountered in entrained flow gasification.

The last of the significant error sources given in the table is the input value for the total surface area of the coal. Coal surface area is used in the initial definition of the pore structure of the coal particles in the model. As this structure is kept through devolatilisation and later gasification reactions, with modifications that change the number and size of pores as reactions occur, it is not surprising that the initial surface area of the particles influences the model predictions. This value was estimated from published correlations and the accuracy of predictions could be improved if experimentally measured coal surface areas were used.

In summary of these findings, it is not possible to say that the predictions of the model are reliable in all instances. Where values for input variables are at the limit of the possible error range, either for experimental measurements or from literature correlations, variations in model predictions of up to 19% carbon conversion were determined. In some cases further model development may provide more accurate estimates of conditions in the gasifier, notably for the wall temperature and slag thickness, but in most cases more accurate experimental data is required for the model, such as that concerning reaction kinetics and volatile yields under gasification conditions.

5.5 Conclusions of Sensitivity Analysis

The findings of this sensitivity analysis have already been partially summarised in previous sub-sections and this section will give only a brief overview. In the first portion of this study it was found that the model defined for entrained flow coal gasification showed sensitivity to most of the tested variables over a wide range of

values. Notably sensitivity was indicated to coal analysis properties, coal particle structure, coal reactivity (in particular carbon dioxide and steam gasification), gas and coal feed rates, gasifier wall temperature and gasifier diameter. Also gasifier performance was predicted to increase with increasing pressure at a rate greater than would be expected if considering the associated increase in residence time only. The significance of coal particle structure variables suggests that shrinking sphere particle reaction models, used in previously published entrained flow gasification models, could introduce significant error into the predictions of these models. In the later part of the study it was found that the possible errors in a number input variables for the model could lead to variations in the model predictions. As a limit it was defined that a variation of greater than 5% predicted carbon conversion was significant. Using this criterion it was determined that coal properties, such as volatile yield, carbon dioxide and steam gasification reactivity parameters, and total surface area, were not known accurately enough to ensure reliable predictions from the model. Similarly, gasifier conditions such as the wall temperature and diameter of the gasifier (if affected by slagging) were imprecise and could produce unreliable predictions. For both sets of variables the values used could be made more accurate either by experimental measurement or more accurate prediction methods.

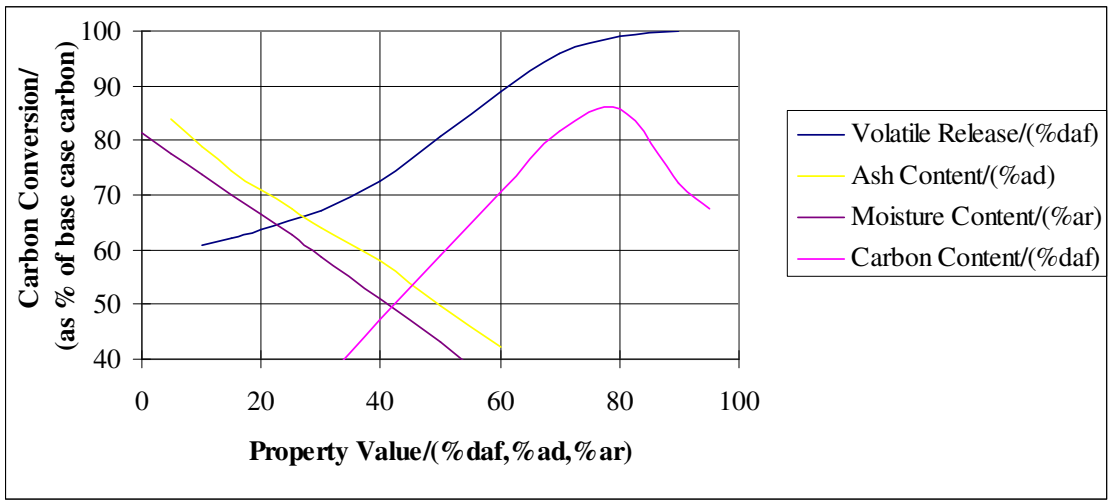

Figure 5.1: Effect of coal property inputs on predicted carbon conversion

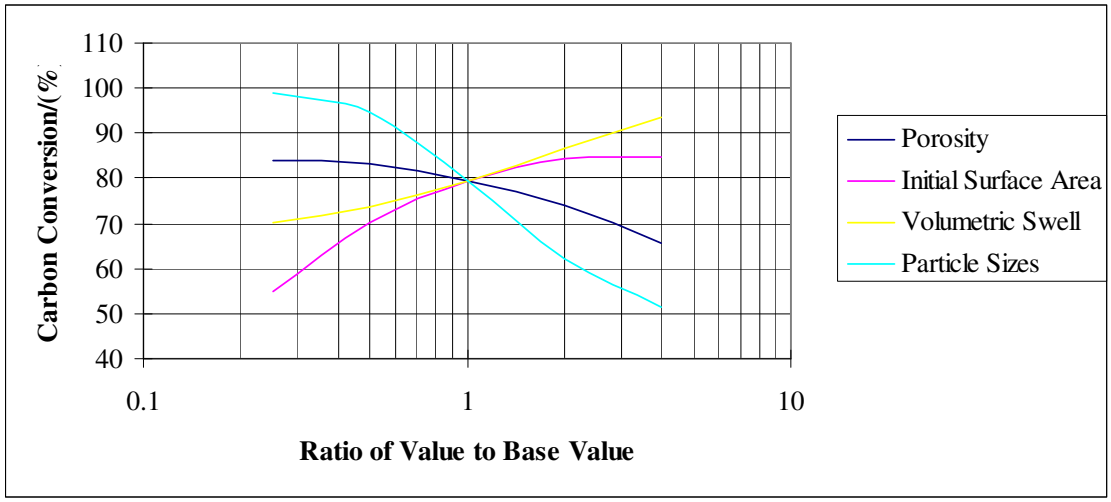

Figure 5.2: Effect of calculated particle properties on predicted carbon conversion

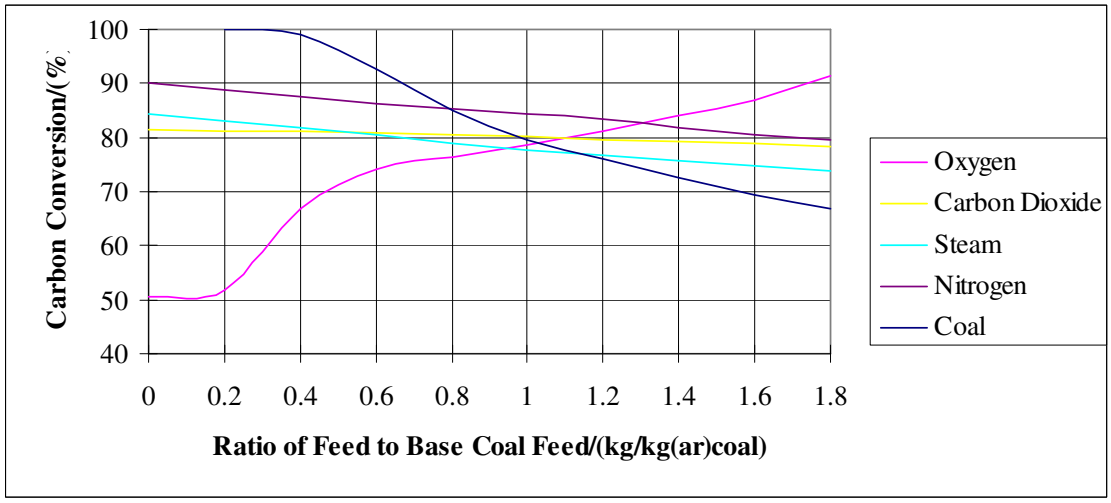

Figure 5.3: Effect of ratio of feeds to base coal input on predicted carbon conversion

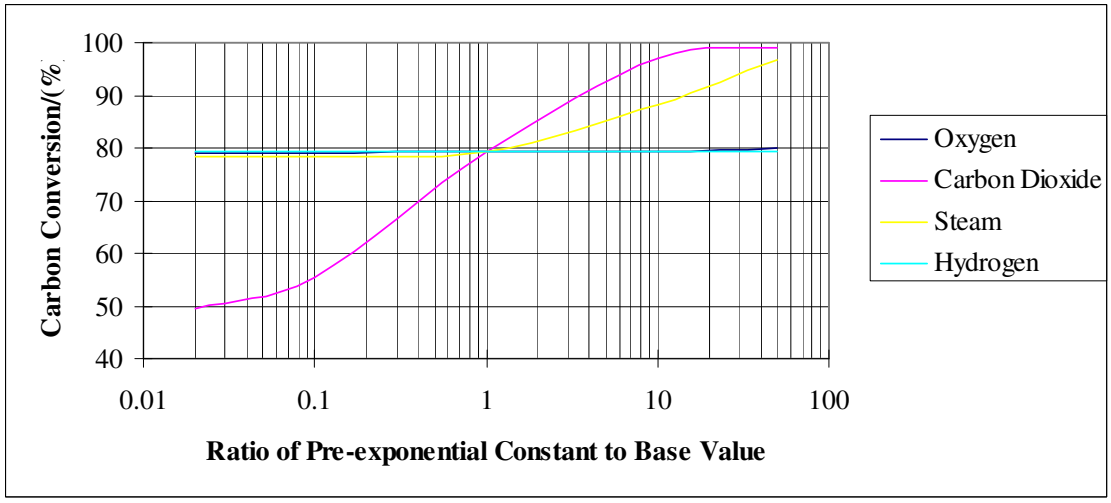

Figure 5.4: Effect of reaction rate pre-exponential constants on predicted carbon conversion

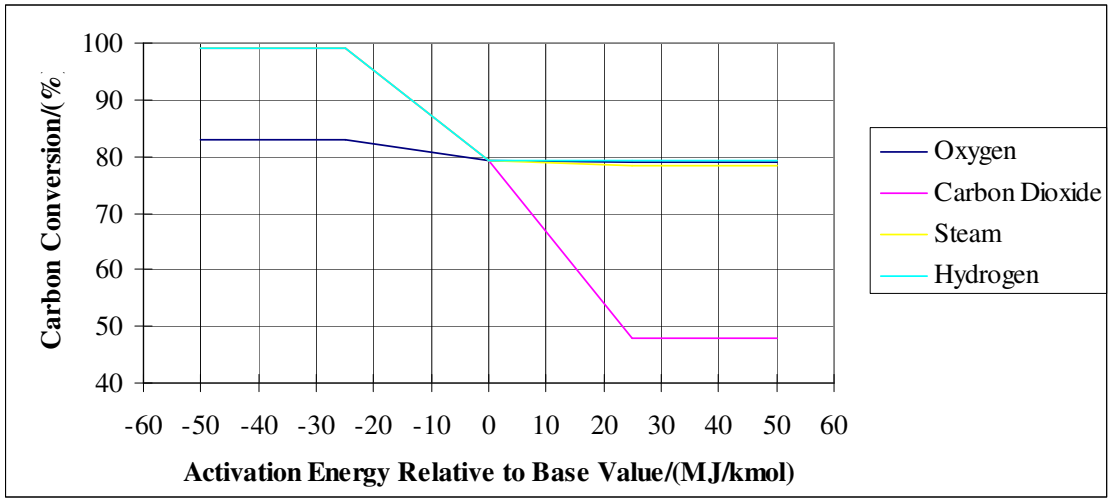

Figure 5.5: Effect of reaction rate activation energies on predicted carbon conversion

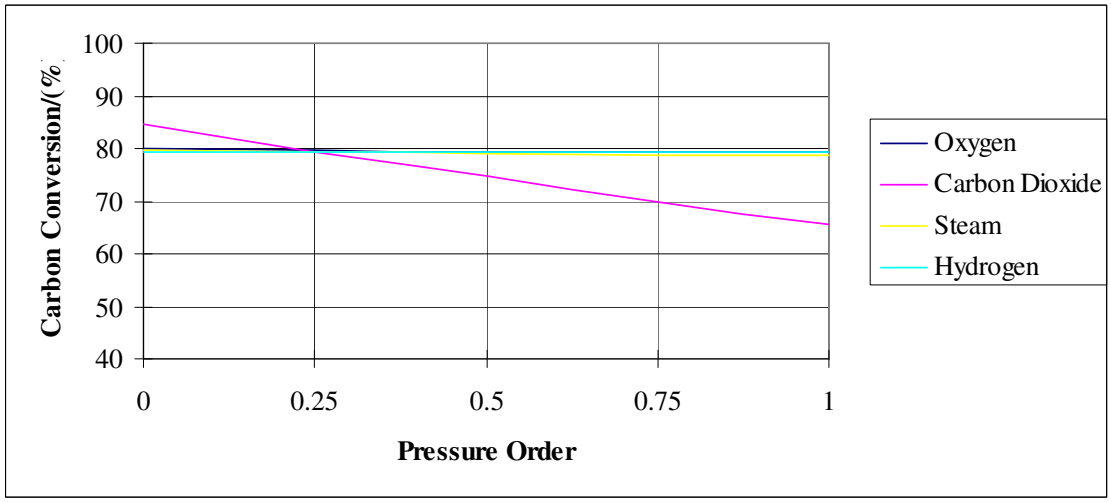

Figure 5.6: Effect of reaction rate pressure orders on predicted carbon conversion

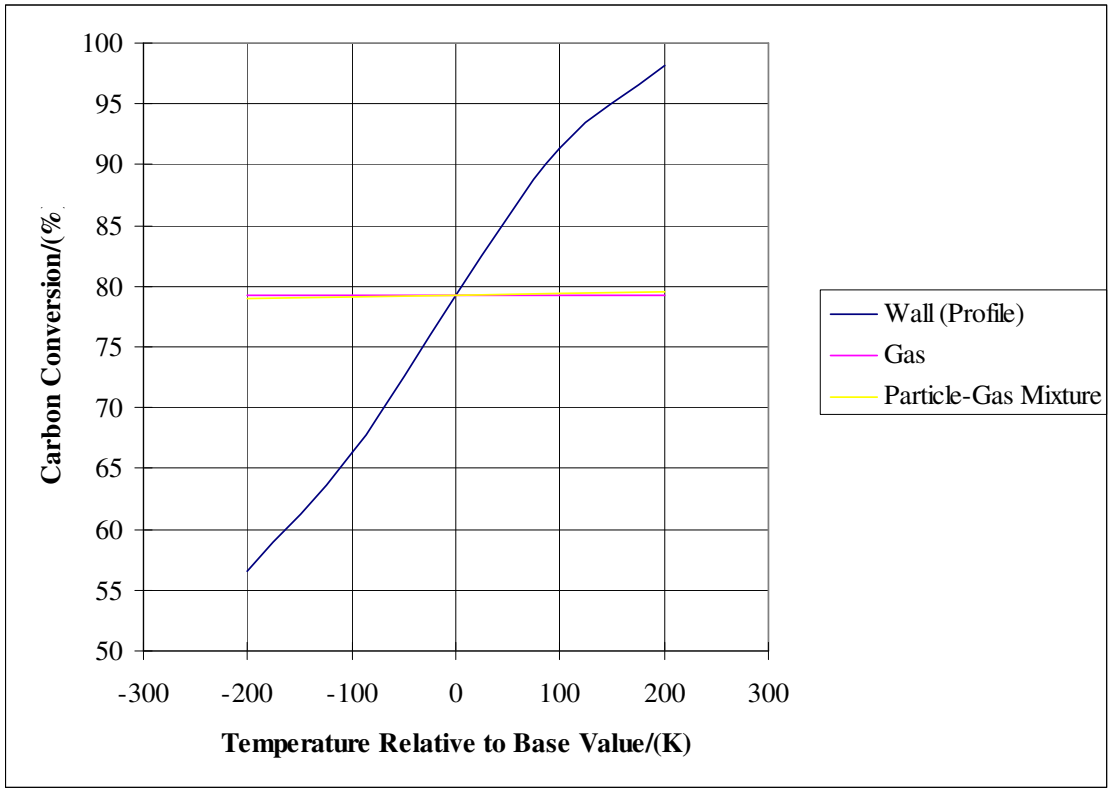

Figure 5.7: Effect of temperature inputs on predicted carbon conversion

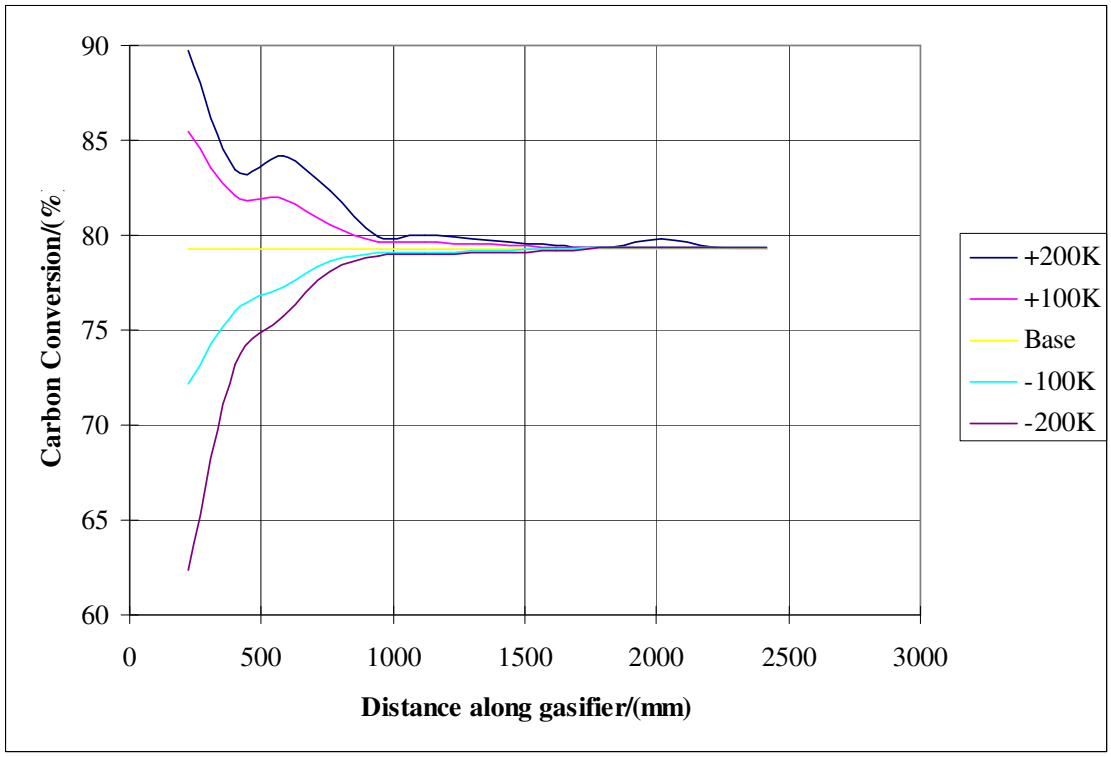

Figure 5.8: Effect of variations in input wall temperatures at different distances along the gasifier on predicted overall carbon conversion

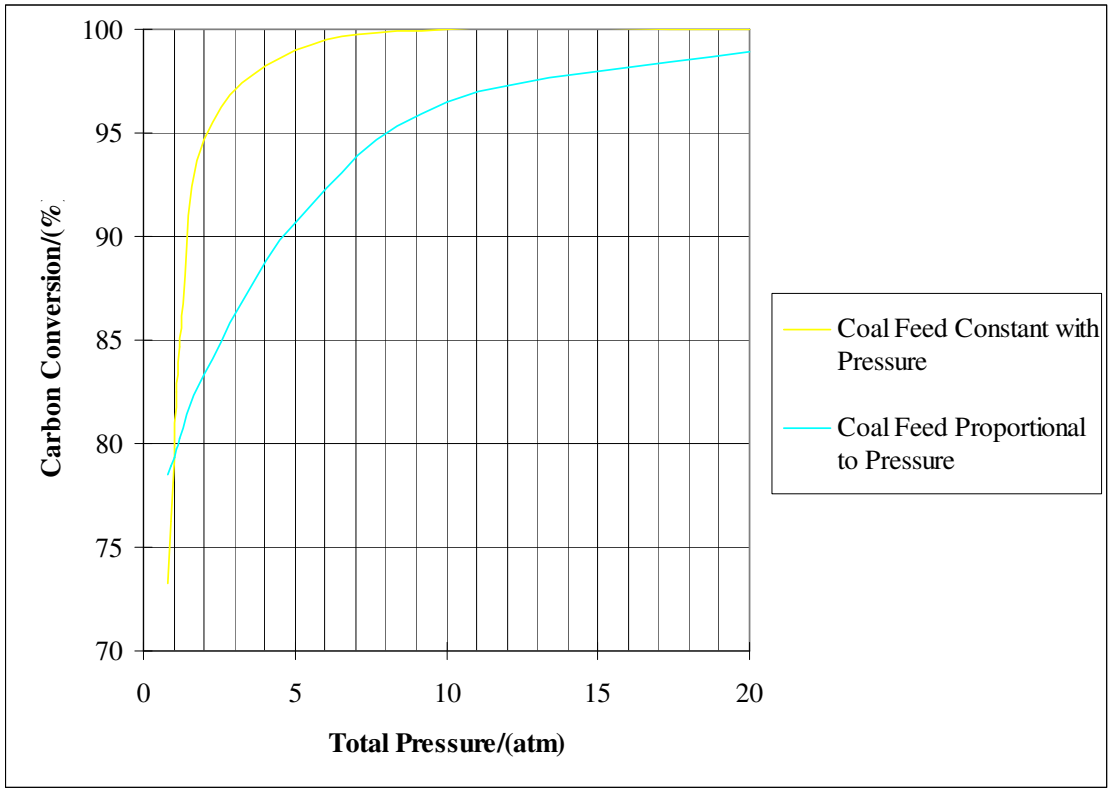

Figure 5.9: Effect of total pressure on predicted carbon conversion

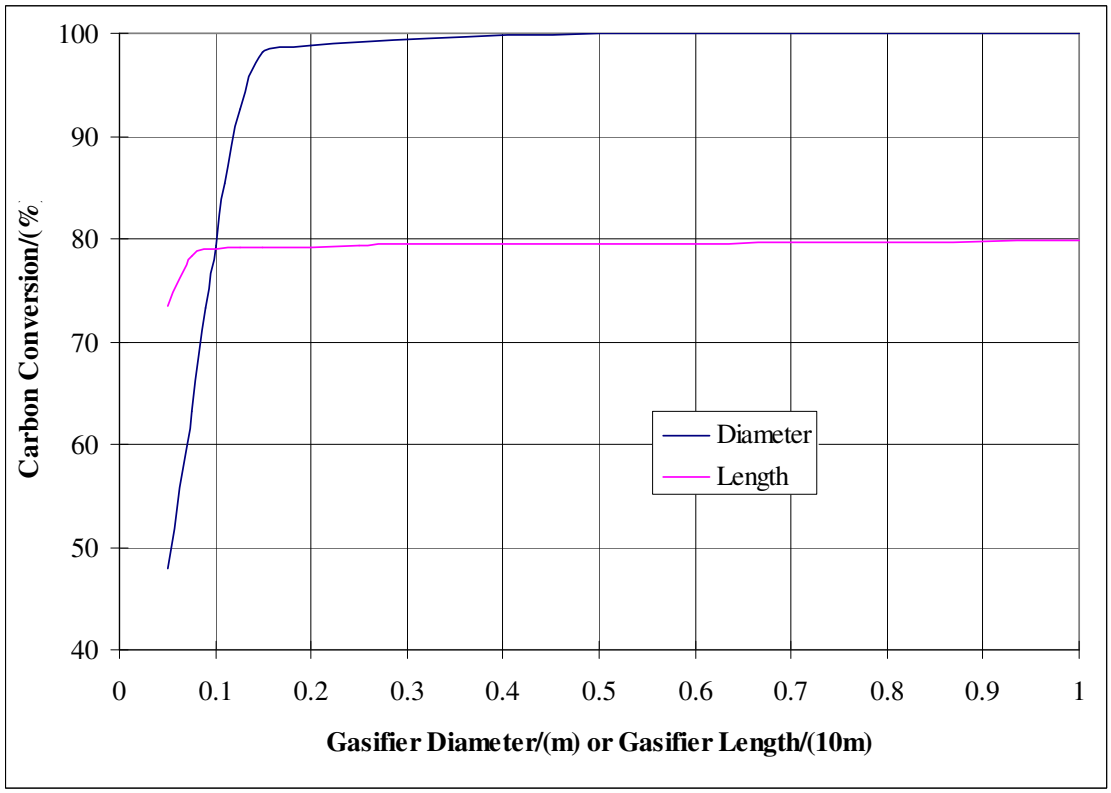

Figure 5.10: Effect of gasifier diameter and length on predicted carbon conversion

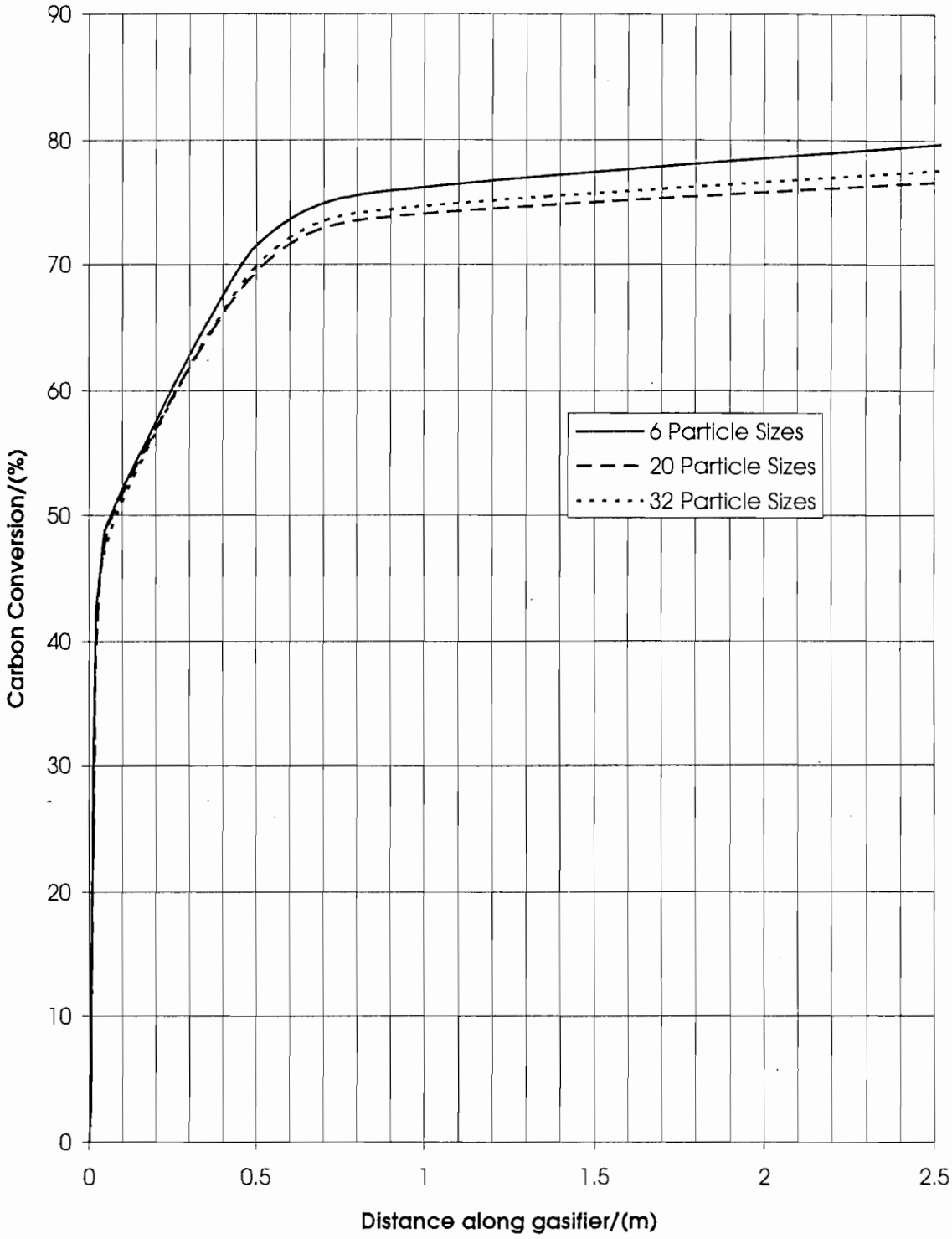

Figure 5.11 : Effect of number of particle sizes modelled on carbon conversion predictions.

6. COMPARISON OF MODEL PREDICTIONS WITH AVAILABLE EXPERIMENTAL MEASUREMENTS

6.1 Introduction

The purpose of preparing a model is to enable prediction of the performance of a particular system either without constructing it or when operating with different conditions to those used experimentally. However the predictions of a model are not reliable unless the model has been verified against results from an experimental system to determine the errors caused by approximations included in the model. This section covers the comparison of model predictions and experimental results for a range of experimental gasifiers. The majority of the experimental work covered is sourced from CSIRO (1995) and covers entrained flow gasification experiments with a selection of eight Australian coals over a wide range of oxygen stoichiometries at atmospheric pressure. Other experimental results have been extracted from the general literature and include work from Brigham Young University, Utah, USA (Brown *et al.* (1988)), United States Bureau of Mines (USBM (1953, 1954)), and the Institute of Gas Technology, USA (IGT (1957)). The inclusion of results from experiments performed over 30 years ago is due to the lack of recent published results that include information on gasifier dimensions, conditions and performance. This is due to a current emphasis on corporate gasification research, complete results of which are not usually released publicly. The major thrust of the model validation is focussed on the CSIRO results as complete details of the experiments were available and the experiments covered a wide range of conditions, using the greatest variety of coals of the available results. Comparisons of experimental results and model predictions were performed for carbon conversion, cold gas efficiency and gas composition for the CSIRO tests while for the other gasifier tests only carbon conversion results were used. It was found that carbon conversion comparison was the best indicator of model performance as cold gas efficiency and gas composition were more susceptible variations due to minor errors in temperatures and gas flows. In this study oxygen stoichiometry is defined with respect to carbon monoxide formation, that is 100% oxygen stoichiometry refers to having sufficient oxygen input to

convert all coal carbon to carbon monoxide. This definition differs from that used in combustion work where stoichiometry is based on carbon dioxide as the product gas.

6.2 Atmospheric Pressure Experimental Gasifiers

6.2.1 CSIRO Experimental Gasifier

6.2.1.1 Description of Gasifier

The experimental gasifier shown in figure 6.1 was constructed and used by CSIRO to study the gasification performance of eight Australian coals at high temperatures and atmospheric pressure in an entrained flow gasifier. Analysis results for the coals used in the study are given in table 6.1. The gasifier design uses the exhaust gases from a burner head combusting propane to heat and gasify coal. Gasification occurs in a 0.1m internal diameter by 2.5m long heated refractory tube with gas and slag cooled by water sprays at the exit. Heating of the refractory tube maintains wall temperatures above 900°C, but in the upper section of the gasifier temperatures are higher due to the high temperature of the exhaust gases from the burner. A wide range of experimental conditions was used in the study covering oxygen stoichiometries from 25 to 150% for each coal with two series of experiments. The first series of experiments varied the quantity of oxygen added, with constant flow rates of other gases and coal, to affect the stoichiometry, and the second series varied coal flow rate, with constant gas flow rates. Measured experimental results from the gasifier were wall temperatures at 11 points, inlet flow rates of gases and coal, gas analysis at the exit, and temperatures at the burner exit and at the coal addition point. Calculated experimental results include carbon conversion and cold gas efficiency, which were calculated from the gas analysis and the assumption that nitrogen flow rate at the exit is identical to the inlet flows, neglecting coal nitrogen.

Table 6.1: Analysis of coals used in the CSIRO gasifier (Harris *et al.* (1995)).

Coal	Moisture /wt%(ad)	Ash /wt%(ad)	Volatile Matter /wt%(daf)	Carbon Content /wt%(daf)	ASTM Rank
A	5.2	9.1	50.2	82.1	High Volatile Bit. B
B	3.0	14.0	41.7	81.4	High Volatile Bit. A
C	2.4	23.9	38.3	83.3	High Volatile Bit. A
D	9.1	11.4	33.3	77.7	Sub-bituminous A
E	2.6	9.6	35.5	84.8	High Volatile Bit. A
F	4.5	9.9	34.3	86.4	High Volatile Bit. A
G	1.6	17.4	25.4	87.0	Medium Volatile Bit.
H	0.8	20.8	11.5	90.3	Semi-Anthracite

6.2.1.2 Prediction Methods

In order to predict results for an experimental gasification run using the model a number of inputs must be made. The model requires data about the coal character, feed rates to the gasifier, temperatures of the feeds and the gasifier wall temperatures. Data on the coal required is the proximate, ultimate and ash analyses, although the ash analysis is not critical and can be approximated, a size analysis and also heterogeneous reactivities of char from the coal, or from a similar coal with the carbon content of that coal. All remaining properties of the coal, such as porosity, internal surface area and volatile release are estimated using techniques previously described. Temperature measurements along the gasifier from the experimental runs are used as wall temperatures as the individual runs were not long enough to allow the wall to reach thermal equilibrium, which would allow calculation of wall temperatures. Gasifier wall temperatures were more dependent on recent conditions experienced by the gasifier, such as preheating, than the characteristics of the experimental run itself. The wall temperature measurements at points along the gasifier are used in the model to generate a complete temperature profile by interpolation of the results. Feed rates of various gases and coal to the gasifier determine the flowrates along the gasifier, as well as the stoichiometry of the run.

Results from the model can be output in any required format but for consistency the carbon conversion, cold gas efficiency and gas composition are calculated on the same basis as the experimental results. This is a dry gas basis using the assumption that the nitrogen flowrate at the exit is identical to that at the inlet. As nitrogen can also be generated from coal nitrogen this introduces an error of up to 2% in the nitrogen flowrate at the exit. Other errors can be estimated from the measurement of inlet flows and on some of the following graphs the range of these errors is indicated as high and low bounds on the experimental results. Similar errors could be implied in the model predictions, arising from the same input data errors, but these are not shown. It is evident that seemingly small errors in input flowrates can have a significant effect on the reliability of calculated results.

Gasification runs, both experimental and modelled, were divided into two groups that are considered separately. One group of runs is referred to as "Standard" and is defined as the series of runs with approximately constant coal feed rate while the gas flowrates were varied to change the run stoichiometry. The other group is referred to as "Equimolar" for the reason that the feed gas flowrate was kept approximately constant, with an equimolar ratio of oxygen and steam, while the coal feed rate was varied to change the run stoichiometry. Differences between the results of these groups of runs will be discussed later.

A number of inputs from experimental data are required by the model in order to give reasonable predictions. For all model predictions the base reactivity values used in the predictions were as given in the description of mathematical model section, with adjustment for the specific coal used. Typical values of these inputs are shown in the following graphs. Figure 6.2 shows the size distributions for the feed coal used in the model. For each coal six distinct particle sizes were used, with the sizing being derived from experimental coal sizing results for each coal. The coal sizing shows that Coal D particles were appreciably smaller than those of the other coals, which may have an impact on results. Average measured gasifier wall temperatures for both types of runs are shown in figures 6.3a and 6.3b as a function of distance along the gasifier and stoichiometry. Variability in temperatures for different runs at the same stoichiometry resulted in the temperatures for the actual run being used in the model, however the

figures show general trends. There is apparent inconsistency in the data as the temperatures do not always increase with stoichiometry, contrary to expectations. Also an obvious decrease in temperature from standard to equimolar runs indicates that higher coal concentrations in the gas for equimolar conditions have cooled the gasifier wall. The temperatures were measured using thermocouples inserted into the refractory lining of the gasifier and thus some of the variability between indicated temperatures could be caused by the thermocouples being slightly different depths into the refractory. The effect of this is that the model wall temperatures will all be underpredicted to varying degrees, which will have some effect on the predicted results. In figures 6.4a and 6.4b gas flowrates as functions of the amount of coal carbon entering the gasifier are shown for the range of stoichiometry considered. These figures show the results for all experimental runs and indicate a higher degree of variability in the standard runs compared to the equimolar. It is obvious that the variability in conditions for different runs will have an impact on comparisons between these runs using the experimental results.

6.2.1.3 Individual Coal Predictions

The following sections will detail comparisons between model predictions and experimental results. Results for each coal are considered separately to determine the accuracy of the model for each coal and in later sub-sections variations between coals will be considered.

A varying number of experimental and model runs were performed for each coal. Several experimental runs were performed under similar conditions in early work to test the repeatability of results and, in some cases, because of problems with equipment. For each coal a selection of runs was modelled to cover the range of stoichiometry considered without the replication required to model every run and, therefore, less model points are shown on the graphs than experimental points.

On examination of the following results it will become obvious that the model performance is better for some coals than others. This is a result of variations in the predicted properties of different coals resulting in prediction errors, such as volatile release or heterogeneous reactivities. In some cases it will be stated in the discussion that particular changes to the model could be performed to improve the

predictions for a particular coal. However these changes were not made in the predictions made in this study as preference was given to presenting the capabilities of the model in its general form as a wide ranging predictive tool. If predictions were required for a specific coal at conditions other than those possible in the present experimental apparatus, the model could be modified using data from previous experiments in order to provide more accurate predictions.

To simplify the following discussion the influence of some factors on gasification will be addressed now. The first is the possible influence of soot formation on measurements and predictions. Soot is considered to be composed of aromatic hydrocarbons arranged in a dense, non-reactive formation. Formation of soot occurs when organic fuels are oxidised under low stoichiometry conditions and, in the case of coal, are commonly formed during combustion of volatiles. While soot particles are of low reactivity they are also very small, even compared to pulverised coal, and due to this, and the high gas temperatures experienced in entrained flow gasification, the soot is likely to be rapidly consumed. However, if soot remains at the gasifier exit, possibly due to lower than expected gasification temperatures, it will not be identified as carbon conversion in the experimental results as the carbon is not in the gas phase. The model, in contrast, does not consider soot as it has no mechanism for calculating the quantity of soot formed, and therefore it appears as converted carbon in the model. Calculation methods that are suitable for calculating quantities of soot formed from coal volatiles are not available in the literature, other than primitive correlations designed for combustion systems that are not applicable to gasification systems.

Another factor that is not considered in the model is slag formation. It is common in high pressure entrained flow gasifiers for liquid slag formed from coal ash and flux to flow down the gasifier walls. In atmospheric pressure gasifier conditions are generally less extreme and slag formation is less common, particularly if unfluxed. In the cases considered below the wall temperatures indicated experimentally would be affected if slag was formed, as it would provide additional insulation between the thermocouples and the hot gases. Therefore use of the measured temperatures in the model would result in low carbon conversion predictions due to the low input temperatures. As high temperatures are required for slag formation this is more likely to

affect high stoichiometry predictions, although residual slag on the gasifier walls could also affect subsequent runs.

The interaction of carbon conversion, gas composition, cold gas efficiency and gas temperature is worthy of definition prior to discussion of experimental results and model predictions. Only gas composition and gas temperature can be measured variables with carbon conversion and cold gas efficiency being calculated from these and other variables. Commonly, and in the model, the composition of the gas at the exit of a gasifier is considered to be the equilibrium composition. Given the feed rates into the gasifier, the exit gas temperature mostly affects only the ratios of carbon monoxide to hydrogen and carbon dioxide to steam, according to the dominant water gas shift reaction. As carbon monoxide has a similar heat of combustion to hydrogen changes in composition due to the water gas shift reaction have only slight effect on the cold gas efficiency. Also the use of gas phase equilibrium means that the composition of the gas can be approximately determined with knowledge of the feeds and carbon conversion alone, as the exit temperature of the gasifier should be known within a small error range. Therefore if, for example, the carbon conversion predicted by the model is similar to that experimentally determined then the gas composition and cold gas efficiency should also be predicted accurately. If this is not the case then an error in the mass balance over the gasifier has occurred experimentally and it is likely that one or more of the measured feed rates to the gasifier are in error. The most likely source of such an error is the coal feed as blockages and uneven flow are more common in a solid feed system and will reflect an experimental error rather than a model inaccuracy.

(i) Coal A

For each of the coals considered in the CSIRO study a similar range of figures will be discussed covering carbon conversion, cold gas efficiency and gas composition predictions and experimental results. For example in figures 6.5a and 6.5b the carbon conversion predictions and results for standard and equimolar tests respectively, plotted against the oxygen stoichiometry of the individual runs. Then figures 6.5c and 6.5d show the predicted and experimental cold gas efficiencies and gas composition respectively for the standard runs, plotted on a similar basis, with figures

6.5e and 6.5f showing the same for the equimolar runs. For the graphs showing either carbon conversion or cold gas efficiency the figures show estimates of errors in experimental values arising from inaccurate measurement of nitrogen flow into the gasifier, nominally a 10% error was allowed. The selection of nitrogen for identification of error was due to its use as a tracer for determining the exit gas flow in the experiments, leading to an enhancement of error when calculating the results. The nitrogen flow was also the least accurately measured flow as it was introduced both with the other gases and as carrier for the coal.

The predictions for Coal A, as shown in Figures 6.5a and 6.5b, show similar trends in carbon conversion to the experimental results with variations within the indicated experimental uncertainty. A consistent overprediction occurs at high stoichiometry, particularly evident for the standard runs. The obvious connection is that the rates of the heterogeneous reactions are slightly overpredicted, as it appears that the volatile release has been reasonably predicted from the agreement between model and experimental results at low stoichiometry.

Figures 6.5c and 6.5d show results for the cold gas efficiencies and gas compositions at the gasifier exit for the standard runs, respectively. This provides an interesting comparison as the gas compositions show good agreement while the cold gas efficiency results have considerable discrepancies. As cold gas efficiency is calculated from the gas analysis this suggests that minor errors in gas composition can be exaggerated in the calculation of cold gas efficiency. The accuracy of cold gas efficiency results is also questionable as it is expected that figure 6.5c should be bell-shaped to produce a region of optimum efficiency for the particular coal, instead a general decline in efficiency with stoichiometry is indicated.

Figures 6.5e and 6.5f show the cold gas efficiency and gas composition results for the equimolar runs. Again disparity exists between experimental and model results for cold gas efficiency, however the experimental results do show some resemblance to the expected bell-shaped curve. The gas composition results are difficult to interpret due to scatter in the experimental results, however general agreement with the model exists.

In summary, the model predictions for Coal A provide a good indication of trends in carbon conversion and exit gas composition but are inconsistent for cold gas efficiency. A slight overprediction in heterogeneous reactivity appears to have influenced results to a minor degree.

(ii) Coal B

A comparison between model predictions and experimental results for carbon conversion in the standard and equimolar runs is given in figures 6.6a and 6.6b, respectively. The model predictions follow the same trends as the experimental results with a minor underprediction of approximately 5%. For this coal a number of experimental runs were performed on different days and this has resulted in some variability in experimental results, particularly evident on the standard plot.

The cold gas efficiency and gas composition graphs for Coal B standard runs are shown in figures 6.6c and 6.6d. Little correlation between model and experimental results is found in either graph, with the gas composition showing wide fluctuations for the experimental runs. Similar results are reflected for the equimolar results in figures 6.6e and 6.6f.

A comparison of model and experimental results for Coal B show good correlation for carbon conversion but poor correlation for cold gas efficiency. Comparison of gas composition is difficult due to variability in experimental gas measurements.

(iii) Coal C

Results for Coal C carbon conversion are given in figures 6.7a and 6.7b for standard and equimolar runs, respectively. Similar trends are identified for both sets of runs with close agreement between model and experimental results for low and high stoichiometries but large underprediction for intermediate stoichiometries. Minor underprediction at low stoichiometries indicates that volatile yield is underpredicted and from the increasing disparity it would be expected that the carbon dioxide and steam gasification rates are also underpredicted. The agreement between model and experiment at high stoichiometry would then have to occur due to overprediction of the heterogeneous combustion rate. In summary it appears that the methods for predicting coal properties used in the model have failed for this particular

coal. Some deviation between the correlations used for predicting the properties and individual coal properties is expected as coal is an extremely complex compound and for some coals these deviations will be significant, as appears to have occurred in this case.

Owing to the variations found in the previous graphs it is unlikely that reasonable comparisons can be found for other features of the runs for this coal. Comparisons of cold gas efficiencies and gas compositions in figures 6.7c, 6.7d, 6.7e and 6.7f show only vague similarities in trends between model and experiment

Model predictions for Coal C appear to indicate minor errors in volatile yield prediction and heterogeneous combustion rates but significant errors in carbon dioxide and steam gasification results. This has lead to general disagreement between model predictions and experimental results over most of the stoichiometry range considered.

(iv) Coal D

Coal D is the lowest rank coal studied in this project and exhibited high levels of conversion during the gasification runs. Results for carbon conversion during different runs are shown in figures 6.8a and 6.8b. Comparison of model predictions with experimental results for the standard runs shows an underprediction at low stoichiometry but overall a good trend indication. However, for the equimolar runs, a slight overprediction occurs at low stoichiometry with underprediction at high stoichiometry. For the equimolar experimental results a large split occurs between results determined on different days. The model has not predicted this change in results using the available data and this suggests that differences in the coal samples used or a difference in gasifier condition between the experimental runs has occurred.

The cold gas efficiency and gas composition results for Coal D are shown in figures 6.8c-f. For the standard runs prediction are good, excepting underprediction of cold gas efficiency at low stoichiometry. The results for the equimolar runs are affected in a similar way to those for carbon conversion.

Model predictions for Coal D are in general agreement with the experimental results, except for an inability to predict a dramatic rise in carbon conversion at mid-stoichiometry for the equimolar runs.

(v) Coal E

As reactivity data was experimentally determined for char from gasifier runs using Coal E the predictions for this coal are susceptible to smaller errors. For this reason further predictions for this coal will be reported in a later section to illustrate additional capabilities of the model. Comparison of the model predictions with the experimental results for carbon conversion are shown in figures 6.9a and 6.9b. There is close agreement between model and experiment for the majority of runs modelled with some noteworthy exceptions. At very low stoichiometry the predicted conversion is approximately 5% above the experimental results, which appear to be lower than the expected volatile release would give. This suggests the possibility of soot formation, which would not show as carbon conversion in the experimental results but would in the model predictions. Another possibility is that the experimental gas temperatures were sufficiently low to reduce the volatile release at these stoichiometries, which is not considered in the model. Another anomaly occurs at high stoichiometry for the standard runs, where the predicted conversion reduces with stoichiometry increase. While the predicted value is within the indicated error margin an examination of possible causes of this conversion decrease identified that the indicated experimental wall temperature decreased as the stoichiometry increased over 120% and also that slag was formed at high stoichiometry for this coal (CSIRO (1995)). These two observations are possibly related as it is expected that liquid slag coating the refractory of the gasifier would insulate the thermocouples measuring the refractory temperature, and therefore result in a low indication of wall temperature, which would affect the model predictions. Fortunately presence of liquid slag is uncommon for unfluxed Australian coals under the conditions experienced in the experimental gasifier so such an effect should not have greatly affected predictions for the subject coals.

The predicted cold gas efficiencies and gas compositions for runs with Coal E are given in figures 6.9c to 6.9f. As is expected, given the good comparisons achieved for conversion, good correlation between model and experiment is achieved for these results as well, excepting mid-range stoichiometry for the equimolar runs. In this range it appears that carbon monoxide concentration has been underpredicted, with a corresponding overprediction of carbon dioxide, giving good

carbon conversion predictions but low cold gas efficiency predictions. This should have been largely corrected by a corresponding rise in hydrogen due to the water gas shift reaction, but this has not occurred which suggests mass balance problems in the experiments.

The predictions for Coal E provided very good comparison with the experimental results, not surprising as experimental reactivity data was determined for chars from this coal. Some anomalies in the results suggest the possibility of soot formation at low stoichiometries and slag production at high stoichiometries, which both are capable of producing errors in the model predictions.

(vi) Coal F

The results for Coal F carbon conversion are shown in figures 6.10a and 6.10b. A similarity in trends exists between this coal and Coal C, as indicated by low predictions in the intermediate stoichiometry range coupled with good predictions at high and low stoichiometries. However predictions are better for Coal F than Coal C and, while poor for the standard runs, are quite close to the experimental results for the equimolar runs. Low predictions in the intermediate stoichiometry range suggest that the carbon dioxide and steam gasification rates have been underpredicted while the combustion rate has been overpredicted to enable overall conversion to be correct at high stoichiometries.

Cold gas efficiency and gas composition predictions, shown in figures 6.10c to 6.10f, indicate large underprediction of cold gas efficiency and carbon monoxide concentration for the standard runs, while predictions for the equimolar runs are very good, in fact probably the best achieved as a set for any coal studied. This disparity between standard and equimolar predictions suggests that some difference in experimental conditions between the two sets of runs may have affected the accuracy of the model predictions.

Coal F predictions exhibit a distinct difference in accuracy between those for the standard runs and those for the equimolar runs. While the predictions for the standard runs have significant underprediction of carbon conversion, cold gas efficiency and carbon monoxide concentration for stoichiometries in the range 60% to 120% stoichiometry, those for the equimolar runs are very close to the

experimental results over the entire stoichiometry range. This inconsistent performance suggests that some unknown experimental effect may have influenced model performance for this coal.

(vii) Coal G

Comparisons of model predictions with experimental results for Coal G carbon conversion are shown in figures 6.11a and 6.11b. The model predictions are generally in good agreement with the experimental results, although some scatter is apparent in the standard run results at higher stoichiometries and a trend of slight underprediction is evident.

Cold gas efficiency and gas composition results are shown in figures 6.11c to 6.11f. Model predictions for the standard runs show general agreement with the experimental results, although carbon dioxide appears to be overpredicted slightly with carbon monoxide being underpredicted accordingly. For the equimolar runs agreement is very close with the exception of low stoichiometry results which show an underprediction of carbon dioxide and an overprediction of cold gas efficiency.

Model predictions for Coal G show very good agreement with the experimental results.

(viii) Coal H

Coal H is the highest rank coal considered in this study and as such has the lowest proximate volatile matter. Comparisons of model predictions with experimental results for carbon conversion are shown in figures 6.12a and 6.12b. It is clear from these figures that the carbon conversion at all but low stoichiometries has been underpredicted. The low stoichiometry conversion relies mostly on volatile release and this appears to have been modelled acceptably while heterogeneous reaction rates, which are important at higher stoichiometry, have been under-estimated. This can result either from underprediction of the char heterogeneous reactivities or misrepresentation of the char structure, both of which are possible considering the assumptions used in modelling.

Comparison of model predictions and experimental results for cold gas efficiency and gas composition are given in figures 6.12c to 6.12f. These

show underprediction of cold gas efficiency and carbon monoxide corresponding to the reduced carbon conversion predictions.

The results for Coal H indicate that, while volatile release was realistically modelled, the predicted carbon conversion was lower than experimentally determined. The most probable cause of this is underestimation of the heterogeneous reaction rates, either by incorrectly estimating reactivities or due to an incorrect pore structure.

6.2.1.3 Trend Analysis for CSIRO gasifier

While previously discussed results have concentrated on discussing individual coals, the major purpose of the model is to predict differences between coals in gasification. It is also useful to know of trends in coal performance based on simple characteristics, such as coal proximate volatile matter and coal rank, and the relationship between gasification conditions and performance.

(i) Effect of Stoichiometry

The effect of stoichiometry has been shown to a large extent in the previous sections however some summarising and identification of trends is warranted. It is clear that stoichiometry has a marked effect on carbon conversion in the experimental gasifier. By detailing some model predictions for Coal E it will become obvious that the effect of adding more oxygen is more complex than simply causing more coal to burn. In figures 6.13a-c and 6.14a-c it can be seen that the increase in stoichiometry over the range 23 to 135% has resulted in only an increase of approximately 30% in total and 7% in combustion carbon conversion (Figures 6.13a and 6.13c). Conversion due to volatile release (Figure 6.13b) has no change in final yield, as this is generally not possible in the model, and only minor variations in release timing, with the lumps in the curves due to release from different particles sizes as heating occurs. The major changes in carbon conversion are predicted to be due to carbon dioxide gasification (Figure 6.14a) presumably as higher concentrations of carbon dioxide are formed at high stoichiometry from combustion of the volatiles. In comparison steam gasification and hydrogen gasification (Figures 6.14b and 6.14c) have

little effect on the overall carbon conversion. Also of interest is the low degree of conversion by heterogeneous reactions at low stoichiometry, which leads to the prediction that volatile release is almost entirely responsible for conversion under these circumstances.

(ii) Relative Performance of Different Coals

In order to simplify the wide range of results shown in the previous section conditions of 100% stoichiometry for both standard and equimolar runs will be considered. Model predictions and experimental results for the 8 coals studied are shown in figures 6.15a and 6.15b for standard and equimolar runs respectively, with a breakdown of predicted carbon conversion showing the reactions attributed responsible for the conversion by the model. In both graphs Coal C conversion is obviously underpredicted and, as the coals are in order of reducing coal volatile matter, it is clear that volatile release has been underpredicted for this coal. Overall prediction of the different performance of different coals in the gasifier correlates well with the experimental results. Exceptions to this are in predictions for Coal C and the equimolar run for Coal D, while underprediction of carbon conversion for Coals F, G and H for the standard runs is significant but the trends followed are still correct. Coal D presents an interesting problem as the standard run is slightly overpredicted while the equimolar run is significantly underpredicted. On examination of the experimental data it appears that the gasifier was markedly cooler for the equimolar run, however the temperature readings may have been affected by slag deposition on the refractory and use of these wall temperatures in the model could cause the observed error.

Performance of the coals in the gasifier can be compared to analysed properties to examine the major influences on gasification efficiency. Comparison of a selection of coal properties with the experimental and modelled gasification performance of the coals is given in the following figures. In all cases the indicated experimental results are for stoichiometries in the range of 85 to 115%, corresponding to a carbon conversion range of approximately 10% so that greater range for individual coals indicates variation in other parameters during the gasification runs. The range of experimental results considered allows for The model predictions on the

figures correspond to the experimental run closest to 100% stoichiometry. Figures 6.16a-c and 6.17a-c show any correlation between proximate analysis results for the coals and the coal performance for the standard and equimolar runs respectively. The equimolar runs show more consistent trends than the standard runs, as well as better model predictions, however significant trends are not clear in the results. A slight trend of increasing carbon conversion with coal volatile matter can be identified but, considering the wide range of volatile matter in the coals, this gives only marginal variation between coals compared to the experimental range of results for individual coals. Coal moisture and ash content have no consistent influence on the carbon conversion. Ultimate coal analysis results are compared with gasification performance in figures 6.18a-c and 6.19a-c for standard and equimolar runs. The best correlator for the experimental results is the carbon content of the coal, which shows a clear inverse relationship to carbon conversion for both standard and equimolar runs. A similar but positive relationship for coal oxygen content is also indicated but coal hydrogen content gives no obvious trend. The carbon and oxygen contents can be taken as a rank effect in the coal, with high rank coals giving lower carbon conversion than low rank coals. Model predictions follow the same trends as the experimental results with regard to these coal properties. Results in figures 6.20a-c and 6.21a-c show the trends in carbon conversion with other miscellaneous coal analyses. The fuel ratio is a calculated coal property often used by Japanese researchers as an indicator of coal performance and is equal to the ratio of coal fixed carbon to volatile matter. Both this and the vitrinite reflectance, an indicator of coal rank, have ill-defined impact on coal performance due to the small range in values for the majority of the coals considered, causing clustering of data on the figures. Coal calorific value also has an uncertain effect, regardless of the data being well spaced.

In summary it can be seen that the model predictions generally show similar trends in performance between coals to the experimental results, with some variations for specific coals. The coal carbon content was found to be the best indicator of gasification performance, with a high carbon content suggesting a low conversion. Coal volatile matter was found to have a lesser effect on gasification performance than was expected.

(iii) Differences Between Standard and Equimolar Runs

Due to the different techniques used for the two sets of runs, the standard runs having constant coal feed rate and the equimolar runs having constant gas feed rates, some differences between both model performance and predicted values are expected. Differences between standard and equimolar runs for individual coals appear to be minimal from previously cited results, excluding those for Coal D which has a marked inconsistency in the equimolar runs. However it should be noted that there appear to be greater differences between coals for the standard runs than for the equimolar. This is possibly due to the higher coal feed rate in equimolar runs raising peak temperatures, as shown in figures 6.22a and 6.22b for model predictions, which would have the effect of masking char reactivity differences by changing rate controlling influences towards diffusion processes. It is curious that the exit temperatures appear to have no connection to the peak temperatures. This can have two possible explanations; namely that with the higher peak temperature the endothermic reactions are accelerated, bring the temperatures down, or the exit temperature is more dependant on the wall temperatures in the second half of the gasifier, which are reasonably constant for all gasifier runs.

The differences between the standard and equimolar series of experimental gasification runs appear to be minor, the major influence on carbon conversion still being stoichiometry. However it appears that the standard run results may be better suited to identifying differences between the coals studied, possibly due to higher peak temperatures experienced in the equimolar runs, as predicted by the model. This allows for better identification of the effect of different reactivities for different coals on the performance of the coals during gasification.

6.2.2 USBM Experimental Gasifier

6.2.2.1 Description of Gasifier

The United States Bureau of Mines (USBM) performed numerous gasification tests under atmospheric pressure conditions during the 1950s. A number of variations in the gasifier design were carried out during the period of the tests with the intent of producing a design which could be scaled to a commercially viable

gasifier. There is some uncertainty as to the actual dimensions of the gasifier due to incomplete labelling of diagrams in the literature but an approximate design is given in figure 6.23 (USBM (1954)). This gasifier is more complex than those previously described being comprised of two different diameter sections of uncertain length with a constriction between the two sections. Details of the arrangement of the feed injection connections is also not given and the refractory of the gasifier walls is water cooled, as is the exit gas. Due to the uncertainties in the gasifier layout it is unclear whether the design can be reasonably approximated by a plug flow model however, given the restricted quantity of data available, an attempt was made assuming that flow through the restriction had negligible affect on the progress of gasification. A limited series of experiments were modelled by restricting the selection to a series performed with five coals under similar reaction conditions in order to test the ability of the model to predict the performance of different coals. Analysis results for these coals are given in table 6.2.

Table 6.2: Analysis of coals used in the USBM atmospheric gasifier (USBM (1954)).

Coal	Moisture /wt%(ad)	Ash /wt%(ad)	Volatile Matter /wt%(daf)	Carbon Content /wt%(daf)	ASTM Rank
Lake de Smet	8.5	11.2	51.4	72.2	Sub-bituminous A
Fries	2.4	12.6	44.4	77.8	High Volatile Bit. A
Roslyn No.3	3.1	18.1	44.9	82.4	High Volatile Bit. A
Sewickley	1.0	14.8	41.1	83.6	High Volatile Bit. A
Pennsylvania	1.0	10.1	7.9	92.5	Anthracite

6.2.3.2 Prediction Methods

Less data is available on the conditions under which the USBM gasification tests were performed, compared to the CSIRO tests. Similar data is available on the properties of the coals used, including sizing analysis, but the exact dimensions of the gasifier and the temperatures inside it are unclear. As a simplification the gasifier was approximated as a cylindrical tube 4.1m long by 0.76m internal diameter. Gasifier wall temperatures were not reported in the reference so an assumption of a near fluid slag layer in the gasifier was made and the wall temperature taken as the ash fluid point for the coal being tested. All other coal properties were estimated, including reactivities, using the same methods used for the CSIRO predictions. Due to the limited number of experimental tests being analysed the comparison of experimental and predicted carbon conversions will be considered in the summary below.

6.2.3 BYU Experimental Gasifier

6.2.3.1 Description of Gasifier

The Brigham Young University (BYU) gasifier has been used for investigation of numerous aspects of gasification, both at atmospheric and higher pressures. Unfortunately full results and conditions have only been made public for a selection of atmospheric pressure tests, with results of a single experimental run for each of four coals given in Brown *et al.* (1988). Analysis results for these coals are given in table 6.3. The dimensions of the gasifier as used for the atmospheric pressure test are indicated in figure 6.24 as a tube approximately 2m long and 0.2m internal diameter (Brown *et al.* (1988)). This gasifier operates under a different set of principles to the CSIRO gasifier as coal and oxygen are added at relatively cool temperatures in the primary feed and, for low moisture coals, steam is added as a secondary stream. The refractory tube of the reactor is also unheated, relying solely on heat produced from the reactions. Again the carbon conversion and cold gas efficiency are calculated from the exit gas composition, utilising argon flow as a tie element in determining the gas composition. In addition char samples were removed from the gasifier via a sample probe prior to the venturi scrubber at the exit. The reference used in this case also

describes a model, previously discussed in the Literature Review section, and compares predictions from this with the experimental results.

Table 6.3: Analysis of coals used in the BYU gasifier (Brown *et al.* (1988)).

Coal	Moisture /wt%(ad)	Ash /wt%(ad)	Volatile Matter /wt%(daf)	Carbon Content /wt%(daf)	ASTM Rank
Utah	2.4	8.3	51.1	77.6	High Volatile Bit. A
North Dakota	19.0	6.1	46.9	61.9	Lignite A
Wyoming	15.0	5.8	49.0	68.7	Sub-bituminous A
Illinois No.6	6.7	10.4	47.5	75.3	High Volatile Bit. A

6.2.3.2 Prediction Methods

The reported results for the experimental tests in this study are not complete due to the absence of any data on the temperatures experienced in the gasifier. As an estimate the wall temperature of the gasifier was set at 1300K for all of the coals in the study. Normal coal analysis results and coal sizing data are presented in the reference, in addition some coal reactivity data was included. As this reactivity data was presented in a different form to that used in the general model, namely gas volume rate of reaction, it was neglected and the reactivities estimated as previously described. Due limited number of results compared to model predictions the comparison will be considered in the summary below.

6.2.4 Summary of Atmospheric Pressure Comparisons

The results of the CSIRO, USBM and BYU atmospheric pressure gasification studies are summarised in figures 6.25, 6.26 and 6.27, respectively, on the basis of carbon conversion relative to the carbon content of the subject coals. Due to the large quantity of data available from the CSIRO study the data shown in figure 6.25 is limited to experimental results from both standard and equimolar runs in the oxygen stoichiometry range of 85 to 115% and average curves are shown for both experimental results and model predictions in this range. The general trends predicted in the figures are similar for all of the studies, carbon conversion decreasing with increasing carbon content for both experimental results and model predictions. Two major exceptions are indicated on the graphs as in figure 6.26 the experimental results for Pennsylvania anthracite are significantly higher than predicted and in figure 6.27 the experimental results for North Dakota lignite are significantly lower than predicted. In both these cases these experimental results contradict the trend of the other experimental results of the same study as well as the general trends of the other experimental studies. Also indicated on figure 6.27 are the model predictions of Brown *et al.* (1988) for the experimental gasification runs. These predictions provide interesting comparison with those of the present study as they display different trends and variations from the experimental results. Both models accurately predict the results of the experimental runs for three of the four coals, with the present study having a significant variation for North Dakota lignite and the Brown *et al.* (1988) study having one for Illinois No.6 bituminous coal. It is possible for all the coals that more experimental data was available for use in modelling than was published, in particular the wall temperature used in the present study was estimated from the experimental conditions, and this could explain differences between the predictions of the two models. This is suspected particularly from the experimental result for North Dakota lignite as it is far below expected values of carbon conversion and may be indicative of a cooler gasifier for this run.

In representing the results for the CSIRO study in the manner shown in figure 6.25 it becomes evident that predictions for the CSIRO gasifier are, on average, low compared to the experimental results for all coals in the study. This was not apparent for comparison of individual runs due to the fluctuations in the experimental

results but is probably caused by underestimation of wall temperatures in the model, as thermocouples were set slightly into the refractory wall of the gasifier. This would affect every model prediction made in a similar manner and result in the observed general underprediction.

In summary, comparison of the model predictions with experimental results from gasification at atmospheric pressure of a variety of coals indicates that the model can be used with reasonable accuracy as a predictive tool. Variations between the model predictions and experimental results occur and are evident in particular for two coals, a very high rank coal from the USBM (1954) study and a very low rank coal from the BYU study (Brown *et al.* (1988)). A general negative relationship between gasification performance, indicated by carbon conversion, and coal carbon content was identified from the summarised results of the three experimental studies. This trend was also followed by the model predictions. A more significant trend of increasing carbon conversion with stoichiometry was identified, but is of little use as high stoichiometry reduces the usefulness of the product gas. Carbon conversion was identified as a more reproducible indicator of gasification performance at a given stoichiometry than cold gas efficiency and exit gas composition. This is due to magnification of experimental errors in feed rates and temperatures when determining the gas phase equilibrium.

6.3 High Pressure Experimental Gasifiers

6.3.1 IGT Experimental Gasifier

6.3.1.1 Gasifier Description

The Institute of Gas Technology (IGT) gasifier was used for numerous experimental runs with a range of coals and pressures between 1.7 and 6.1 atmospheres (IGT (1957)). The design of the gasifier is represented in figure 6.28 and a gasification region of approximately 0.46m internal diameter and 1.8m length is indicated. In this gasifier the coal, air and steam are injected tangentially in a mixing region with oxygen being added axially. After this initial mixing region flow is restricted into a roughly cylindrical reaction volume. The refractory wall of the gasifier is neither

heated nor cooled and is surrounded by a pressure vessel. A selection of experimental runs were modelled over a range of pressures for the four coals given in table 6.4.

Table 6.4: Analysis of coals used in the IGT pressurised gasifier (IGT (1957)).

Coal	Moisture /wt%(ad)	Ash /wt%(ad)	Volatile Matter /wt%(daf)	Carbon Content /wt%(daf)	ASTM Rank
Illinois (A)	1.7	8.4	37.9	82.0	High Volatile Bit. A
Illinois (B)	2.5	7.2	32.5	80.9	High Volatile Bit. A
West Virginia Federal	0.7	9.2	34.8	83.8	Medium Volatile Bit.
West Virginia Ameagle	0.5	7.7	27.2	86.8	High Volatile Bit. A

6.3.1.2 Prediction Methods

In the reference indicated details on the operating conditions and coal properties are given in detail for numerous experimental tests. Only a selection of these tests will be modelled with an aim to study the effects of pressure and coal on the accuracy of model predictions. A range in stoichiometry from 63 to 105% was used in the tests analysed, with wall temperatures in the gasifier reported as ranging from 1500 to 1900K. All other variables were calculated as previously defined. The model predictions and experimental results are considered in the later summary.

6.3.2 USBM Experimental Gasifier

6.3.2.1 Gasifier Description

A second gasifier was operated by the United States Bureau of Mines (USBM) in the 1950s, but at high pressures. The series of experiments planned for the gasifier was terminated when the establishment was closed due to a change in government policy and the experimental results made public were sparse due to initial

difficulties with failure of plant items. A series of experiments were performed with a single coal using the gasifier design indicated in figure 6.29 at pressures ranging between 7.8 and 21.4 atmospheres. The reactants were injected axially into the gasifier via a set of concentric tubes with reaction in a tube of approximate internal diameter of 0.25m and length 0.94m before the flow was quenched by water sprays. In this gasifier the refractory lining of the gasifier was heavily cooled with water. The analysis results for the coal used in these experiments varied slightly between runs but is essentially the same as for Sewickley coal in table 6.3

6.3.2.2 Prediction Methods

A range of data is supplied in the reference for the coal analysis and conditions in the experimental gasifier tests. Again temperatures inside the gasifier were not reported so the wall temperatures were taken as the slag fluid temperature. Coal properties were calculated as described previously. Comparison of the model predictions and experimental results is given in the summary below.

6.3.3 Summary of High Pressure Comparisons

The comparisons of experimental results with model predictions for the IGT and USBM pressurised gasifiers are shown in figures 6.30 and 6.31, respectively. In figure 6.30 a varied range of predictions are shown for four coals in the IGT gasifier with grouping of the coals into either Illinois Non-coking or West Virginia Coking types. The tests are ordered in terms of reaction pressure for each coal in sequence from left to right. For the series of runs 19A to 19D and 51A to 52D the only variable of the tests to change significantly was the pressure, as given on the figure. It is evident that predictions for the first set of Illinois coal runs accurately reflect the experimental results with increasing carbon conversion with pressure. The second set of Illinois coal results are less accurate but approximately correct. In contrast the predictions for the West Virginia coals are generally inaccurate with most predicted carbon conversions far greater than the experimental results. The reasons for this are not obvious but may relate to the coking nature of the coals. This can have two possible reasons, either the experimental results were unpredictably low or the model incorrectly

represents the coals. Experimental results for coking coals can be affected by feeding difficulties due to the coal swelling and agglomerating in the burner section. This could cause the observed variations by reducing carbon conversion. Conversely the model predictions can be influenced by any number of incorrect assumptions relating to the reactivity and swelling of the coals. The predictions for the USBM high pressure gasifier shown in figure 6.31 show very good correlation with the experimental results. There is no systematic error obvious in the deviations between model and experimental, although the comparisons are generally less accurate at high pressures. Sources of error in the experimental gasifier results are undetermined but can be expected to be significant due to the less sophisticated instrumentation available at the time of the experiments. The obvious queries to be made about the model predictions relate to the clustering of predictions about the 90% conversion level regardless of the variation in experimental results significantly above and below this value for the P-19 and P-21 runs. On examination of the data for these runs there is no clear reason for these variations in the experimental results and it is possible that experimental, rather than model, errors result in the differences between model and experimental values.

There are no conclusive findings on the model performance arising from the comparison of model predictions with experimental results for the IGT and USBM pressurised gasifier. Performance of the model was generally good, with the exception of predictions for the coking coal runs in the IGT gasifier, however the range of coals used in the comparisons was relatively small at only three distinctively different coals. The ability to predict performance of gasifiers over a range of pressures was excellent for the Illinois coal in the IGT gasifier for pressures from 1.7 to 5.1 atmospheres. Carbon conversion is also predicted accurately over the range of pressure from 7.8 to 21.4 atmospheres for the USBM gasifier tests but owing to the small range in carbon conversions indicated this is less conclusive.

6.4 Testing of Individual Model Components

It is difficult to analyse the accuracy of individual components of the model due to the interaction of different effects on the reactions occurring in the gasifier. The simplest method of determining the accuracy of a model component is to study the

difference in performance between two experimental and modelling runs in which a single variable is changed. In a practical system this is clearly not possible as, for example, when reaction stoichiometry is changed it tends to change reaction temperatures as well as the concentration of reactant gases and increasing oxygen input will also increase carbon dioxide and steam concentrations in the later stages of the gasifier. Therefore the analysis comparing the performance of model components relative to the experimental results will be mostly qualitative. An exception is the volatile yield model which can be compared directly with experimental results at low stoichiometry, where carbon conversion due to heterogeneous reactions is expected to be minimal. For all of the following discussion the results of the CSIRO experimental gasification study will be used, except where noted, due to the wide range of stoichiometry and coals used. The discussion will also be limited to the influence of model components that were identified in the sensitivity analysis as liable to produce significant errors in the model predictions as it is not possible to distinguish minor influences given the scatter of experimental results. Also it is not possible to validate the accuracy of individual model components at high pressures owing to the limited experimental data available. High pressures are expected to influence the performance of the volatile yield sub-model and the calculation of heterogeneous reaction rates.

6.4.1 Volatile Yield Sub-Model

The volatile sub-model used in the modelling work can be compared with the experimental carbon conversion from the CSIRO gasifier at low stoichiometries using the eight different coals of the study. In the sub-model the volatile yield is predicted using the ultimate analysis according to the method of Neoh and Gannon (1984) and the composition of the volatiles is calculated so that all hydrogen, oxygen, sulfur and nitrogen in the coal is released in the volatiles, with the balance of the volatiles being carbon. From this the carbon conversion involved with volatile release constitutes only a proportion of the volatile yield, but can be calculated simply from the ultimate analysis of the coals. The carbon conversions calculated for the volatile yield sub-model using this method are shown in figure 6.32 with the range of experimental results for the same coals under low stoichiometry conditions in the CSIRO gasifier. The

range of stoichiometries taken as being low varies for each coal but are in the range of 20 to 40% oxygen stoichiometry. This should be sufficiently low to prevent oxygen reacting directly with the coal particles and lower temperatures will reduce the reaction rates of the other reactant gases. It is therefore assumed that negligible carbon loss due to heterogeneous reactions occurs at these stoichiometries. An exception to this may be Coal D, which is the lowest ranking coal of the CSIRO study and also has the smallest paticle sizing. Coal D would therefore be expected to be more reactive and experimental results have also proven to be widely scattered. The figure indicates that the range of carbon conversions for each coal is less than 10% except for Coal D which has an approximately 25% range. All of the volatile yield carbon conversion predictions are within the experimental range of results, although the prediction for Coal C is on the lower boundary so may be suspect. This suggests that the possible error of 19% in carbon conversion due to inaccuracy in the volatile yield estimate calculated in the sensitivity analysis was not approached for the coals of this study and an error in the range of 5 to 10% appears more realistic for the predictions.

6.4.2 Factors Related to Heterogeneous Reaction Rates

The accuracy of the methods used to predict heterogeneous reaction rates is difficult to determine as the reaction rate is influenced by temperature, gas composition and particle structure, as well as coal reactivity. Therefore it is only possible to state the observation, previously made about the results in figure 6.25, that average carbon conversion predictions for each of the eight coals in the CSIRO study were lower than the average experimental results by up to 10%. The likely causes of this, as determined in the sensitivity analysis, are inaccurate gasifier wall temperature measurements, incorrect carbon dioxide and steam gasification reactivities, and slag deposition on the gasifier wall. As it appears that all coals have been affected similarly, that is for all the average predictions are lower than the average experimental results, it is most likely that the model predictions were affected in a consistent manner by low wall temperature inputs. This is suggested as it is unlikely that for eight coals the reactivities were all underpredicted, with none overpredicted, and slag deposition was only evident for some of the coals, and generally at higher stoichiometries than used in the figure.

Wall temperature measurements would be similarly affected for most experimental runs without slagging as the error would relate to the depth into the refractory of the wall that the thermocouples were buried. As the gasifier refractory was rarely replaced during the sries of experiments the thermocouple locations would remain constant for most of the experimental runs. From this reasoning it appears likely that the general underprediction of carbon conversion by the model was caused by input of inaccurate wall temperatures, however other errors of smaller magnitudes may also be masked by this larger error. The maximum error in carbon conversion prediction expected due to wall temperature inaccuracy was 14%, from the sensitivity analysis, and from figure 6.25 it appears that the error is less than 10%. Variations in the size of this error between different coals can be taken as indicative of errors in reactivity estimates for the coals, if slagging is neglected. In this case the errors in reactivities are estimated to account for errors of up to 8% in carbon conversion predictions, compared to possible errors of up to 15% indicated in the sensitivity analysis.

6.4.3 Conclusions of Model Component Validation

It is difficult to verify the accuracy of individual components of the model due to the interaction of conditions in gasification. The most conclusive validation is of the volatile yield sub-model which indicates that an error 5 to 10% in carbon conversion prediction is likely to be caused by inaccuracy in the model, rather than the 19% possible error calculated in the sensitivity analysis. The other possible error sources can be less readily quantified, but hypothesis suggested an error of up to 10% in carbon conversion predictions arising from errors in the measured gasifier wall temperatures and an error of up to 8% in carbon conversion predictions arising from coal heterogeneous reactivity inaccuracies. These are less than the possible errors of 14 and 15%, respectively, calculated in the sensitivity analysis. This suggests that these model components may be more accurate than assumed in the sensitivity analysis, but definite findings are not possible.

6.5 Conclusions from Comparison Study

In concluding the validation study it can be stated that predictions made by the model at atmospheric pressure are reliable for most coals and a wide range of conditions. Improved model performance was identified when more accurate reactor and coal property data are available.

Due to the limited experimental data available for high pressure gasification it is not possible to conclusively verify the model performance at high pressures. The model showed some aptitude in prediction at high pressures but the same degree of confidence in predictions as those for atmospheric pressures cannot be recommended. It is expected that predicted variations in performance for changes in coals and gasification conditions at high pressures will be accurate. However, results from further experimental work are required to validate the predictions for specific gasification runs and the variations in performance between different gasifiers.

In comparison with the possible errors in predictions from the model indicated in the sensitivity analysis, the differences between model predictions and experimental results were generally within acceptable magnitudes. Less error than expected was determined to arise from the volatile yield sub-model, wall temperature measurements and reaction rate calculations used in the model.

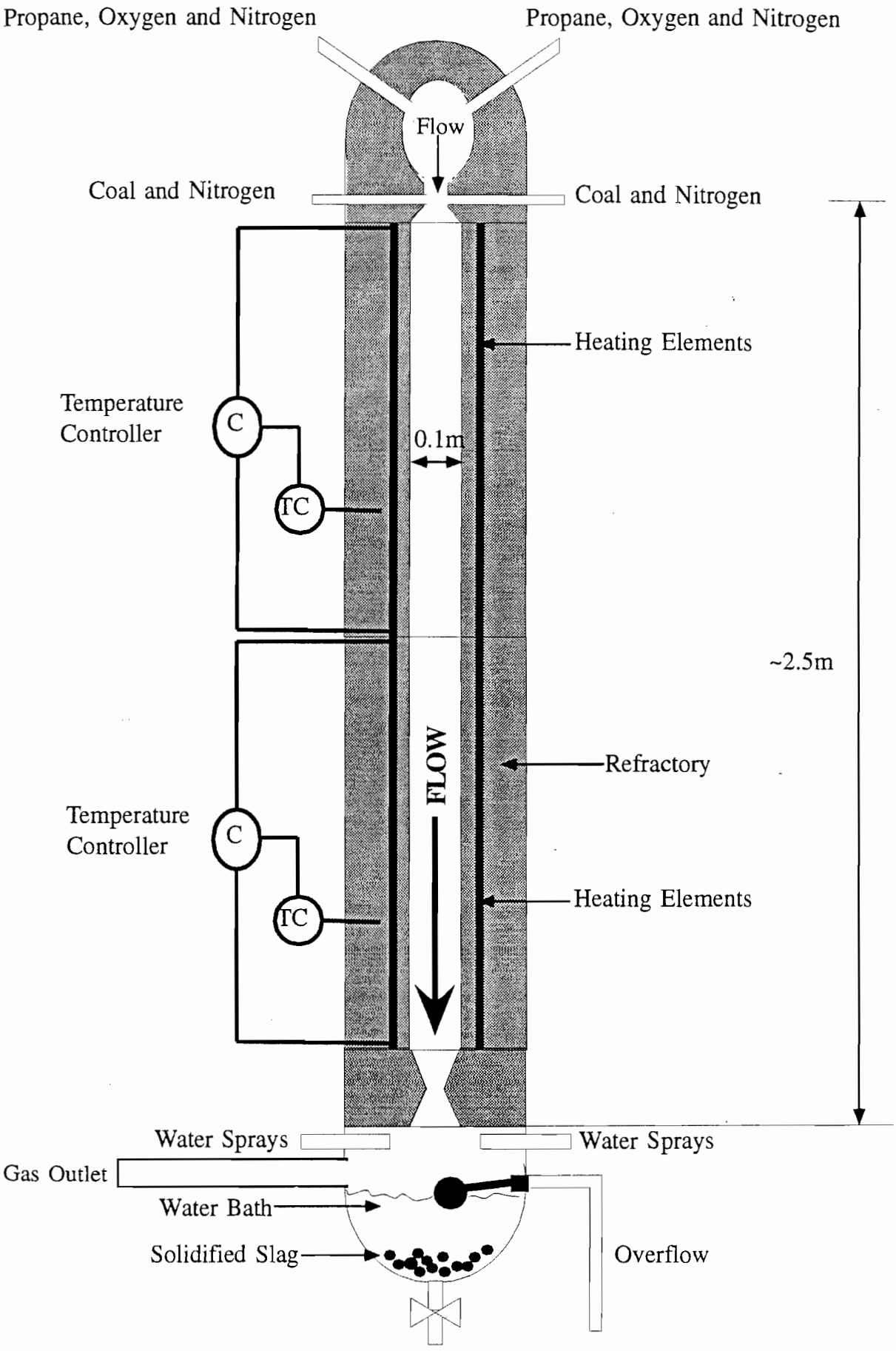

Figure 6.1 : CSIRO experimental atmospheric pressure gasifier (CSIRO (1995))

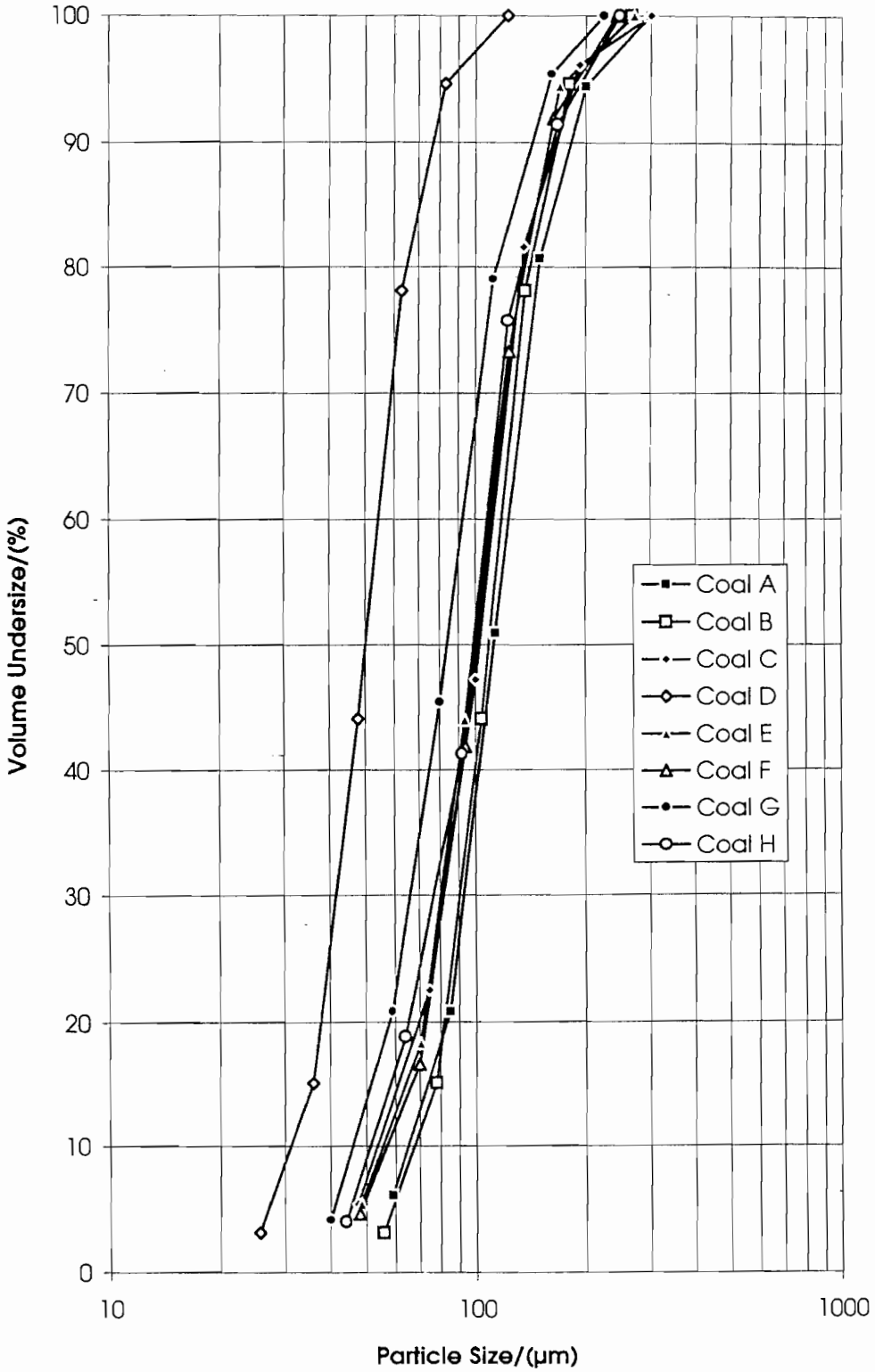

Figure 6.2: Modelled size distribution of coals used in CSIRO gasifier (CSIRO (1995))

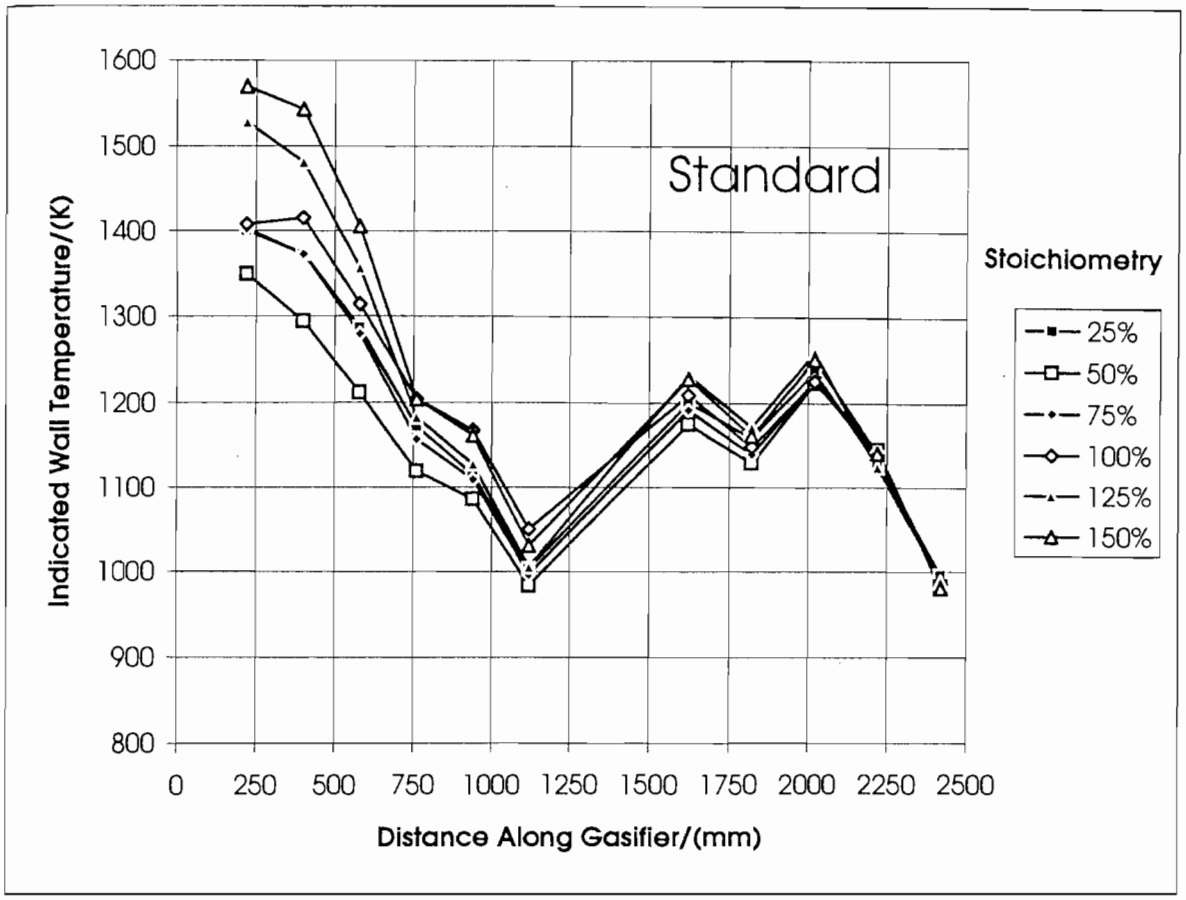

Figure 6.3a : Average gasifier wall temperatures for Standard runs.

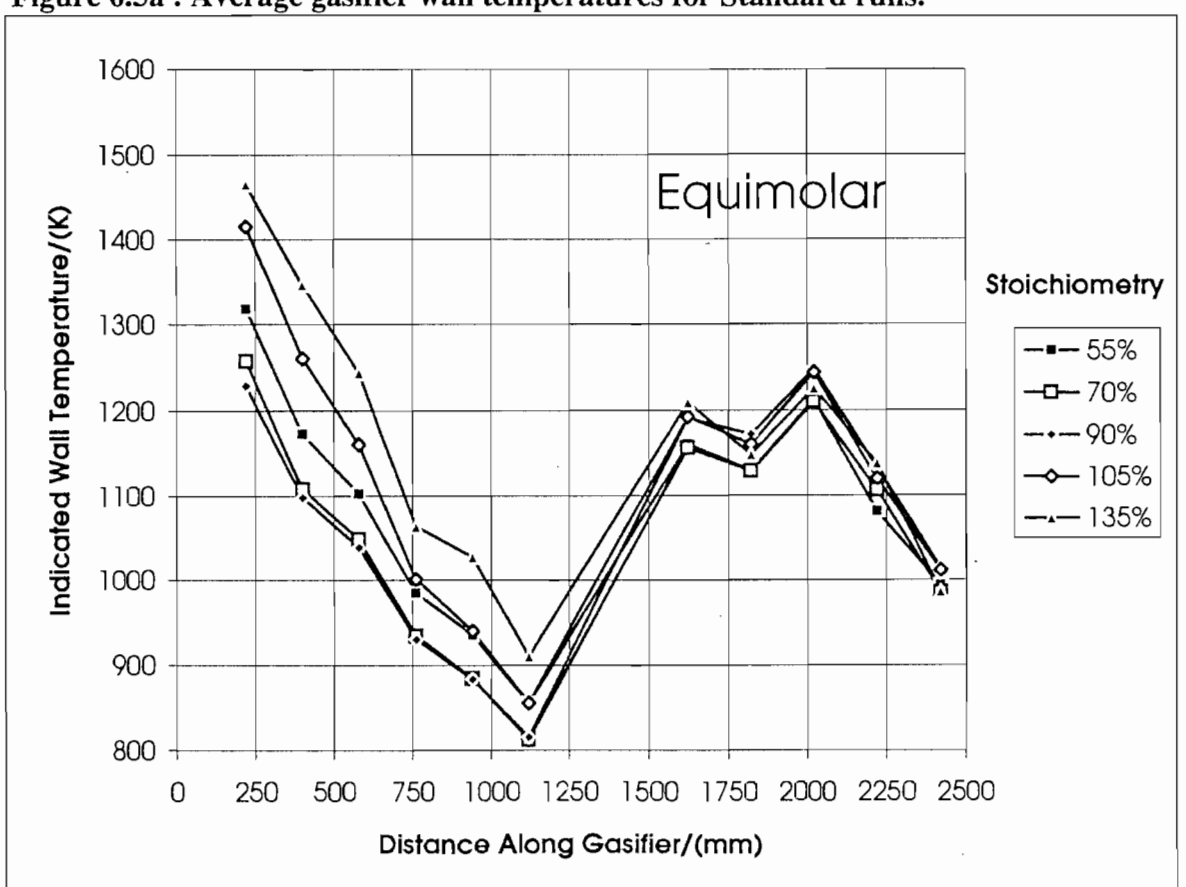

Figure 6.3b : Average gasifier wall temperatures for Equimolar runs.

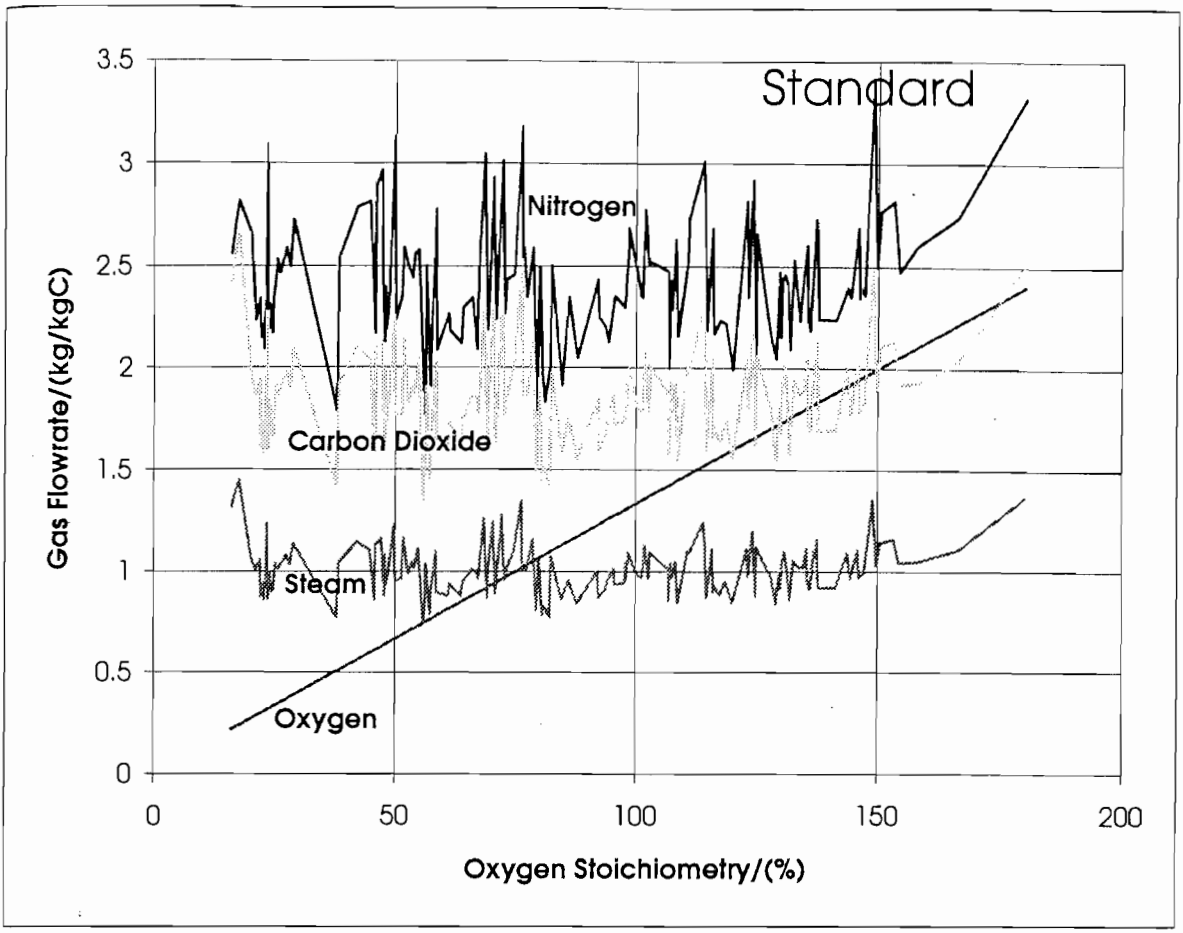

Figure 6.4a : Gasifier feed gas flowrates for Standard runs.

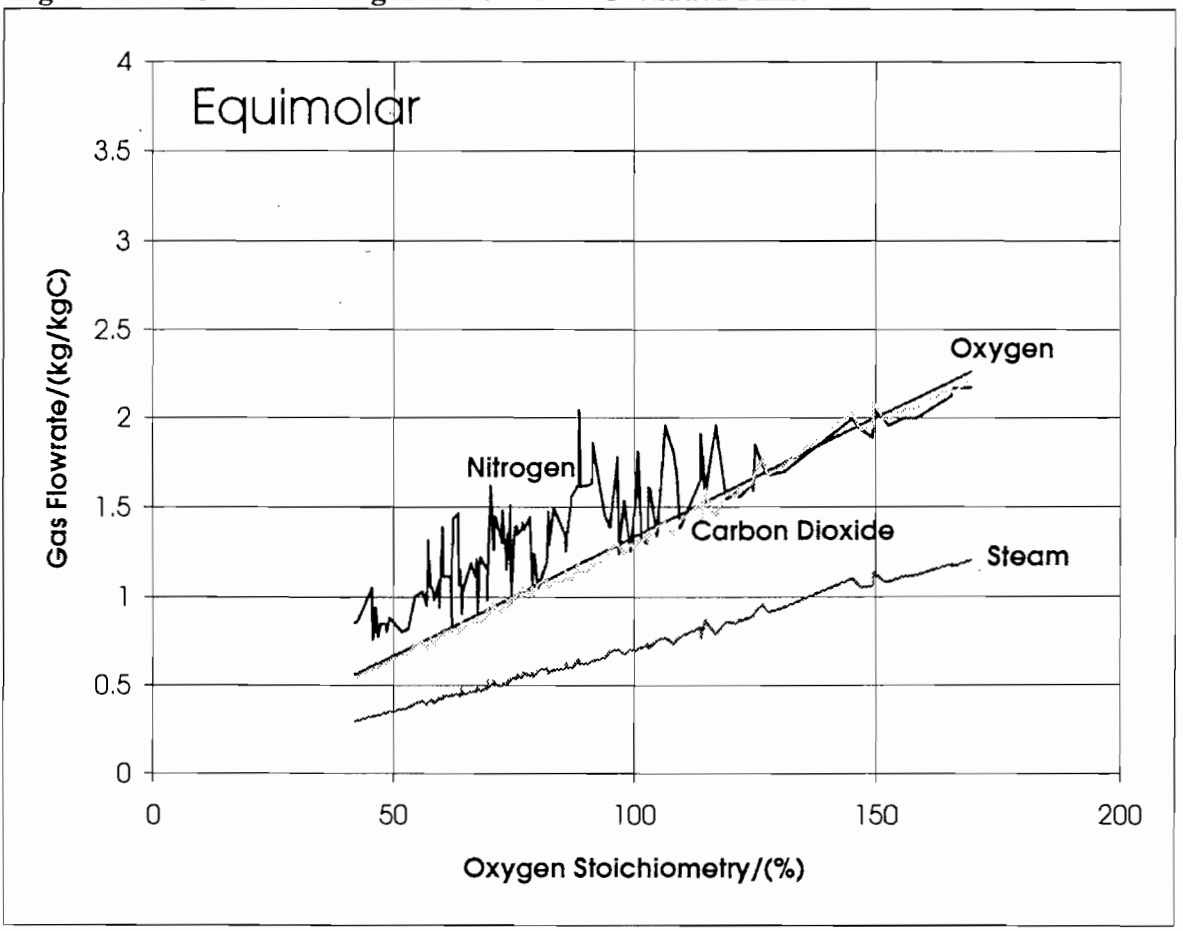

Figure 6.4b : Gasifier feed gas flowrates for Equimolar runs.

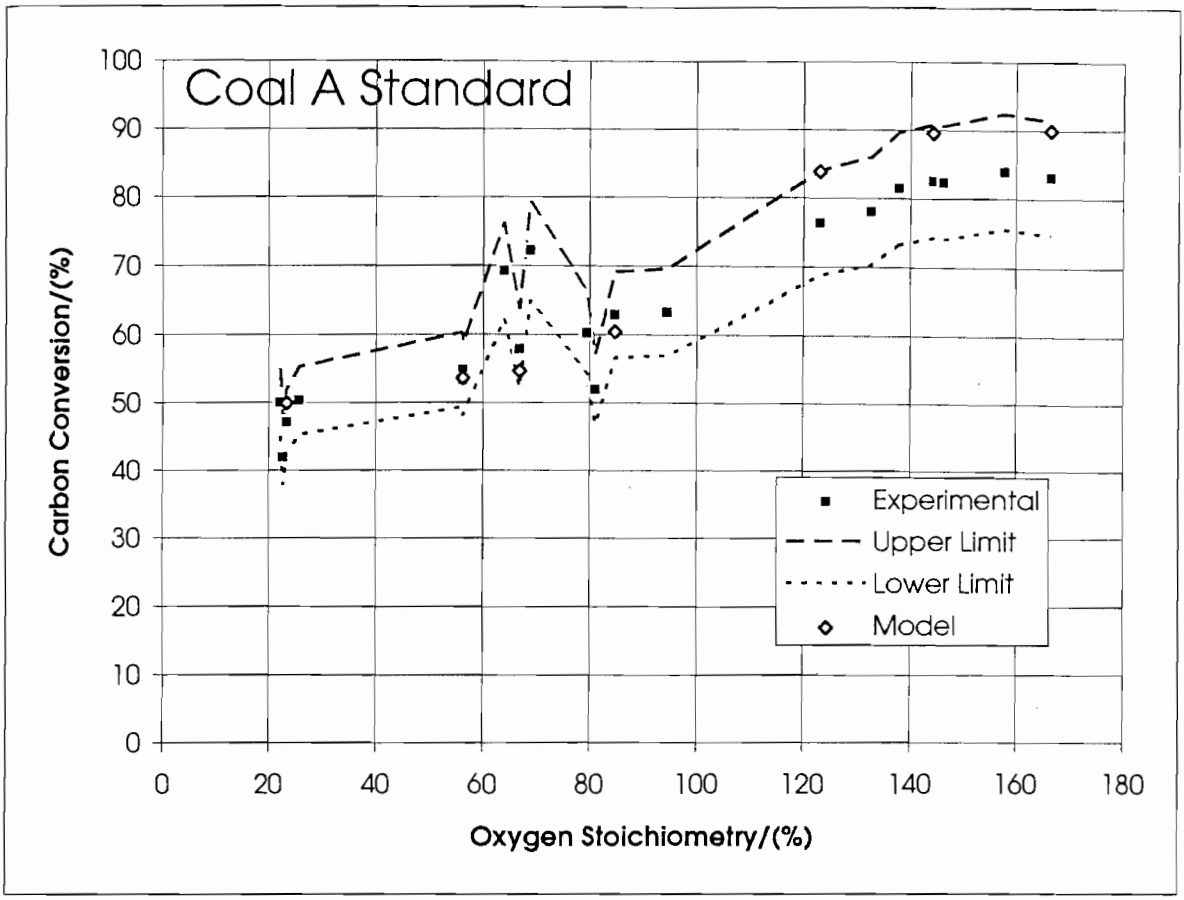

Figure 6.5a : Carbon conversion results and predictions for Coal A Standard runs

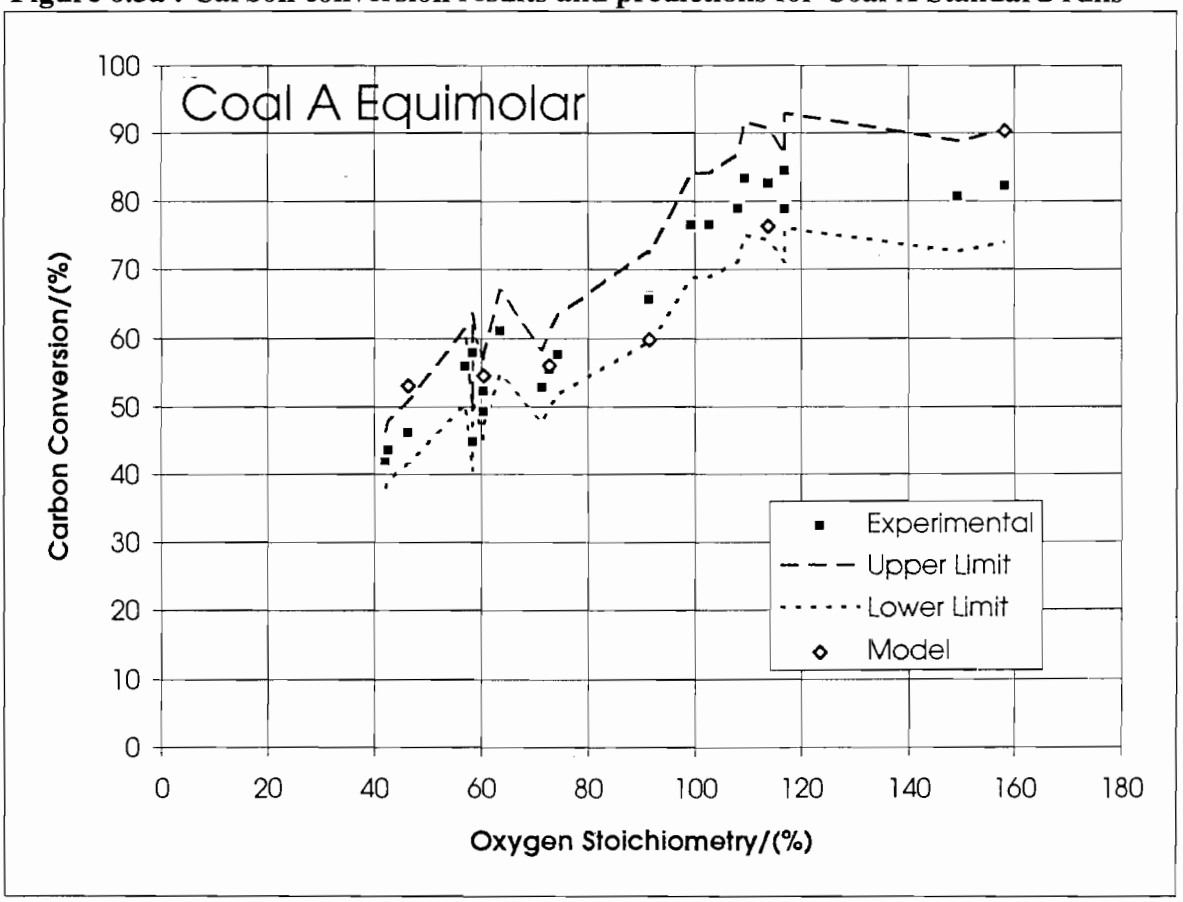

Figure 6.5b : Carbon conversion results and predictions for Coal A Equimolar runs

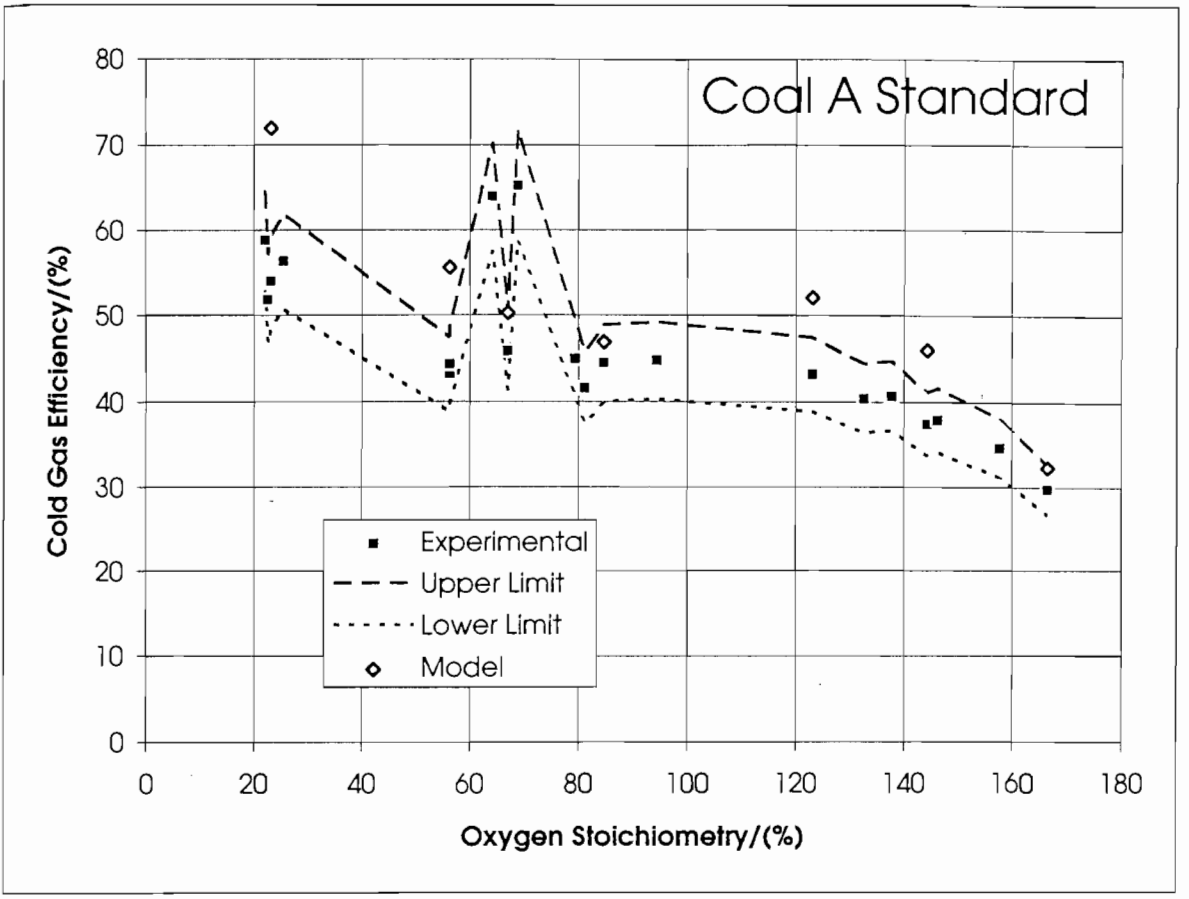

Figure 6.5c : Cold gas efficiency results and predictions for Coal A Standard runs

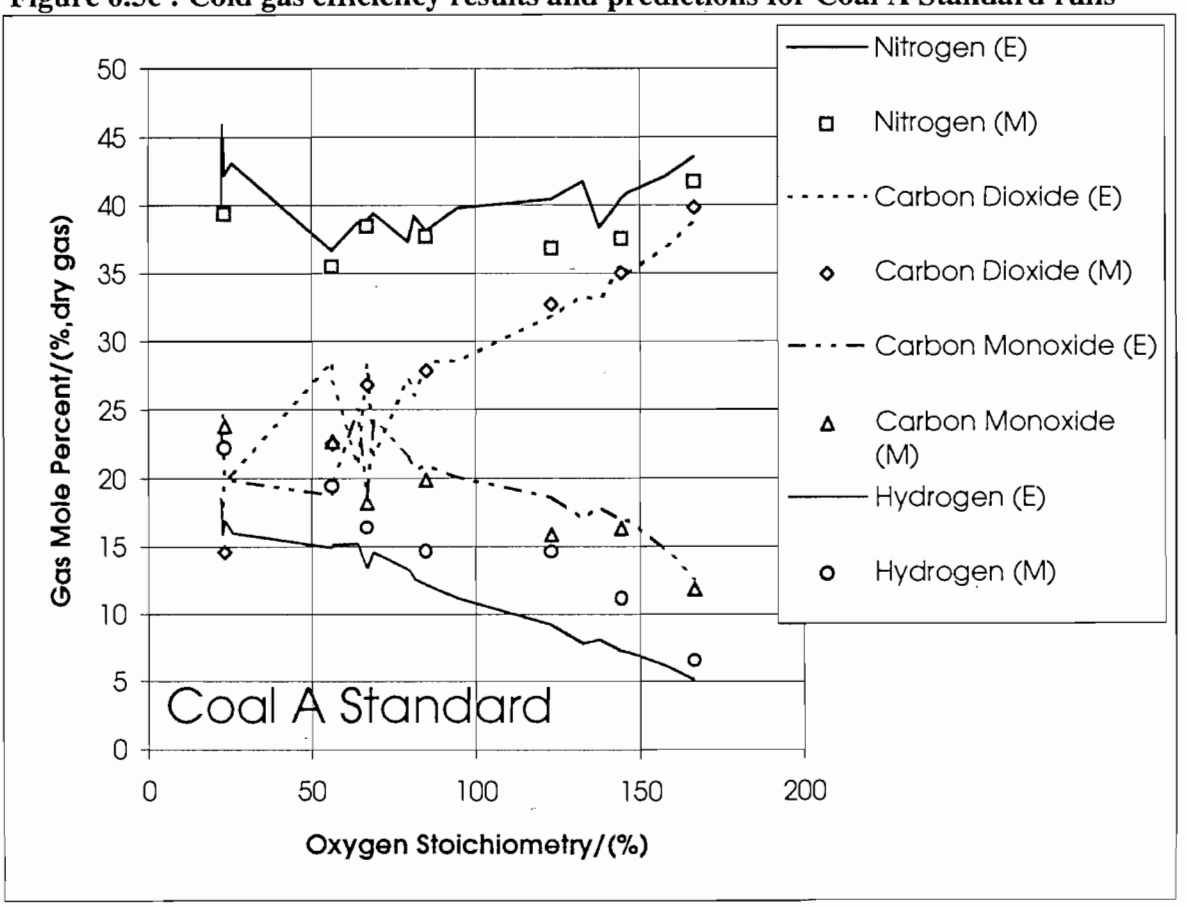

Figure 6.5d : Gas composition results and predictions for Coal A Standard runs

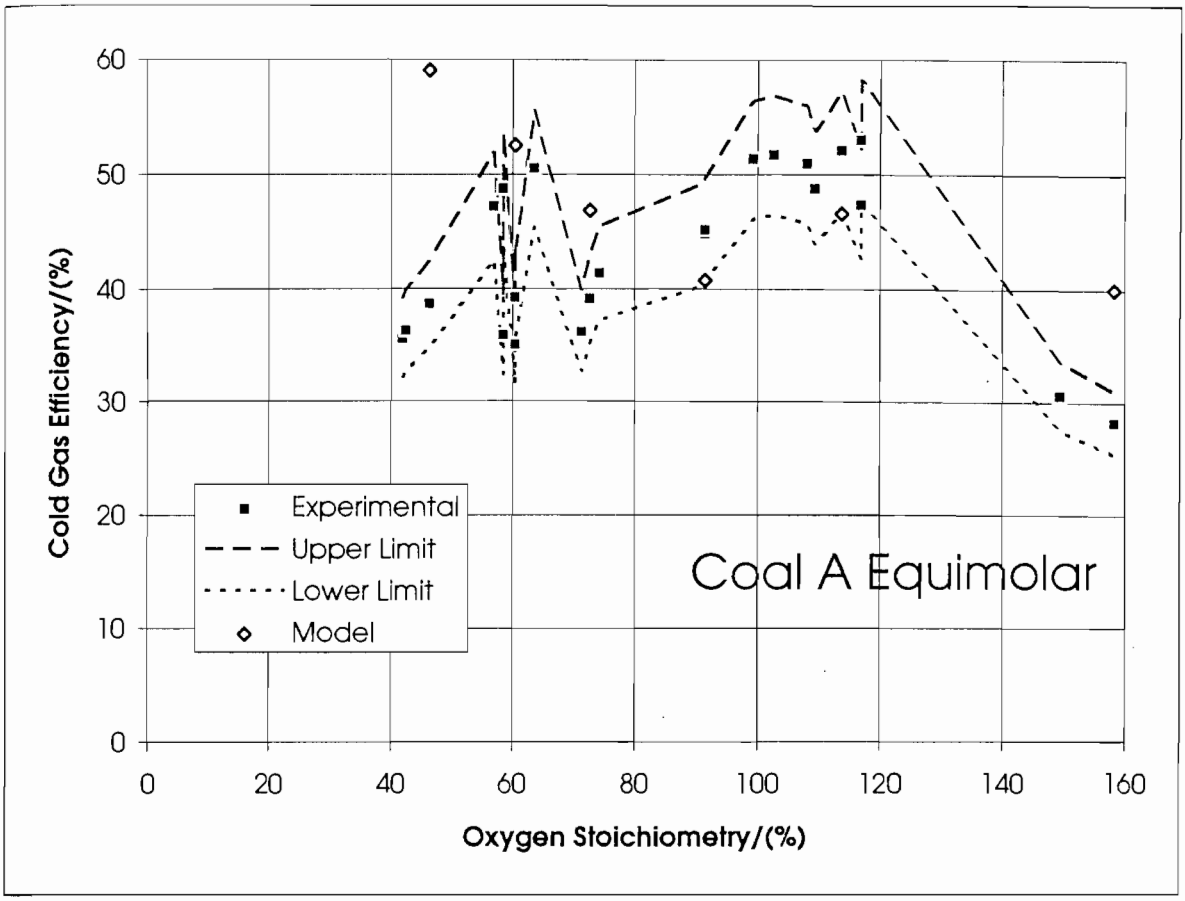

Figure 6.5e : Cold gas efficiency results and predictions for Coal A Equimolar runs

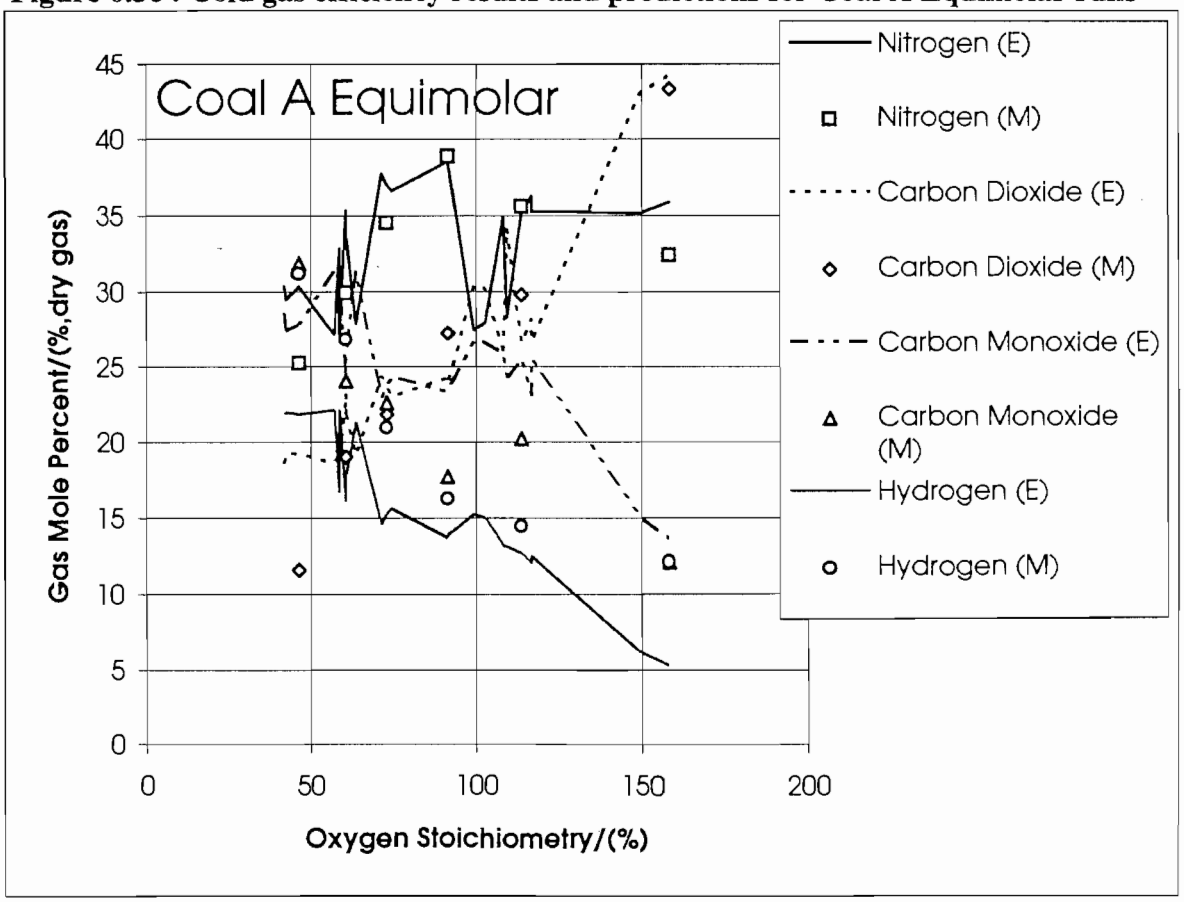

Figure 6.5f : Gas composition results and predictions for Coal A Equimolar runs

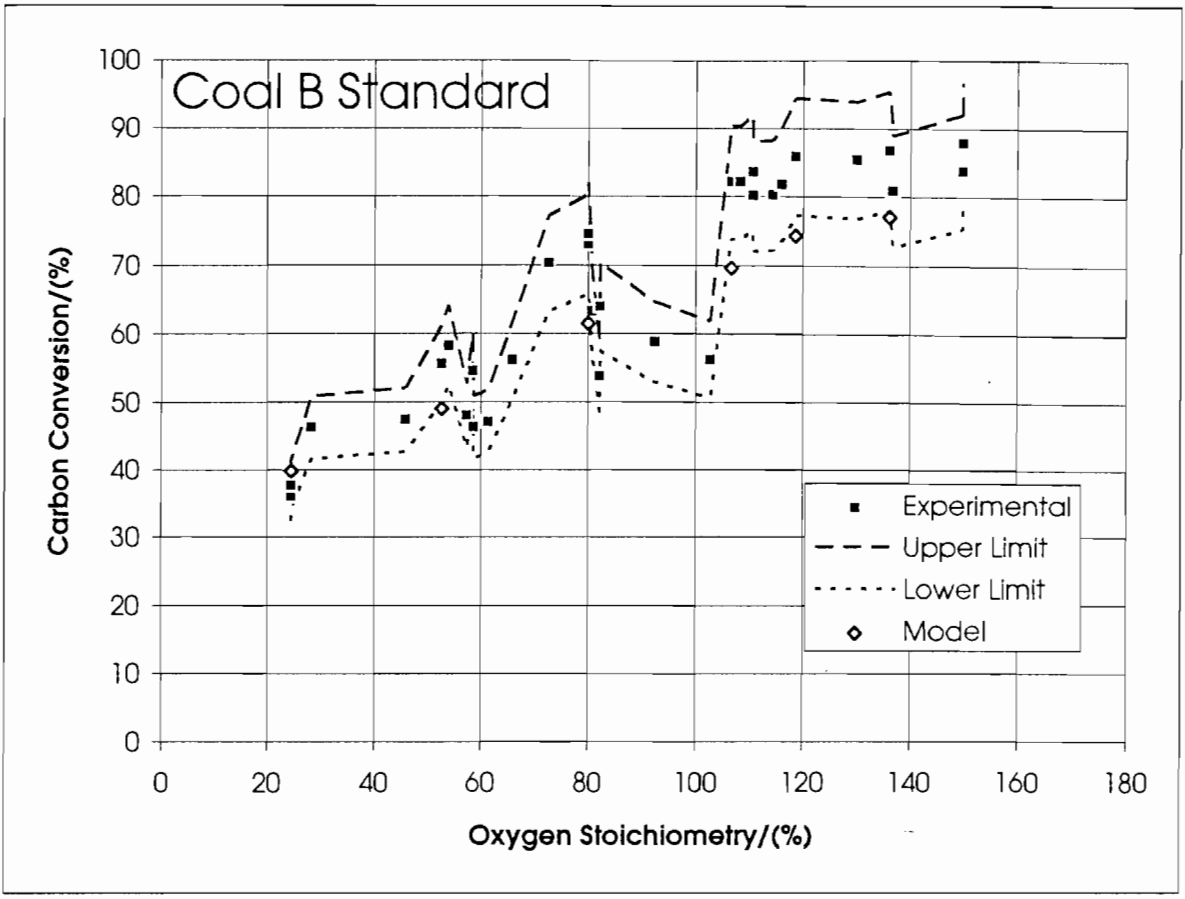

Figure 6.6a : Carbon conversion results and predictions for Coal B Standard runs

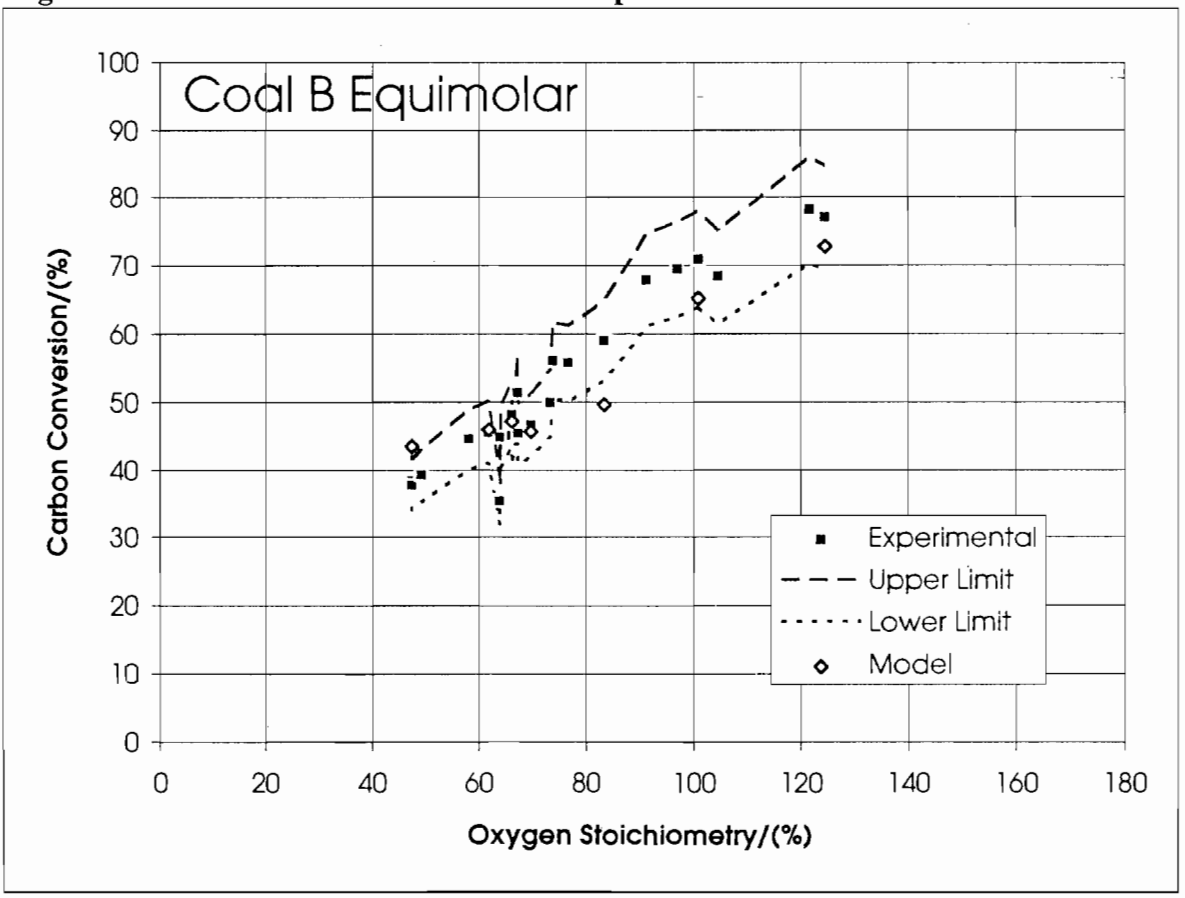

Figure 6.6b : Carbon conversion results and predictions for Coal B Equimolar runs

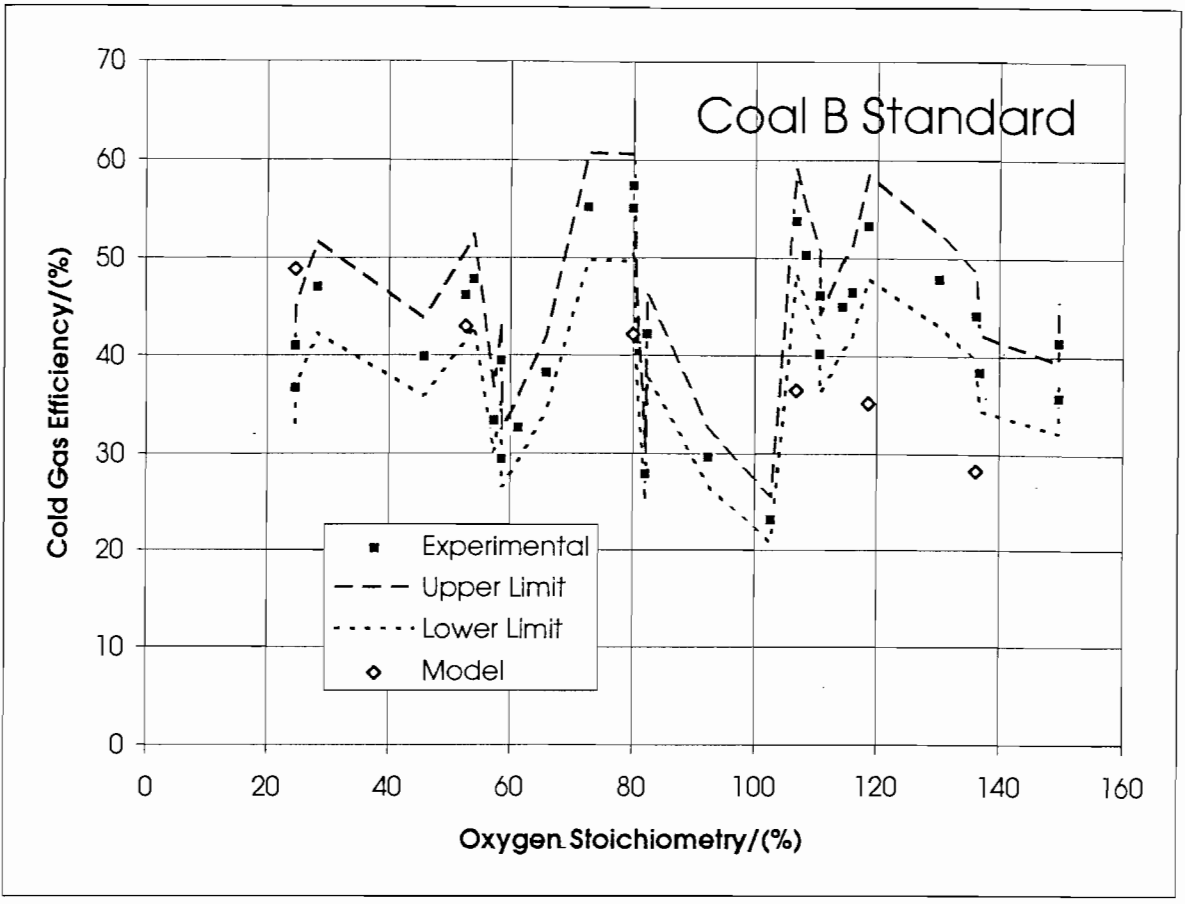

Figure 6.6c : Cold gas efficiency results and predictions for Coal B Standard runs

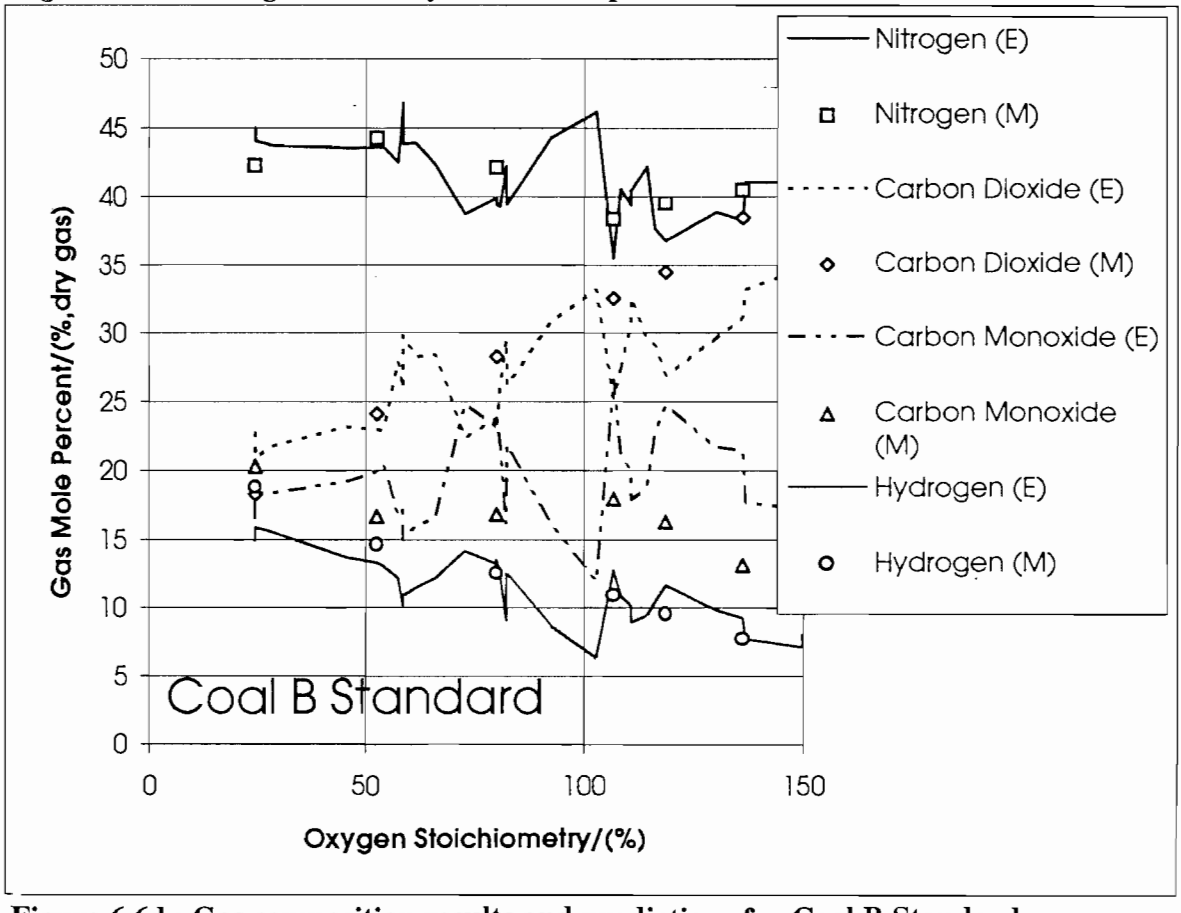

Figure 6.6d : Gas composition results and predictions for Coal B Standard runs

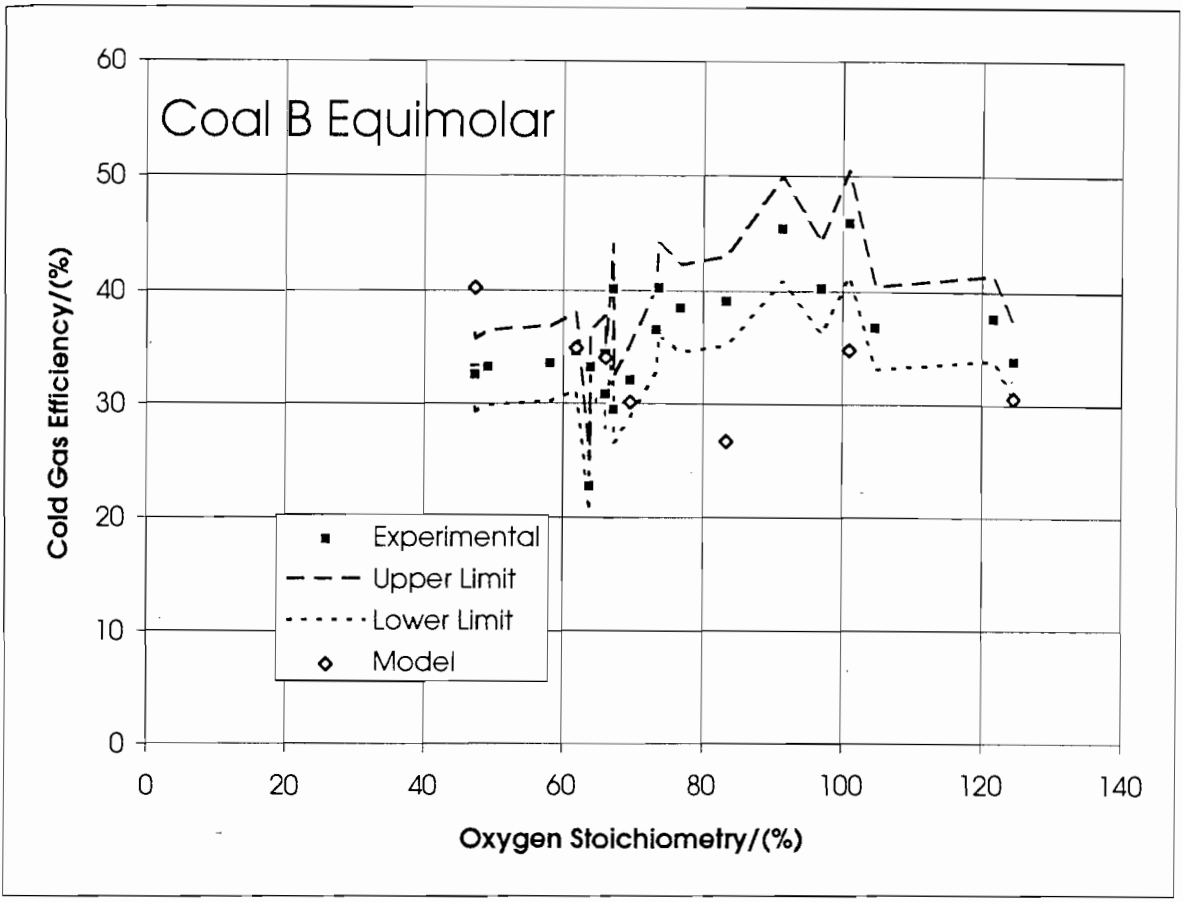

Figure 6.6e : Cold gas efficiency results and predictions for Coal B Equimolar runs

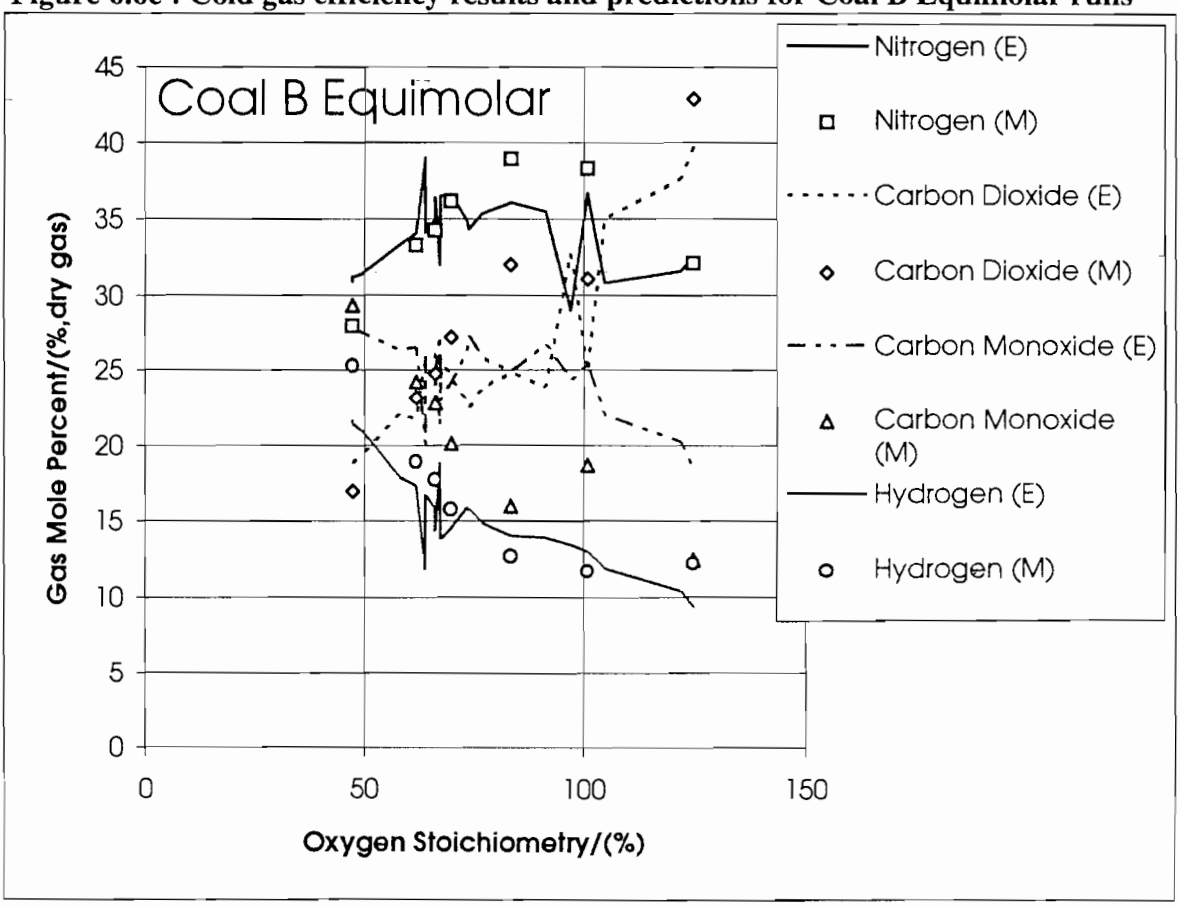

Figure 6.6f : Gas composition results and predictions for Coal B Equimolar runs

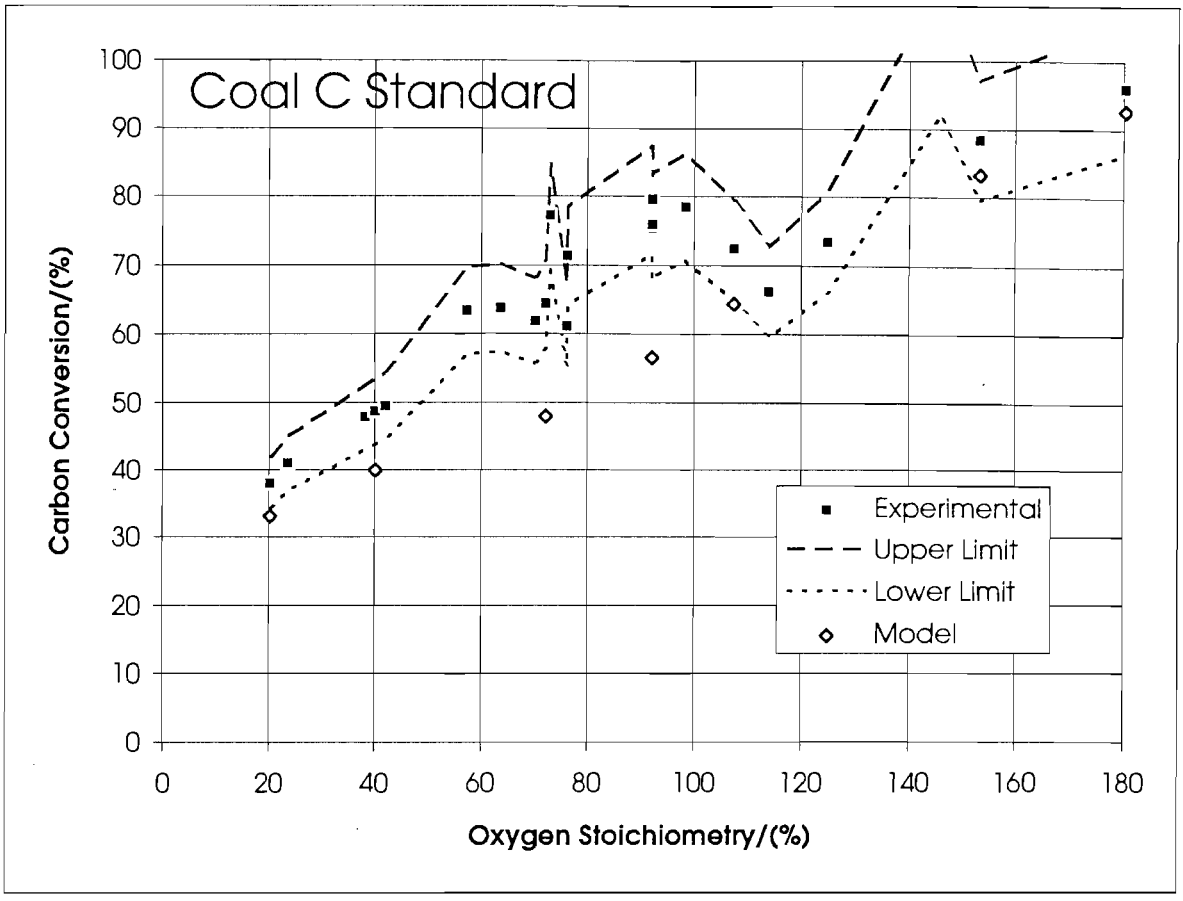

Figure 6.7a : Carbon conversion results and predictions for Coal C Standard runs

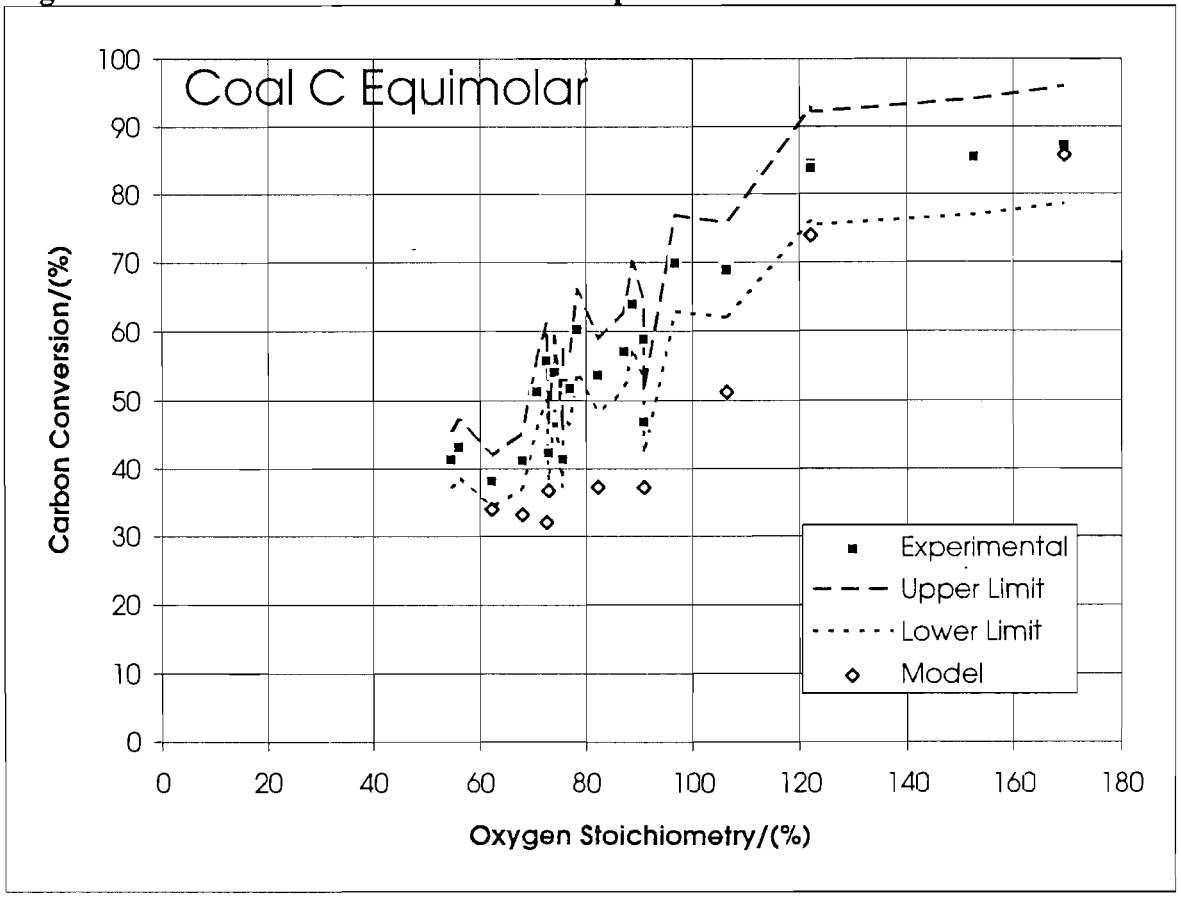

Figure 6.7b : Carbon conversion results and predictions for Coal C Equimolar runs

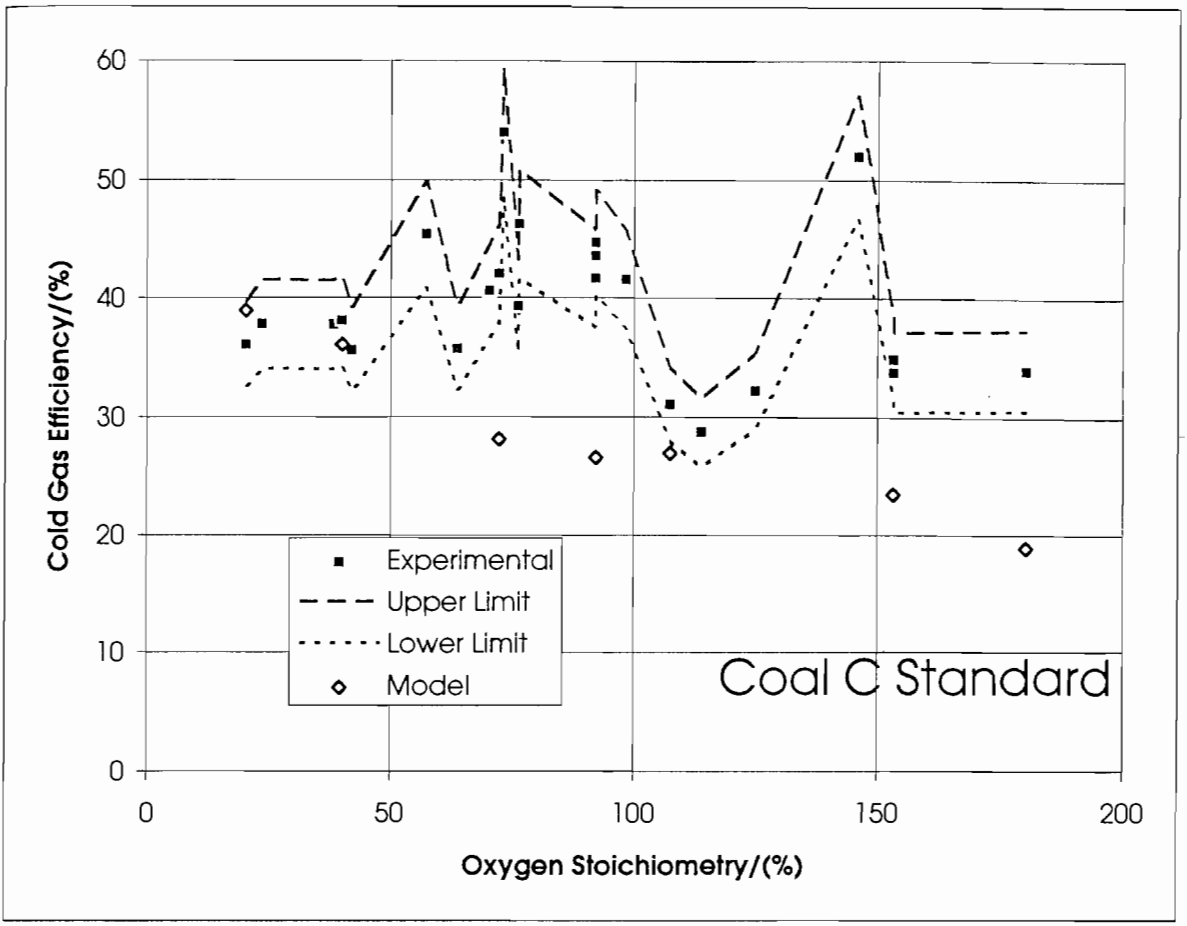

Figure 6.7c : Cold gas efficiency results and predictions for Coal C Standard runs

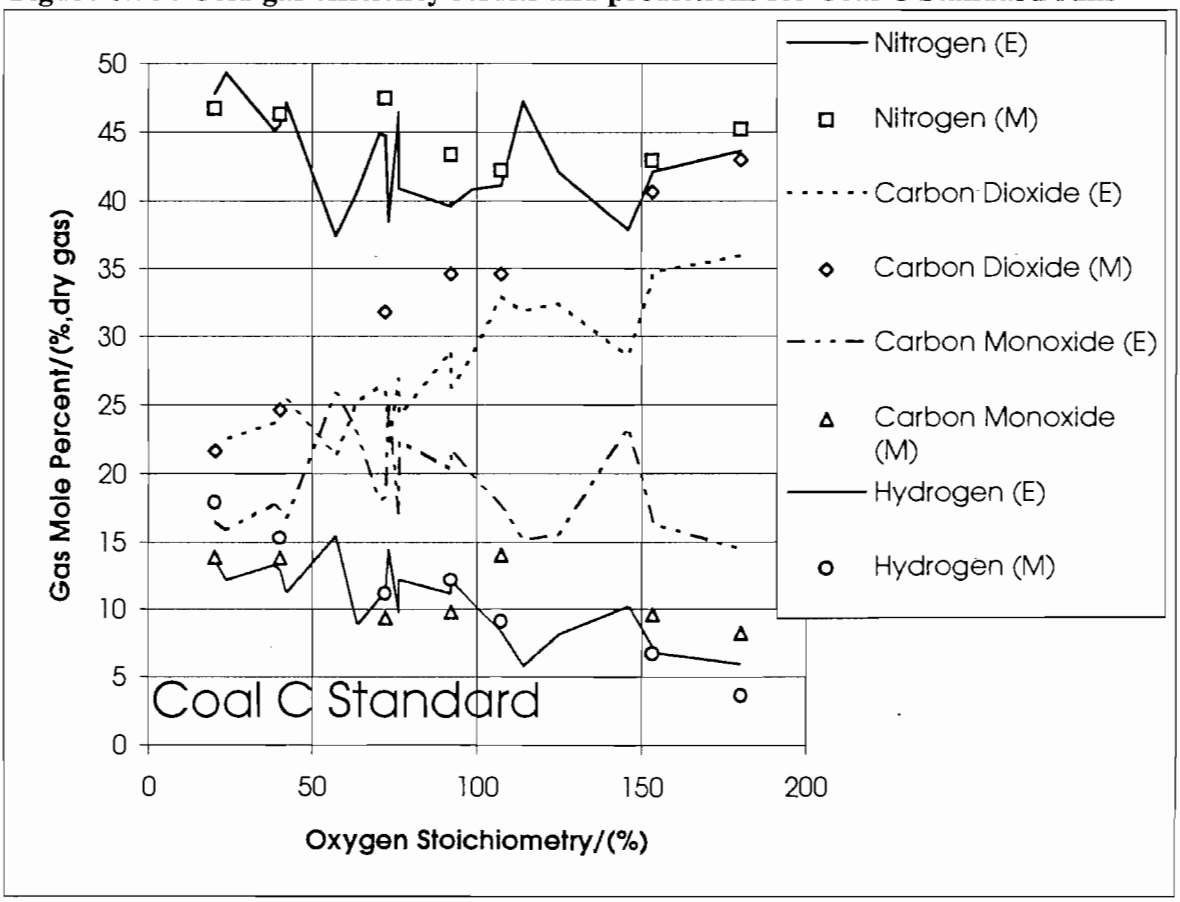

Figure 6.7d : Gas composition results and predictions for Coal C Standard runs

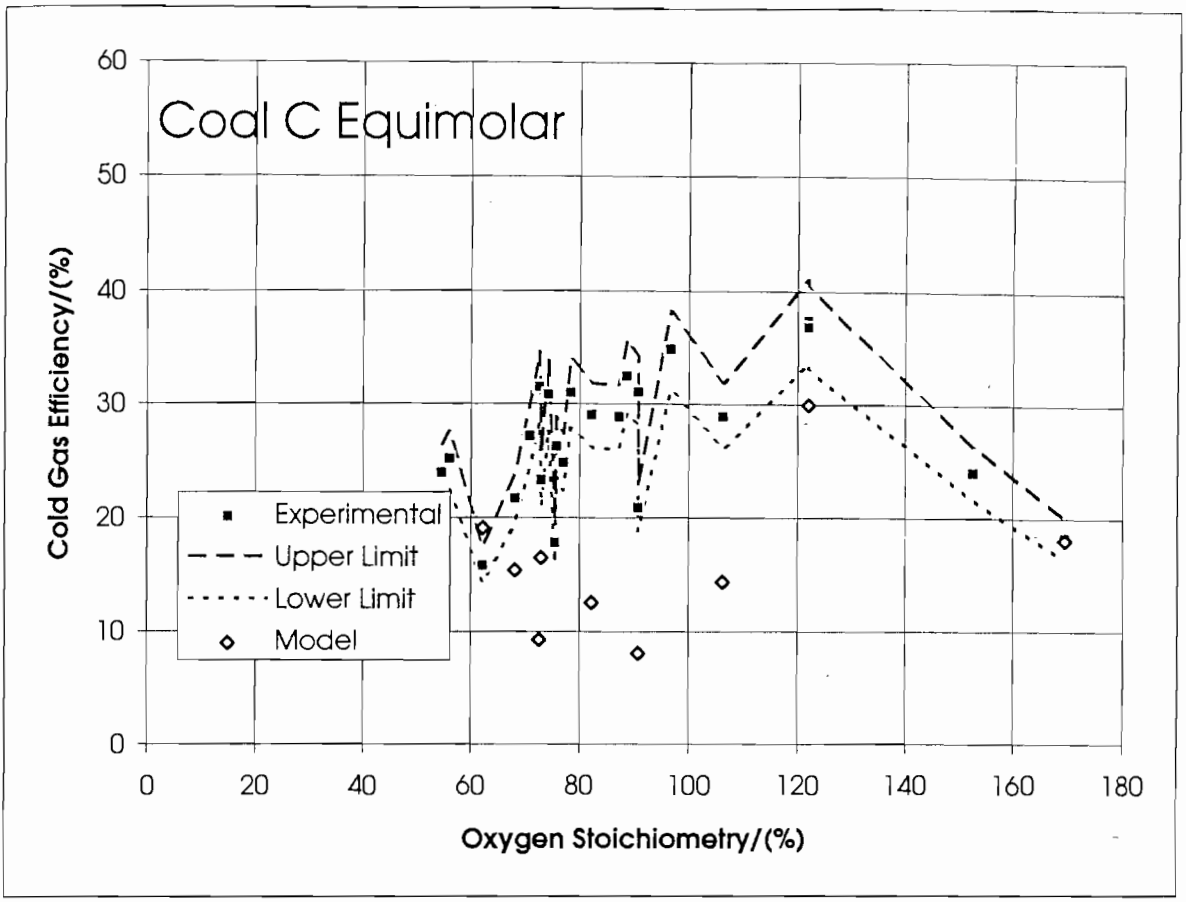

Figure 6.7e : Cold gas efficiency results and predictions for Coal C Equimolar runs

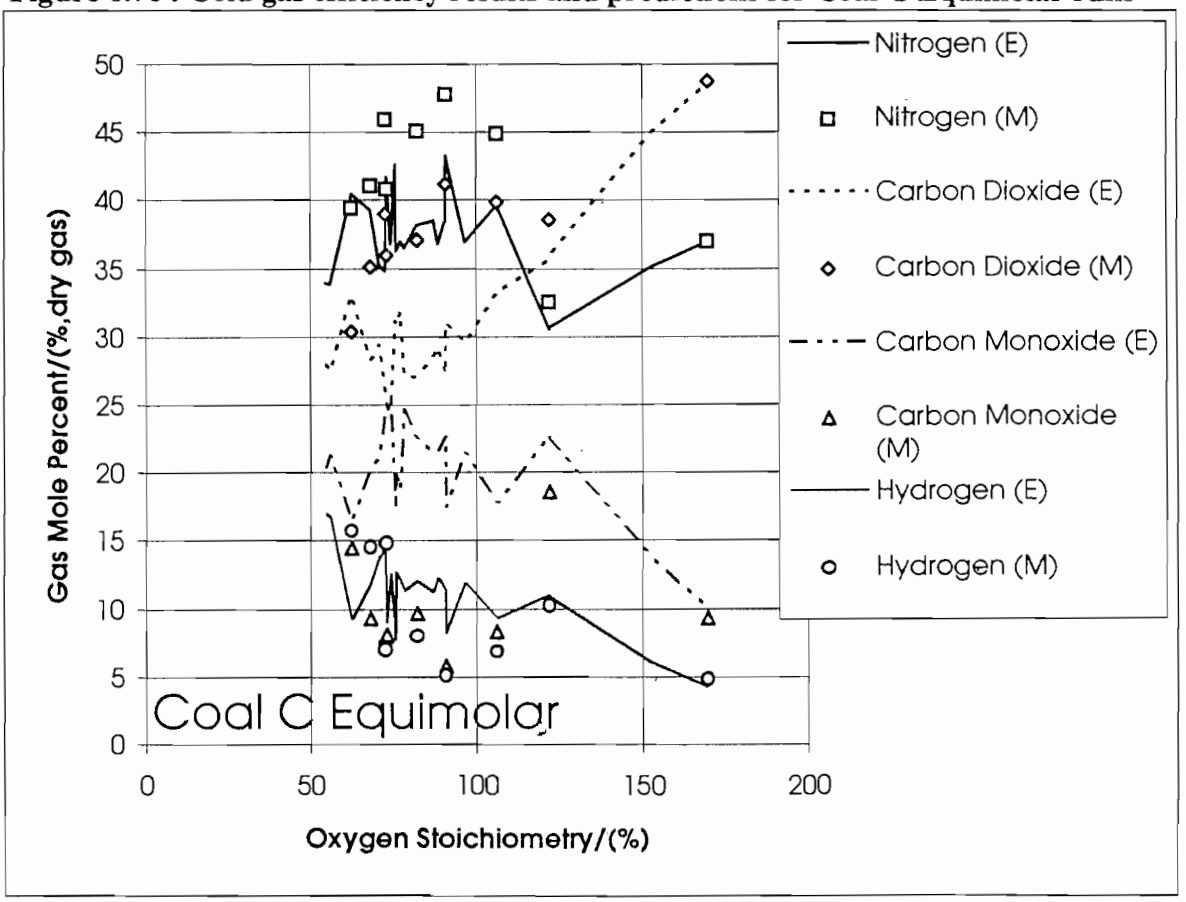

Figure 6.7f : Gas composition results and predictions for Coal C Equimolar runs

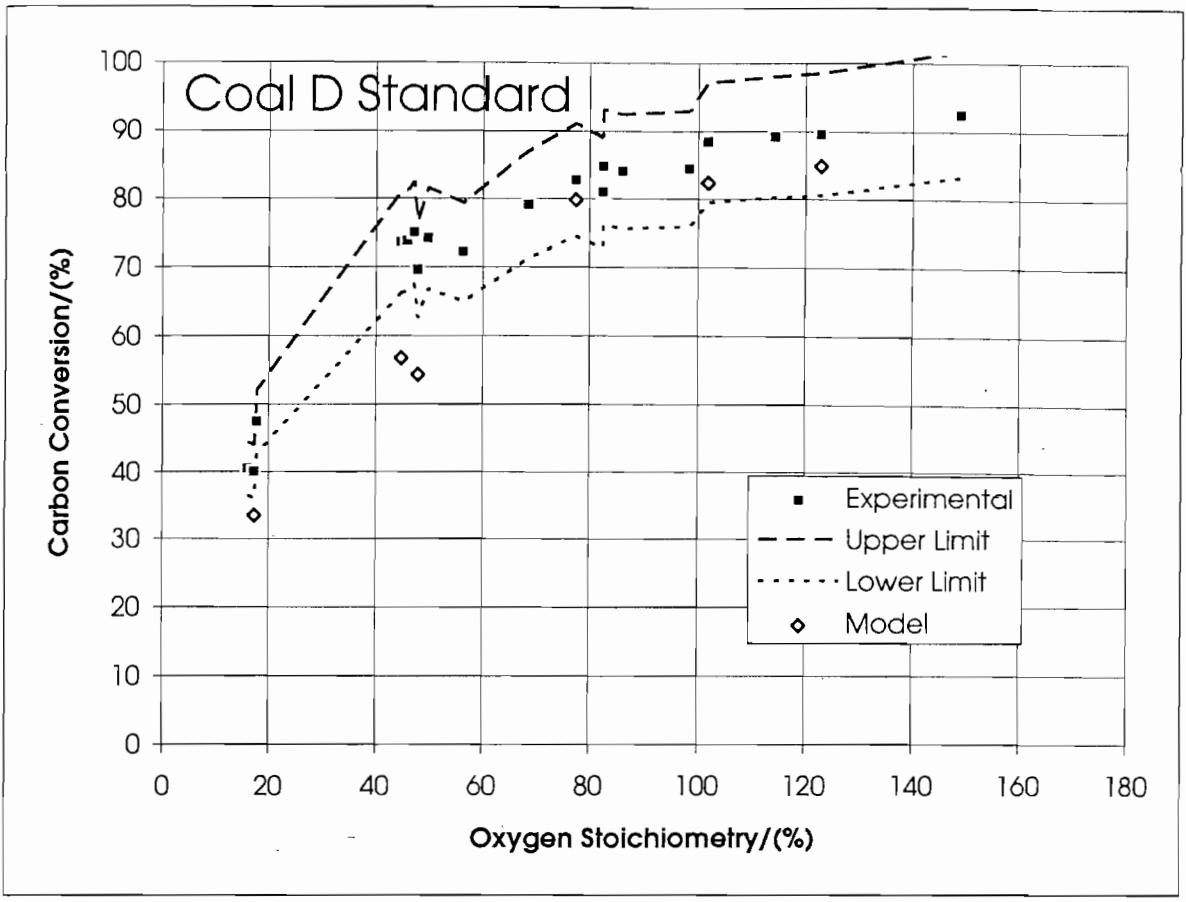

Figure 6.8a : Carbon conversion results and predictions for Coal D Standard runs

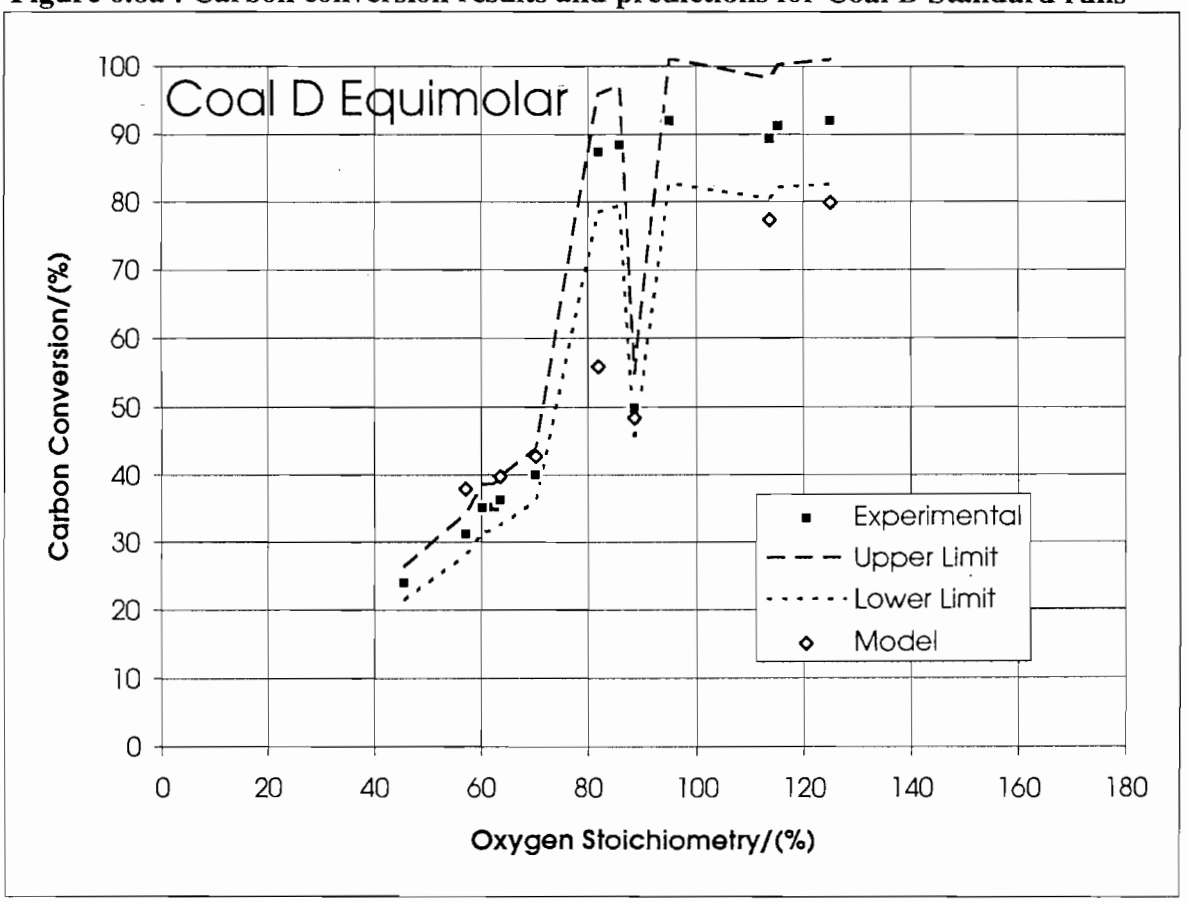

Figure 6.8b : Carbon conversion results and predictions for Coal D Equimolar runs

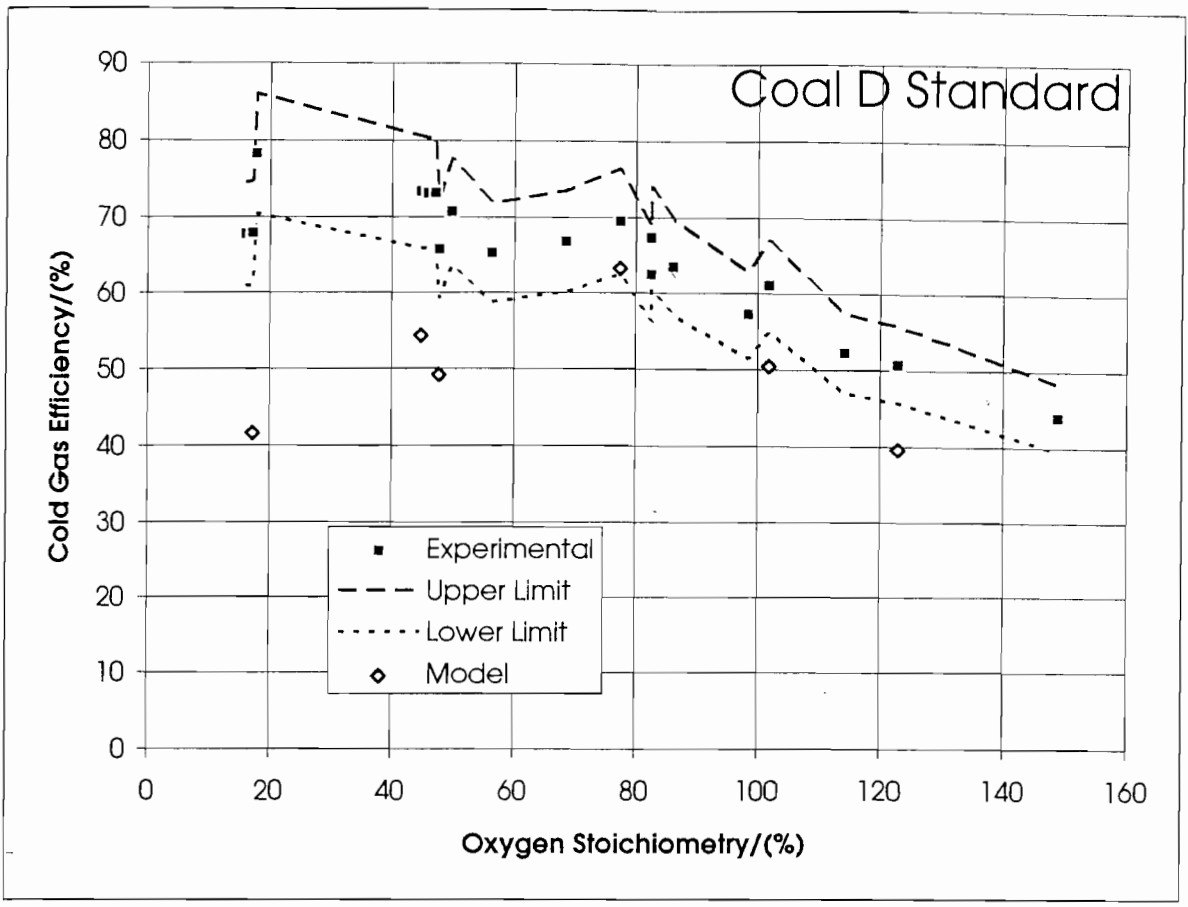

Figure 6.8c : Cold gas efficiency results and predictions for Coal D Standard runs

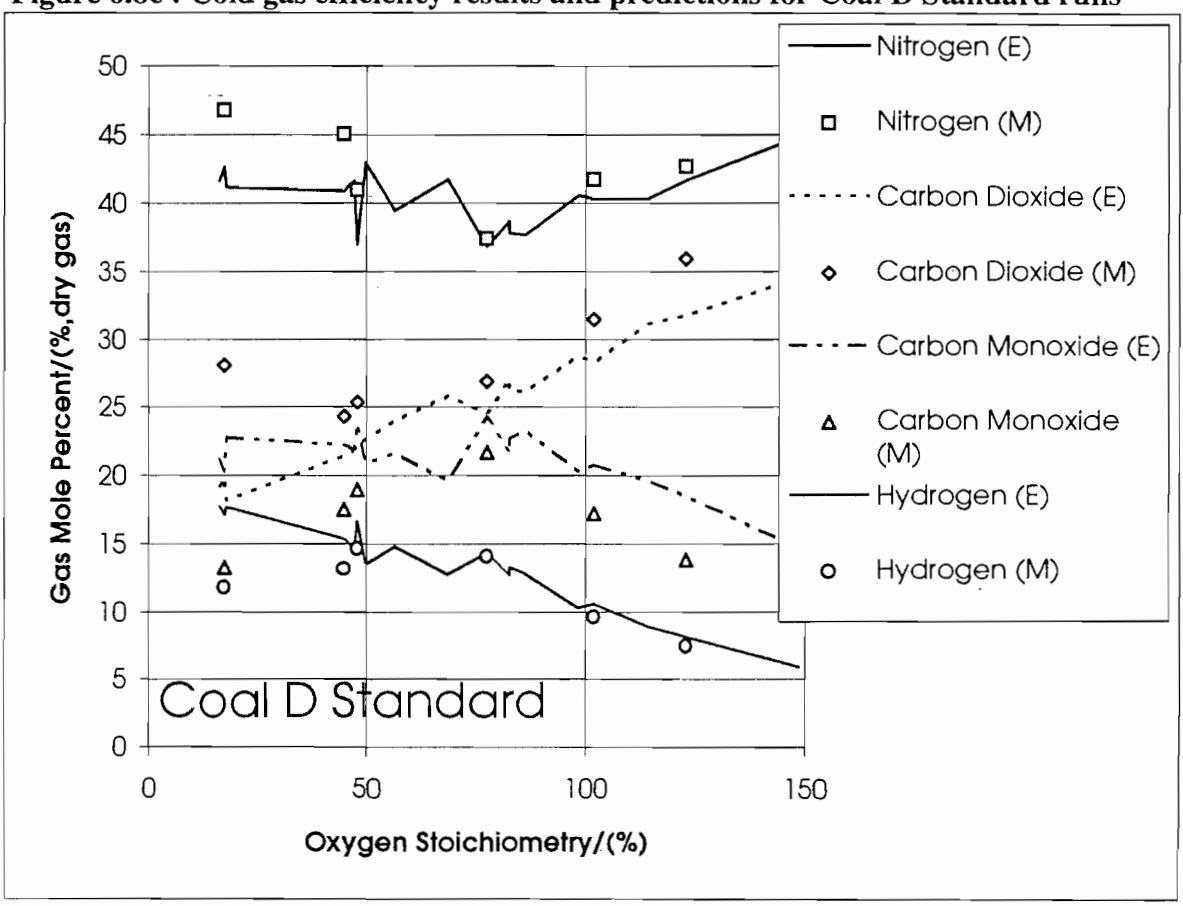

Figure 6.8d : Gas composition results and predictions for Coal D Standard runs

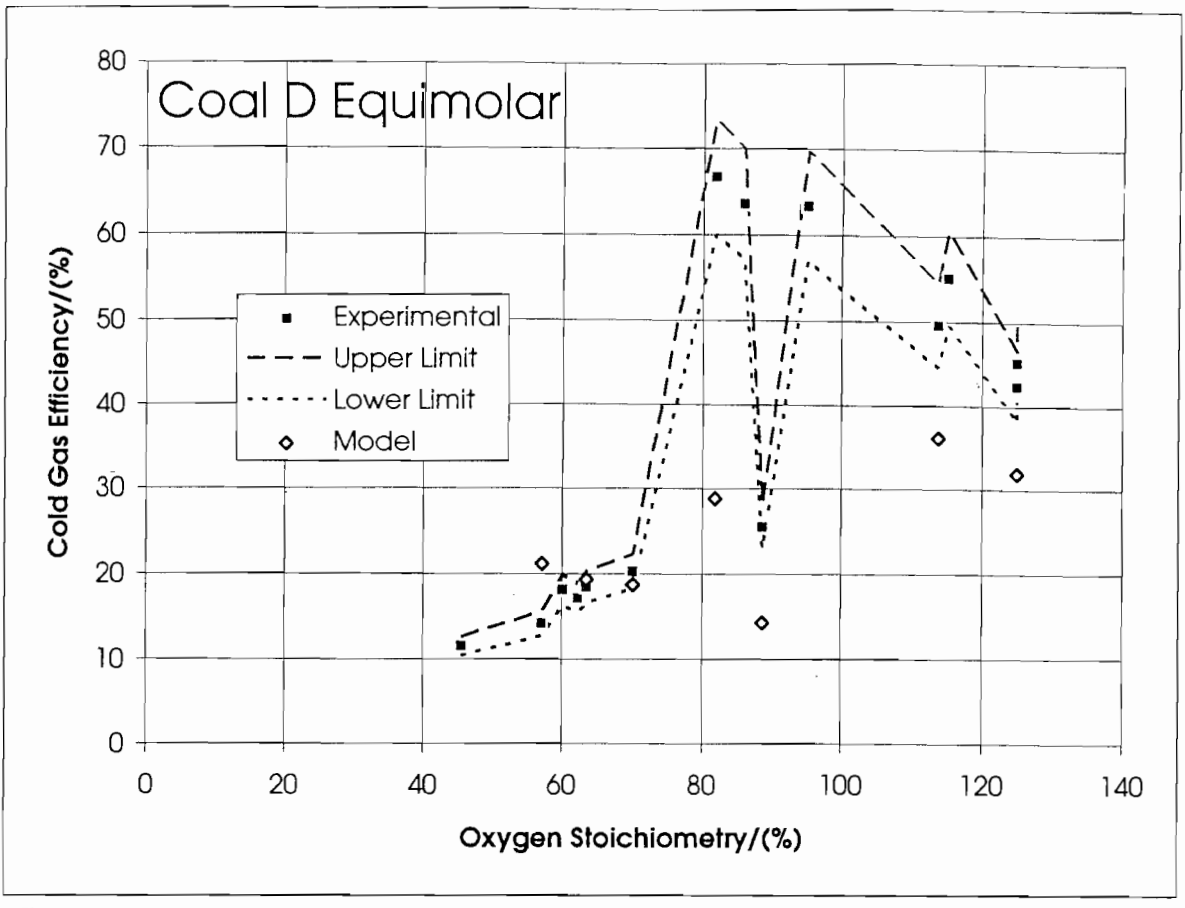

Figure 6.8e : Cold gas efficiency results and predictions for Coal D Equimolar runs

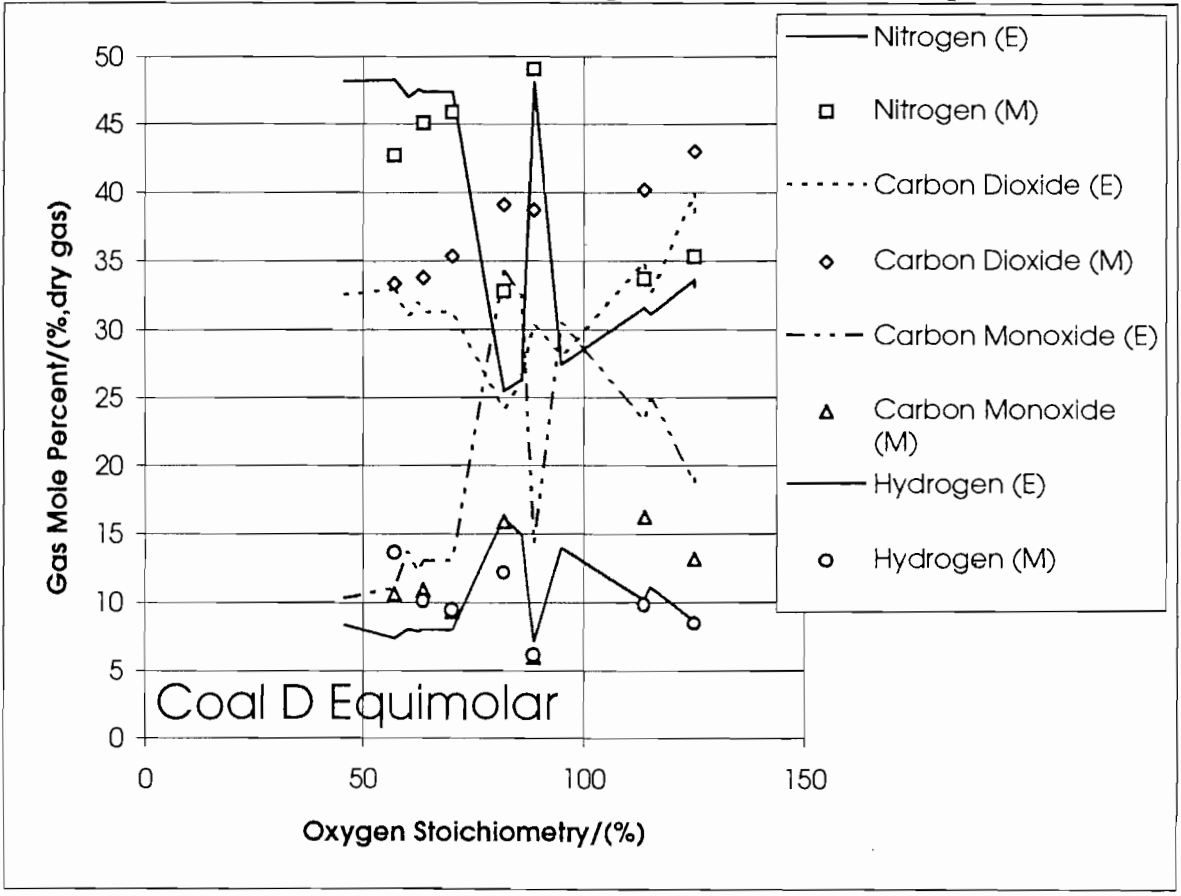

Figure 6.8f : Gas composition results and predictions for Coal D Equimolar runs

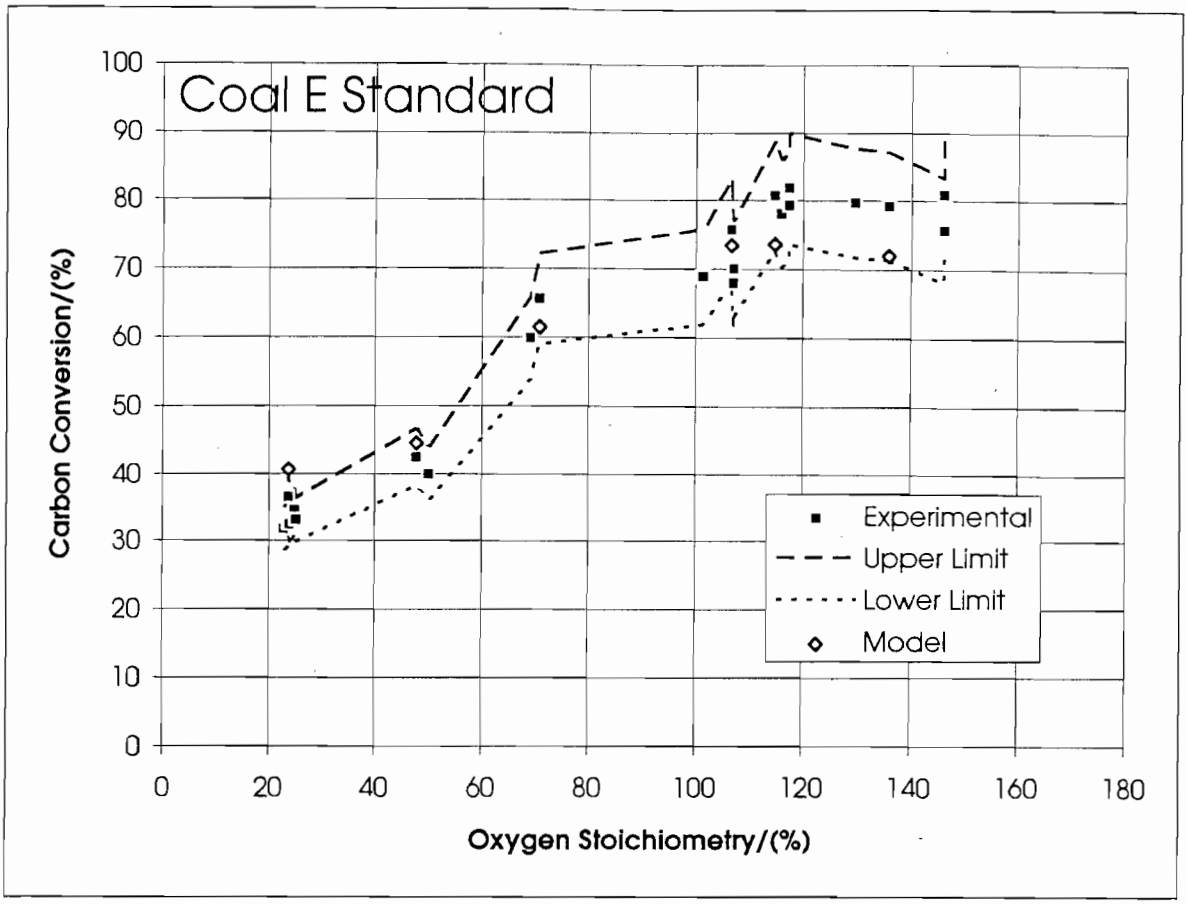

Figure 6.9a : Carbon conversion results and predictions for Coal E Standard runs

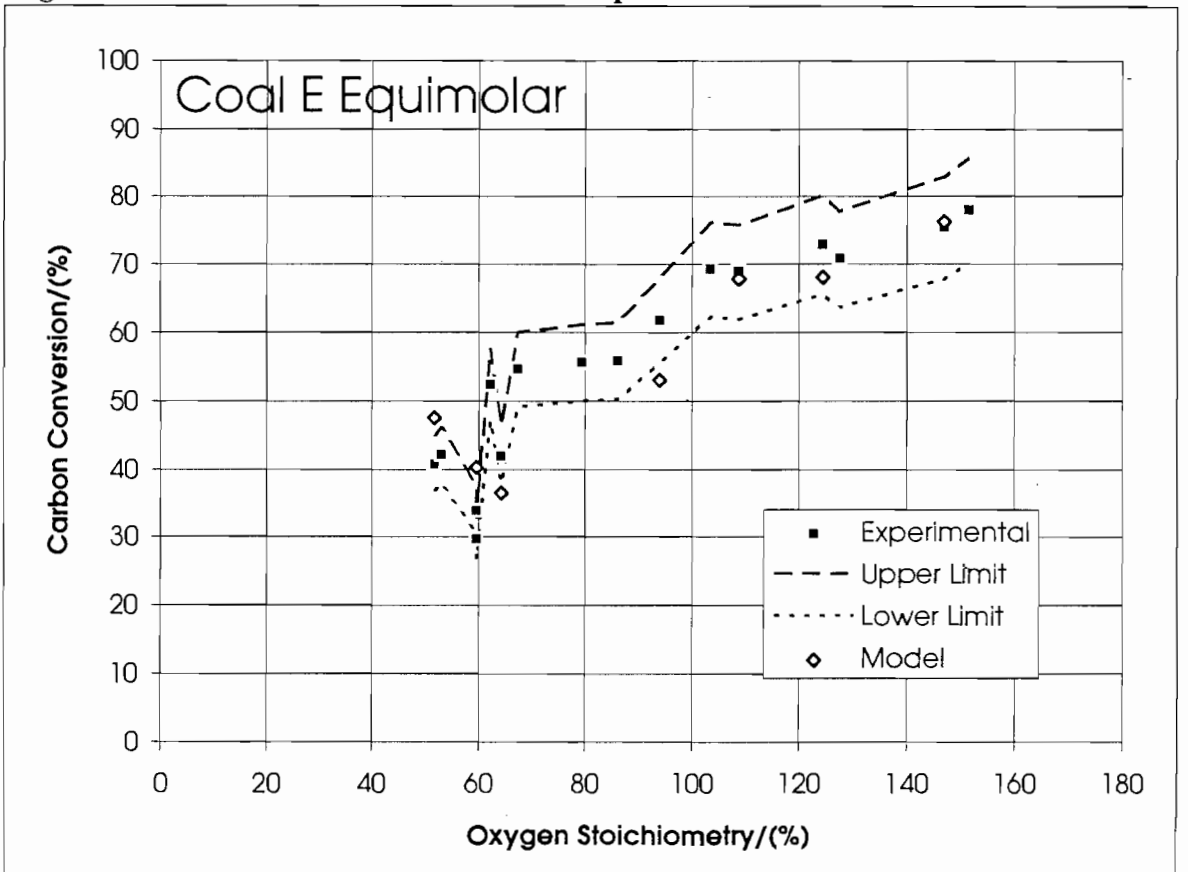

Figure 6.9b : Carbon conversion results and predictions for Coal E Equimolar runs

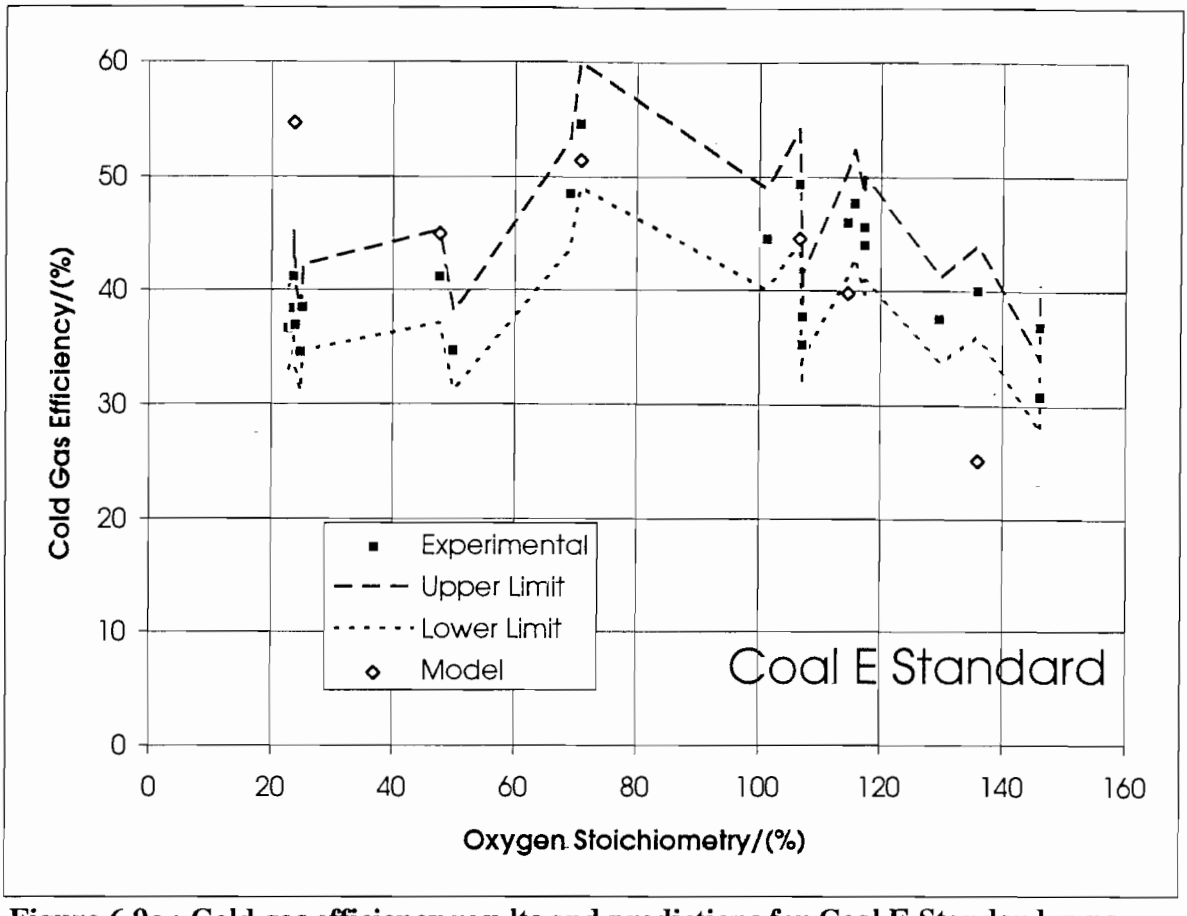

Figure 6.9c : Cold gas efficiency results and predictions for Coal E Standard runs

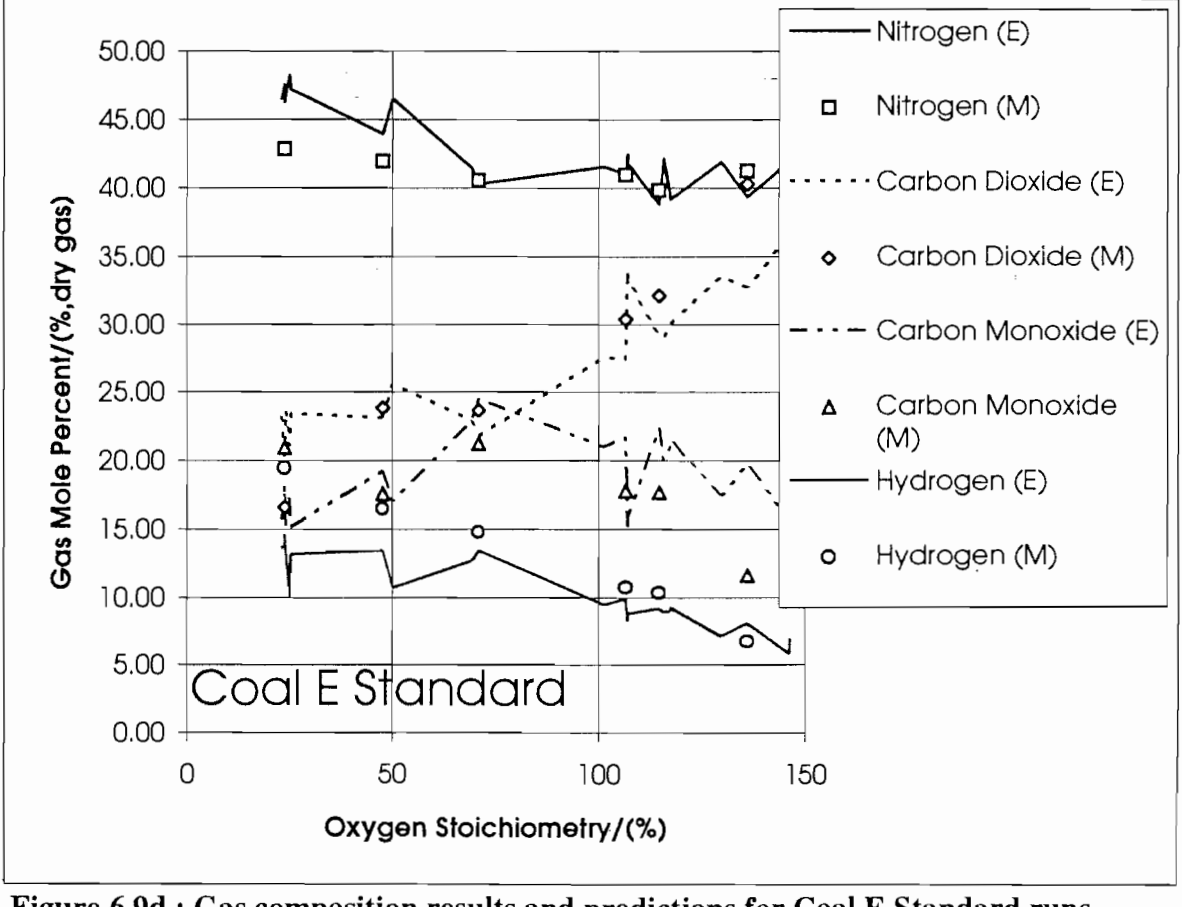

Figure 6.9d : Gas composition results and predictions for Coal E Standard runs

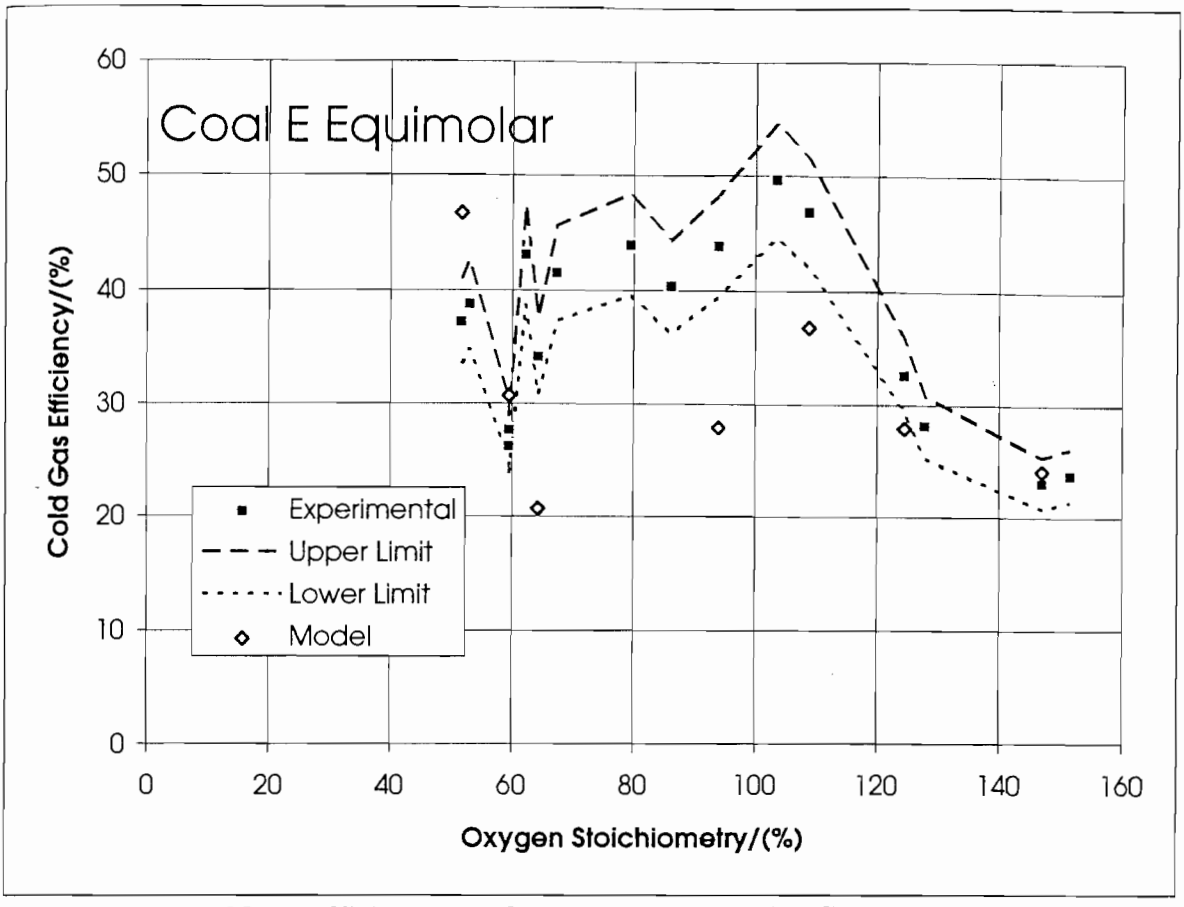

Figure 6.9e : Cold gas efficiency results and predictions for Coal E Equimolar runs

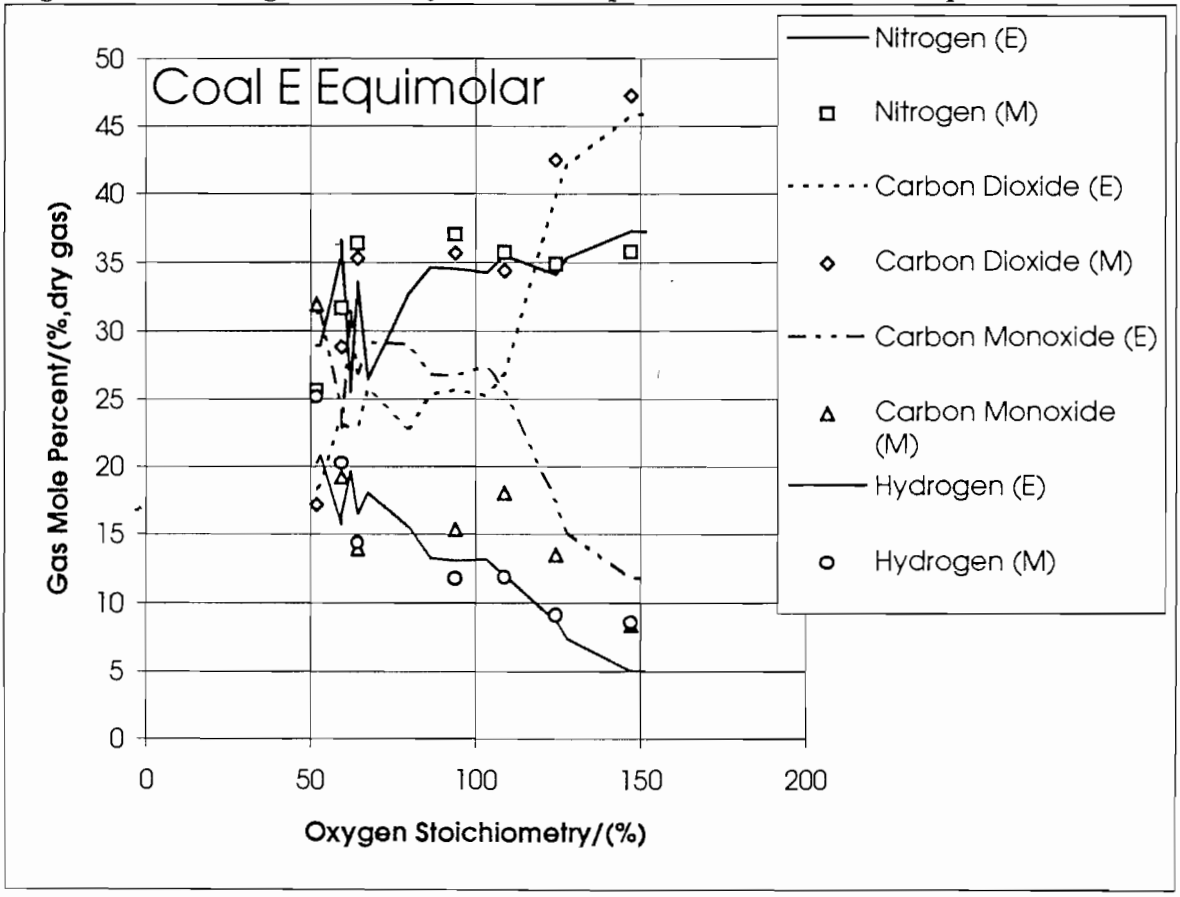

Figure 6.9f : Gas composition results and predictions for Coal E Equimolar runs

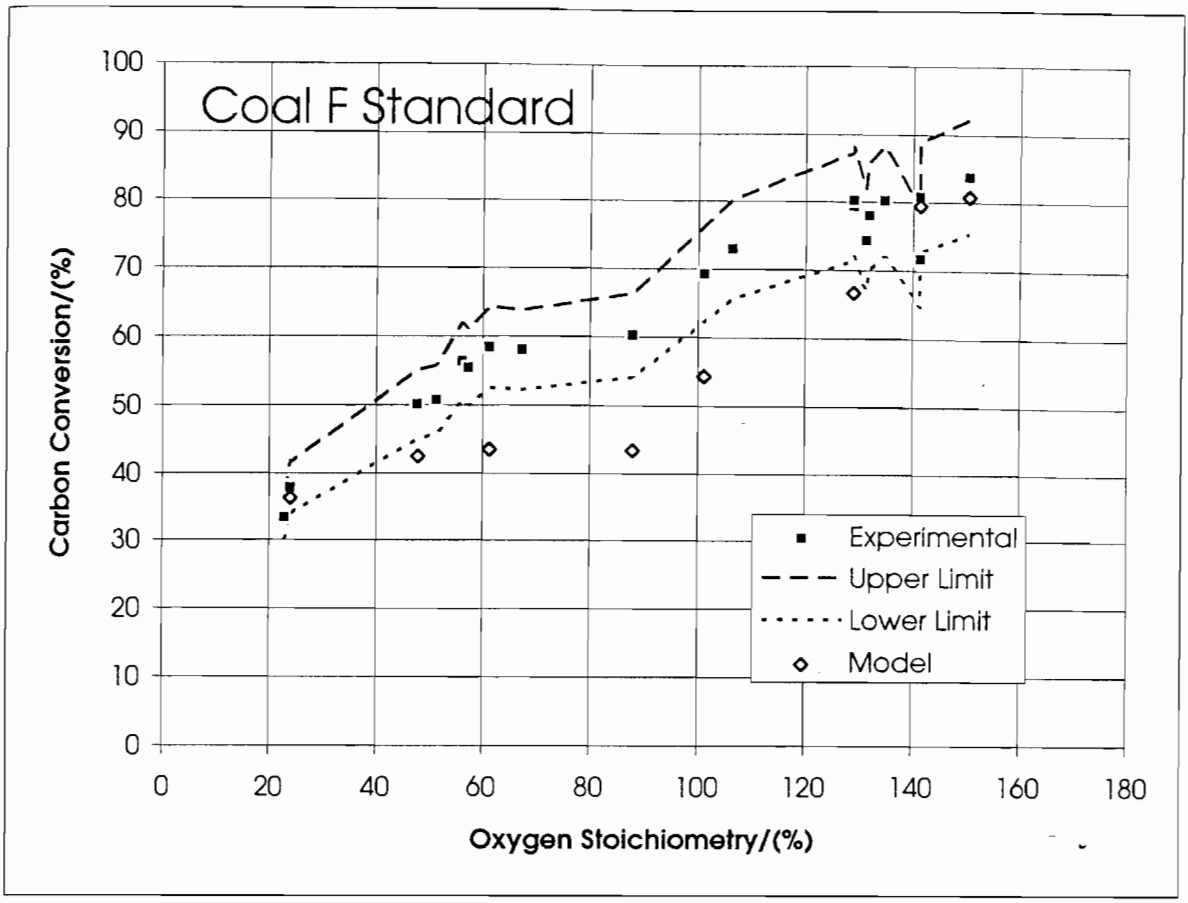

Figure 6.10a : Carbon conversion results and predictions for Coal F Standard runs

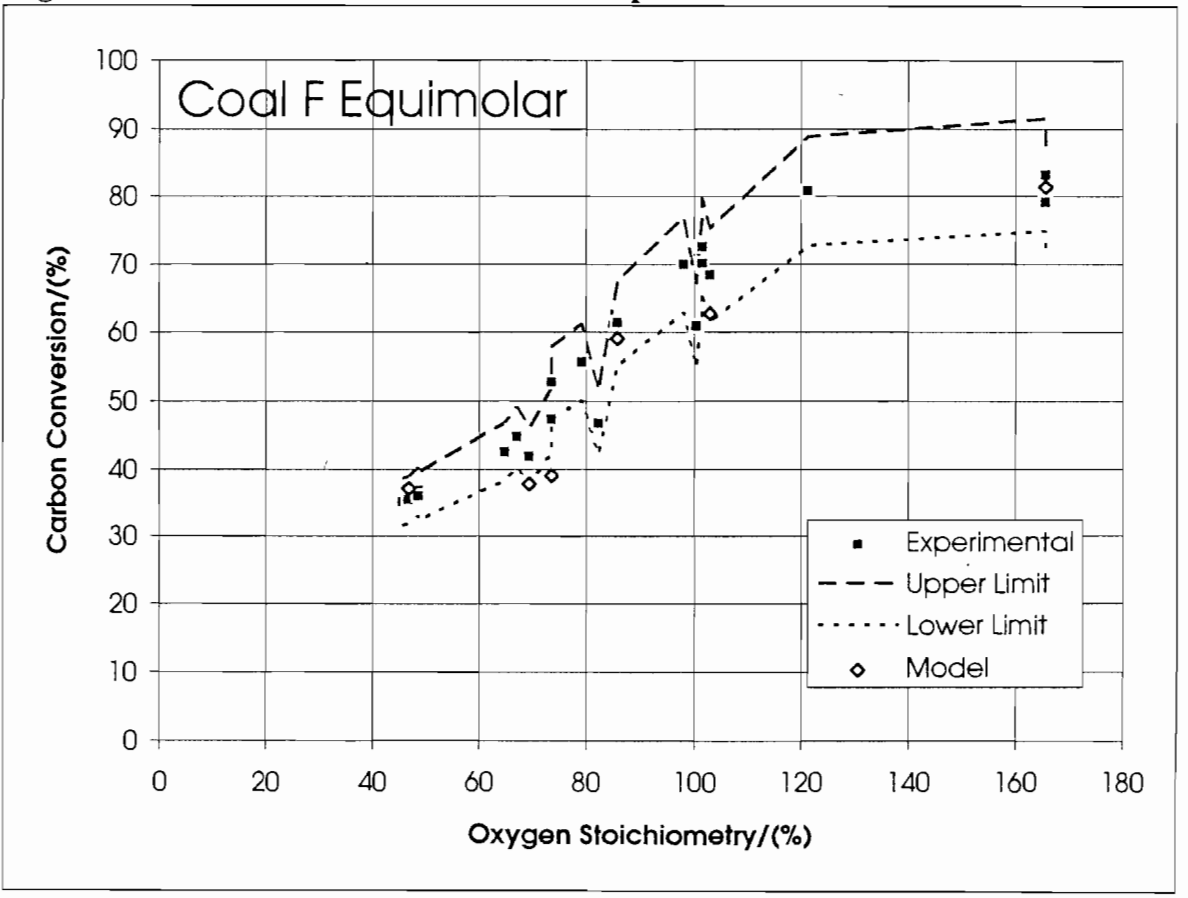

Figure 6.10b : Carbon conversion results and predictions for Coal F Equimolar runs

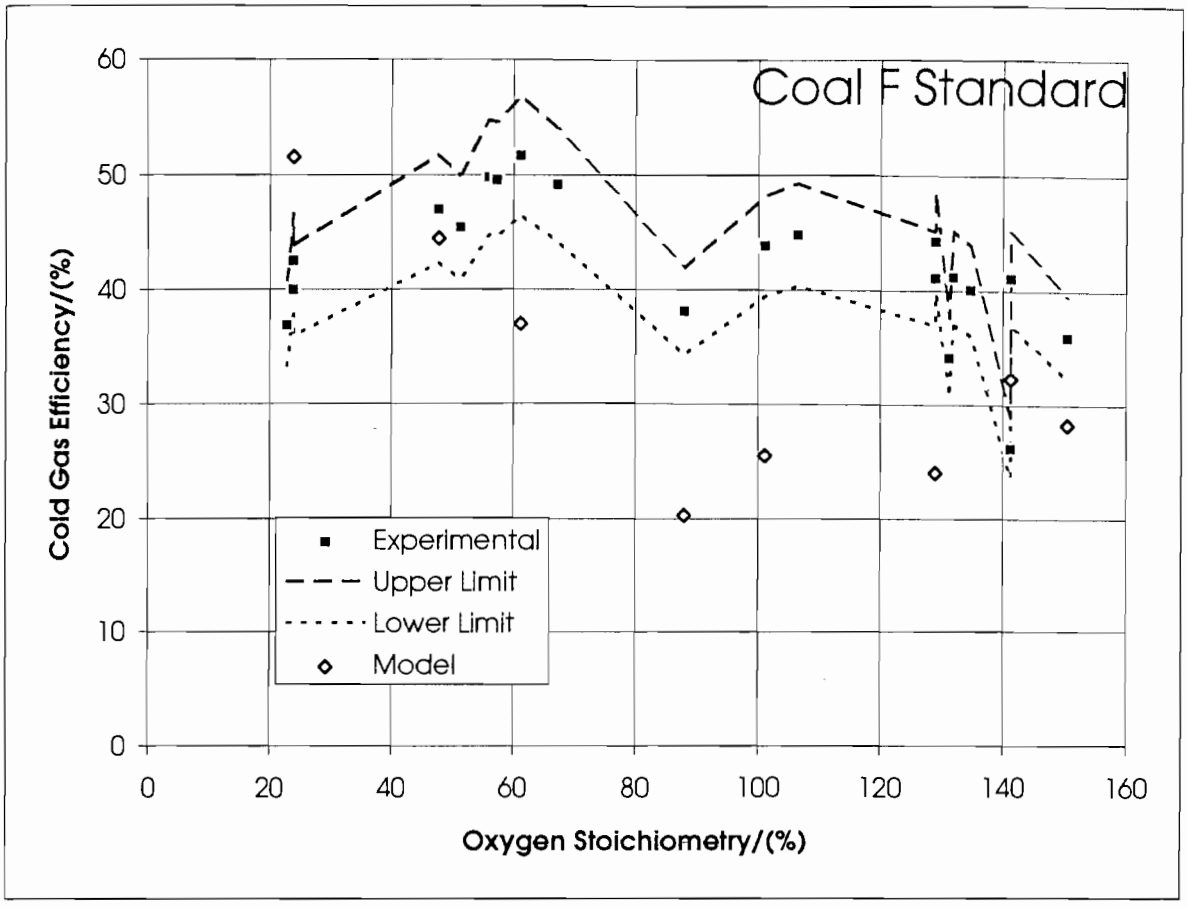

Figure 6.10c : Cold gas efficiency results and predictions for Coal F Standard runs

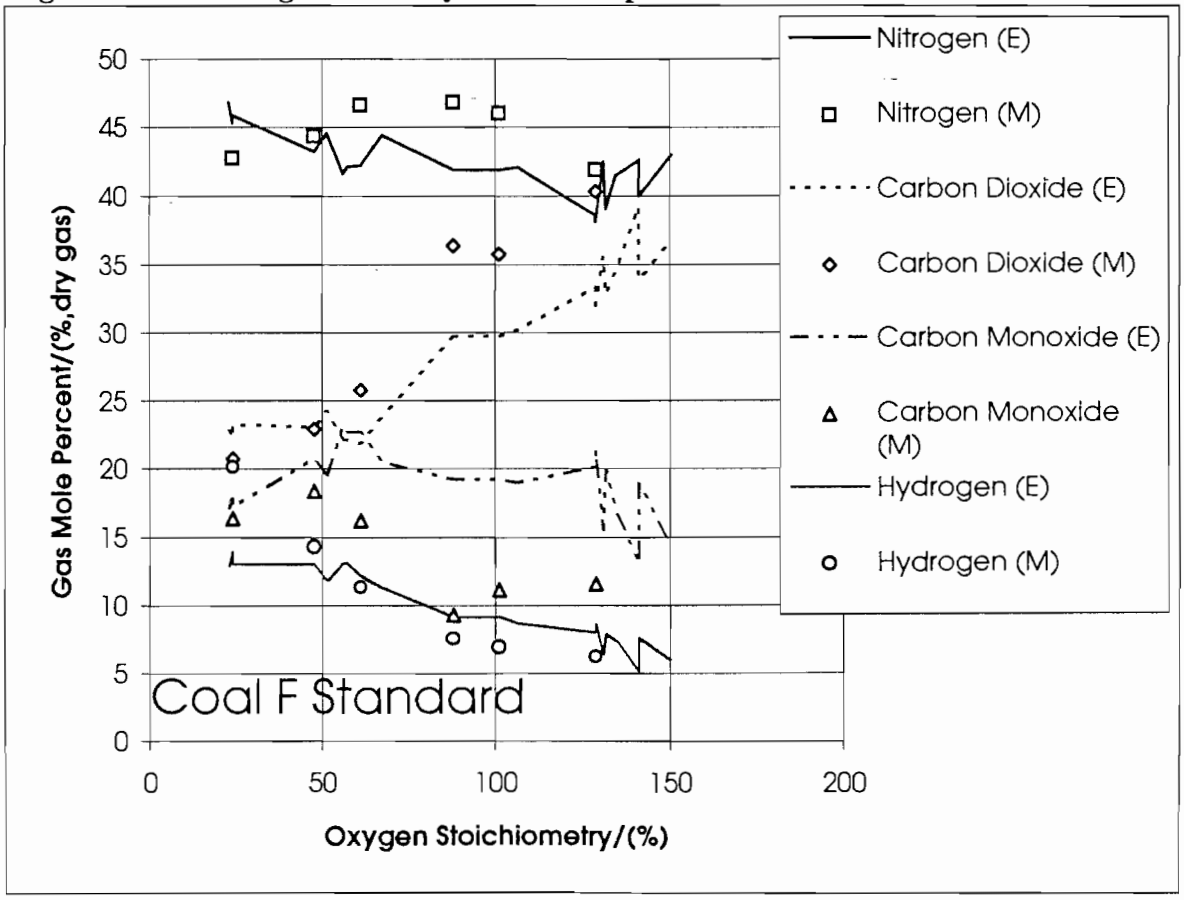

Figure 6.10d : Gas composition results and predictions for Coal F Standard runs

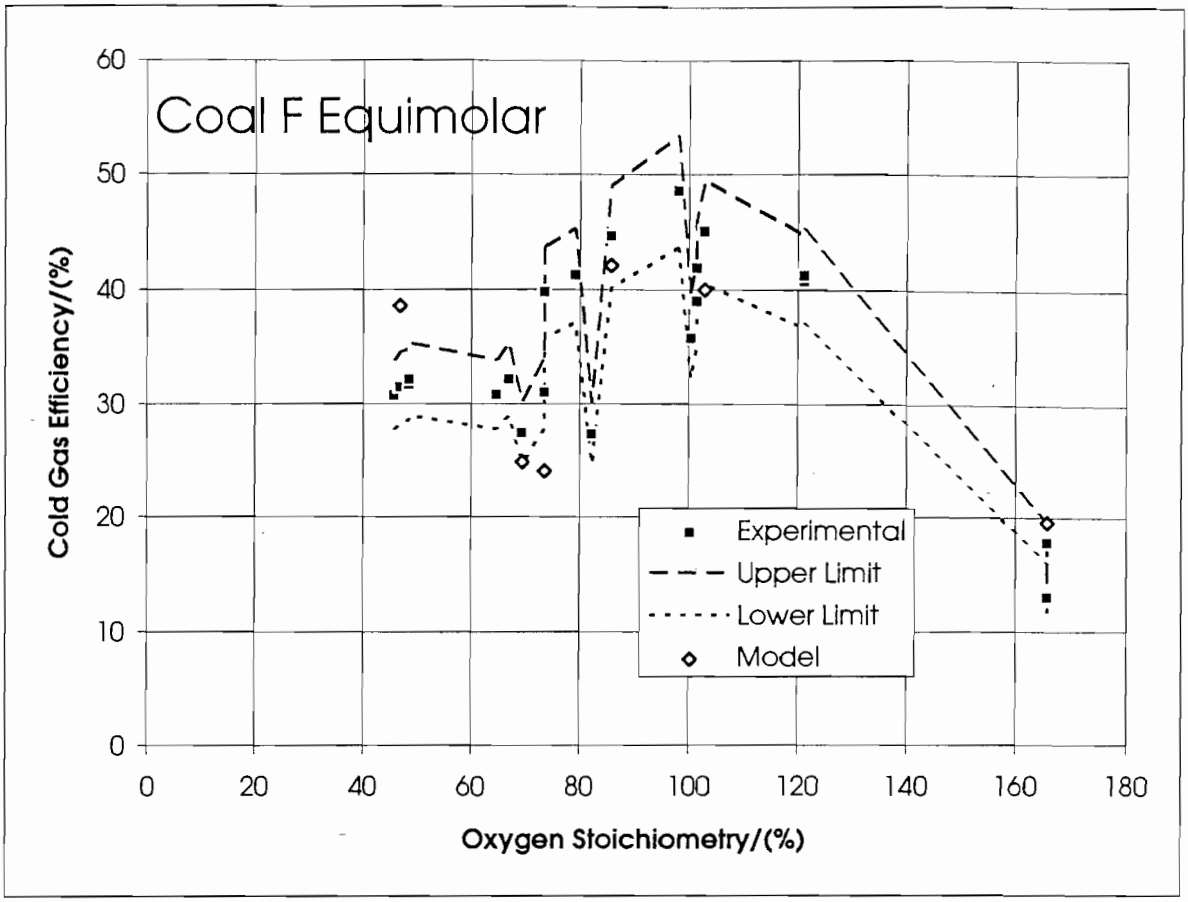

Figure 6.10e : Cold gas efficiency results and predictions for Coal F Equimolar runs

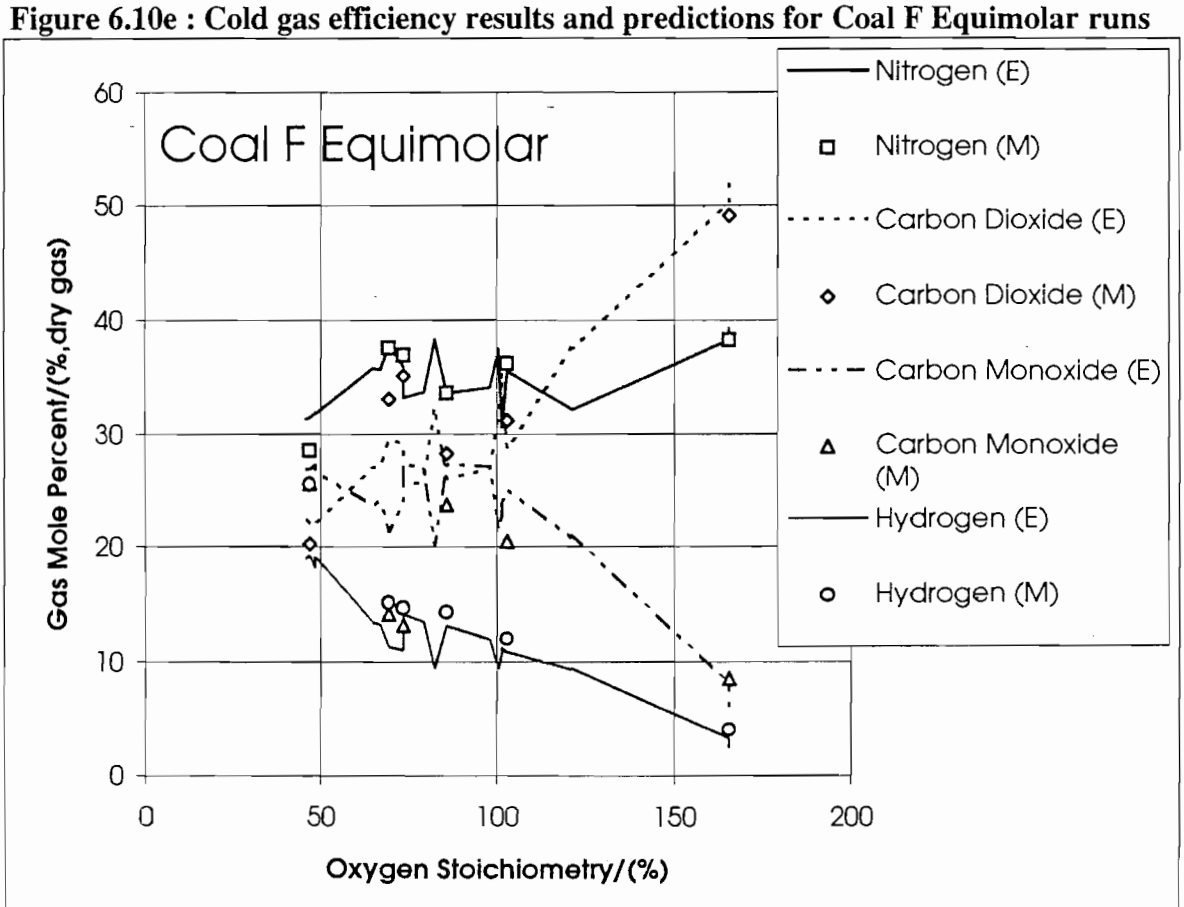

Figure 6.10f : Gas composition results and predictions for Coal F Equimolar runs

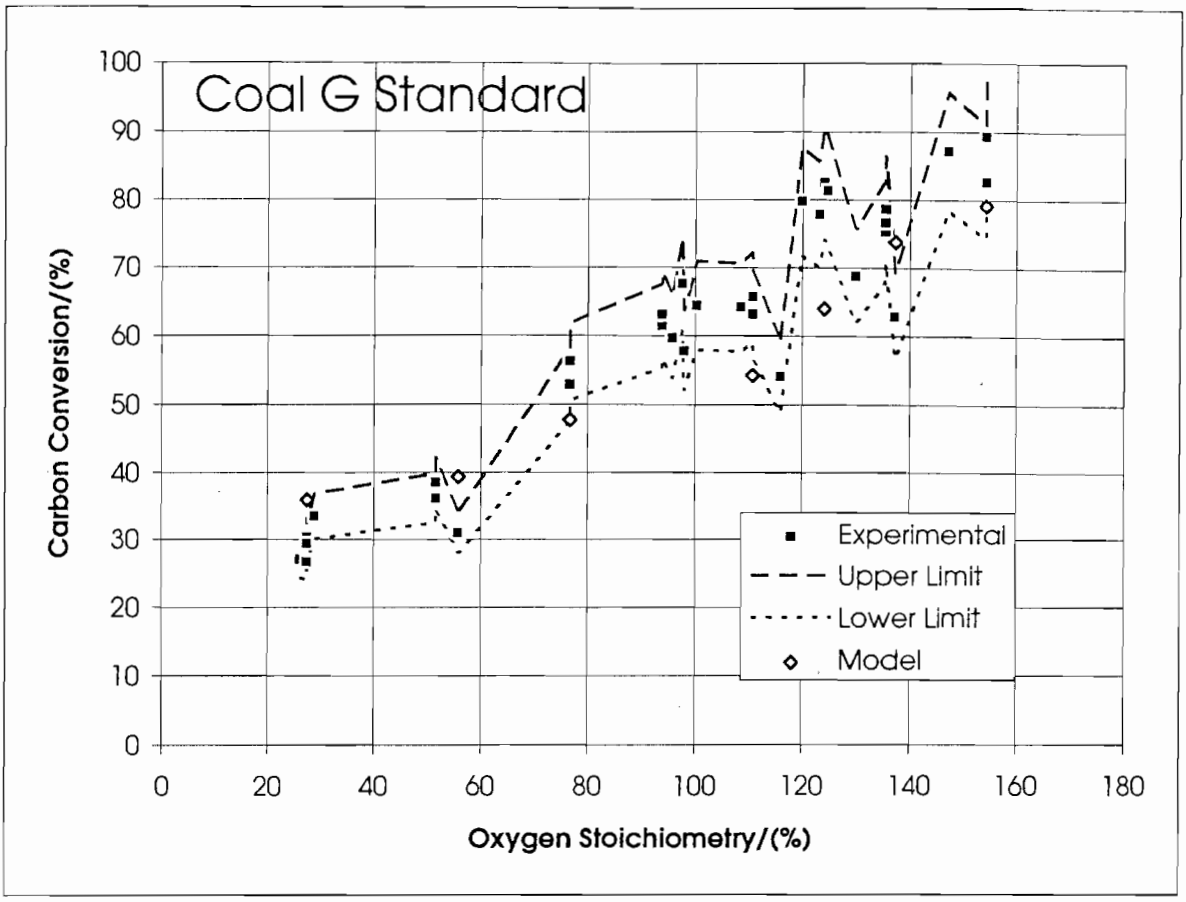

Figure 6.11a : Carbon conversion results and predictions for Coal G Standard runs

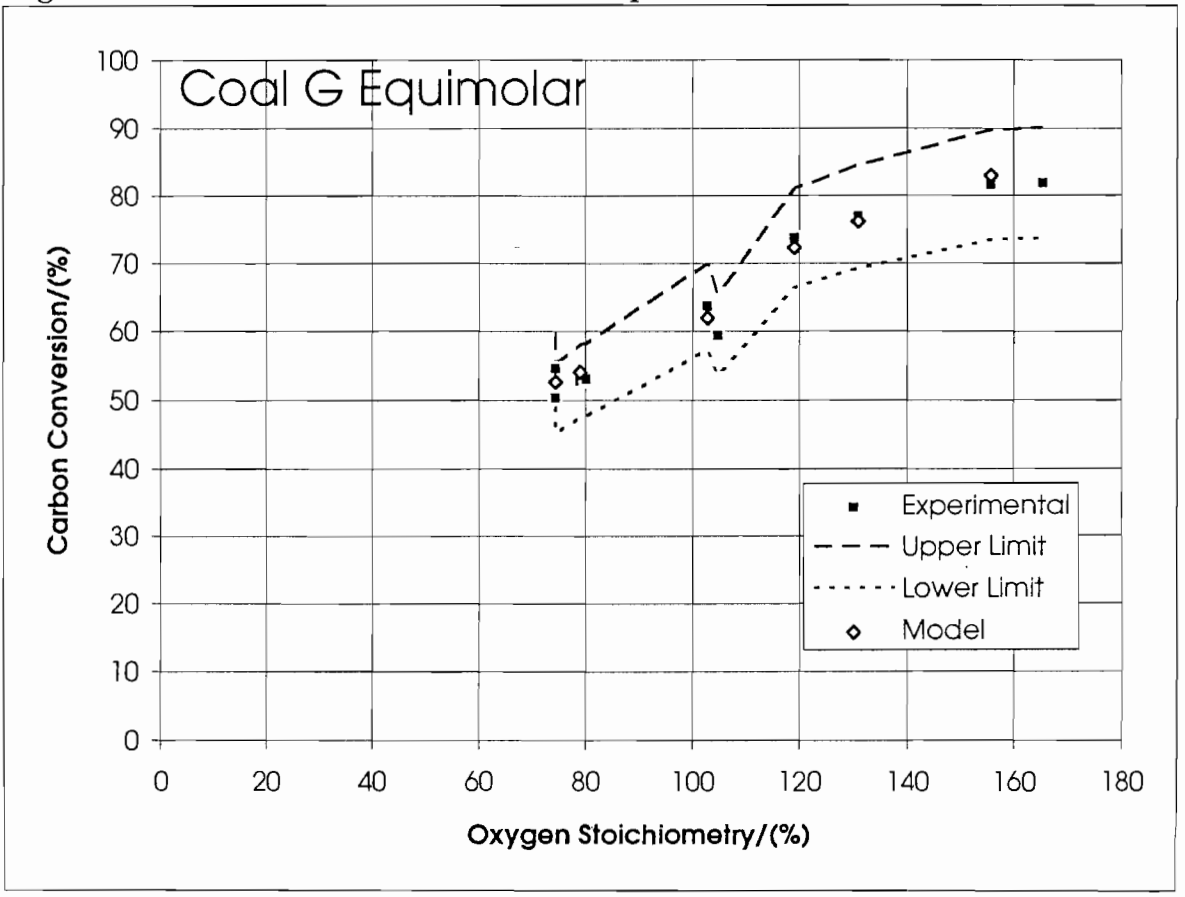

Figure 6.11b : Carbon conversion results and predictions for Coal G Equimolar runs

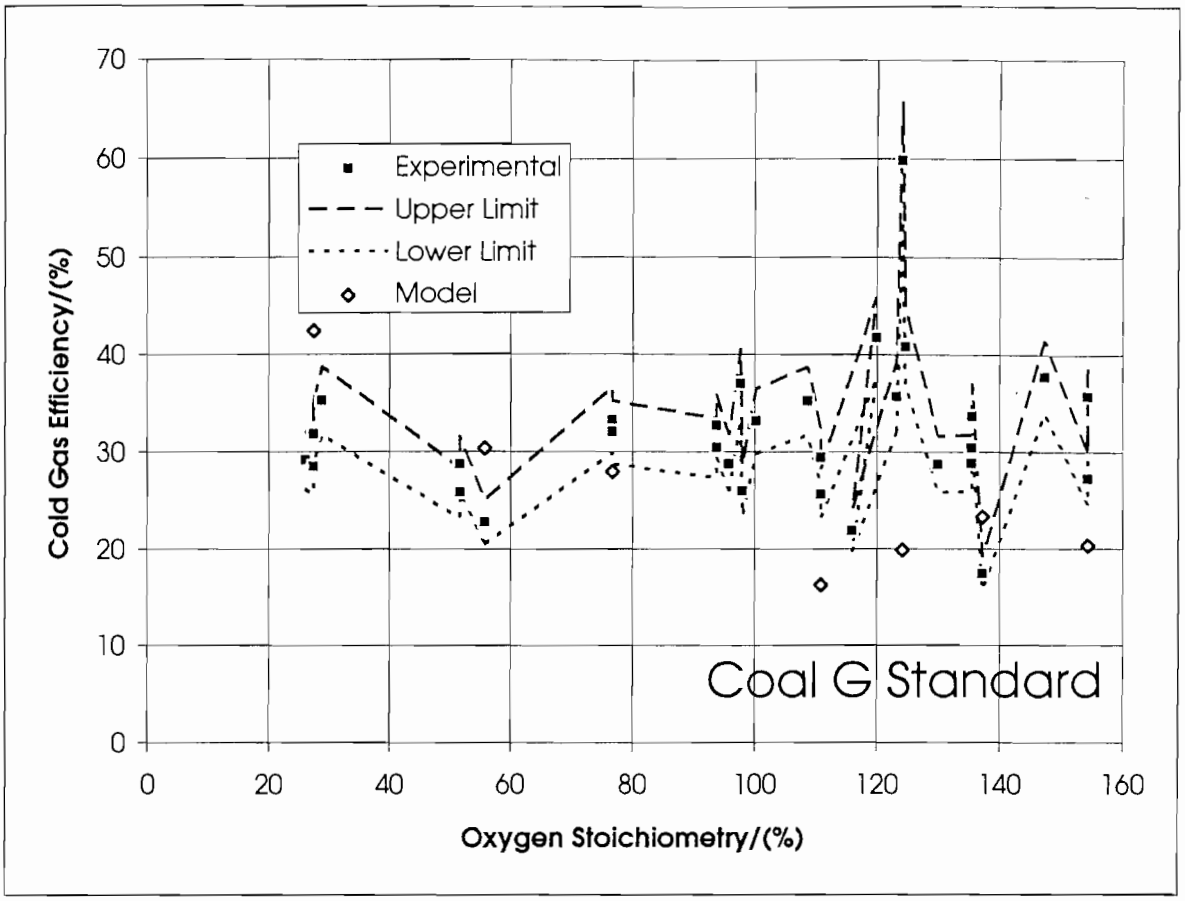

Figure 6.11c : Cold gas efficiency results and predictions for Coal G Standard runs

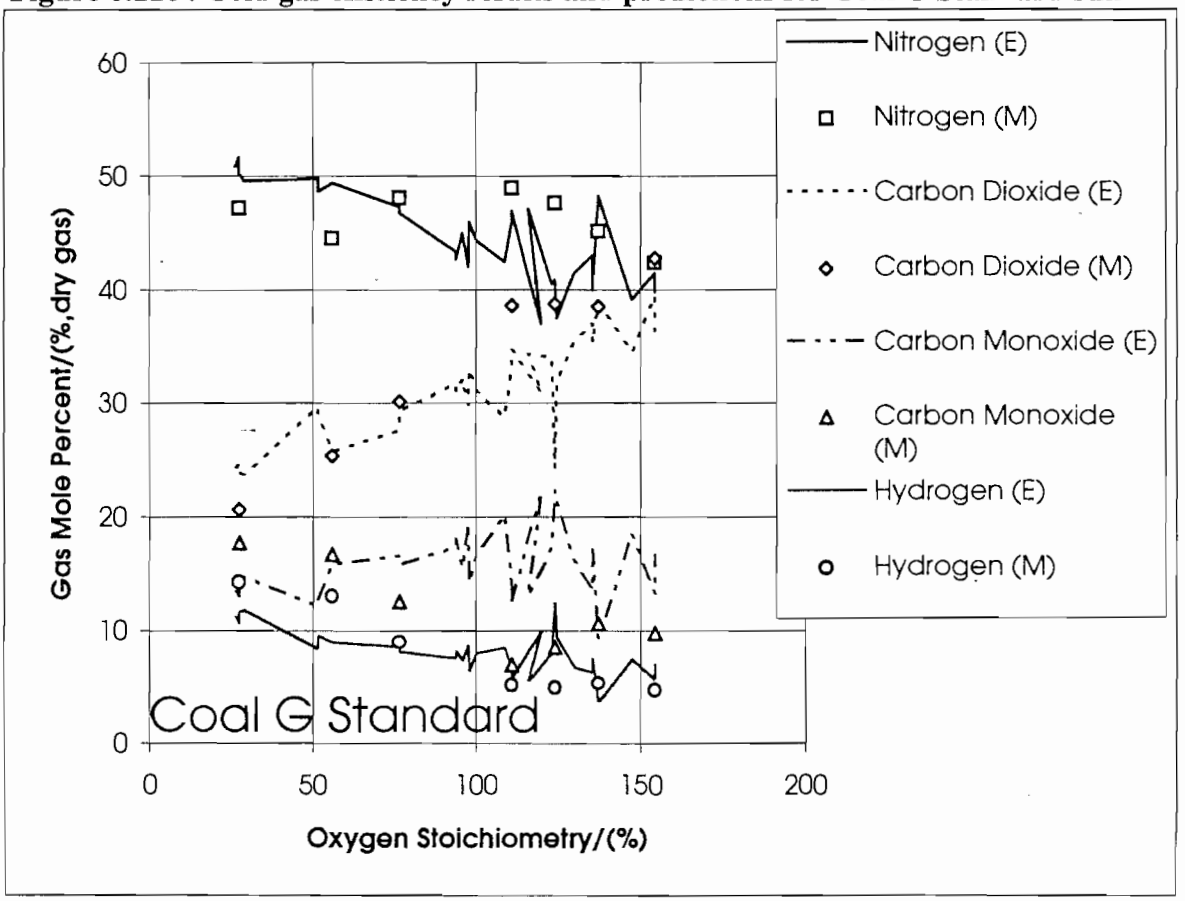

Figure 6.11d : Gas composition results and predictions for Coal G Standard runs

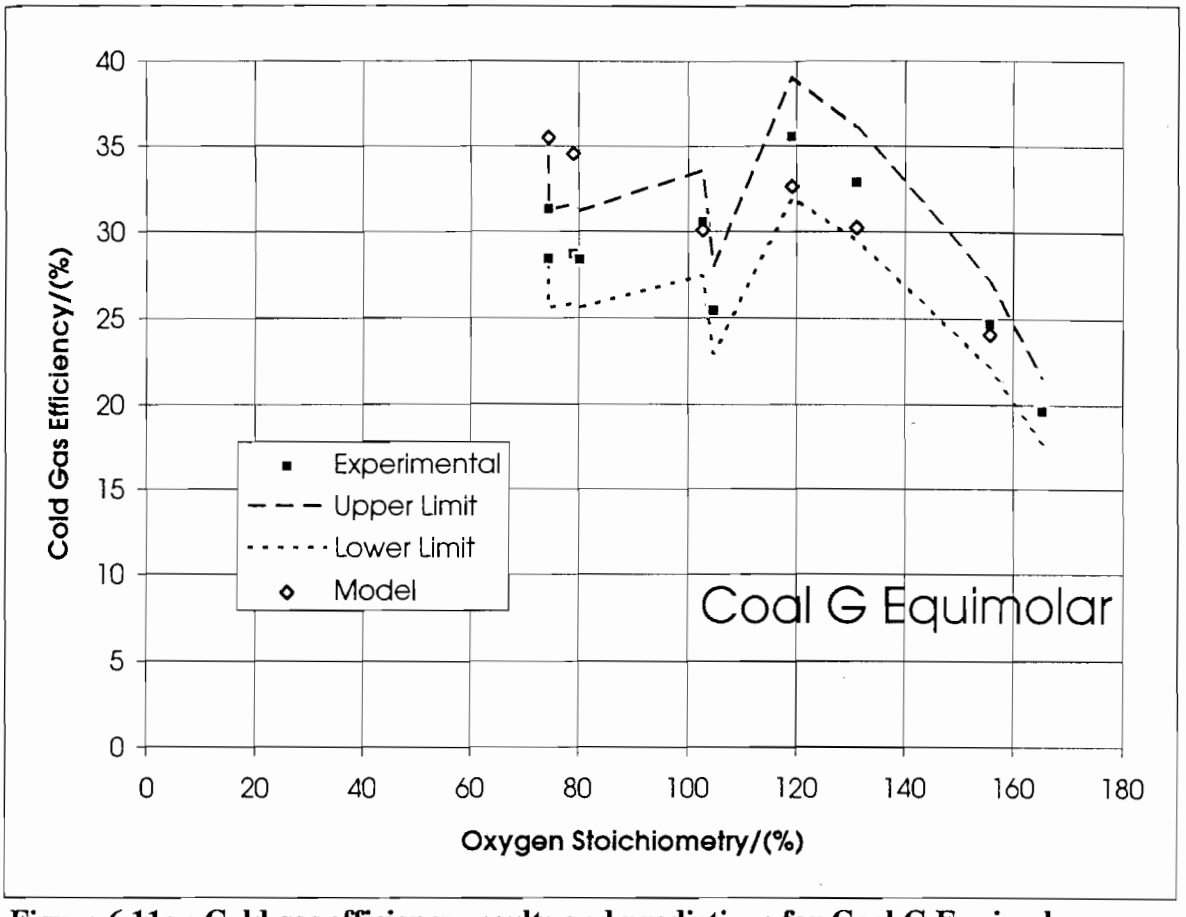

Figure 6.11e : Cold gas efficiency results and predictions for Coal G Equimolar runs

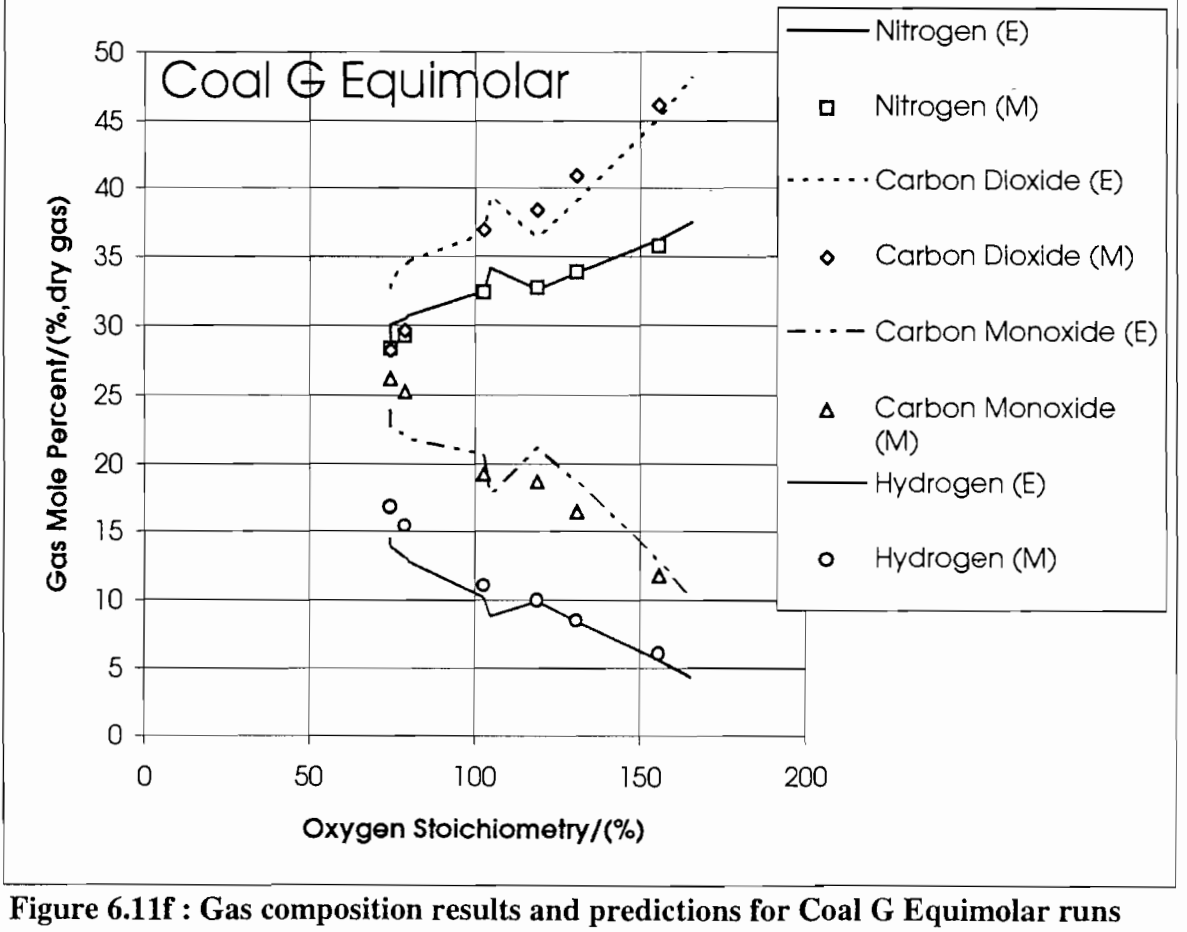

Figure 6.11f : Gas composition results and predictions for Coal G Equimolar runs

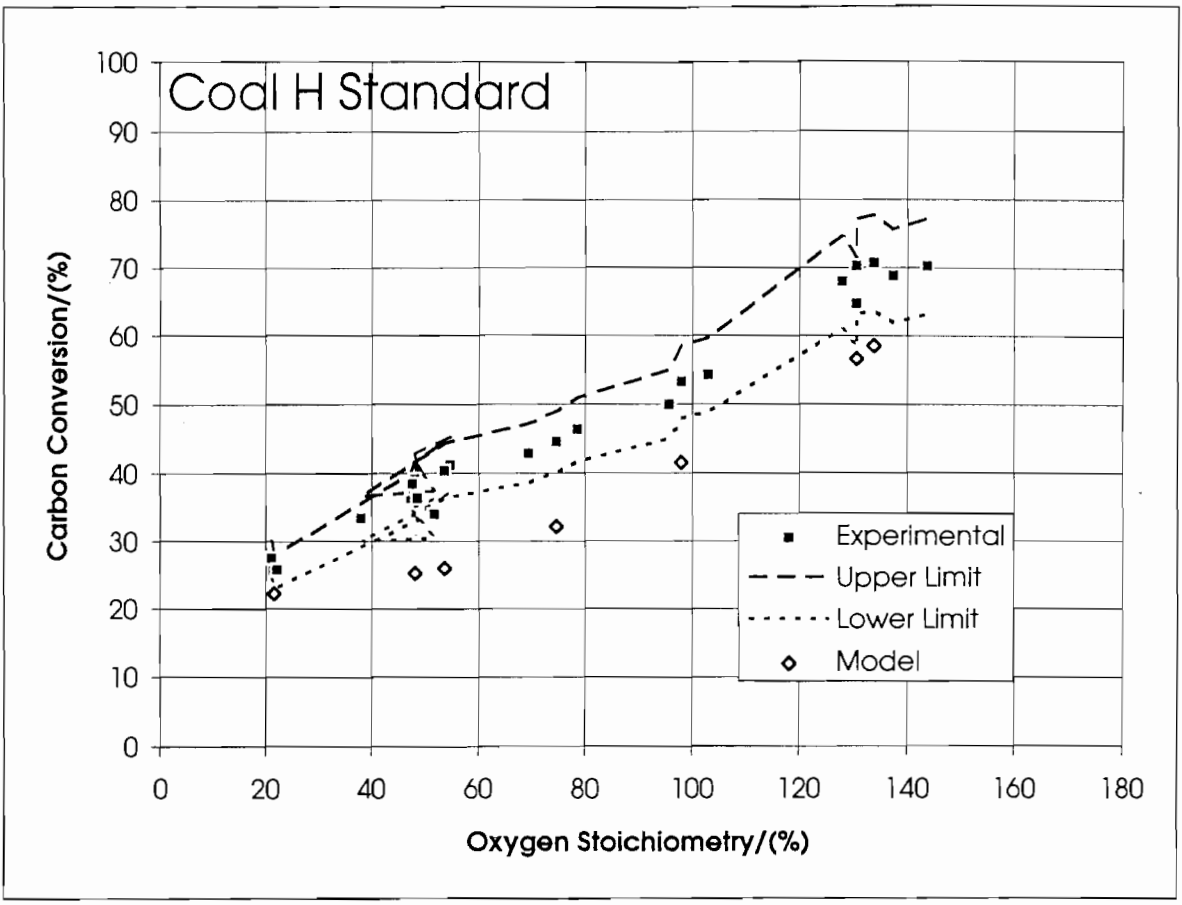

Figure 6.12a : Carbon conversion results and predictions for Coal H Standard runs

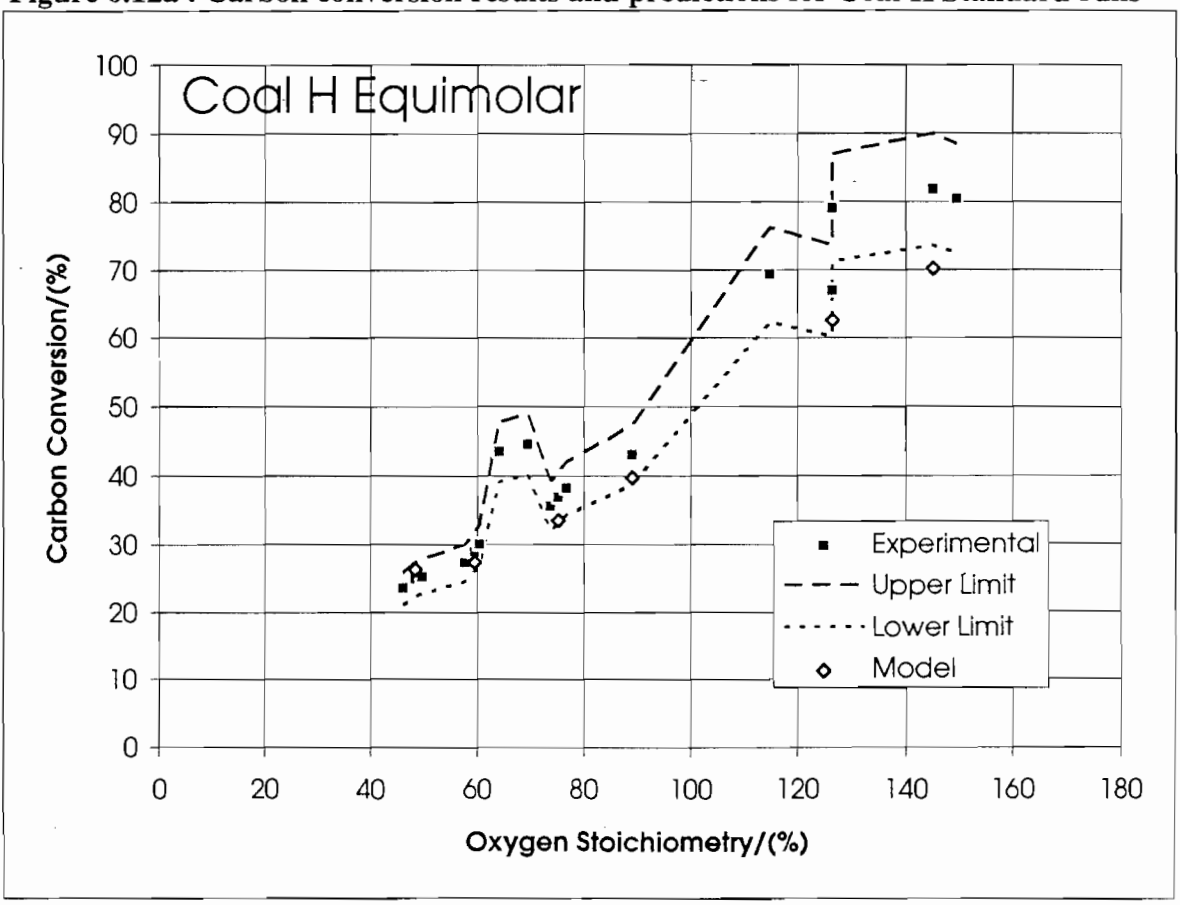

Figure 6.12b : Carbon conversion results and predictions for Coal H Equimolar runs

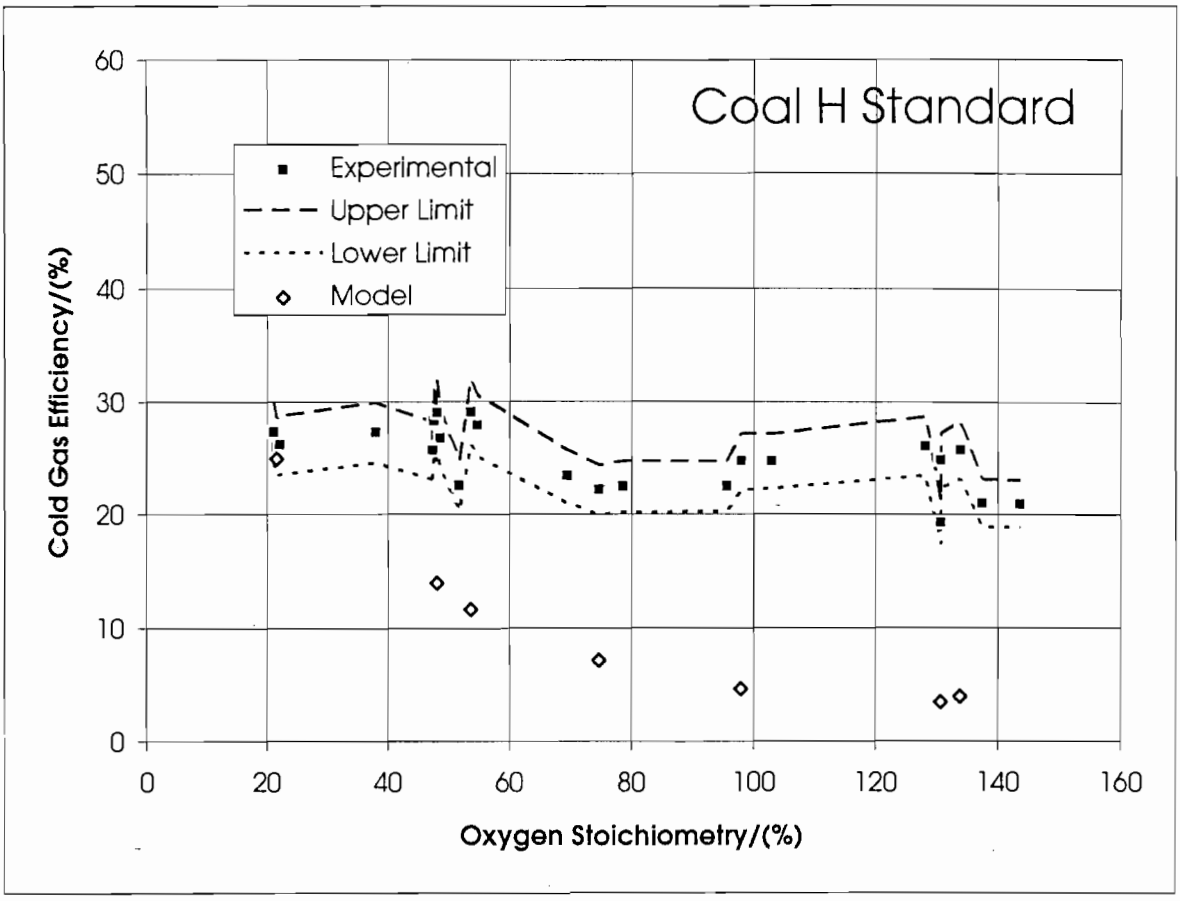

Figure 6.12c : Cold gas efficiency results and predictions for Coal H Standard runs

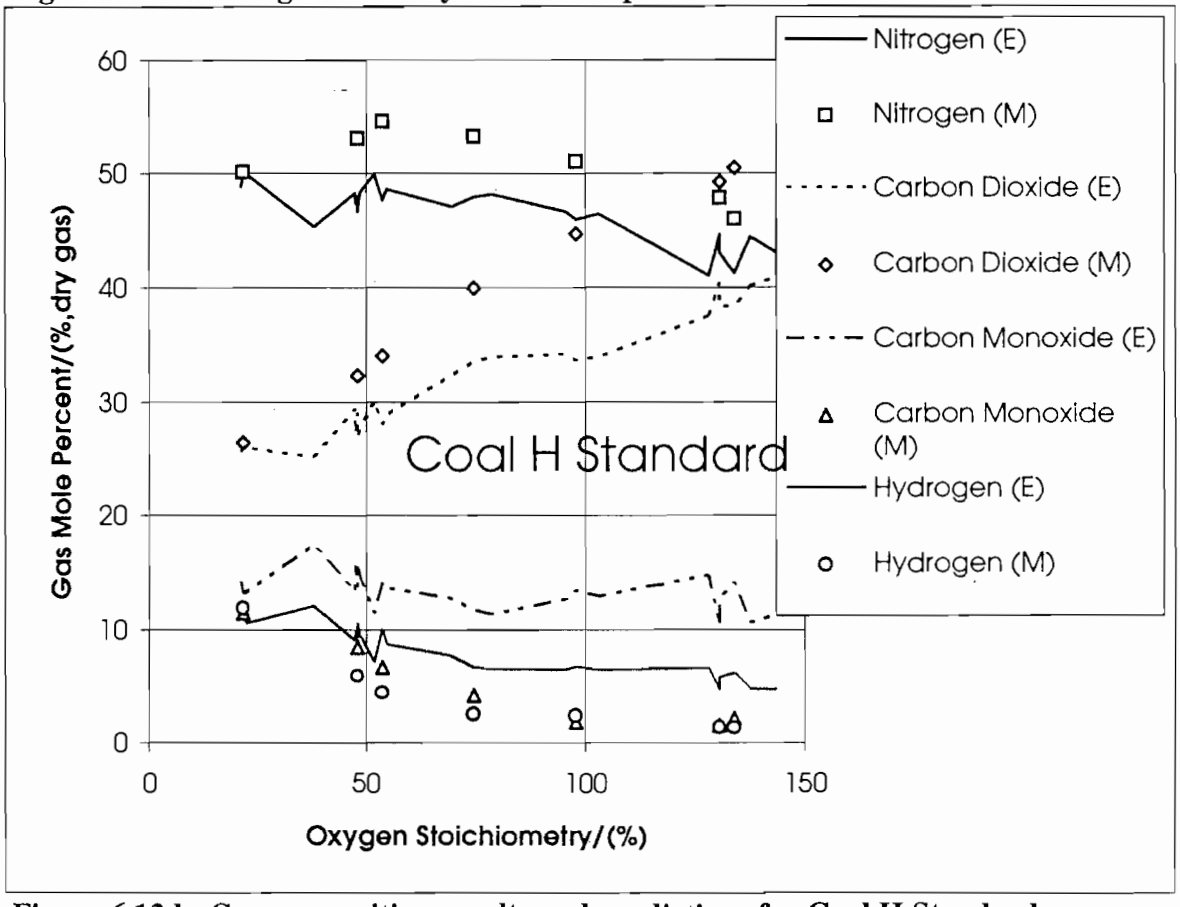

Figure 6.12d : Gas composition results and predictions for Coal H Standard runs

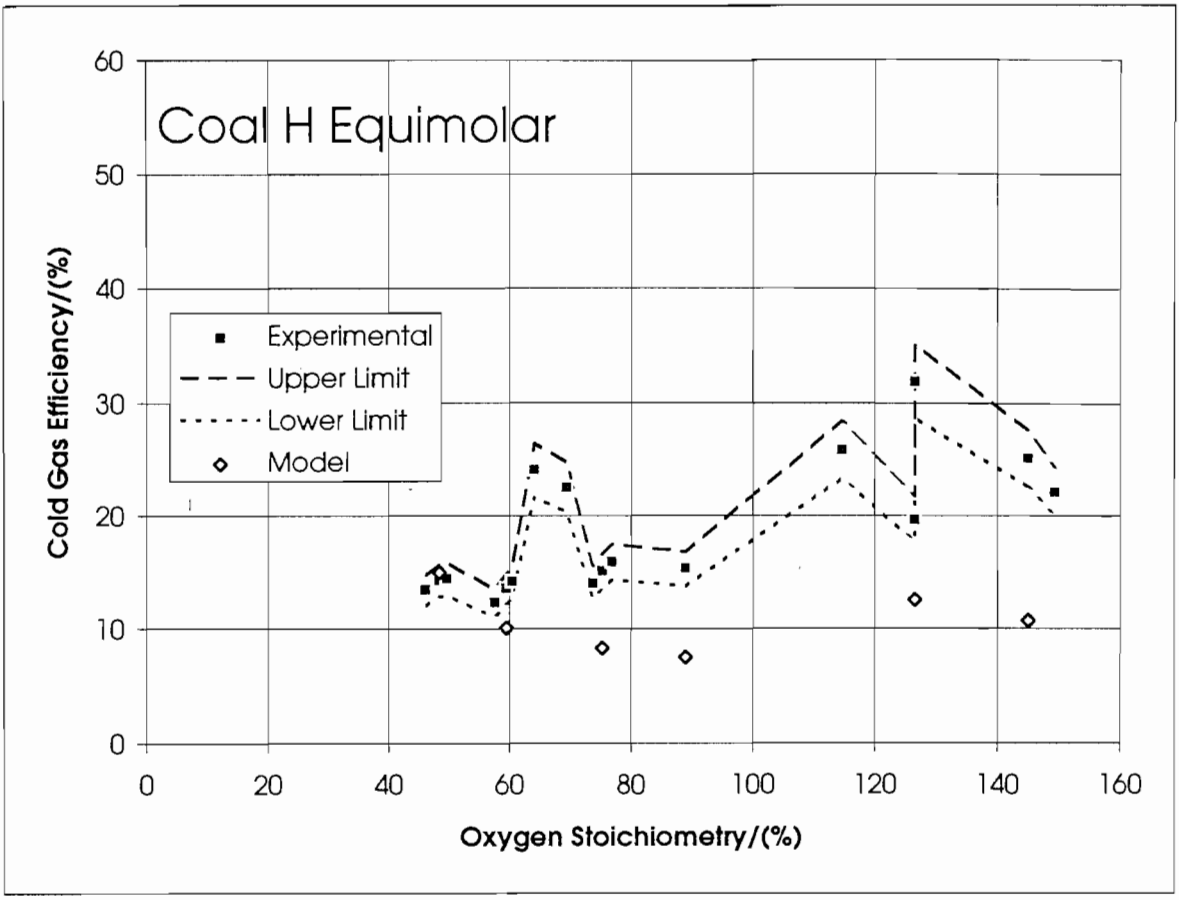

Figure 6.12e : Cold gas efficiency results and predictions for Coal H Equimolar runs

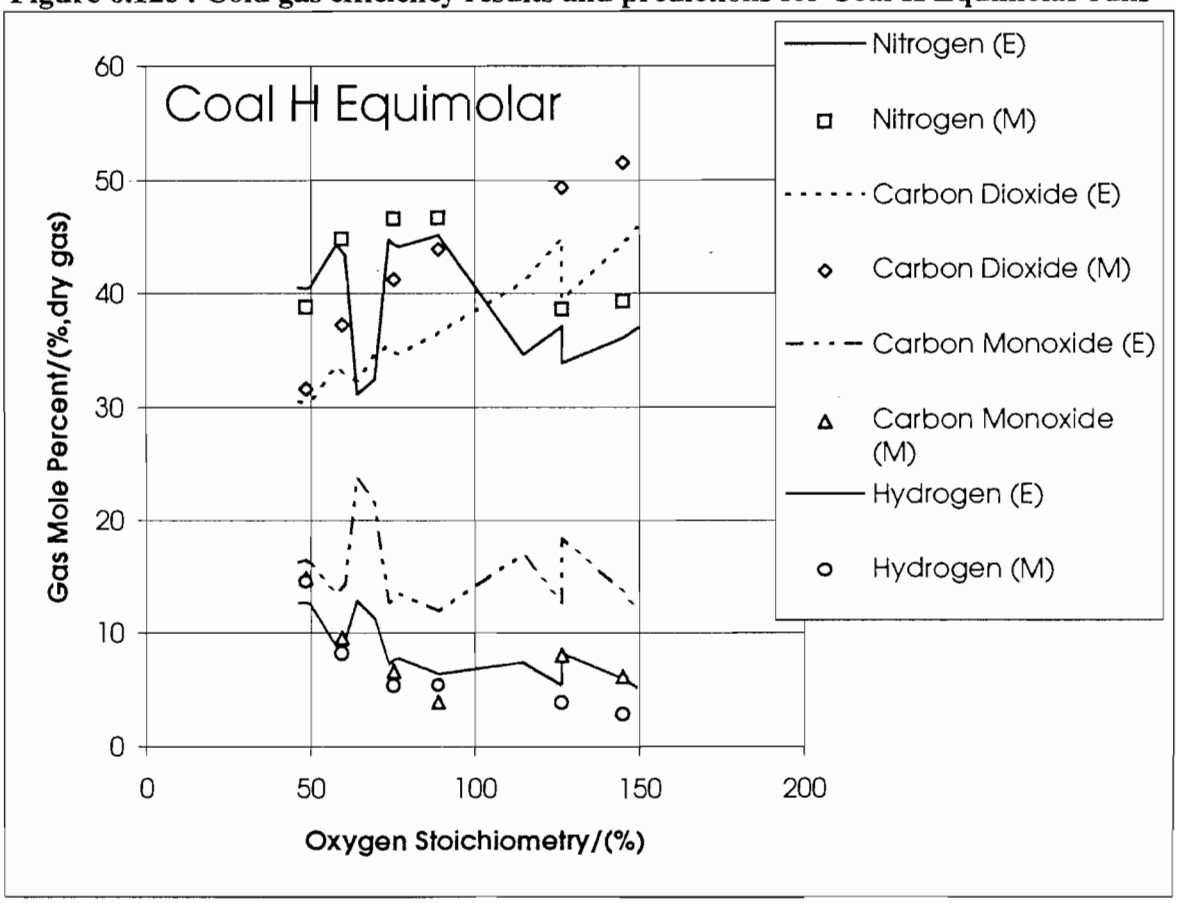

Figure 6.12f : Gas composition results and predictions for Coal H Equimolar runs

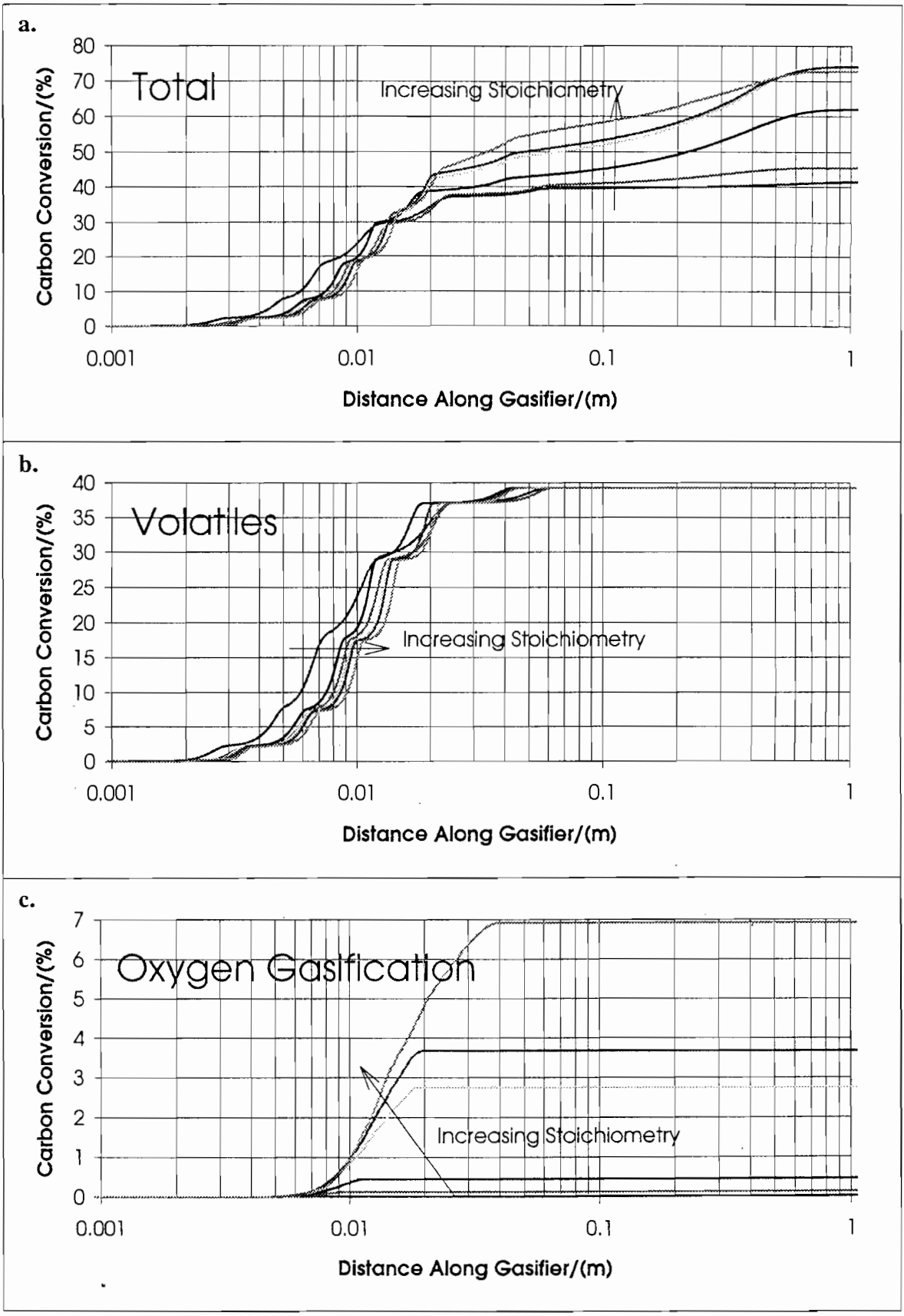

Figure 6.13a-c : Predicted carbon conversion by individual processes with varying stoichiometry (Coal E Standard runs)
a. Total, b. Volatiles, c. Oxygen gasification

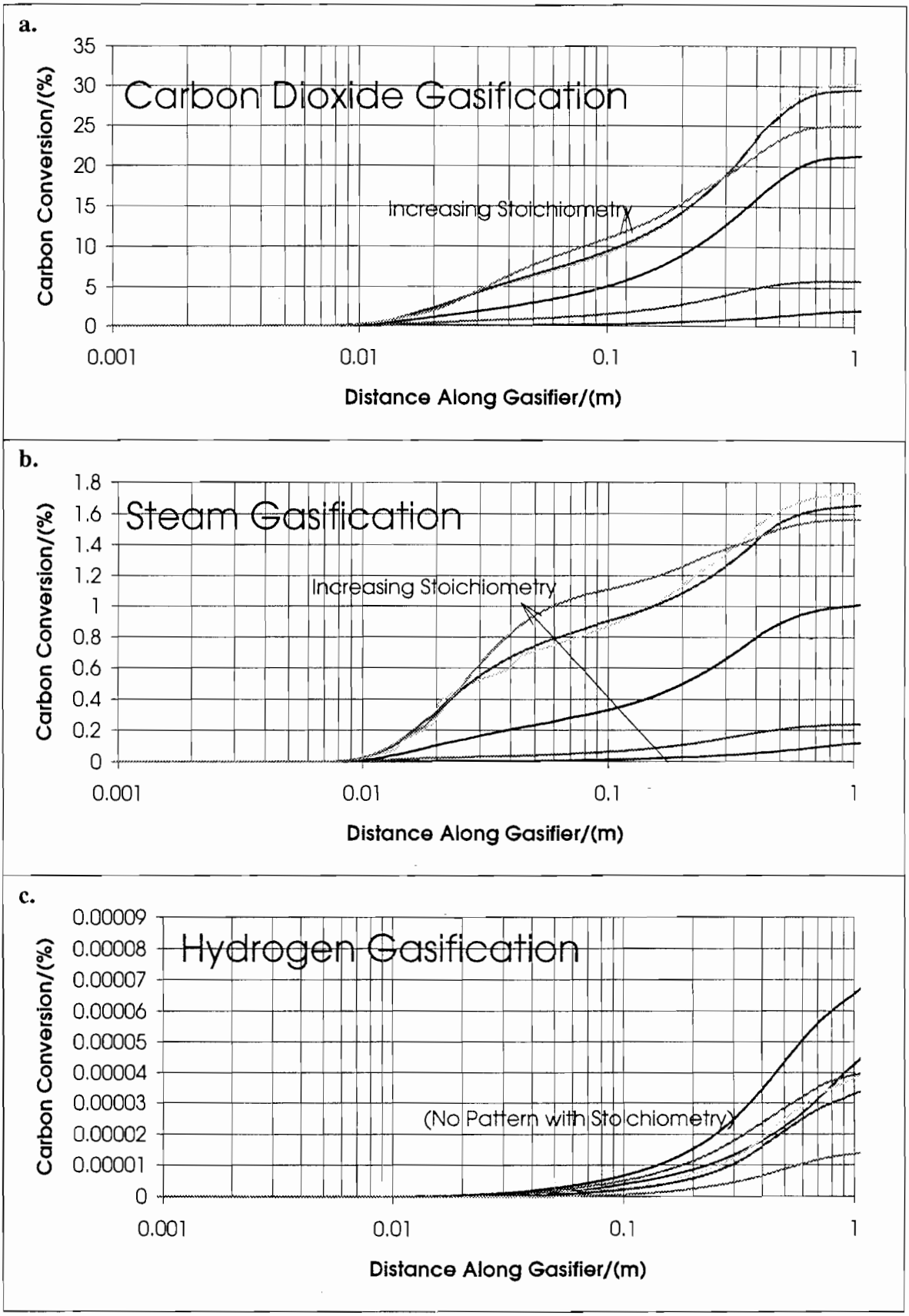

Figure 6.14a-c : Predicted carbon conversion by individual processes with varying stoichiometry (Coal E Standard runs)
a. Carbon Dioxide, b. Steam, c. Hydrogen gasification

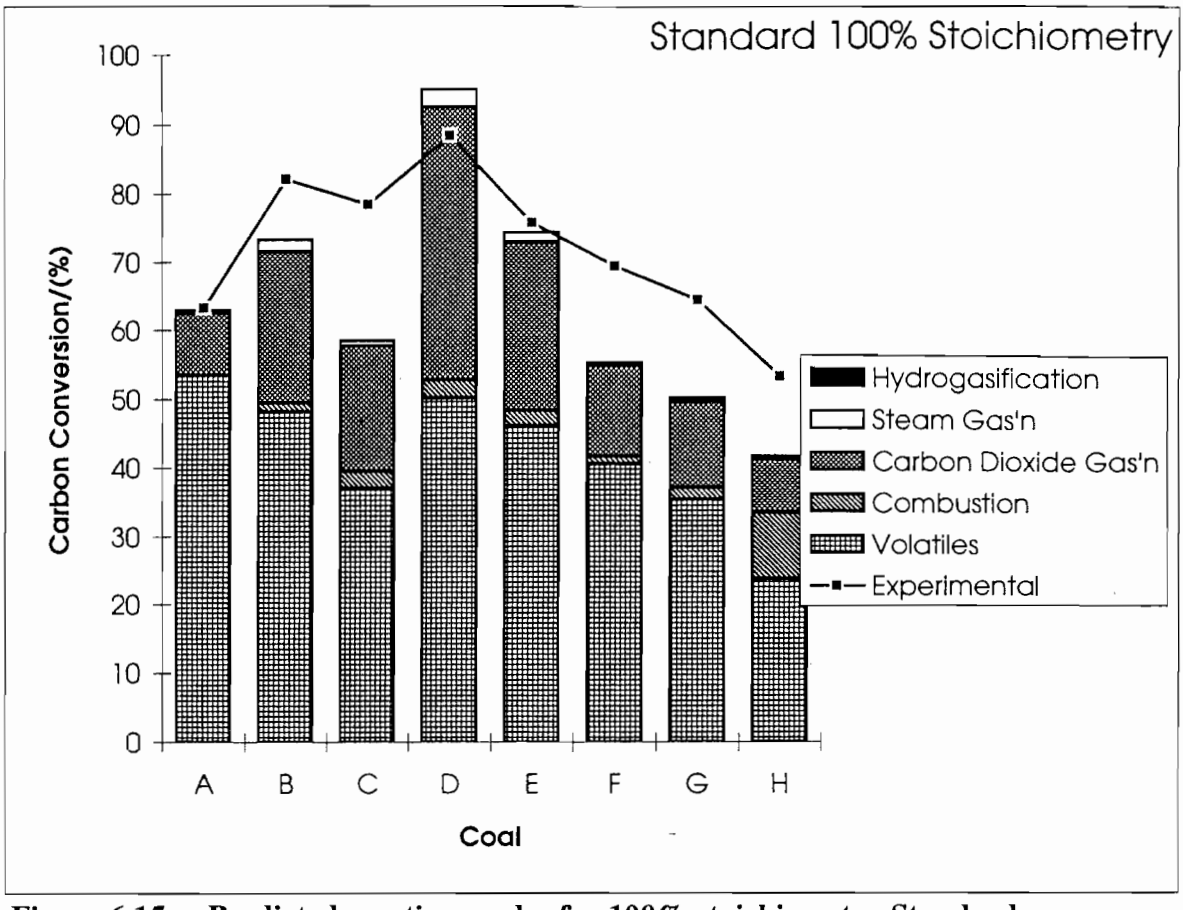

Figure 6.15a : Predicted reaction modes for 100% stoichiometry Standard runs.

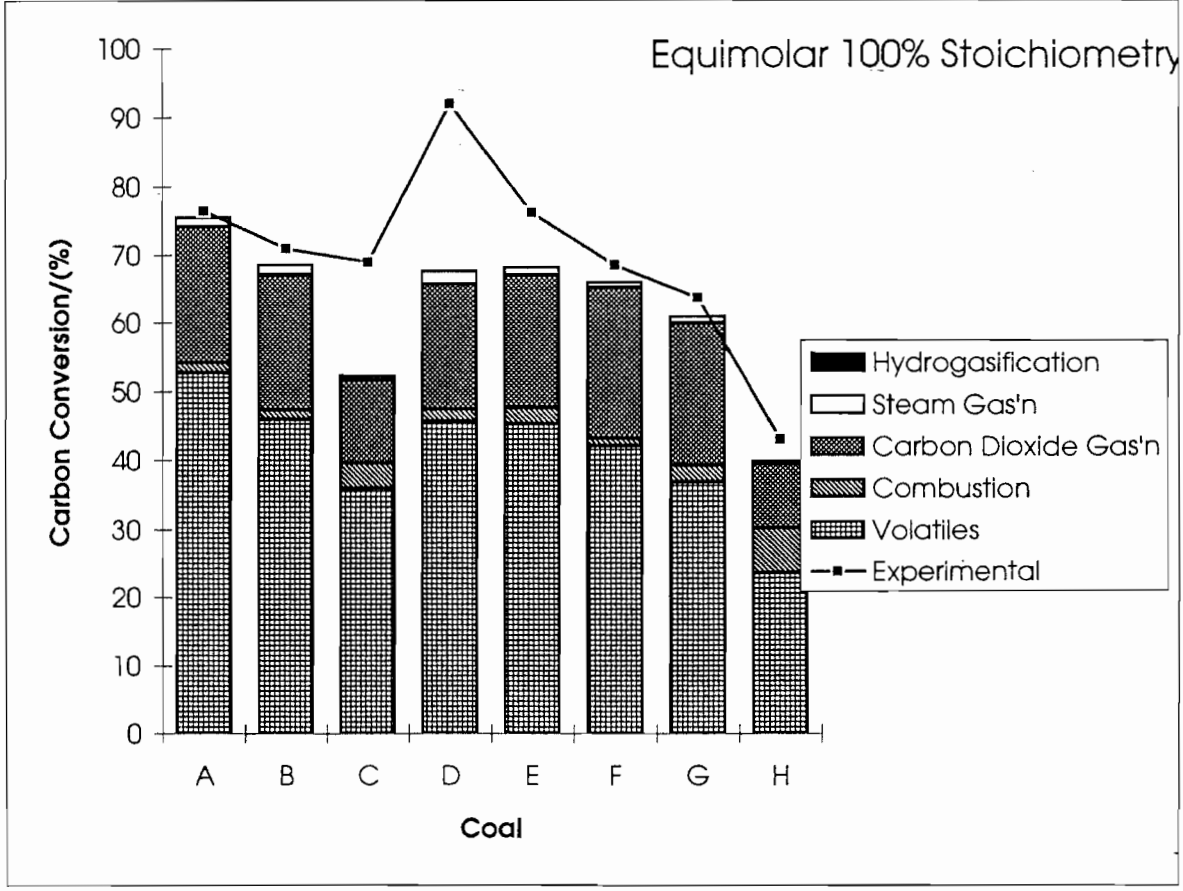

Figure 6.15b : Predicted reaction modes for 100% stoichiometry Equimolar runs.

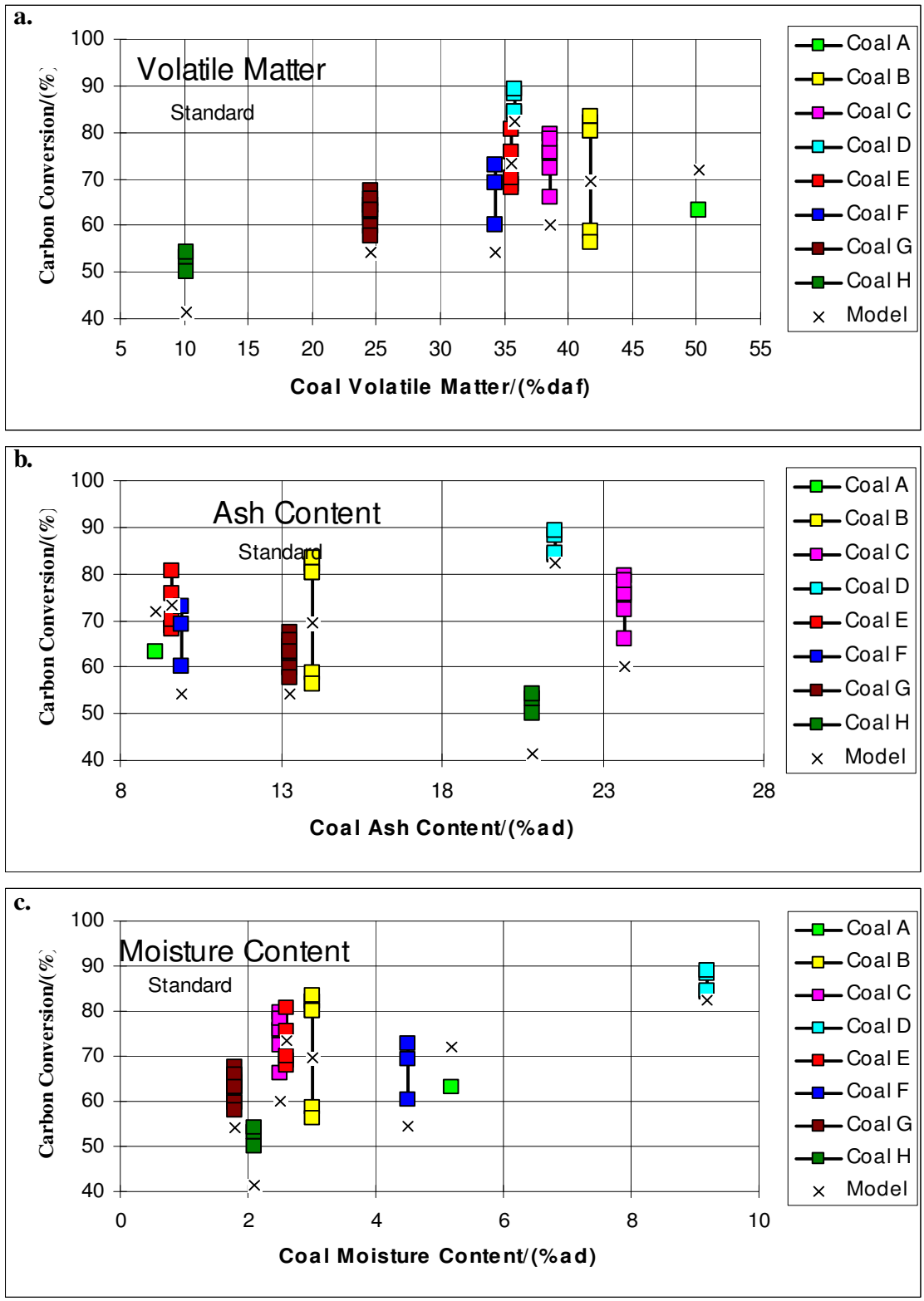

Figure 6.16a-c: Experimental and predicted carbon conversion for Standard runs plotted against some proximate analysis results a. Volatile Matter, b. Ash Content, c. Moisture Content of coal

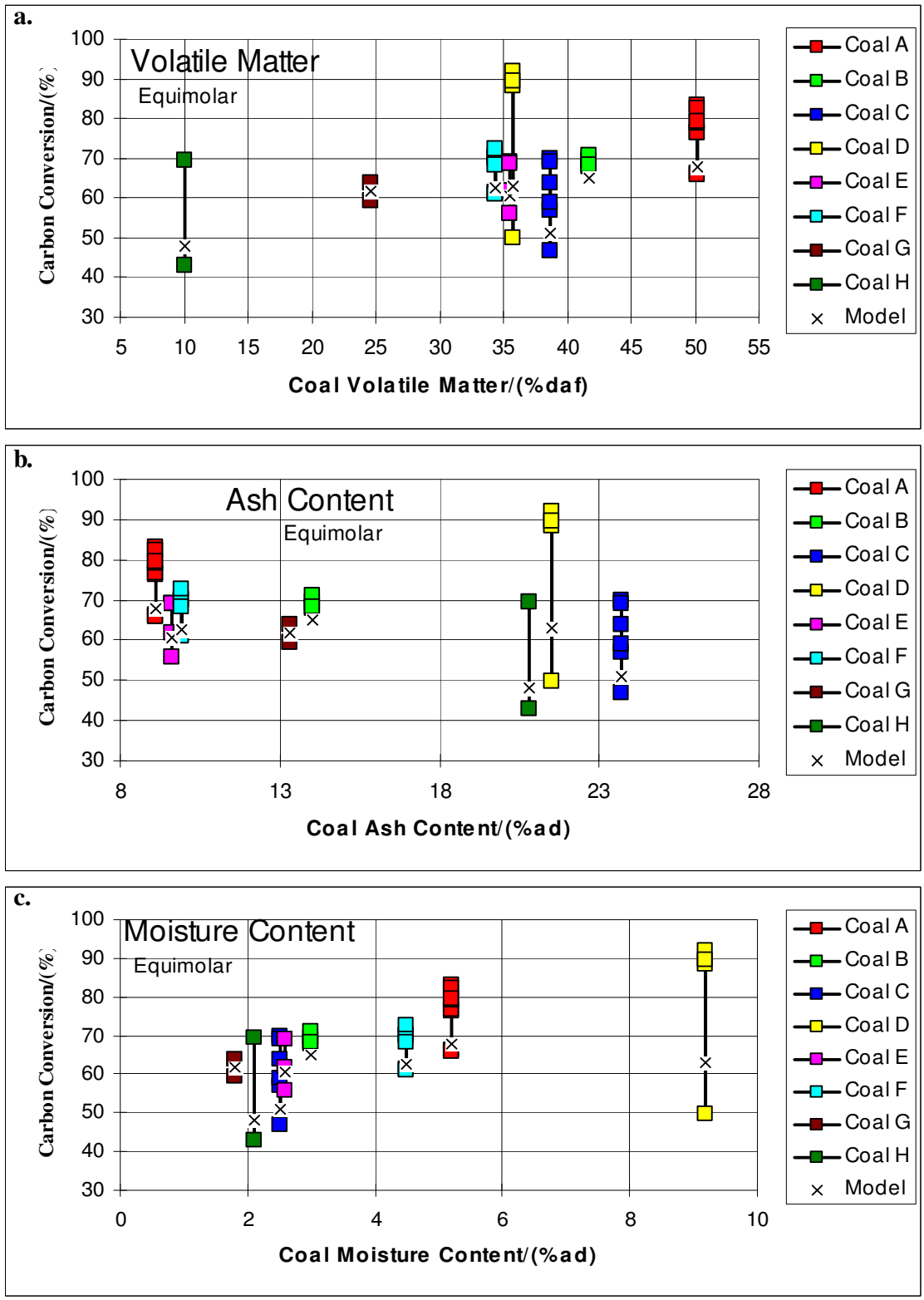

Figure 6.17a-c: Experimental and predicted carbon conversion for Equimolar runs plotted against some proximate analysis results a. Volatile Matter, b. Ash Content, c. Moisture Content of coal

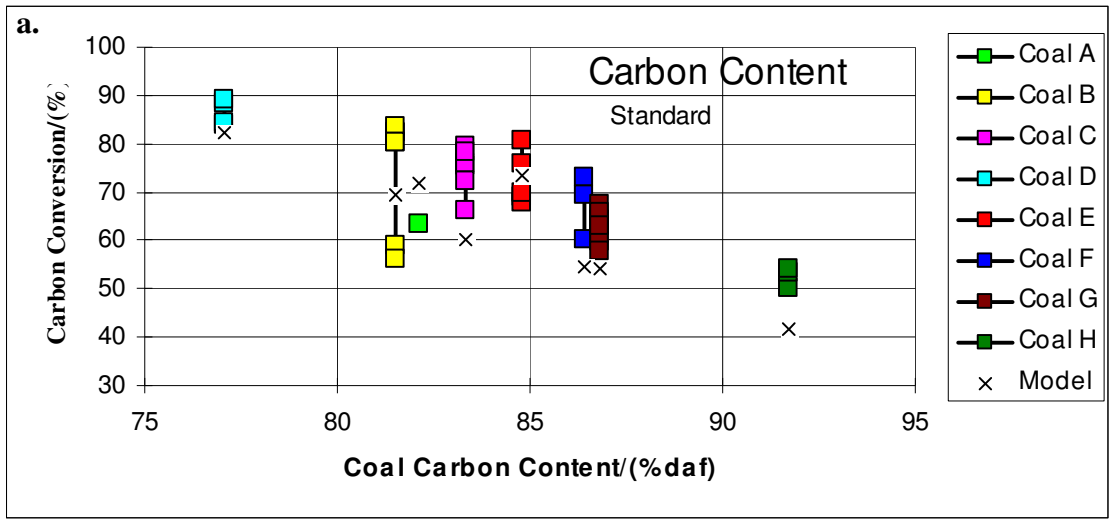

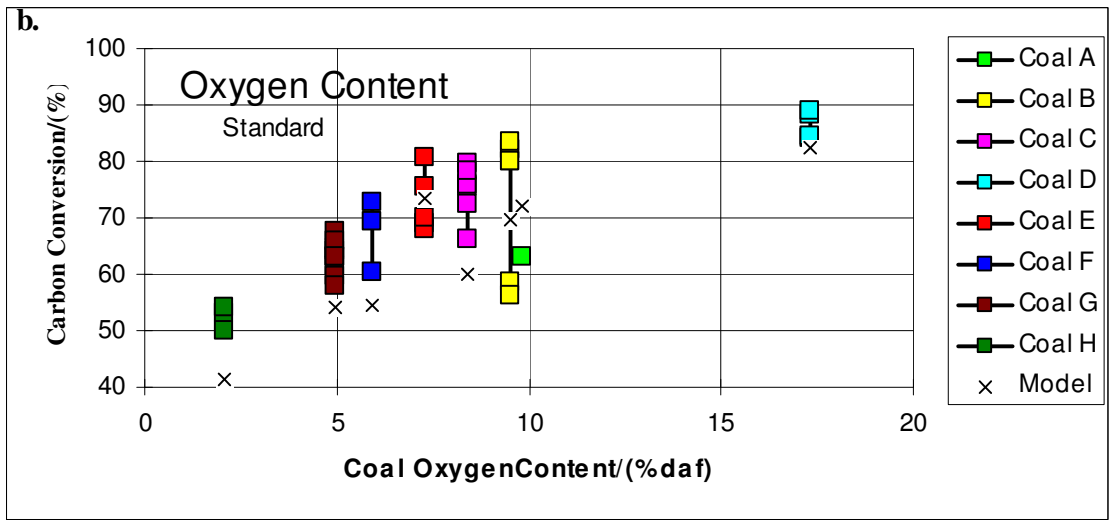

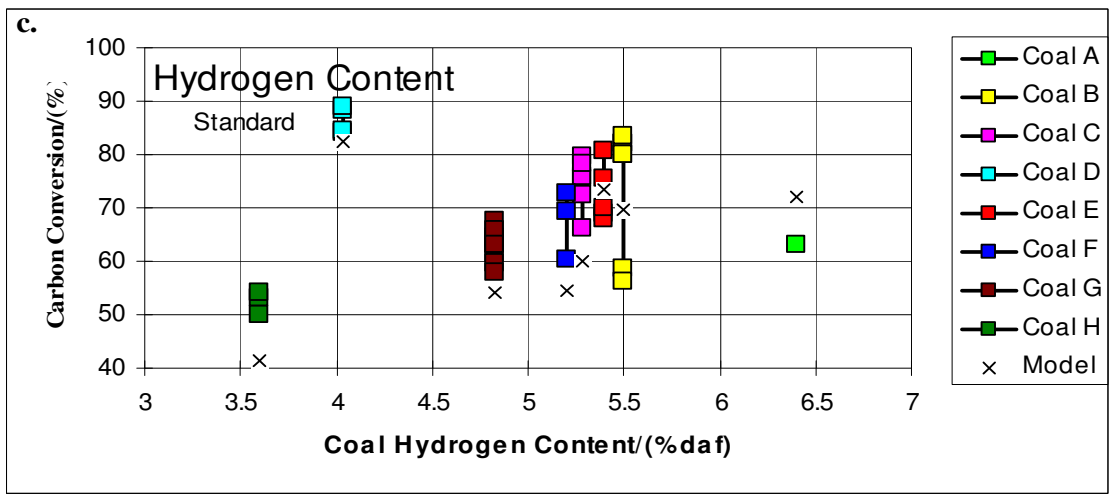

Figure 6.18a-c: Experimental and predicted carbon conversion for Standard runs plotted against some ultimate analysis results a. Carbon Content, b. Oxygen Content, c. Hydrogen Content of coal

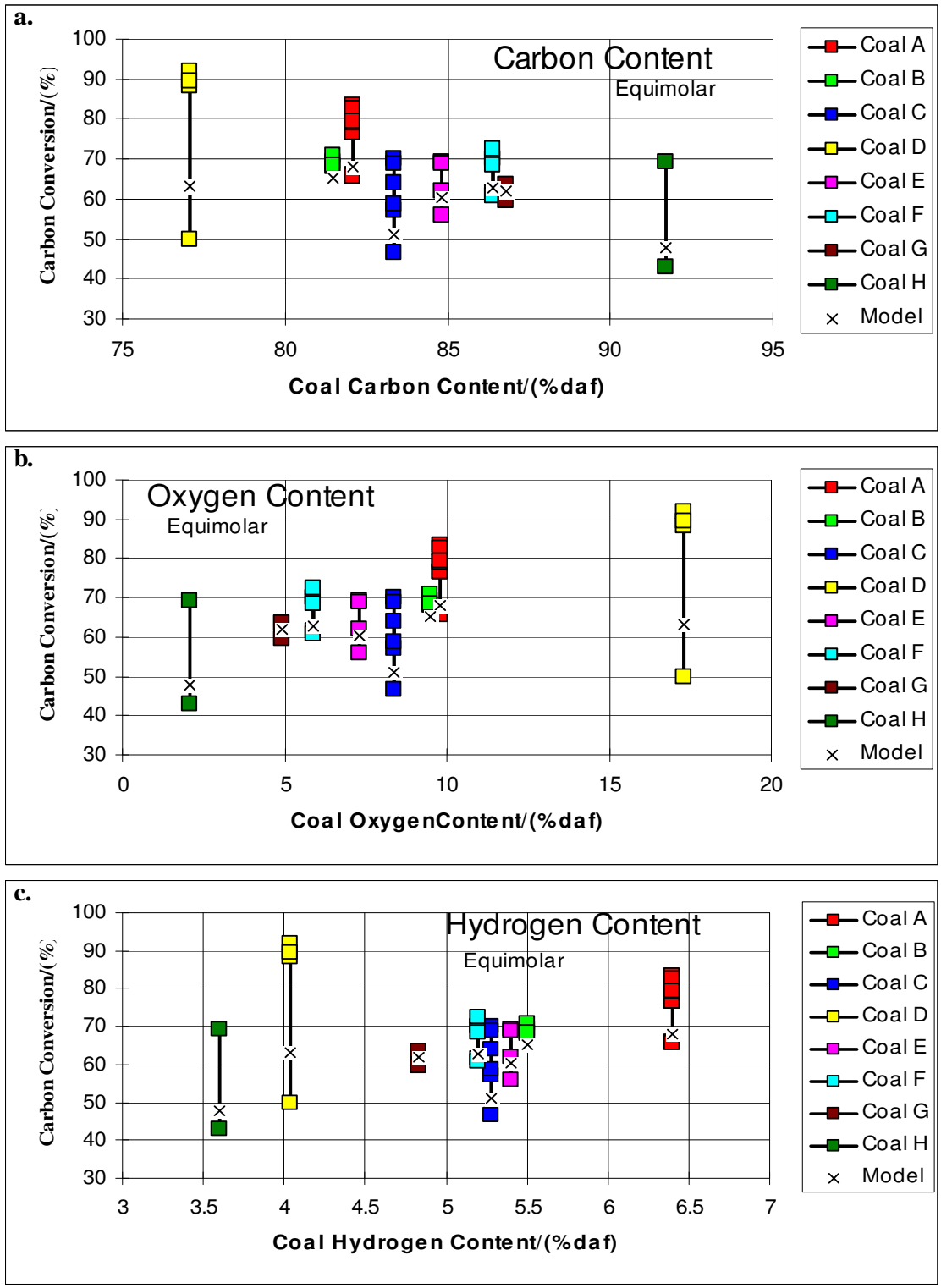

Figure 6.19a-c: Experimental and predicted carbon conversion for Equimolar runs plotted against some ultimate analysis results a. Carbon Content, b. Oxygen Content, c. Hydrogen Content of coal

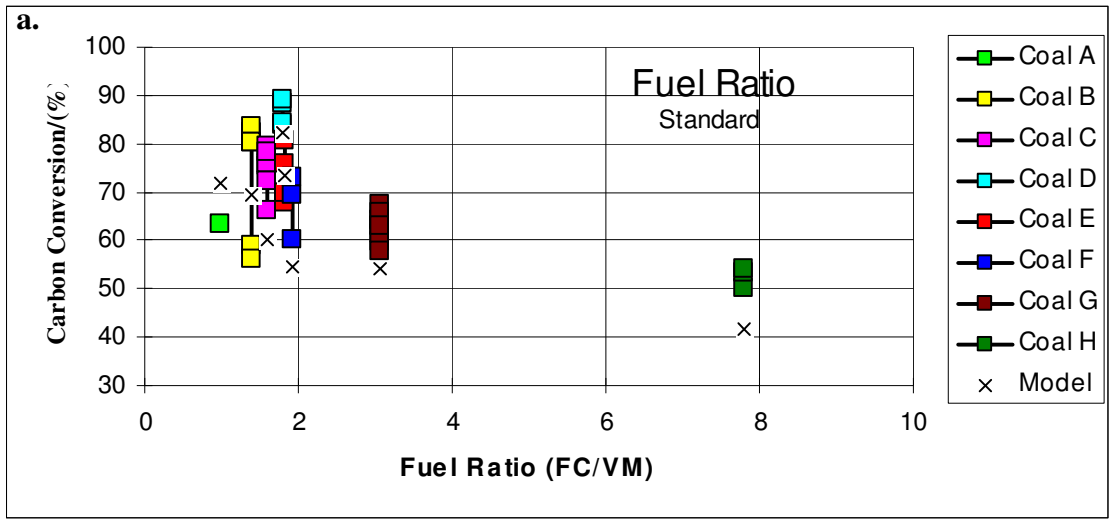

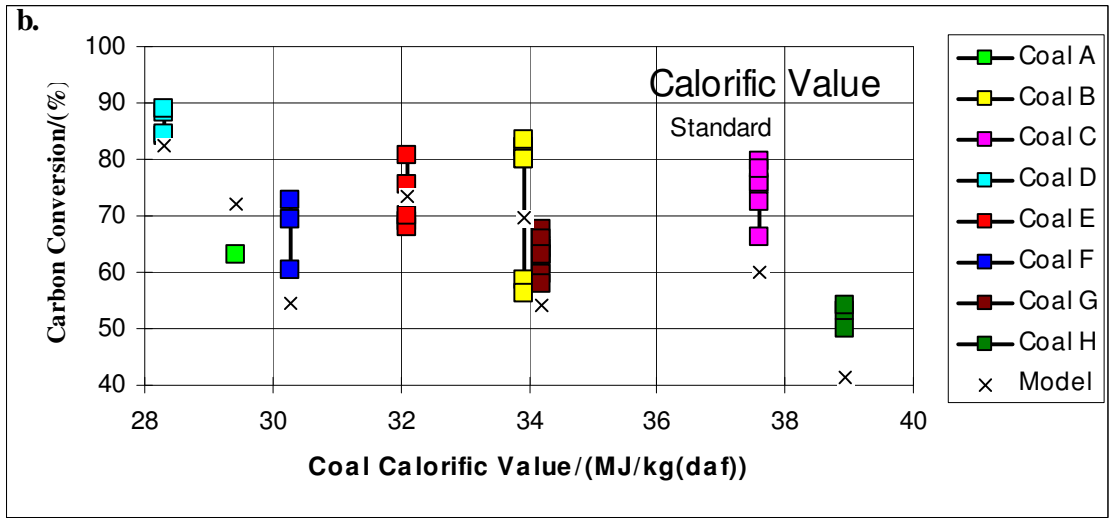

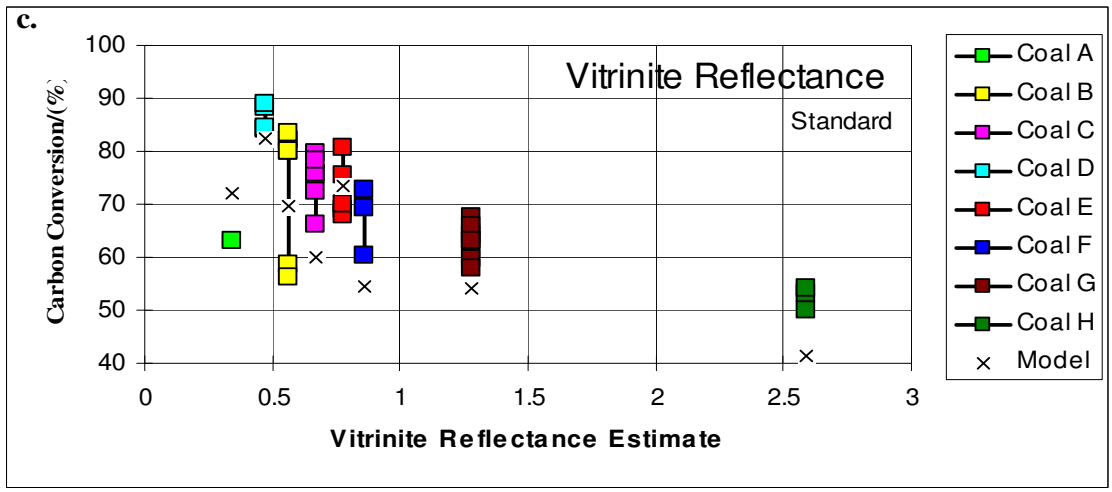

Figure 6.20a-c: Experimental and predicted carbon conversion for Standard runs plotted against some miscallaneous analysis results a. Fuel Ratio, b. Calorific Value, c. Vitrinite Reflectance of coal

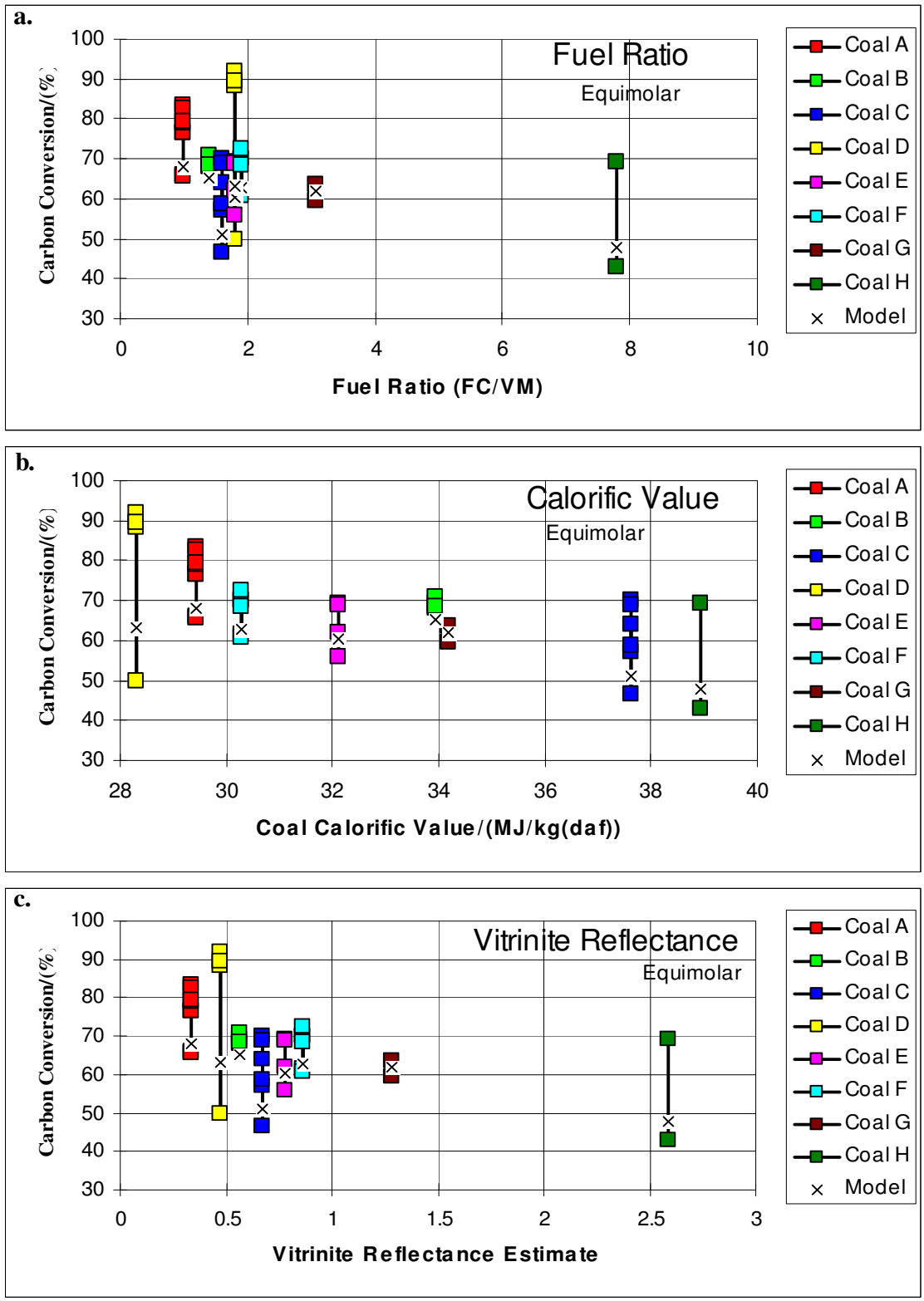

Figure 6.21a-c: Experimental and predicted carbon conversion for Equimolar runs plotted against some miscallaneous analysis results a. Fuel Ratio, b. Calorific Value, c. Vitrinite Reflectance of coal

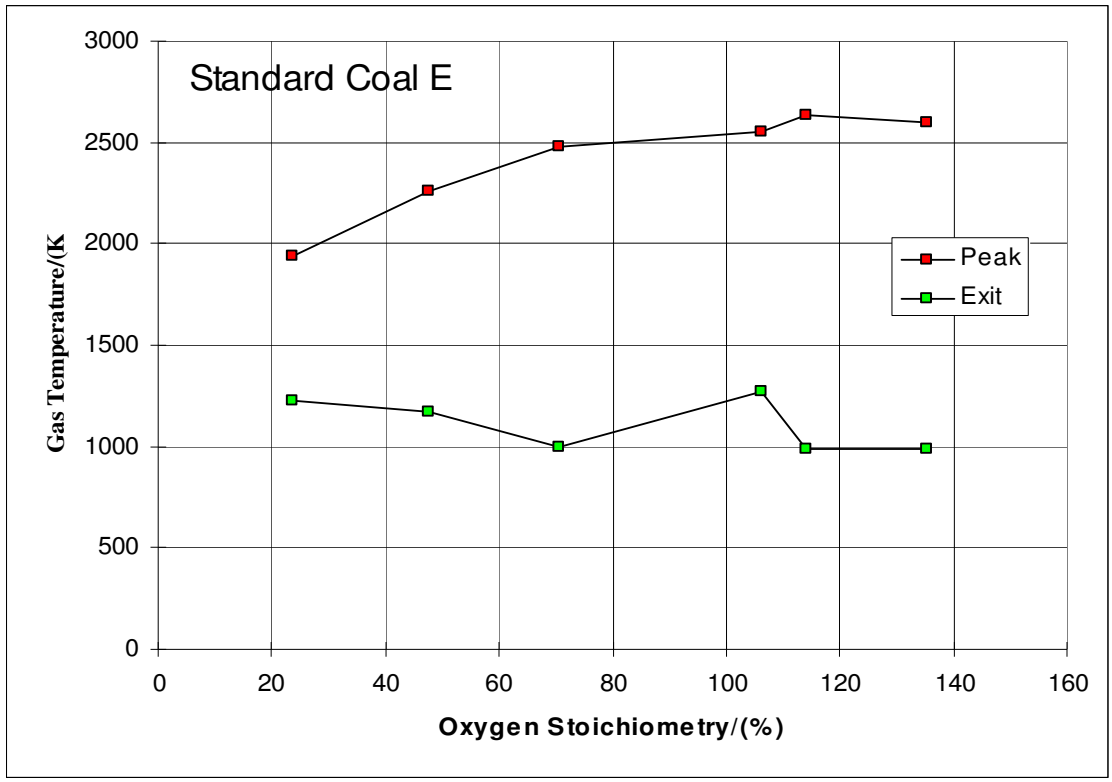

Figure 6.22a: Gas temperatures for Standard runs with different stoichiometries

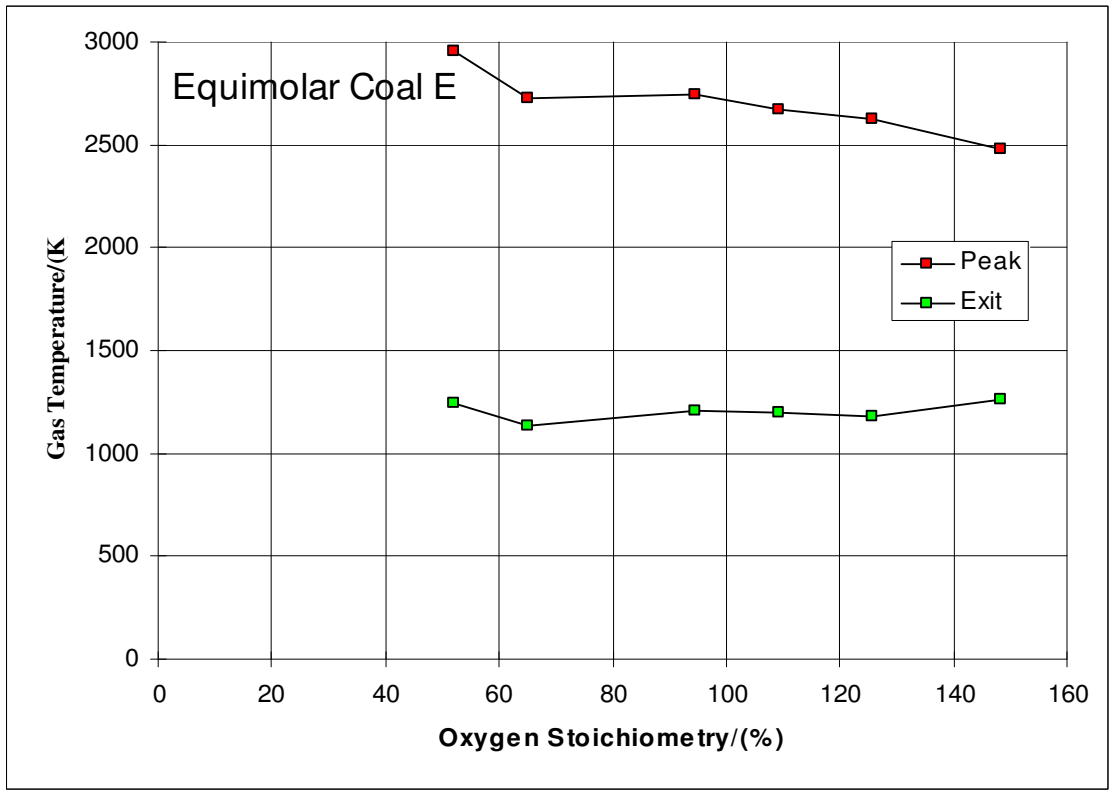

Figure 6.22b: Gas temperatures for Equimolar runs with different stoichiometries

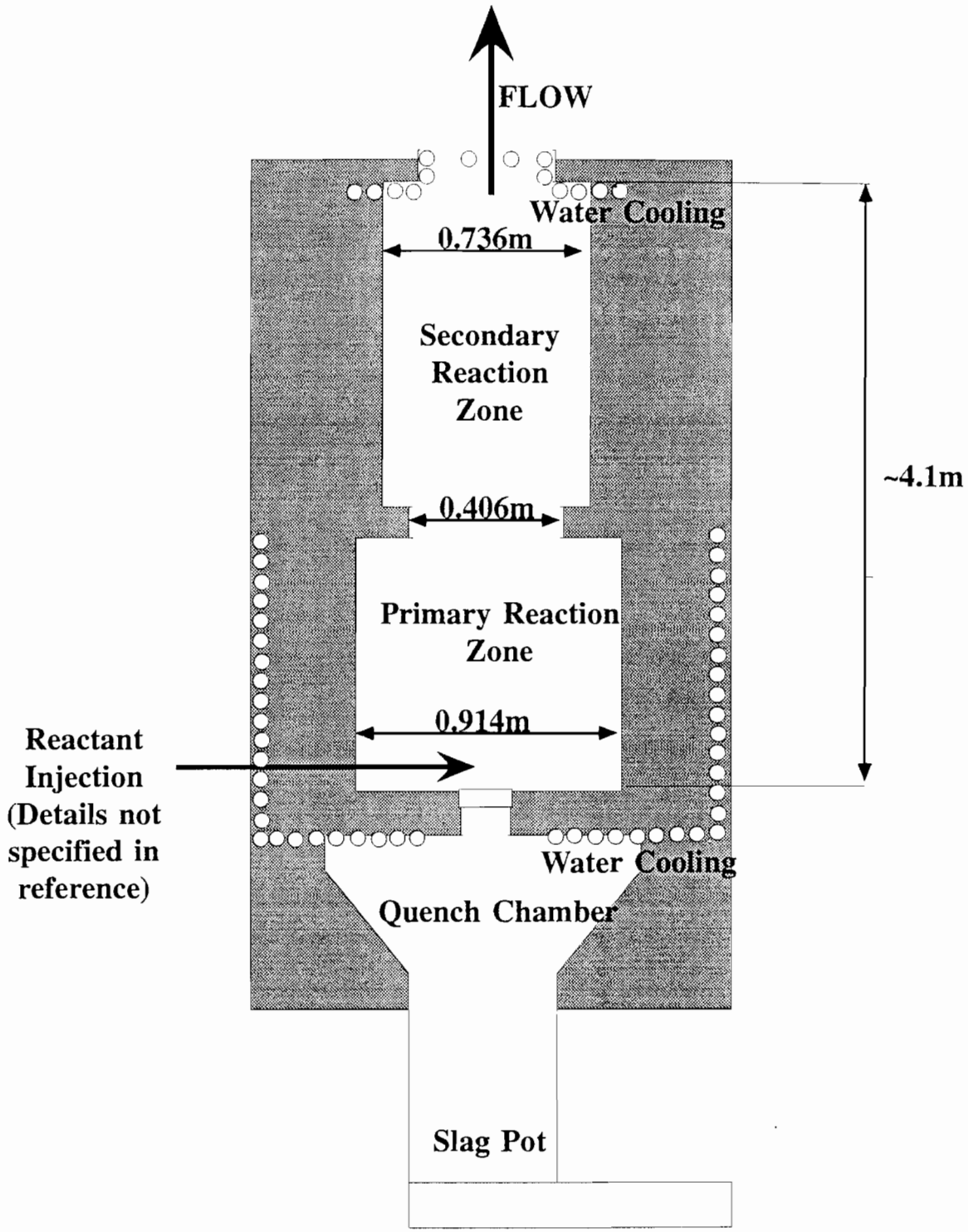

Figure 6.23: USBM atmospheric pressure gasifier (USBM (1954)) 192

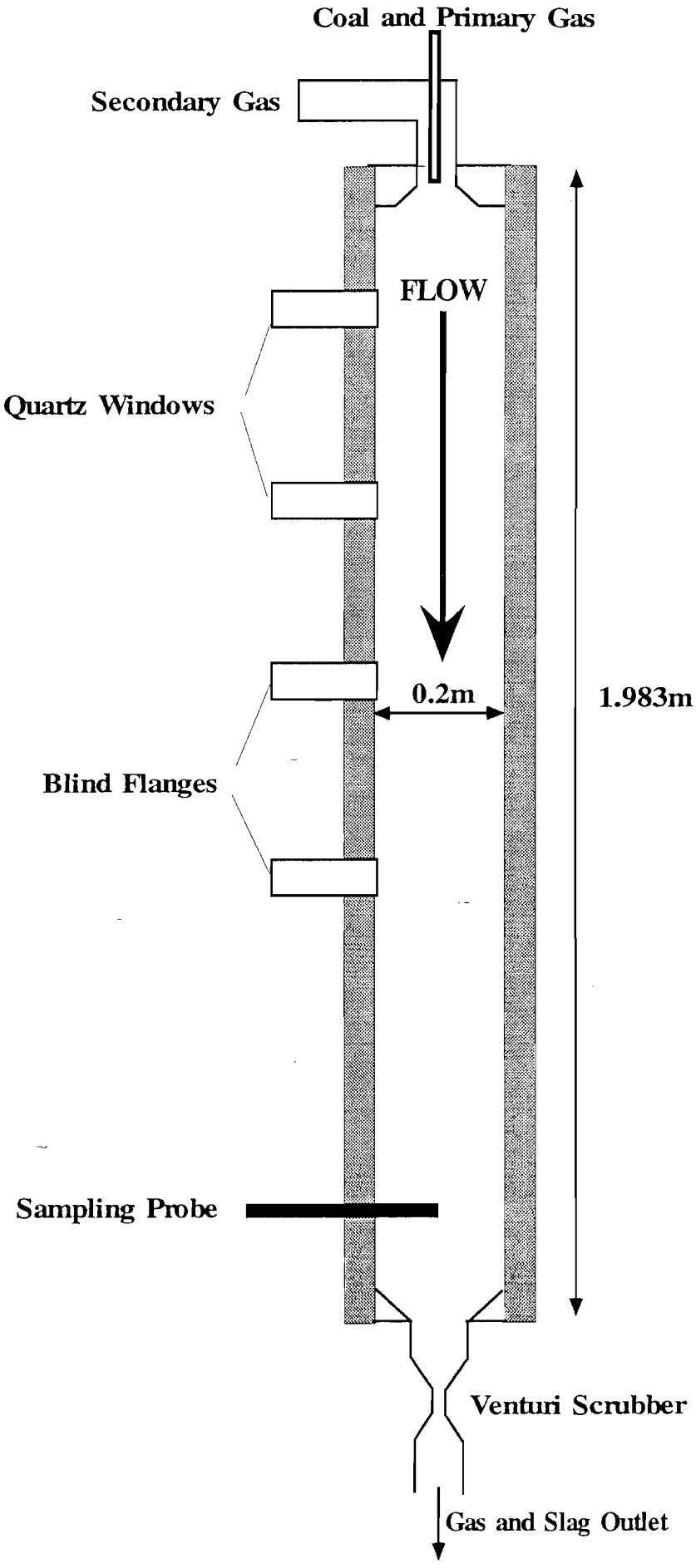

Figure 6.24:BYU laboratory scale gasifier (Brown *et al.* (1988))

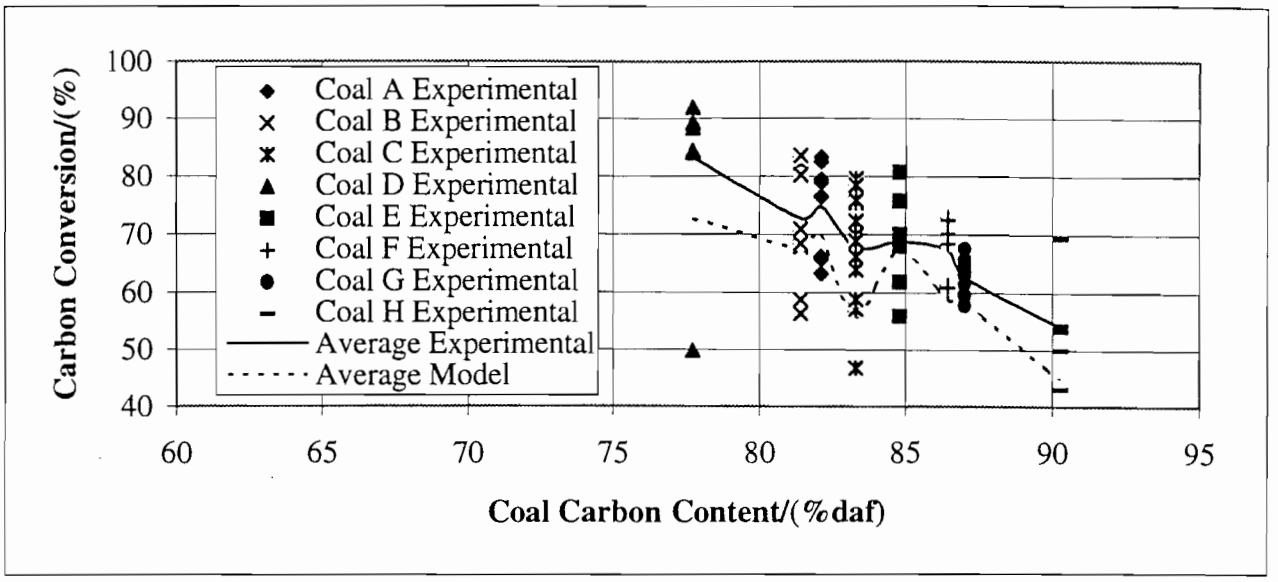

Figure 6.25: Comparison of model predictions with CSIRO (1995) experimental results.

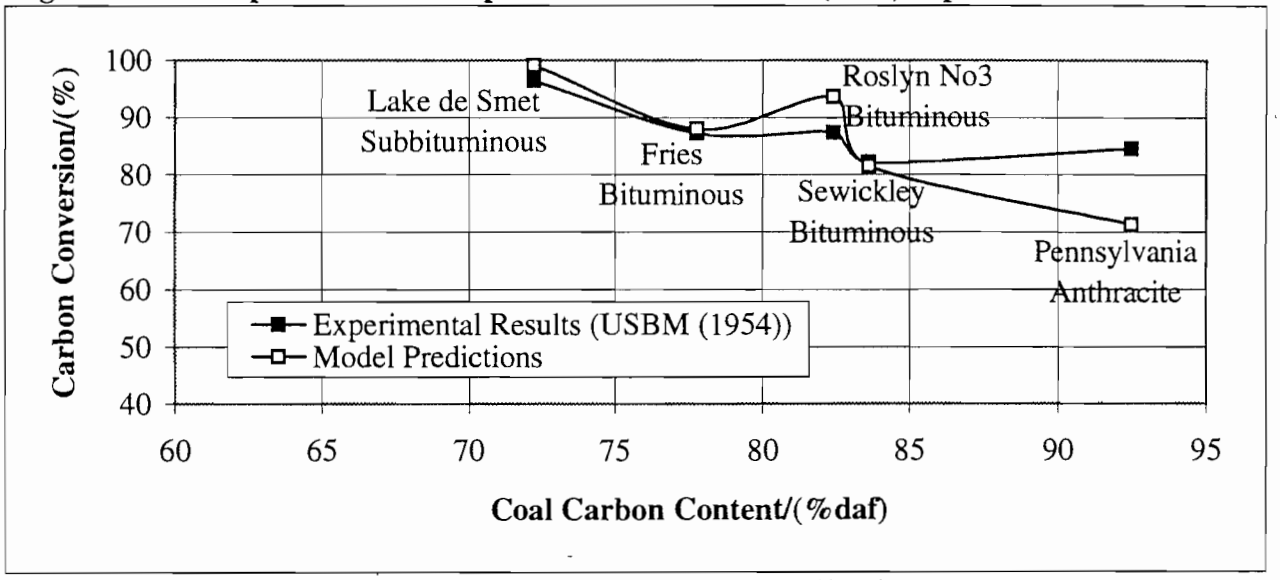

Figure 6.26: Comparison of model predictions with USBM (1954) experimental results.

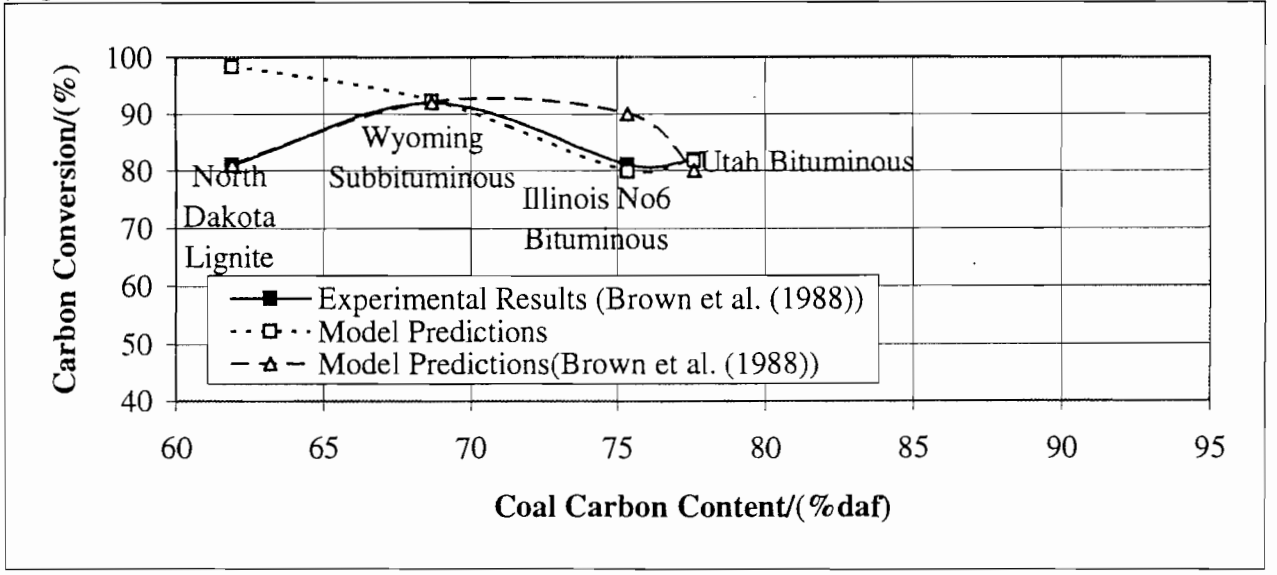

Figure 6.27: Comparison of model predictions with Brown *et al.* (1988) experimental results and model predictions.

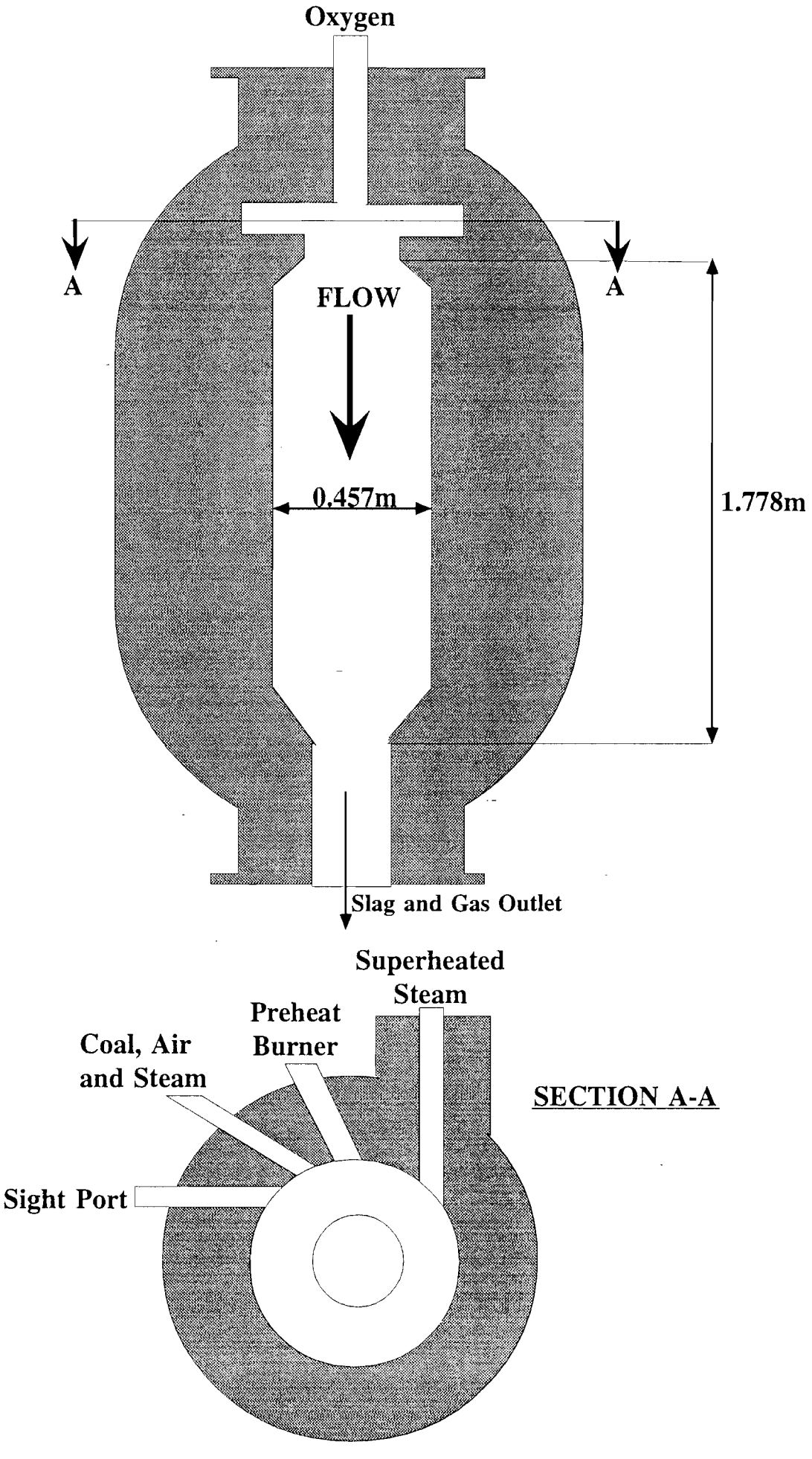

Figure 6.28: IGT pressurised experimental gasifier (IGT (1957))

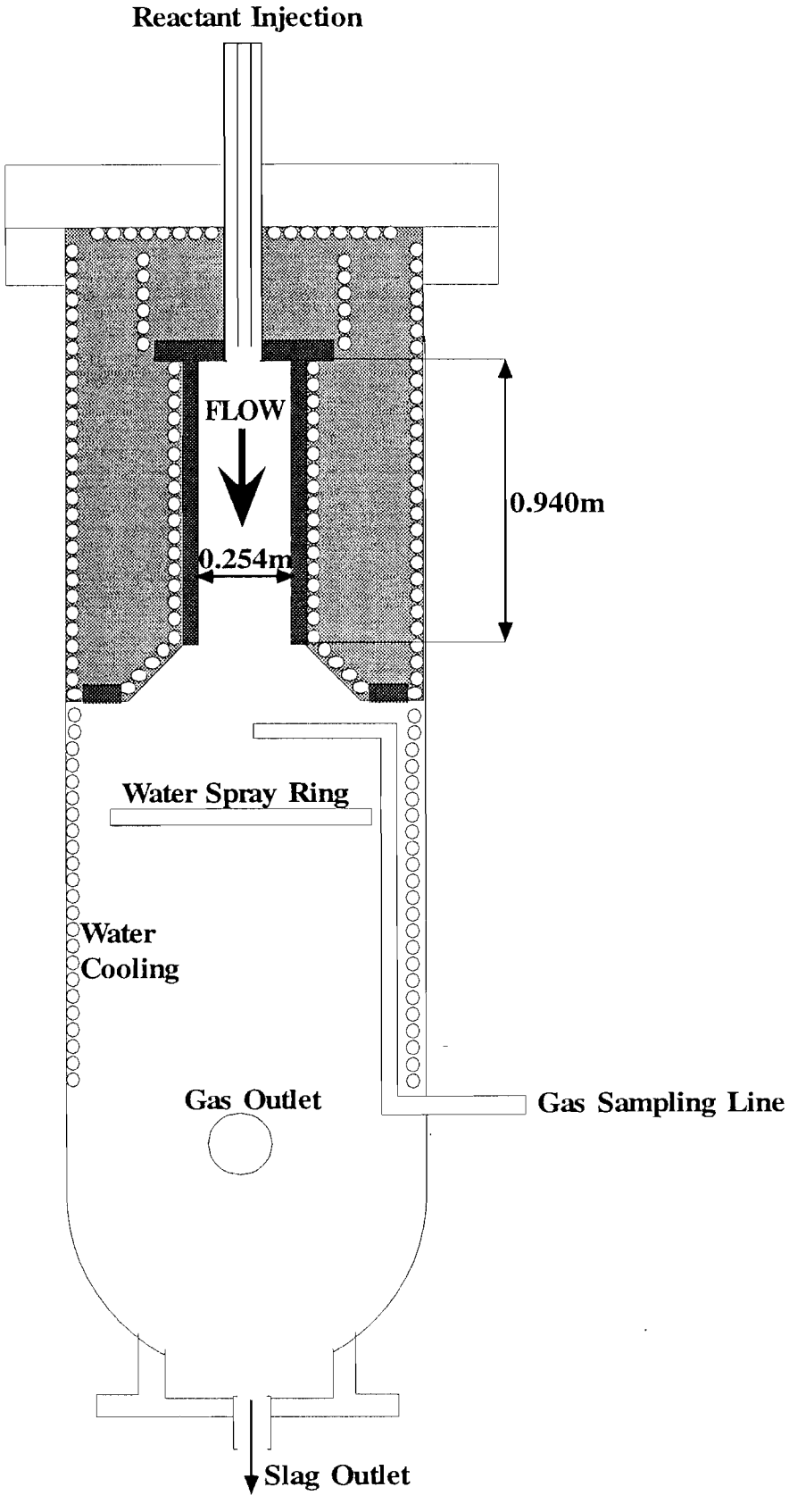

Figure 6.29: USBM pressurised gasifier (USBM (1953))

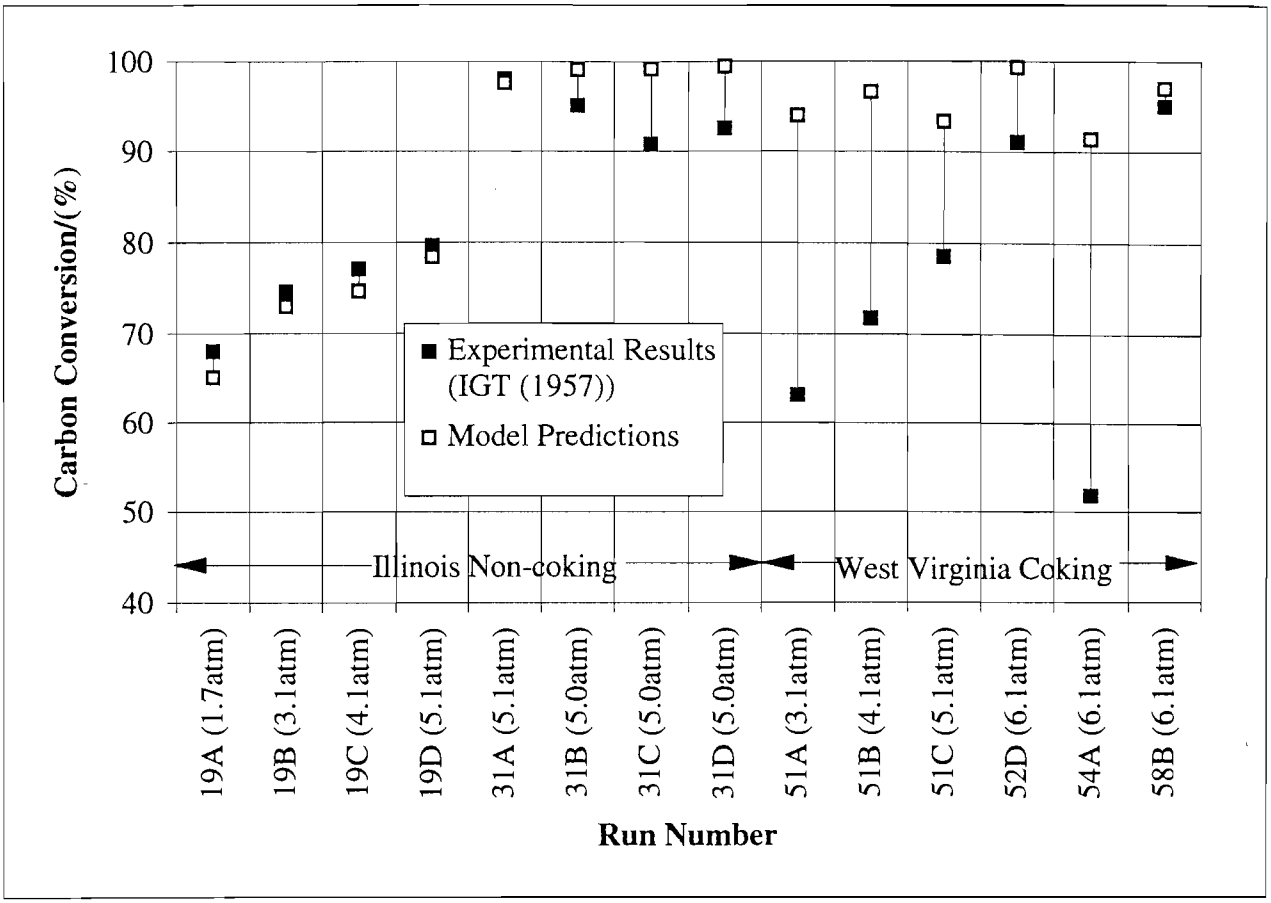

Figure 6.30: Comparison of model predictions with intermediate pressure IGT (1957) experimental results.

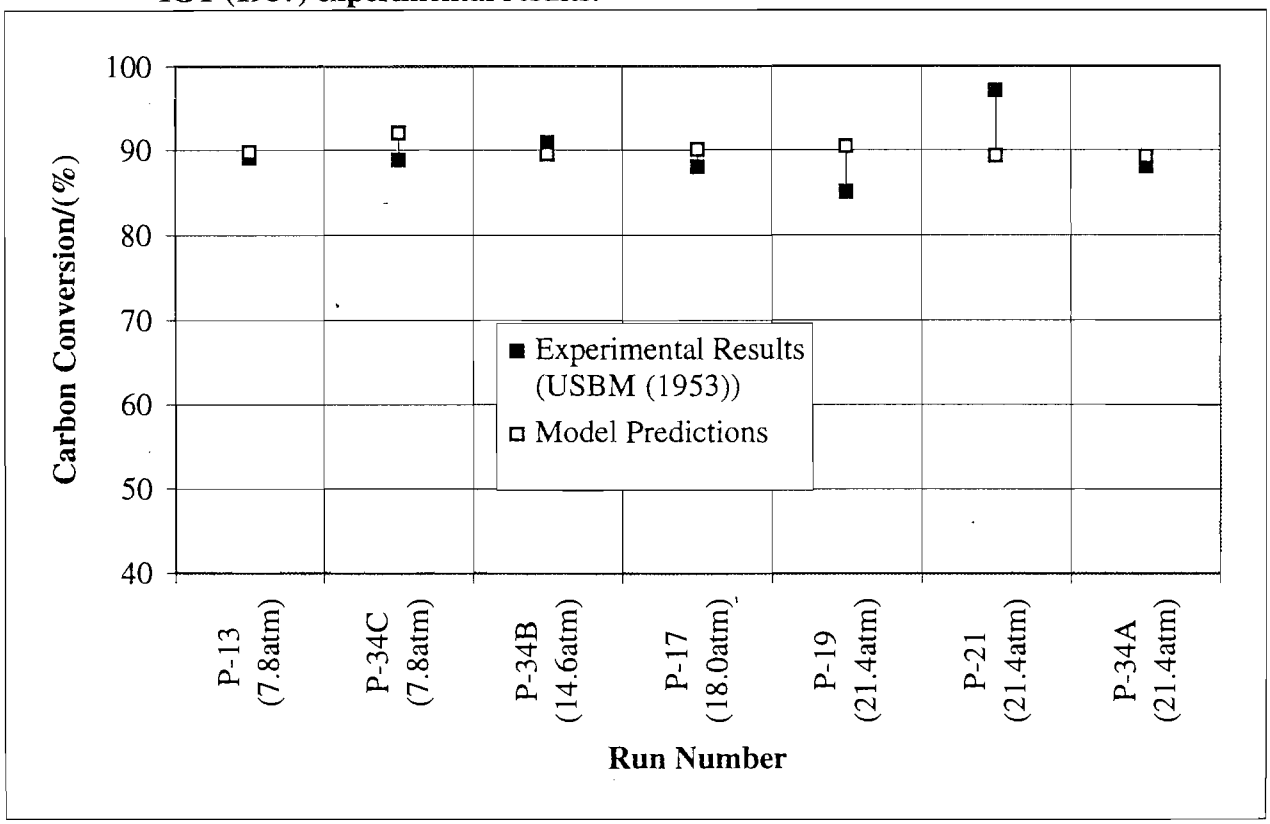

Figure 6.31: Comparison of model predictions with high pressure USBM (1953) experimental results.

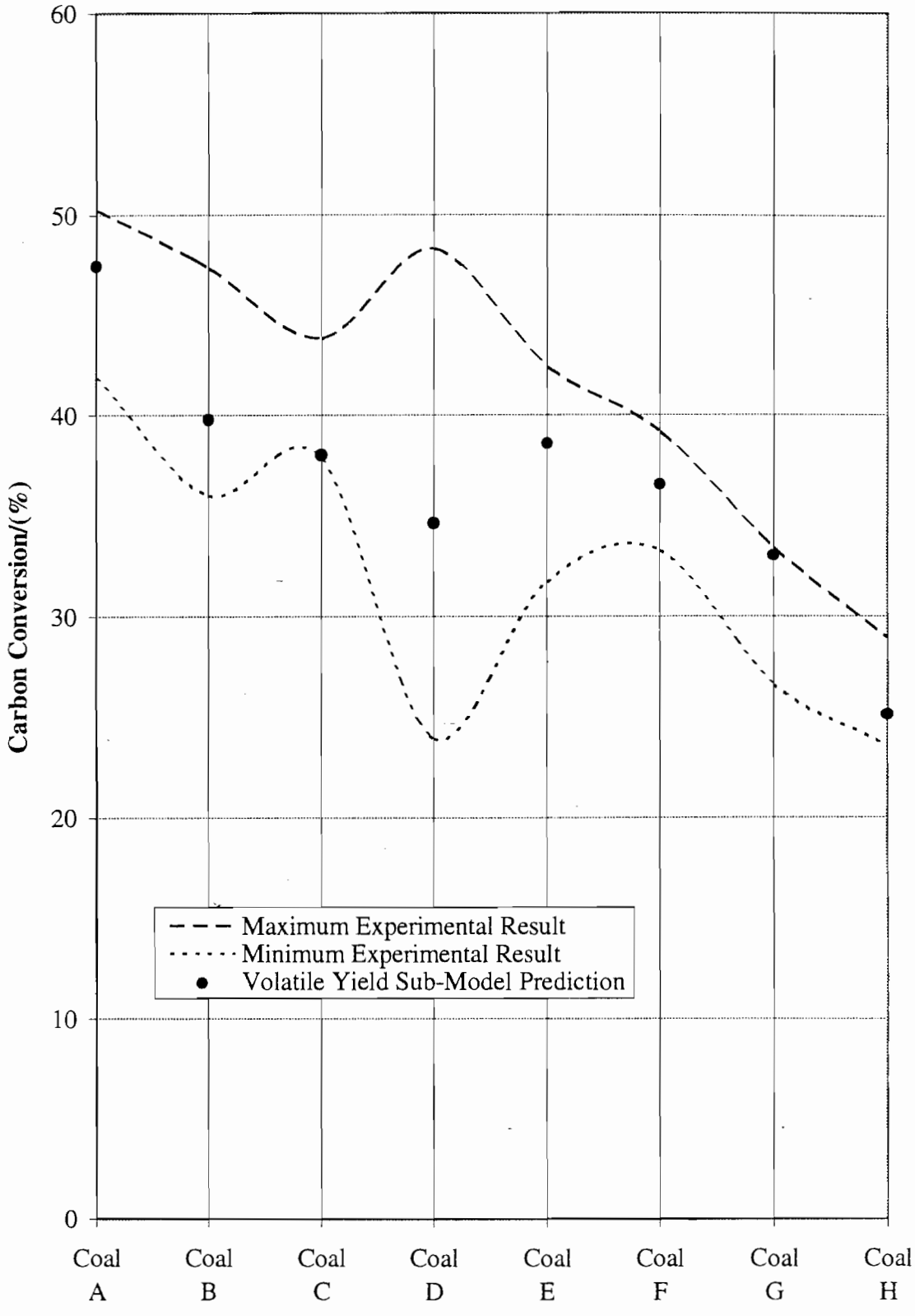

Figure 6.32: Comparison of volatile yield sub-model predictions with overall carbon conversion experimental results at low stoichiometry.

7. USE OF MODEL PREDICTIONS TO DETERMINE REACTION MECHANICS AND OPTIMUM GASIFIER FEED MIXTURES

7.1 Introduction

It is the aim of this section to provide illustrative examples of the capabilities of the model developed. In previous sections the predictions of the model have been focussed on variables that can be compared with experimental results, but it is also possible to make predictions that can aid in the understanding of processes occurring in the gasifier or the design and operation of gasifiers. Two specific areas will be examined in this section, namely the predicted modes of the gasification reactions and the influence of changes in gasification conditions on the optimum mixture of feed gases. Reaction modes is a generic term covering the reaction regimes and interaction of different gasification reactions. Optimum gasification feed mixture is defined by the ratios of oxygen and steam to coal at which gasifier performance is at a maximum, for a given gasifier design. Variations in gasification conditions that are considered are gasifier pressure, gasifier diameter and feed coal.

The major work of this model has been in attempting to accurately model the progress of particle reactions and to allow for realistic progress of reactions only a limited number of assumptions have been made. Foremost of these is the assumption of only a single pore size for each particle, for simplification of pore diffusion calculations, and also the assumption that ash from converted portions of the particles does not interfere with reactions. As the temperatures experienced in the initial stages of gasification are considerably higher than common ash fusion temperatures it is assumed that the coal ash will melt and the droplets of molten slag will occupy only a small proportion of the external particle area, some support for this assumption can be found in Lin *et al.* (1994) although results in that study vary depending on the particular coal and reaction temperature used. In other aspects of the particle reaction modelling a 'natural' interaction of influences on heterogeneous reaction rates is allowed by modifying the diffusion rates of reactant gases to the particles due to hindrance by the flux of volatiles and product gases away from the particles. Due to this is possible for the model to

predict if heterogeneous reactions occur prior to or during devolatilisation, and whether different heterogeneous reactions occur simultaneously or are sequenced due to differences in reaction and diffusion rates.

Another aspect of the model purpose that has only fleetingly been considered in previous sections is the selection of operating conditions to provide optimum gasification conditions. In the broad sense the operating conditions of a gasifier can include elements of the gasifier design, such as diameter, and the mixture of gases input with the coal. When varying conditions in a hypothetical situation, where comparison with experimental results is not required, gasifier performance is best considered in terms of cold gas efficiency. It was shown in an earlier section that cold gas efficiencies determined from results of small scale gasifiers can be inaccurate, however it is a better indicator of the performance of gasifiers than carbon conversion as it describes the value of the product gas and is therefore more commonly used for larger gasifiers. By varying the coal used in the model and identifying the ratios of oxygen and steam to coal for which the predicted cold gas efficiencies are maxima the influence of the feed coal on the operating conditions of a gasifier can be estimated, and also a preferred coal for gasification can be selected.

7.2 Reaction Rate Study

7.2.1 Influence of Reaction Modelling on Predictions

The model can be used to predict the influence of individual reactions on the rate of carbon conversion in a gasifier. Using as an example the same experimental run as was used previously in the sensitivity analysis, that is the CSIRO gasifierwith Coal E at 106% oxygen stoichiometry, the individual reaction rates can be shown from the model predictions. In figures 7.1 and 7.2 predicted carbon conversion rates and total carbon conversion due to individual reactions are shown as functions of distance along the gasifier. Please note that the axis indicating distance along the gasifier is on a logarithmic basis so as to provide better definition in the early stages of the gasifier.

Figure 7.1 shows the rates of carbon conversion due to volatile release and heterogeneous reactions, while figure 7.2 gives the predicted carbon

conversion due to each of the reactions, both as functions of distance along the gasifier. The most pronounced mechanism of carbon conversion is volatile release that is indicated by six distinct peaks in figure 7.1, denoting the six particle sizes used in the model. Volatile release is predicted to occur rapidly in the initial stages of the gasifier with the largest particle size being completely devolatilised by 0.05m into the gasifier. In the modelling of devolatilisation no direct allowance for particle size was considered and the separation of the peaks is therefore dependant solely on a difference in heating rate of the particles with size. In figure 7.2 it is indicated that a total carbon conversion of approximately 38% was predicted for volatile release.

In contrast to volatile release, the curves shown for the predicted rates of carbon conversion due to the heterogeneous reactions in figure 7.1 do not exhibit the influence of different particle sizes in the gasifier. This is due to the slower rates and influence of gas composition on the reactions leading to overlap between peaks in reaction rate of different particle sizes. Oxygen gasification, as expected due to its more rapid rate, commences noticeably before the other heterogeneous reactions and ceases when the oxygen is depleted. Carbon dioxide and steam gasification commence at similar distances along the gasifier, overlapping with the region in which oxygen gasification occurs. Carbon dioxide is predicted to have a much greater rate than the steam gasification and occurs at significant rates up to approximately 0.5m along the gasifier. The influence of this is more accurately portrayed in figure 7.2 as carbon dioxide gasification is predicted to account for approximately 31% carbon conversion. Oxygen gasification, which peaked at higher rates than carbon dioxide gasification but only briefly, is predicted to account for a carbon conversion of only 3%. Steam gasification was predicted to proceed at slow rates and accounted for only 2% carbon conversion. This largely explains the pronounced sensitivity to carbon dioxide gasification rates found in the sensitivity analysis.

To further clarify the interaction of reactions at the particles a single particle size, namely 97μm, is considered in figures 7.3 to 7.5. In figure 7.3 the predicted gas, particle and wall temperatures are shown with distance along the gasifier. Similarly, in figure 7.4 reactant gas concentrations are shown and in figure 7.5 the volatile release and heterogeneous reaction rates are shown. The figures are shown on

the same distance scale to facilitate comparison between the different variables. Volatile release is indicated to occur rapidly, commencing when particle temperature exceeds 750K, and the flux of volatiles away from the particle prevents diffusion of reactant gases to the particles. This is indicated by the lack of heterogeneous reactions during devolatilisation when the reactant gas concentrations are indicated as high. While devolatilisation is proceeding, the concentration of oxygen decreases due to combustion of the volatiles, and possibly due to oxygen gasification of smaller particles. This raises gas and, to a lesser extent, particle temperatures. Oxygen gasification commences immediately after devolatilisation ceases and peaks rapidly then ceases with the depletion of oxygen. During devolatilisation and oxygen gasification the steam and carbon dioxide concentrations increase, coming to a maximum at the point of oxygen depletion. Carbon dioxide and steam gasification commence during oxygen gasification, but rise to maximum rate only after all oxygen is consumed. Although the concentration of steam is indicated as being slightly higher than that of carbon dioxide, carbon dioxide gasification is predicted to be approximately eight times faster than steam gasification under these conditions. As carbon dioxide and steam gasification are endothermic the gas and particle temperatures drop while these reactions dominate. This appears to be responsible for a decline in both rates and when the wall temperature drops below 1500K the gas and particle temperatures also drop and the reaction rates decrease to insignificant levels. The concentrations of carbon dioxide and steam are still significant in the later sections of the gasifier but little reaction occurs. Hydrogen concentrations rise after the depletion of oxygen but hydrogen gasification is predicted to be insignificant for the entire length of the gasifier.

From the predictions discussed in this section it appears that reaction sequencing occurs in the gasifier, but with some overlap. The model calculates that the flux of volatiles through the particle boundary layer is sufficiently high to prevent diffusion of reactant gases to the coal particles. When devolatilisation ceases the remaining oxygen is predicted to react rapidly with the particles. Carbon dioxide and steam also react with the particles during oxygen gasification but their peak rates are delayed until all oxygen is depleted, at which time temperatures, as well as carbon dioxide and steam concentrations, are maximum. Due to the influence of endothermic

reactions the gas and particle temperatures drop with carbon dioxide and steam reacting, resulting in decreasing reaction rates. When the gasifier wall temperatures drop below 1500K reaction rates drop to insignificant levels. Hydrogen gasification is of no significance under these conditions.

7.2.2 Influence of Pressure on Reaction Rate Modelling

In all of the previous modelling predictions the area of the coal particles accessible to reactant gases has been calculated using a complex particle effectiveness factor. This factor includes terms to account for the reaction and diffusion rates, including the influence of pressure order and product gas flows. To indicate the influence of temperature and pressure on the values used in the model for effectiveness factors the component graphs in figure 7.6 have been prepared from the reaction rate sub-model. Each graph in the figure shows the variations in effectiveness factor for one of the heterogeneous gasification reactions. As noted the partial pressure of reactant gas is taken as 80% of the total pressure for each case, also the particle size was taken as 100μm with 1μm diameter pores. All of the reactions show similar trends in effectiveness factor with variations in the positioning of the curves relative to temperature and pressure, and in all cases the influence of temperature on effectiveness factor is more evident than that of pressure. Simple trends are evident as high temperatures decrease the effectiveness factors and high pressures increase them. As the effectiveness factors describe a relationship between reaction rate and diffusion the reasoning behind this is obvious. With increasing temperature the reaction rates increase at a greater rate than diffusion, so the effectiveness factor decreases as reactant gases are consumed before diffusing far into the particle pores. Conversely, with increasing pressure the diffusion rate increases roughly proportionally to the pressure while, with fractional pressure orders, the reaction rate increases to a lesser degree to result in higher effectiveness factors.

Each of the gasification reactions has a distinctive pattern of effectiveness factor variations with temperature and pressure. Hydrogen gasification is shown as a simpler relationship as the slower reaction rate leads to high effectiveness factors over most of the graph, only decreasing at very high temperatures. Oxygen

gasification effectiveness factors decrease rapidly for temperatures greater than 500K and are approximately zero by 1750K. Carbon dioxide factors are similar but decrease at 1000K and are near zero above 2250K, due to a slower reaction rate than oxygen. Steam gasification factors have a more gradual decrease with temperature, decreasing from 1250K onwards and approaching zero above 2750K. The slower decrease for steam gasification probably arises due to its unusual variations in physical properties at high temperatures. The influence of pressure on effectiveness factors produces increases of up to 0.22 from atmospheric pressure to 41 atmospheres pressure for the different reactions.

While the previous figure indicates only a mild influence of pressure of the effectiveness factors of gasification reactions the resultant impact on the modelling methods used could be significant. In figure 7.7 three different sets of modelling predictions have been prepared to indicate the influence of effectiveness factor calculations on the predictions. The basic prediction used is for the CSIRO gasifier Coal E 106% stoichiometry run, used previously in the sensitivity analysis, with a calculated particle effectiveness factor for each of the heterogeneous reactions. Additional predictions were made using simplified reaction rate modelling that either assume that the heterogeneous reactions were either limited by the chemical reaction rate (effectiveness factor unity) or that the diffusion of gases to the particles (effectiveness factor zero). Carbon conversion predictions from these three different models are shown in figure 7.7a as functions of distance along the gasifier. As shown in this figure the predicted carbon conversion from the normal model is approximately 5% below the chemically limited model prediction while the diffusion limited model predicts much higher carbon conversion. This indicates that the normal model calculated that pore diffusion hindered the reactions significantly. The other two parts of figure 7.7, b and c, show the same predictions assuming gasifier pressure was 10 and 30 atmospheres respectively, with feed rates increasing proportionately to pressure. These figures indicate that the predictions assuming chemical rate limitation and the normal model approach each other as pressure increases. This suggests that a simplified model that neglects pore structure and diffusion, excepting the particle pore area, could be applicable at high pressures with the introduction of minimal error. This is significant in the development of complex models

that include fluid dynamics modelling as the inclusion of complex particle calculations adds excessively to computation time in these models.

7.3 Gas Feed Mixture

A number of variables can influence the selection of optimum feed mixture to a gasifier. In the following studies the modelled gasifier is based upon the CSIRO experimental gasifier previously discussed but with a uniform wall temperature of 1500K and the feed mixture used contains only oxygen, steam and nitrogen, as is typical of large gasifiers. More realistic temperatures for gas and particle input streams to the gasifier of 800 and 500K respectively were also selected. The assumed coal feed rate has a marked impact on predictions in many cases and variations in the input values affect the residence times in the gasifier. In each series of predictions the coal feed rate is varied to allow for logical comparison between predictions, however comparison between different series of predictions is not generally possible as variations in the coal feed rates can lead to nonsensical conclusions. For example several figures in the following sections show the variations in cold gas efficiency with changes in feed mixtures for Coal E at 20 atmospheres pressure in a 0.1m diameter gasifier, however all vary slightly due to variations in the coal feed rate assumptions for each series of predictions. Therefore each set of figures should only be considered in the context of the section it is contained in.

As an explanatory note about the graphs shown in the following sections the effects of inputs of oxygen and steam into a gasifier should be discussed. The simplest effect of changing the quantity of gas added to a gasifier is the variation in residence time. Also greater quantities of gas have a dilution effect that reduces the peak temperatures experienced in the gasifier, and therefore the reaction rates. This means that, as a general rule, the total input of gas should be minimised to improve the gasifier performance. Contradicting this is the requirement for reactant gases to be added in order to convert carbon from the coal particles into carbon monoxide. In this case oxygen is the most efficient additive, as it reacts more rapidly than other gases and, as oxygen gasification is exothermic, raises the gasifier temperatures for faster reaction. However oxygen alone as a reactant can lead to two product gases, carbon monoxide and carbon

dioxide, and to achieve optimum gasification efficiency it is not possible to add sufficient oxygen to gasify all carbon as this will lead to excessive carbon dioxide formation. When all oxygen is consumed other gases, such as carbon dioxide and steam, will react with the carbon and therefore it can be beneficial to add steam to the gasifier. Steam has two effects on gasification in that it can gasify carbon but will also lower the gasifier temperature as the reaction is endothermic. Therefore a balance in the quantity of steam and oxygen added must be found to maintain gasifier temperatures at a high enough value to allow gasification to proceed at an acceptable rate and also to minimise the concentration of carbon dioxide in the exit gases. In the following graphs an optimum region of operation based on oxygen and steam feeds is usually clearly defined, however the location of this region can vary depending on other operating conditions, gasifier design and coal properties.

7.3.1 Pressure Effects

The influence of pressure on model predictions was considered in a previous section and it was indicated that only a slight improvement in gasifier performance was expected if gasifier feed rates were altered proportionally to the pressure changes. In figures 7.8 to 7.11 the effect of varying the ratio of feed gases to coal on the predicted cold gas efficiency at pressures from 1 to 30 atmospheres is considered. In all cases the feed rate of coal is adjusted to be in proportion to the gasifier pressure. On each of the graphs the location of the maximum cold gas efficiency is identified by a 'X' with the corresponding cold gas efficiency given below the legend. It is obvious that the constraints determining the optimum feed ratios varies with pressure as the maximum cold gas efficiency moves from 0.5 kg of oxygen and 0.5 kg of steam, per kg of coal (dry, ash free basis) at 1 atmosphere pressure to 1.0 kg oxygen and 0.4 kg steam at 10, 20 and 30 atmospheres. The likely reason for this is the predicted fall in volatile yield at high pressures. At atmospheric pressure the heterogeneous reaction rates are slower and the optimum cold gas efficiency arises from devolatilisation with minimal oxidation of volatiles by oxygen. Steam is added to provide additional gasification reactant after the oxygen has been consumed but can also adjust the equilibrium gas composition. At higher pressures the lower volatile yields lead to a dependence on

heterogeneous reactions to convert carbon into carbon monoxide, therefore significant quantities of oxygen are required to increase carbon conversion by oxygen gasification, and indirectly carbon dioxide and steam gasification. Again steam is required to increase carbon conversion by gasification and to adjust the equilibrium gas composition. In contrast to the predicted influence of pressure on carbon conversion at the same gas feed rates, it is indicated that the maximum cold gas efficiency decreases from atmospheric pressure to higher pressures, although by 30 atmospheres pressure the cold gas efficiency has risen to approximately the same value. This again is related to the predicted change in volatile yield with pressure.

7.3.2 Gasifier Size

In a previous section it was shown that model predictions were insensitive to gasifier length after some critical value, when the endothermic reactions reduce the temperatures so that reaction rates become negligible, so this study will concentrate on the influence of gasifier diameter on the optimum feed mixture, at constant gasifier length. This corresponds to a scale-up in gasifier size and, to keep residence times approximately constant with varying gasifier diameter, the feed rates were adjusted to maintain proportionality to the cross sectional area of the gasifier. In figures 7.12 to 7.15 the influence of gasifier feed ratios on predicted cold gas efficiencies is shown for gasifier diameters of 0.1m, 0.5m, 1.0m and 2.0m. All predictions were made at 20 atmospheres total pressure. For each of the graphs the optimum mixture of feed gases is indicated by an 'X' and is in the range of 0.8 to 0.9 kg of oxygen and 0.3 kg of steam, per kg of coal (dry, ash free basis). The values of cold gas efficiency predicted at the optimum feed mixture vary with gasifier diameter, rising from 69.0% for a 0.1m diameter gasifier to 80.2% for a 1.0m diameter gasifier then dropping to 75.2% for a 2.0m gasifier. The reasons for this are not certain but a number of effects could influence the predictions. Obviously for larger size gasifiers the impact of wall temperatures on gasification will be reduced due to the lower ratio of wall area to gasifier gas volume. This reduces the heat exchange between wall and the gas-particle mixture, both in initial stages of gasification when gas and particles are heated and later when hot gases lose energy to the walls. The relative influence of these changes on the gasifier performance

could vary as the diameter is increased so that with initial diameter increases the reduced loss of heat to the walls improves efficiency while at larger diameters the slower heating of the feed gases reduces efficiency to a greater extent. It is also possible that some components of the model have exceeded their range of realistic operation at the higher diameters. The most likely components for this failure are heat transfer and physical properties. Heat transfer modelling can become unrealistic when the path length for radiative transfer is larger than acceptable in the algorithm for calculating gas emissivity. This can occur in large diameter and high pressure gasifiers with high concentrations of steam or carbon dioxide. In large diameter gasifiers the reduced heat transfer to the gasifier walls can lead to excessively high gas temperature predictions. This is largely a limitation of the physical property calculations for the gas as the methods used do not allow for dissociation of gases at high temperatures, which affects reaction rate and other calculations in the model. Inclusion of dissociation in the model is complex as dissociation is affected by both temperature and pressure, affects all of the gas physical properties and introduces an additional set of possible gasification reactions involving dissociated species. It is likely therefore that the predictions indicated in figure 7.15, and possibly figure 7.14, are outside the range of design of the model and additions to the model must be made to confidently model large high pressure gasifiers.

7.3.3 Coal Effects

To illustrate the impact of coal properties on the optimum input rates of oxygen and steam to gasifier predictions for the series of coals used in the CSIRO study were compared (see table 6.1 for analysis results). The predicted cold gas efficiencies with changing oxygen and steam inputs are shown in figures 7.16 to 7.23 for the eight coals. In this case the amount of coal fed to the gasifier was kept constant between coals on a dry, ash free basis and the gasifier pressure was set as 20 atmospheres. The maximum cold gas efficiencies found for each coal and the gas feed ratios at which this occurred are summarised in table 7.1 in order of decreasing cold gas efficiency. Values are given as ranges due to the inaccuracy involved in generation of the graphs from a finite number of data points, a grid spacing of predictions with gas ratios varied in steps of 0.1kg/kg (daf) coal. Therefore the optimum gas ratio is indicated in a

range, with the locations indicated on the figures being the closest grid intersections. The range in maximum cold gas efficiency was then estimated from the gradients in cold gas efficiency surrounding the selected grid points.

Table 7.1: Summary of optimum gas feed ratios for CSIRO study coals.

Coal	Maximum Cold Gas Efficiency/(%)	Optimum Oxygen /(kg/kg (daf) coal)	Optimum Steam /(kg/kg (daf) coal)
D	86.0-88.2	0.7-0.8	0.1-0.2
A	74.6-75.6	0.8-0.9	0.3-0.4
E	69.2-72.6	0.8-0.9	0.2-0.3
B	64.4-66.0	0.8-0.9	0.2-0.3
F	63.5-66.0	0.9-1.0	0.2-0.3
G	61.2-63.0	1.0-1.1	0.3-0.4
C	52.4-53.8	0.9-1.0	0.2-0.3
H	47.2-47.5	1.0-1.1	0.2-0.3

It is difficult to make precise conclusions from the predictions indicated in the figures and summarised in table 7.1, however some general observations can be made. For the majority of the coals studied the optimum gas feed mixture appears to be 0.8 to 1.0 kg of oxygen and 0.2 to 0.4 kg of steam, per kg of coal (dry, ash free basis). Exceptions are Coal D, which requires less steam, and Coals G and H, which require more oxygen. In the case of Coal D the variation is probably due to the higher moisture content of the coal contributing steam with the coal, or alternatively could be due to the higher reactivity for a lower rank coal resulting in lower steam requirement to achieve equivalent conversion to the other coals. Coals G and H are both higher rank coals and this may mean that a higher oxygen input is required to give higher temperatures to result in higher reaction rates. With regard to the ranking of coals on the basis of predicted maximum cold gas efficiency possible in the gasifier, it appears that a number of competing influences makes correlation with coal characteristics difficult. The best performing of the coals is Coal D that differs from the other coals mostly in being lower rank, with a higher predicted reactivity, and the conversely the worst

performing coal is Coal H that is of high rank, therefore causing prediction of low reactivity. Coal C is indicated as the second worst performing coal, however previous comparison of experimental results with model predictions indicated that the model significantly underpredicted results for this coal so it will be neglected. The predictions for the other coals are within a range of 10% cold gas efficiency, with the exception of Coal A that is a very high volatile matter coal and has the second best performance of the coals. The coals that are grouped mid-range in the predicted cold gas efficiencies, Coals E, B, F and G, are linked by having similar volatile matter contents. This may be indicate one controlling influence of gasification performance as the coal volatile matter, with another being large variations in reactivity as predicted due to coal rank differences. The optimum gas feed mixtures found in this study are comparable with those reported in EPRI (1993) for a Shell entrained flow gasifier which, for a range of 18 different feed materials (including lignites and petroleum coke but mostly bituminous coals), indicated optimum feed ratios of 0.84 to 1.04 kg of oxygen per kg of coal (daf) and 0.10 to 0.33 kg of steam (and moisture from the coal) per kg of coal (daf). The moisture from the coal was included in the steam input for these coals for the purpose of comparison as the CSIRO coals were air dried prior to gasification so the studies cannot be compared directly. The model predictions for optimum feed mixture therefore appear to be realistic.

7.4 Conclusions from Model Predictions

In the study of reaction rate modelling the influence of individual reactions on carbon conversion were predicted. From these predictions it appears that sequencing of particle reactions occurs, although overlaps occur with more than one reaction occurring simultaneously. Initially devolatilisation is rapid and the flux of volatiles prevents reactant gases diffusing to the coal particles. As devolatilisation ends any remaining oxygen is rapidly consumed by oxygen gasification of the coal and the rapid rate of this reaction, compared to the other heterogeneous gasification reactions, leads to it dominating conversion until the oxygen is consumed. With declining oxygen concentration in the gasifier the carbon dioxide and steam gasification rates rise, with carbon dioxide gasification rate being predicted as almost an order of magnitude higher

than the steam gasification rate. As these reactions are endothermic temperatures decline in the gasifier and correspondingly reaction rates drop to negligible values in the second half of the gasifier. Hydrogen gasification rates are not significant at any stage in the gasifier. Another finding of the reaction modelling study was that at high pressures a simpler reaction model, chemically rate limited, can be used instead of the complex pore effectiveness factor model normally used without significant change in model predictions.

In the other part of this study the optimum gas feed combinations for a variety of pressures, gasifier sizes and coals were predicted on the basis of maximum cold gas efficiency for the predicted product gas. Under varying pressure conditions, with the coal feed kept proportional to pressure, it was indicated that lower oxygen input at low pressures is required than at high pressures. This is probably due to the prediction of reducing volatile yield at higher pressures meaning that more heterogeneous reaction is required to gasify carbon at higher pressures. A further series of predictions were made with varying gasifier diameter, coal feed rate being maintained as constant with respect to gasifier cross-sectional area, a general rise in cold gas efficiency is predicted with the optimum mix of feed gases remaining constant. At high diameters a drop in efficiency occurs which is probably related to exceeding the useable range of some model components. The most susceptible model components are the heat transfer calculations, as a maximum path length for radiative transfer is reached, and physical property calculations for the gases, as high temperatures lead to dissociation of the gases which is not modelled. For accurate modelling of large gasifiers at high pressures some improvement of the model is advised. The last series of predictions considered the differences in maximum cold gas efficiency and optimum feed gas mixtures for different coals. While maximum cold gas efficiencies varied significantly for different coals definite trends with coal properties were not determined. Tentative conclusions were that predicted performance is related to coal volatile matter but they can also be influenced by variations in predicted heterogeneous reactivity.

Figure 7.1: Carbon conversion rates for individual reactions in gasifier
Figure 7.2: Carbon conversion due to individual reactions in gasifier

8. CONCLUSIONS

This study has described the development, testing and specific predictions of a mathematical model for entrained flow coal gasification. Most components of the model were developed using methods described in published literature, although in some cases the methods were developed in this study from published experimental results. The resultant mathematical model was tested for sensitivity to expected errors in the values of common inputs and then predictions from the model compared with an extensive range of experimental gasification results at atmospheric pressure. Predictions were also compared with a limited range of experimental results for higher pressure entrained flow gasifiers. Additional predictions were made to establish the capabilities of the model and suggest trends in gasifier performance with changes in gasification pressure, gasifier dimensions and feed coal.

8.1 Errors Sources Associated with Modelling Methods

The development of the mathematical model from literature results involved an extensive literature review considering a wide range of topics. While some of these topics are related to methods used in coal combustion modelling additional data is required to correct for additional gas species present in high concentrations in gasification and also for the higher pressures used in many gasifiers. The key areas of an entrained flow gasification model that require extensive modification in modelling techniques, compared to a combustion model, are volatile yield, heterogeneous reaction rate, homogeneous reactions, radiative heat transfer and gas physical properties.

While volatile yield has been studied by numerous researchers under both atmospheric and higher pressures, no universal correlation has been shown to be capable of predicting volatile yield for any coal under different temperature and pressure conditions. In this study a method was used which combines a correlation for predicting volatile yield at high temperatures and atmospheric pressure, for any coal, with another correlation to predict the change in volatile yield with devolatilisation pressure, based on experimental results for a single coal. It was estimated that errors in the predicted volatile yield from this method can occur, with resultant significant errors in model

predictions. Comparison of predicted and experimental volatile yields during gasification, possible with some assumptions at low stoichiometry, indicate that the method worked accurately for the majority of coals considered.

Two possible methods for heterogeneous reaction rate prediction were considered in the study, namely Arrhenius expressions including pressure order terms to account for the influence of high pressure reactant gases and Langmuir-Hinshelwood expressions. Both types of expression have deficiencies, with the pressure orders being difficult to fit to high pressure experimental data and Langmuir-Hinshelwood expressions being untested at high temperatures. Due largely to the inconsistencies between different literature sources of data for Langmuir-Hinshelwood expressions, Arrhenius expressions including pressure order terms were used to model the reaction rates. The values for pressure orders for each of the reactions were determined from literature values for high pressure experimental rates. Values for the activation energies were also selected from literature but the pre-exponential constants were modified according to the rank of the coal using a literature correlation. This correlation relies upon knowledge of the reactivity of a coal char formed under similar conditions to the subject char. Again this leads to the possibility of errors in model predictions, and for some coals studied significant errors in char reactivity prediction appear to have occurred.

Particle structure must be considered due to the use of intrinsic reaction rate expressions in the heterogeneous reaction modelling. Numerous pore structure models were considered in the literature review but a simple single average pore size model was selected for use in the model due to the lack of data available for most of the subject coals. The errors associated with use of this model were shown to be minimal, compared to more complex models, in the literature.

Homogeneous reaction modelling was performed in the model by a combination of assuming some reactions are instantaneous and that others are always in equilibrium. This method was derived by using literature values of rates and equilibrium constants. In general gas phase reactions involving oxygen are considered to be instantaneous while other reactions are considered to be in equilibrium. The errors involved in this modelling technique are not readily defined and comparison of

experimental and predicted gas compositions indicate erratic variations for no obvious reasons.

The range of temperatures experienced in entrained flow coal gasifiers make radiant heat transfer and convection significant. Convective transfer modelling can be performed using standard literature techniques but in gasification the modelling requirements for radiative heat transfer are more complex. This is due to the high concentrations of emissive gases present at various stages of gasification, in particular in high pressure gasification. An algorithm presented in the literature (Modest (1993)) was used in the model to estimate a grey gas emissivity at each stage of gasification and radiative transfer calculations were adapted to allow for absorption and emission of radiant energy by the gas. The algorithm used for gas emissivity is that the path length for radiative transfer cannot be excessively large, so the model can only be used for a limited range of gasifier sizes and operating pressures. While the experimental results available are for small diameter gasifiers it was estimated that significant errors will arise in the range of 1 to 2 metre diameter gasifiers operating at 20 atmospheres pressure.

Physical properties for the gases were calculated using correlations derived from experimental results for pure gases at high temperatures and pressures. At temperatures exceeding 2500K at atmospheric pressure, and higher temperatures for high pressures, a significant degree of dissociation of gases can occur. This was not considered in the model as it adds significantly to the complexity of modelling gas properties and reactions, so predictions made under situations where very high temperatures are predicted are subject to error. These extremes of predicted temperature are most likely to occur in large diameter gasifiers operating at high pressures due to the higher energy density and lower heat losses to the gasifier walls. This adds another source of error in predictions for this class of gasifier.

8.2 Accuracy of Model Predictions Compared with Experimental Results

Model predictions were made for comparison with a selection of experimental gasification results. Under atmospheric pressures an extensive range of experimental results was available from three different gasifiers using a total of 17 different coals and a wide range of varying feed stoichiometries and temperatures. At

higher pressures a limited range of results was available from two gasifiers operating at pressures ranging from 1.7 to 21.4 atmospheres pressure with five different coals. A general result of the study was that comparison of model predictions and experimental results was best performed on the basis of carbon conversion as this was less susceptible to exaggeration of experimental errors than cold gas efficiency or gas composition.

The large quantity of available experimental data for atmospheric pressure gasification allowed comprehensive comparison with model predictions. Comparison indicated that accurate predictions were made for the majority of the coals considered and almost all predictions were within an estimated error margin of the experimental results. From these results general trends of increasing carbon conversion with increasing coal volatile matter content and decreasing coal carbon content were identified. The coal carbon content is an indicator of coal rank and can be used as an inverse correlator of coal reactivity.

At high pressures the limited experimental data available prevented any general findings on model performance. The predictions for the majority of the experimental results were accurate but results were only available for a limited range of experimental conditions and coals. Predictions for gasification of two similar coking coals differed greatly from the experimental results. Whether this is due to experimental difficulties, which are common with coking coals, influencing the results or model inaccuracy cannot be determined.

8.3 Prediction of Reaction Mechanics and Optimum Feed Mixture

More detailed analysis of model predictions in the absence of supporting experimental data can suggest likely sequencing of carbon converting reactions and variations in optimum feed mixtures depending on gasification conditions.

The model predicts that reactions occurring at the coal particles are sequenced but with some overlap at the transition from one reaction to another. Devolatilisation of the particles is predicted to occur first, followed by oxygen gasification then steam and carbon dioxide gasification. Hydrogen gasification was not found to be significant at any stage. The flux of volatiles through the particle boundary layer during devolatilisation was predicted to reduce diffusion of reactant gases to the

particles so that heterogeneous reaction rates were negligible. After devolatilisation oxygen gasification was far more rapid than the other gasification reactions, until oxygen was depleted. Steam and carbon dioxide gasification commenced while oxygen gasification was occurring and reached peak rates when the particle temperatures were highest, coinciding with oxygen depletion. The rates of steam and carbon dioxide gasification dropped as the temperatures decreased due to the endothermic nature of the reactions.

Optimum feed mixtures, defined as the ratios of oxygen and steam to coal, for specific gasification conditions were predicted on the basis of the model cold gas efficiency. Changes in the predicted optimum mixture were identified for changing gasification pressure, gasifier diameter and feed coal. For example, with increasing pressure the quantity of oxygen required was predicted to increase from 0.5 kg per kg of coal (daf) at atmospheric pressure to 1.0 kg per kg of coal (daf) at total pressures higher than 10 atmospheres. The changes with gasification pressure were predicted largely because of the predicted changes in volatile release from the coal. With increasing gasifier diameter, maintaining constant gasifier length and varying feed rates proportionally to gasifier cross-sectional area, the optimum feed mixture showed little variation but the maximum cold gas efficiency was indicated to increase for gasifier diameters up to 1 metre. This was suggested to occur due to the reduced heat losses from larger gasifiers resulting in higher gasification temperatures and therefore higher carbon conversion. At larger diameters a decrease in the cold gas efficiency occurred and this is suspected to have been caused either due to exceeding the maximum path length allowed in the calculation of gas emissivity or excessive temperatures leading to errors in other calculated gas physical properties. In the study of the effects of feed coal on the gasifier optimum feed mixture it was predicted that the optimum steam addition would vary with the moisture content of the coal and the oxygen addition may be connected to the reactivity of the coal. The maximum predicted cold gas efficiency of the coal appeared to be related to a combined effect of coal volatile matter content and coal reactivity, as predicted from coal carbon content. High volatile matter content is indicated as improving performance of coals in gasification while high carbon content reduces the performance.

9. RECOMMENDATIONS FOR FURTHER WORK

In the selection of methods and data from the literature for use in the development of the model some specific research areas appear to have been neglected, resulting in the extrapolation of correlations beyond the range of experimental results. As this introduces ill-defined error sources into the model predictions it is recommended that further research in these areas is required to improve the reliability of gasification models. Areas that appear to require further research are listed below. In addition further development of the model is possible in a number of key areas to improve model predictions and expand the range of model predictions possible.

(a) High Temperature and Pressure Heterogeneous Reaction Kinetics.

Little experimental work involving carbon gasification reactions at both high temperature and high pressure has been published, and that which has been has been inconclusive. This research is required to allow accurate modelling of the reactions and the variation in reactivity between different coal chars under these conditions.

(b) High Pressure Devolatilisation Yields.

While a significant quantity of data has been published for high pressure devolatilisation little has been applicable to the rapid heating rate and high temperature conditions of entrained flow gasification. Sufficient data is required to allow accurate prediction of volatile yield for any given coal under a wide range of pressures and temperature conditions applicable to entrained flow gasification.

(c) Gas Physical Properties.

It was indicated in several prior sections that errors in the model predictions could be caused by inadequate modelling of gas physical properties. A key property is the emissivity of the gas mixture that was calculated using the only correlation for grey gas emissivity published for high pressure gases at path lengths approaching those used in larger gasifiers. It is expected that in large gasifier modelling path lengths exceed the range of this correlation, which means that an improved correlation will be required if modelling of large gasifiers is to be attempted. It was also suggested that the high peak temperatures experienced in gasification at high pressures in large diameter

gasifiers mean that further development of gas property correlations, perhaps encompassing gas dissociation effects, will be required as part of further model development work.

(d) Slag Layer Modelling.

Inclusion of a slag layer model in future gasification modelling is suggested as a means of more accurate prediction of gasifier dimensions and the wall temperatures. A simple model is described and tested in Appendix B but was considered not suitable for inclusion in the present model, in large part due to the absence of a fluid slag layer under the experimental conditions experienced in most of the cases modelled in this study. At the higher temperatures experienced in large gasifiers such a model may be required as liquid slag will coat the walls and wall temperatures will therefore be difficult to estimate from other data.

(e) Fluid Dynamics Modelling.

Improvements in the model predictions in larger gasifiers could be achieved by incorporation of modelling of fluid dynamics, including motion of particles, in the model. This would enable prediction of the impact locations of coal and ash particles with the gasifier wall, which could be used in slag layer modelling. The limitations on reaction rates caused by the rates of mixing of reactants can also be considered in this type of model, which may have significant impact on predictions.

10. REFERENCES

Adanez, J., Labiano, F. G., 1990, "Modeling of Moving-Bed Coal Gasifiers", Ind. Eng. Chem. Res, V29, pp2079-2088.

Adschiri, T., Shiraha, T., Ogawa, K., Furusawa, T., 1985, "Unified interpretation of CO_2 and steam gasification rates of coal chars", Int. Conf. Coal Sci., pp288-294.

Adschiri, T., Shiraha, T., Kojima, T., Furusawa, T., 1986, "Prediction of CO_2 gasification rate of char in fluidized bed gasifier", FUEL, V65, pp1688-1695.

Adschiri, T., Kojima, T., Furusawa, T., 1987, "Estimation of dynamic change in gasification rate of chars- I. A common formulation of dynamic change in experimentally observed surface area during steam gasification of char & II. Overlapped grain model", Chem. Eng. Sci., V42, pp1313-1317, pp1319-1322.

Anon., 1990, "Clean Coal Technology", reprinted from Int. Power Generation, May 1990.

Anon., 1992, "Product Guide : Coal Gasification Systems", Modern Power Systems, June, pp53-57.

Anthony, D. B., Howard, J. B., Hottel, H. C., Meissner, H. P., 1976a, "Rapid devolatilisation and hydrogasification of bituminous coal", FUEL, V55, pp121-128.

Anthony, D. B., Howard, J. B., 1976b, "Coal Devolatilization and Hydrogasification", AIChE J., V22, pp625-656.

Aris, R., 1957, "On shape factors for irregular particles-I The steady state problem. Diffusion and reaction", Chem. Eng. Sci., V6, pp262-268.

Arri, L. E., Amundson, N. R., 1978, “An analytical study of Single Particle Char Gasification”, AIChE J., V24, pp72-87.

AS1038, 1986, “Methods for the analysis and testing of coal and coke: Part 6 Ultimate analysis of higher rank coal - determination of carbon and hydrogen”, Australian Standards Association, North Sydney, NSW.

AS1038, 1989, “Methods for the analysis and testing of coal and coke: Part 3 Proximate analysis of higher rank coal”, Australian Standards Association, North Sydney, NSW.

AS1038, 1992, “Methods for the analysis and testing of coal and coke: Part 1 Higher rank coal - total moisture”, Australian Standards Association, North Sydney, NSW.

Babcock and Wilcox Company, 1978, “Steam : Its Generation and Use”, Babcock and Wilcox Company, New York.

Badzioch, S., Hawksley, P. G. W., 1970, “Kinetics of Thermal Decomposition of Pulverised Coal Particles”, Ind. Eng. Chem. Process Des. Dev., V9, pp521-530.

Balci, S., Dogu, G., Dogu, T., 1987, “Structural Variations and a Deactivation Model for Gasification of Coal”, Ind. Eng. Chem. Res, V26, pp1454-1458.

Ballal,G., Li, C.-H., Glowinski, R., Amundson, N. R., 1989, “Single Particle Char Combustion and Gasification” Comp. Meth. Appl. Mech. Eng., V75, pp467-479.

Ballal, G., Zygourakis, K., 1987, “Evolution of Pore Surface Area during Non-Catalytic Gas-Solid Reactions, 1. Model Development & 2. Experimental Results and Model Validation”, Ind. Eng. Chem. Res., V26, pp911-921, pp1787-1796.

Batchelder, H. R., Sternberg, J. C., 1950, “Thermodynamic study of coal gasification”, Ind. Eng. Chem., V42, pp877-882.

Batchelder, H. R., Busche, R. M., Armstrong, W. P., 1953, “Kinetics of coal gasification, Proposed mechanism of gasification”, Ind. Eng. Chem., V45, pp855-862.

Batchelder, H. R., Busche, R. M., Armstrong, W. P., 1953, “Kinetics of coal gasification, Development of reaction rate equations”, Ind. Eng. Chem., V45, pp1863-1867.

Batchelder, H. R., Busche, R. M., Armstrong, W. P., 1953, “Kinetics of coal gasification, Development of heat transfer equations and method of calculation”, Ind. Eng. Chem., V45, pp1868-1871.

Batchelder, H. R., Busche, R. M., Armstrong, W. P., 1953, “Kinetics of coal gasification, Calculated relation between gasifier yields and process variables”, Ind. Eng. Chem., V45, pp1872-1878.

Batchelder, H. R., Busche, R. M., 1954, “Kinetics of coal gasification, Design of atmospheric pressure gasifiers”, Ind. Eng. Chem., V46, pp2501-2508.

Biederman, D. L., Miles, A. J., Vastola, F. J., Walker, P. L. Jr., 1976, “Carbon-Carbon Dioxide Reactions : Kinetics at low pressures and hydrogen inhibition”, Carbon, V14, pp351- 356.

Blackwood, J. D., McGrory, F., 1958, “The Carbon-Steam reaction at high pressure”, Aust. J. Chem., V11, pp16-33.

Blackwood, J. D., 1959, “The reaction of carbon with hydrogen at high pressure”, Aust. J. Chem., V12, pp14-28.

Blackwood, J. D., Ingeme, A. J., 1960, “The reaction of carbon with carbon dioxide at high pressure”, Aust. J. Chem., V13, pp194-209.

Blackwood, J. D., 1962, “The kinetics of the system carbon-hydrogen-methane”, Aust. J. Chem., V15,pp397-408.

Bliek, A., Lont, J. C., van Swaaij, W. P. M., 1986, “Gasification of coal-derived chars in synthesis gas mixtures under intraparticle mass-transfer controlled conditions”, Chem. Eng. Sci., V41, pp1895-1909.

Bliek, A., 1984, “Mathematical modeling of a cocurrent fixed bed coal gasifier”, PhD Thesis, Twente University, Netherlands.

Brown, T. D., 1982, “Coal gasification - combined cycles for electricity production”, Prog. Energy Combust. Sci., V8, pp277-301.

Brown, B. W., Smoot, L. D., Smith, P. J., Hedman, P. O., 1988, “Measurement and Prediction of Entrained-Flow Gasification Processes”, AIChE Journal, V34, pp435-446.

Caram, H. S., Fuentes, C., 1982, “Simplified Model for a Countercurrent Char Gasifier”, Ind. Eng. Chem. Fund., V21, pp464-472.

Chang, Y. H., 1988, “A mathematical model for the gasification of a single particle of coal”, Int. Chem. Eng., V28, pp520-526.

Charpenay, S., Serio, M. A., Solomon, P. R., 1992, “The Prediction of Coal Char Reactivity Under Combustion Conditions”, Int. Comb. Symp., Sydney.

Chen, S. G., Yang, R. T., Kapteijn, F., Moulijn, J. A., 1993, “A new surface oxygen complex on carbon : Toward a unified mechanism for carbon gasification reactions”, Ind. Eng. Chem. Res., V32, pp2835-2840.

Chi, W.-K., Perlmutter, D. D., 1989, “The Effect of Pore Structure on the Char-Steam Reaction”, AIChE J., V35, pp1791-1802.

Chin, G., Kimura, S., Tone, S., Otake, T., 1983, "Gasification of coal char with steam, (Part 1): Analysis of Reaction Rate & (Part 2): Pore Structure and Reactivity", Ind. Eng. Chem., V23, pp105-112, pp112-120.

CSIRO, 1995, private communications, (Contact: Dr. David Harris, Manager Coal Combustion and Gasification, Division of Coal and Energy Technology, North Ryde, Sydney, Australia.)

Dave, N., Duffy, G. J., 1992, "Final report on an assessment of integrated gasification combined cycle power generation", State Energy Research and Development Fund (NSW).

Denn, M. M., Yu, W.-C., Wei, J., 1979, "Parameter Sensitivity and Kinetics-Free Modelling of Moving Bed Coal Gasifiers", Ind. Eng. Chem. Fund., V18, pp286-288.

Doraiswamy, L. K., Gokarn, A., 1988, "Less Known Behaviour of Gas-Solid Reactions: The Expanding Core Model in Catalytic and Non-Catalytic Systems", Chem. Eng. Tech., V11, pp438-447.

Du, Z., Sarofim, A. F., Longwell, J. P., Tognotti, L., 1991, "The CO/CO2 Ratio in the Products of the Carbon-Oxygen Reaction", in "Fundamental Issues in the Control of Carbon Gasification Reactivity", Elsevier, Netherlands, pp91-106.

Dutta, S., Wen, C. Y., Belt, R. J., 1977, "Reactivity of coal and char. 1. In a carbon dioxide atmosphere", 1977, Ind. Eng. Process Des. Dev., V16, pp20-30.

Edwards, D. K., Matavosian, R., 1984, "Scaling rules for total absorptivity and emissivity of gases", J. of ASME, V106, pp684-689.

EPRI, 1978, “Economic Studies of Coal Gasification Combined Cycle Systems for Electric Power Generation”, EPRI AF-642, Electric Power Research Institute, Palo Alto, California.

EPRI, 1993, “Shell Coal Gasification Project : Final Report on Eighteen Diverse Feeds”, EPRI TR-100687, Project 2695-01, Final Report, July 1993, Electric Power Research Institute, Palo Alto, California.

Ergun, S., Menter, M., 1966, “Reactions of carbon with carbon dioxide and steam”, Chem. and Phys. of Carbon, V1, pp203-263.

Essenhigh, R. H., 1981, “Fundamentals of Coal Combustion”, in “Chemistry of Coal Utilization”, Second Suppl. Vol., Elliott, M. A. (Ed).

Evans, R., Thompson, B. H., Hiller, H., Vierrath, H. E., 1985, “The British Gas/ Lurgi slagging gasifier status, application and economics”, Coaltech ’85, London, pp659-687.

Field, M. A., 1969, “Rate of combustion of size-graded fractions of char from a low-rank coal between 1200°K and 2000°K”, Combustion and Flame, Vol 13, pp237-248.

Field, M. A., 1970, “Measurements of the effect of Rank on Combustion Rates of Pulverised Coal”, Comb. Flame., V14, pp237-248.

Foster, M. D., Jensen, K. F., 1990, “Small angle X-ray scattering investigations of pore structure changes during gasification”, FUEL, V69, pp88-96.

Frederick, W. J., Wag, K. J., Hupa, M. M., 1993, “Rate and Mechanism of Black Liquor Char Gasification with CO_2 at Elevated Pressures”, Ind. Eng. Chem., V32, pp1747-1753.

Fuertes, A. B., Pis, J. J., Perez, A. J., *et al.*, 1989, “Variation of the textural properties of a coke during gasification”, Vacuum, V39, pp67-681.

Fung, D. P. C., Kim, S. D., 1984, “Chemical reactivity of Canadian coal-derived chars”, FUEL, Vol 63, pp1197-1201.

Gadsby, J., Long, F. J., Sleightholm, P., Sykes, K. W., 1948, “The mechanism of the carbon dioxide-carbon reaction”, Proc. Royal Soc., A193, pp357-376.

Gan, H., Nandi, S. P., Walker, P. L. Jr., 1972, “Structural properties of a selection of coal derived chars”, FUEL, V51, pp272-281.

Gavalas, G. R., 1980, “A Random Capillary Model with Application to Char Gasification at Chemically Controlled Rates”, AIChE J., V26, pp577-585.

Govind, R., Shah, J., 1984, “Modeling and Simulation of an Entrained Flow Coal Gasifier”, AIChE J., V30, pp79-92.

Goyal, A., Zabransky, R. F., Rehmat, A., 1989, “Gasification kinetics of Western Kentucky bituminous coal char”, Ind. Eng. Chem. Res., V28, pp1767-1778.

Haga, T., Nishiyama, Y., 1988, “Influence of Structural parameters on coal char gasification, 1. Non-catalytic gasification”, FUEL, V67, pp743-747.

Hampartsoumian, E., Murdoch, P. L., Pourkashian, M., Williams, A., 1993, “The reactivity of coal chars produced under various pyrolysing conditions”, in “Recent Advances in Combustion Modelling”, B. Larrouturou (Ed.), World Scientific, Singapore.

Hashimoto, K., Miura, K., Xu, J.-J., Tezen, Y., Nagai, H., 1987, “Reactivities of various coals and demineralized chars under steam gasification”, 1987 Int. Conf. Coal Sci., Ed. J. A. Moulijn *et al.* , Elsevier, Amsterdam, pp507-510.

Haynes, H. W. Jr., 1982, “An Improved Single Particle Char Gasification Model”, AIChE J., V28, pp517-521.

Hippo, E., Walker, P. L. Jr, 1975, “Reactivity of heat-treated coals in carbon dioxide at 900°C”, FUEL, Vol 54, pp245-248.

Hobbs, M. L., Radulovic, P. T., Smoot, L. D., “Modeling fixed-bed coal gasifiers”, AICHE J., V38, pp681-702.

Hottel, H. C., Sarofim, A. F., 1967, “Radiative Transfer”, McGraw-Hill Book Company, New York, p453, p354-357.

Hoy, H. R., Wilkins, D. M., 1958, “Total gasification of coal”, BCURA Monthly Bulletin, Volume XXII, Feb/Mar Part I, pp57-109.

Huleatt, M. B., 1991 “Handbook of Australian black coals: geology, resources, seam properties, and product specifications”, Australian Government Publishing Service, Canberra.

IGT, 1957, “Gasification of Pulverized Coal in Suspension”, Inst. Gas Tech., Research Bulletin 7.

Kasaoka, S., Sakata, Y., Tong, C., 1985, “Kinetic evaluation of the reactivity of various coal chars for gasification with carbon dioxide in comparison with steam”, Int. Chem. Eng., V25, pp160-175.

Kayembe, N., Pulsifer, A. H., 1976, “Kinetics and catalysis of the reaction of coal char and steam”, FUEL, V55, pp211-219.

Kehoe, J. P. G., Aris, R., 1973, “Communications on the theory of diffusion and reaction-IX. Internal pressure and forced flow for reactions with volume change”, Chem. Eng. Sci., Vol 28, pp2094-2098.

Khan, M. R., Jenkins, R. G., 1986, “Swelling and plastic properties of coal devolatilized at elevated pressures : an examination of the influences of coal type”, FUEL, pp725-731.

Knight, A. T., Sergeant, G. D., 1982, “Reactivity of Australian coal-derived chars to carbon dioxide”, FUEL, V61, pp145-149.

Kojima, T., Adshiri, T., Kawaguchi, H., Furusawa, T., 1986, “Experimental and theoretical investigations of experimental fluidized bed char gasifier by model taking account of adsorption dynamics of reactant”, Chem. Eng. Sci., V41, pp813-820.

Kosky, P. G., Floess, J. K., 1980, “Global Model of Countercurrent Coal Gasifiers”, Ind. Eng. Chem. Pro. Des. Dev., V19, pp586-592.

Kovacik, G., Chambers, A., Ozum, B., 1991, “CO_2 Gasification Kinetics of Two Alberta Coal Chars”, Canadian J. Chem. Eng., V69, pp811-815.

Kwon, T.-W., Kim, S. D., Fung, D. P. C., 1988, “Reaction kinetics of char-CO_2 gasification”, FUEL, V67, pp530-535.

Laurendeau, N. M., 1978, “Heterogeneous kinetics of coal char gasification and combustion”, Prog. Energy Combust. Sci., V4, pp221-270.

Leckner, B., 1972, “Spectral and total emissivity of water vapour and carbon dioxide”, Comb. and Flame, V19, pp33-48.

Lee, C. W., Scaroni, A. W., Jenkins, R. G., 1991, “Effect of pressure on the devolatilisation and swelling behaviour of a softening coal during rapid heating”, FUEL, V70, pp957- 965.

Lee, C. W., Jenkins, R. G., Schobert, H. H., 1992, “Structure and reactivity of char from elevated pressure pyrolysis of Illinois No6 bituminous coal”, Energy and Fuels, 6, pp40-47.

Lim, C. J., Lucas, J. P., Haji-Sulaiman, M., Watkinson, A. P., 1991, “A mathematical model of a Spouted Bed Gasifier”, Canadian J. Chem. Eng., V69, pp596-610.

Lin, S. Y., Hirato, M., Horio, M., 1994, “The Characteristics of Coal Char Gasification at Around Ash Melting Temperature”, Energy & Fuels, V8, pp598-606.

Linares-Solano, A., Mahajan, O. M., Walker, P. L. Jr, 1979, “Reactivity of heat-treated coals in steam”, FUEL, Vol 58, pp327-332.

Littlewood, K., 1977, “Gasification: Theory and Application”, Prog. Energy Combust. Sci., V3, pp35-71.

Long, F. J., Sykes, K. W., 1948, “The mechanism of the steam-carbon reaction”, Proc. Royal Soc., A193, pp377-399.

Mahagaokar, U., Krewinghaus, A. B., 1990, “Shell coal gasification - Recent performance results on Drayton, Buckskin, Blacksville No2 and Pyro No9 coals”, ASME/IEEE Power Gen. Conf., Boston MA, Oct 21-25.

Maloney, D. J., Monazam, E. R., Ramanathan, S., 1993, “Evaluation of errors resulting from particle shape assumptions applied in coal combustion modeling”, in “Recent advances in combustion modelling”, Larrouturou, B. (Ed.), World Scientific, Singapore.

Mangold, E. C., Muradaz, M. A., Ouellette, R. P., Farah, O. G., Cheremisiniff, P. N., 1982, “Coal Liquefaction and Gasification Technologies”, Ann Arbor Science, Michigan, USA.

Mann, R., Almeida, J. J., Mugerwa, M. N., 1986, “A random pattern extension to the stochastic network pore model”, Chem. Eng. Sci., V41, pp2663-2671.

Matsui, K., Tsuji, H., Makino, A., 1983, “The effects of water vapor concentration on the rate of combustion of an artificial graphite in humid air”, Comb. Flame, V50, pp107-118.

Matsui, K., Tsuji, H., Makino, A., 1986, “A further study of the effects of water vapor concentration on the rate of combustion of an artificial graphite in humid air flow”, Comb. Flame, V63, pp415-427.

Matsui, I., Kunii, D., Furusawa, T., 1987, “Study of char gasification by carbon dioxide. 1. Kinetic study by thermogravimetric analysis”, Ind. Eng. Chem. Res., V26, pp91-95.

Merrick, D., 1984, “Coal Combustion and Conversion Technology”, Energy Alternatives Series, Macmillan, London.

Miccio, F., Salatino, P., 1992, “Monte-Carlo simulation of combustion-induced percolative fragmentation of carbons”, Comb. Symp. (Int.), Sydney.

Mills, K. C., Rhine, J. M., 1989, “The measurement and estimation of the physical properties of slags formed during coal gasification, 1. Properties relevant to fluid flow, 2. Properties relevant to heat transfer”, FUEL, V68, pp173-200, pp904-910.

Miura, K., Hashimoto, K., Silveston, P. L., 1989, “Factors affecting the reactivity of coal chars during gasification and indices representing reactivity”, FUEL, V68, pp1461-1475.

Modest, M. F., 1993, “Radiative Heat Transfer”, McGraw-Hill, Inc., New York.

Monazam, E. R., Johnson, E. K., Zondlo, J. W., 1992, "Modeling and simulation of a crossflow coal gasifier", Fuel Sci. and Tech. Int., V10, pp51-73.

Monson, C. R., Germane, G. J., Blackham, A. U., Smoot, L. D., 1995, "Char Oxidation At Elevated Pressures", Comb. and Flame, V100, pp669-683.

Morell, J. I., Amundson, N. R., Park, S.-K., 1990, "Dynamics of a Single Particle during Char Gasification", Chem. Eng. Sci., V45, pp387-401.

Muhlen, H.-J., van Heek, K. H., Juntgen, H., 1985, "Kinetic studies of steam gasification of char in the presence of H_2, CO_2 and CO", FUEL, V64, pp944-949.

Neoh, K. G., Gannon, R. E., 1984, "Coal volatile yield and element partition in rapid pyrolysis", FUEL, Vol 63, pp1347-1352.

Ni, Q., Williams, A., 1995, "A simulation study on the performance of an entrained-flow coal gasifier", FUEL, V74, pp102-110.

Niksa, S., 1988, "Rapid coal devolatilisation as an equilibrium flash distillation", AIChE J., V34, pp790-802.

Niksa, S., Kerstein, A. R., 1991, "FLASHCHAIN theory for Rapid Coal Devolatization Kinetics, 2. Impact of Operating Conditions", Energy & Fuels, V5, pp665-673.

Oh, M. S., Peters, W. A., Howard, J. B., 1989, "An experimental and modeling study of softening coal pyrolysis", AIChE J., V35, pp775-792.

Osafune, K., Marsh, H., 1988, "Gasification kinetics of coal chars in carbon dioxide", FUEL, V67, pp384-388.

Radovic, L. R., Lizzio, A. A., Jiang, H., 1991, “Reactive Surface Area : An old but new concept in carbon gasification”, in “Fundamental Issues in Carbon Gasification Research”, Elsevier, Netherlands, pp235-255.

Raghunathan, K., Yang, R. Y. K., 1989, “Unifaction of coal gasification data and its applications”, Ind. Eng. Chem. Res., V28, pp518-5123.

Ranish, J. M. and Walker, P. L. Jr., 1993, “High Pressure Studies of the Carbon-Oxygen Reaction”, Carbon, V31, pp135-141.

Reyes, S., Jensen, K. F., 1986, “Percolation Concepts in Modelling of Gas-Solid Reactions, I-Application to Char Gasification in the Kinetic Regime & II-Application to Char Gasification in the Diffusion Regime”, Chem. Eng. Sci., V41, pp333-343, pp345-354.

Ruprecht, P., Schafer, W., Wallace, P., 1988, “A computer model of entrained coal gasification”, FUEL, V67, pp739-742.

Saffer, M., Ocampo, A., Laguerie, C., 1988, “Gasification of coal in a fluidized bed in the presence of water vapor and oxygen; an experimental study and a first attempt at modeling the reactor”, Int. Chem. Eng., V28, pp46-61.

Sandmann, C. W., Zygourakis, K., 1986, “Evolution of pore structure during gas-solid reactions : Discrete Models”, Chem. Eng. Sci., V41, pp733-739.

Schafer, W., Trondt, M., Langhoff, J., Konkol, W., Hibbel, J., 1988, “The Texaco Coal Gasification Process for Syngas and Fuel Gas Generation”, Energy Progress, V8, pp28-38.

Schwartz, C. W., 1982, “Combined Cycle Coal Gasification”, Energy Progress, V2, pp207- 212.

Shah, N., Ottino, J. M., 1987, “Transport and Reaction in Evolving, Disordered Composites, I. Gasification of Porous Solids”, Chem. Eng. Sci., V42, pp63-72.

Shaw, J. T., 1977, “Theoretical work on reaction sequences in the gasification of coke by CO_2 and by steam in conditions remote from equilibrium”, FUEL, V56, pp134-136.

Shufen, L., Ruizheng, S., 1994, “Kinetic studies of a lignite char pressurized gasification with CO_2, H_2 and steam”, FUEL, V73, pp413-416.

Simons, G. A., Finson, M. L., 1979, “The Structure of Coal Char: Part I. Pore Branching & Part II. Pore Combination”, Comb. Sci. & Tech., V19, pp217-225, pp227-235.

Simons, G. A., 1983, “The Role of Pore Structure in Coal Pyrolysis and Gasification”, Prog. Energy Comb. Sci., V9, pp269-290.

Singh, C. P. P., Saraf, D. N., 1977, “Simulation of high-temperature water-gas shift reactors”, Ind. Eng. Chem. Process Des. Dev., pp313-319.

Smith, I. W., 1978, “The Intrinsic Reactivity of Carbons to Oxygen”, FUEL, V57, pp409-414.

Smith, I. W., 1982, “The combustion rates of coal chars: a review”, 19th Symp. (Int.) on Combustion, The Combustion Institute, pp1045-1065.

Smith, I. W., Tyler, R. J., 1972, “Internal burning of pulverized semi-anthracite: the relation between particle structure and reactivity”, FUEL, V51, pp312-321.

Smith, I. W., Tyler, R. J., 1974, “The reactivity of a porous brown coal char to oxygen between 630 and 1812°K”, Comb. Sci. and Tech., V9, pp87-94.

Smoot, D., Smith, J., 1985, “Pulverised-Coal Combustion and Gasification”, Plenum, New York.

Solomon, P. R., Hamblen, D. G., 1984, “Finding Order in Coal Pyrolysis Kinetics”, Prog. Energy Comb. Sci., V9, pp323-360.

Solomon, P. R., Hamblen, D. G., Carangelo, R. M., Serio, M. A., Deshpande, G. Y., 1988, “General Model of Coal Devolatilization”, Energy and Fuels, V2, pp405-420.

Solomon, P. R., Serio, M. A., Suuberg, E. M., 1992, “Coal Pyrolysis: Experiments, Kinetic Rates and Mechanisms”, Prog. Energy Combust. Sci., V18, pp133-220.

Sotirchos, S.V., Amundson, N., 1984, “Dynamic Behaviour of a Porous Char Particle Burning in an Oxygen-containing Environment.Part I : Constant Particle Radius.Part II : Transient Analysis of a Shrinking Particle”, AIChE J., V30, pp537-549, pp549-556.

Srinivas, B., Amundson, N. R., 1980, “A Single-Particle Char Gasification Model”, AIChE J., V26, pp487-496.

Stillman, R., 1979, “Simulation of a Moving Bed Gasifier for a Western Coal”, IBM J. Res. Dev., V23, pp240-252.

Su, J.-L., Perlmutter, D. D., 1984, “Evolution of Pore Volume distribution during Gasification”, AIChE J., V30, pp967-973.

Su, J.-L., Perlmutter, D. D., 1985, “Effect of Pore Structure on Char Oxidation Kinetics”, AIChE J., V31, pp973-981.

Szekely, J., Evans, J. W., Sohn, H.Y., 1976, “Gas-Solid Reactions”, Academic Press, New York.

Tingey, G. L., 1966, “Kinetics of the water-gas equilibrium reaction. I. The reaction of carbon dioxide with hydrogen”, J. of Phys. Chem., V70, p1406-1412.

Tognotti, L., Longwell, J. P., Sarofim, A. F., 1990, “The products of the high temperature oxidation of a single char particle in an electrodynamic balance”, 23rd International Combustion Symposium, pp1207-1213.

Tomita, A., Mahajan, O. P., Walker, P. L. Jr, 1977, “Reactivity of heat-treated coals in hydrogen”, FUEL, Vol 56, pp137-144.

Tseng, H. P., Edgar, T. F., “The Change of the Physical Properties of Coal Char during Reaction”, FUEL, V68, pp114-119.

Ubhayakar, S. K., Stickler, D. B., Gannon, R. E., 1977, “Modelling of entrained-bed pulverised coal gasifiers”, FUEL, V56, pp281-291.

Unsworth, J. F., Barratt, D. J., Roberts, P. T., 1991, “Coal quality and combustion performance: An international perspective”, Elsevier, Amsterdam.

USBM, 1954, “Synthetic Liquid Fuels. Annual report of the Secretary of the Interior for 1953. Part I.- Oil from Coal”, Report of Investigations 5043, US Bureau of Mines.

USBM, 1953, “Progress report on operation of pressure-gasification pilot plant utilizing pulverized coal and oxygen”, Report of Investigations 4971, US Bureau of Mines.

Valix, M. G., Harris, D. J., Smith, I. W., Trimm, D. L., 1992, “The intrinsic combustion reactivity of pulverised coal chars: The use of experimental pore diffusion coefficients”, 24th Combusion Symposium (Int.), Sydney, Australia.

Vamvuka, D., Woodburn, E. T., Senior, P. R., 1995, "Modelling of an entrained flow coal gasifier, 1. Development of the model and general predictions", FUEL, V74, pp1452-1460.

Vamvuka, D., Woodburn, E. T., Senior, P. R., 1995, "Modelling of an entrained flow coal gasifier, 1. Effect of operating conditions on reactor performance", FUEL, V74, pp1461-1465.

van Heek, K. H., 1990, "Advanced Coal Conversion by Pyrolysis and Hydrogenation", Third Flame Research Course, IFRF, Sept 1990, Netherlands.

van Krevelan, D. W., 1993, "Coal", Elsevier, Amsterdam, Table 7.5 p204.

Wall, T. F., *et al.*, 1988, "Ignition of low volatile and low rank coals", End of grant report 875, National Energy Research, Development and Demonstration Program, Dept. of Primary Industries and Energy, Australia.

Watkinson, A. P., Lucas, J. P., Lim, C. J., 1991, "A prediction of performance of commercial gasifiers", FUEL, V70, pp519-527.

Weeda, M., Abcouwer, H. H., Kaptejn, F., Moulijn, J. A., 1993, "Steam gasification kinetics and burn-off behaviour for a bituminous coal derived char in the presence of H_2", Fuel Proc. Tech., V36, pp235-242.

Wen, C. Y., Chuang, T. Z., 1979, "Entrainment Coal Gasification Modelling", Ind. Eng. Chem. Process Des. Dev., Vol 18, pp684-695.

Wen, C. Y., Dutta, S., 1979, in Wen, C. Y., Lee, E. S. (Eds), "Coal Conversion Technology", Addison Wesley Publishing Co., New York.

Wheeler, A., 1951, “Reaction Rates and Selectivity in Catalyst Pores”, in “Advances in Catalysis V III”, Academic Press Inc., New York, pp258-260.

Yoon, H., Wei, J., Denn, M. M., 1978, “A Model for Moving-Bed Coal Gasification Reactors”, AIChE J., V24, pp885-903.

Zhi-hua, M., Cheng-fang, Z., Zi-bin, Z., Er-li, S., 1992, “A study on the intrinsic kinetics of steam gasification of Jincheng coal char”, Fuel Proc. Tech., V31, pp69-76.

Zygourakis, K., Arri, L., Amundson, N. R., 1982, “Studies on the Gasification of a Single Char Particle”, Ind.Eng.Chem.Fund., V21, p1-12.

APPENDIX A: DETERMINATION OF INTRINSIC REACTIVITIES

A.1 Introduction

Intrinsic reactivities were determined experimentally for three char samples from CSIRO gasifier runs with Coal E. A fixed bed apparatus was used with monitoring of the gas composition to determine the rate of carbon gasification for reactant gases containing either oxygen, carbon dioxide or steam.

A.2 Experimental Procedure

A typical reactivity measurement is performed by preparing a char sample of approximately 1 gram in the fixed bed and flushing the entire system, including sample, with nitrogen. The sample is then inserted into a preheated furnace with nitrogen still flowing through the sample. When thermal equilibrium is reached the nitrogen flow is stopped and a mixture of nitrogen and reactant gas is connected to the sample. Reaction rates are continuously monitored by analysis of the exit gas stream for carbon monoxide and carbon dioxide. When stable conditions have been reached, or a desired carbon conversion figure achieved, the furnace is turned off and the reactor allowed to gradually cool. The dependence of reaction rate on temperature is performed by monitoring the rate as the reactor cools. The remaining char is weighed in order to check the level of conversion calculated from the gas analysis and the surface area of the char measured using a standard BET analysis with nitrogen. If the reactions were maintained in the chemically limited regime the intrinsic reactivities can be simply determined from the rates as functions of temperature and the total surface area of the samples.

The peak temperatures used for measuring the reactivity to different reactant gases vary depending on the reaction rate of the gas. In all cases a controlled rate of reaction is required to ensure that the reactions proceed slowly and are chemically limited. This is relatively easy with carbon dioxide and steam reactions as the slower rates and endothermic nature lead to stable reaction rates. For oxygen reacting however, the rate can easily become excessive, resulting in rapidly rising temperature and complete near-instantaneous reaction. For these reasons the temperature for the oxygen reaction is kept below 400°C, while temperatures of 800-950°C are used for the carbon dioxide and steam reactions.

A.3 Experimental Reactivities

The experimental reactivities of char from CSIRO gasifier runs with Coal E at approximate stoichiometries of 25, 50 and 125% were determined. Carbon dioxide reactivities were determined for all three chars while oxygen and steam reactivities were determined for the 25% stoichiometry char only. Char reactivities can be reported on a number of bases and figure A.1 represents the simplest of these, mass per mass rate, for all determinations. Each point on the graph represents an instantaneous rate determined from gas analysis at a particular temperature as a function of the mass of char remaining, which is calculated from the accumulated mass loss over the length of the experiment. In figure A.2 the rates from figure A.1 are converted to intrinsic rate form using the concentration of reactant gas fed to the reactor and the measured nitrogen BET surface area of the char. The pressure orders are assumed for this study as literature results indicate that values found at atmospheric pressure may not be accurate and do not represent the effect of pressure on rate at high reactant gas pressures. The terms of the intrinsic rate expressions fitting the data shown in figure A.2 are given in table A.1 to fit the general rate expression, equation A.1.

$$Rate_a = \eta . A . \exp\left(\frac{-E}{RT}\right) . P_a^n \qquad \text{Equation (A.1)}$$

Table A.1: Terms for intrinsic rate expressions for CSIRO gasifier Coal E chars.

Char	Reactant Gas	Pressure Order, n	Pre-exponential Factor, A /(kg/m^2/s/atm^n)	Activation Energy, E /(MJ/kmol)
25% Stoichiometry	Oxygen	0.8	0.002852	93.2
”	Steam	0.2	2.745	205.8
”	Carbon Dioxide	0.25	689.0	243.3
50% Stoichiometry	Carbon Dioxide	0.25	758.0	245.0
125% Stoichiometry	Carbon Dioxide	0.25	407.6	238.7

A.4 Discussion and Conclusions

The results obtained for the reactivities of Coal E chars are a combination of experimental and literature, due to the inclusion of literature pressure orders obtained over a wider range of pressures than was possible in the available experimental apparatus. While the carbon dioxide reactivities given in table A.1 suggest changes in reactivity with the char formation stoichiometry, it is evident in figure A.2 that these reactivities are in reality nearly identical and any of the three sets of values is a reasonable approximation of the carbon dioxide reactivity of all three samples. The near linear relationship of the points for each reactivity determination in figure A.2 indicates a consistent reactivity determination in each case, and for steam and carbon dioxide gasification the activation energies are close to commonly reported literature values. However, the oxygen reactivity a lower activation energy was found for the char than is common, although a wide range of literature values for other chars indicates that it is not abnormal. As the terms in table A.1 would extrapolate to a much lower reactivity for oxygen at high temperatures than would be expected from literature results, general reactivity data for oxygen gasification of carbonaceous material will be introduced in the mathematical model development section instead of the experimentally obtained terms.

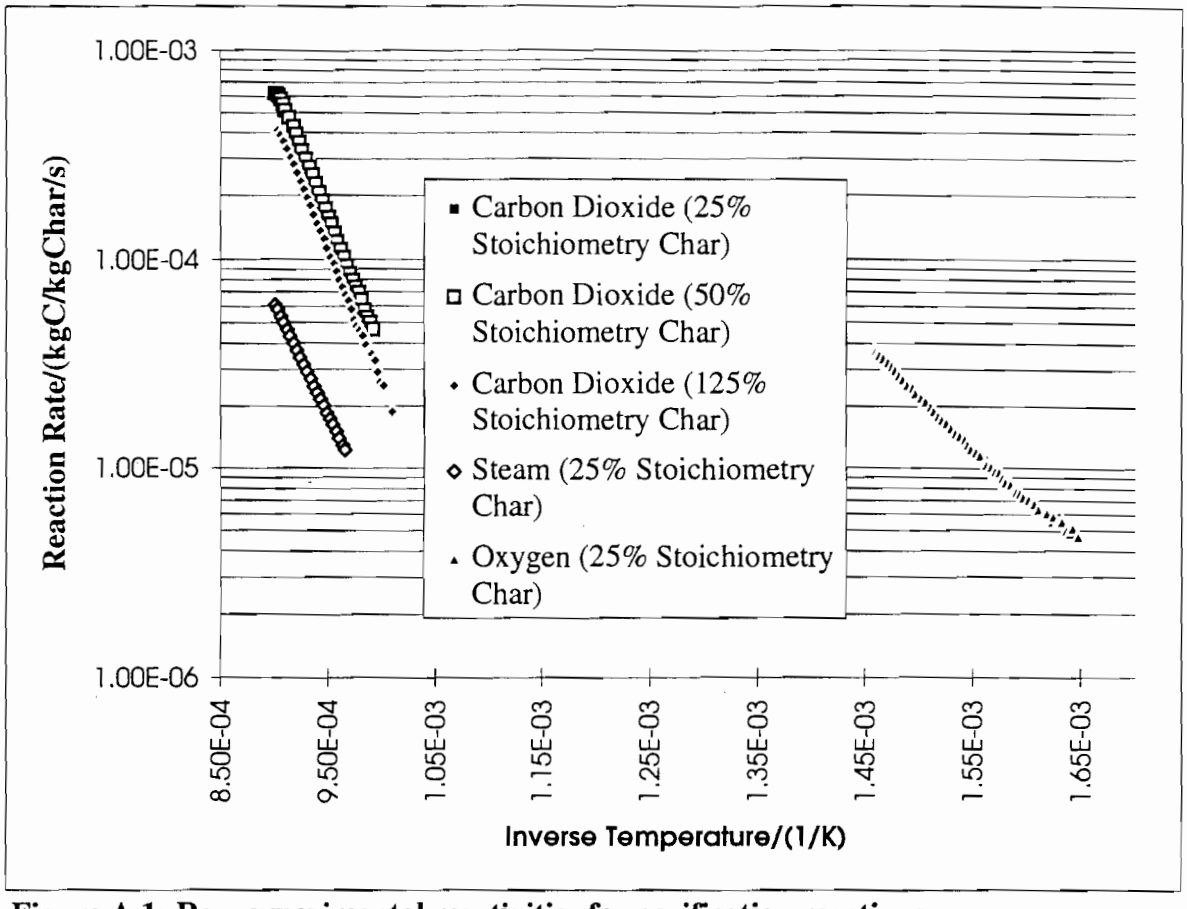

Figure A.1: Raw experimental reactivities for gasification reactions.

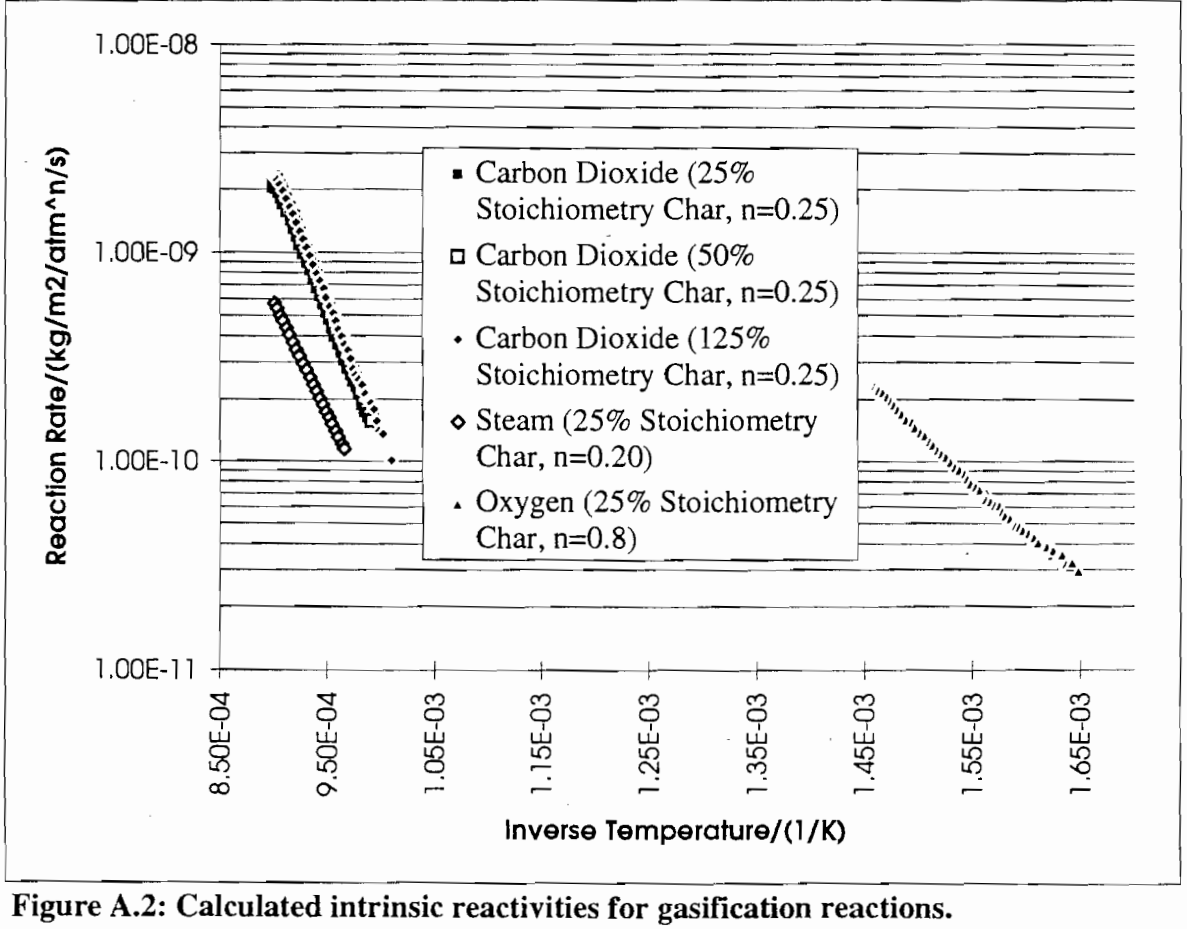

Figure A.2: Calculated intrinsic reactivities for gasification reactions.

APPENDIX B: SLAG LAYER MODEL

B.1 Introduction

A simple model to predict the thickness and temperature of a fluid slag layer flowing down a gasifier wall was studied for potential use as a sub-model of the gasification model developed in this study. This slag layer model was previously published by Schoen (1993) and is based on basic heat and mass balance criteria. A diagrammatic representation of a slag layer on a gasifier wall is shown in figure B.1 with temperatures, dimensions, heat fluxes and mass fluxes. The key point of figure B.1 are that a distinct slag melting temperature, T_m, is assumed so that slag is solid below this temperature and fluid above it. This is a simplifying approximation as slag is a multicomponent substance that will have a melting range rather than a distinct point. The model estimates the thickness of the fluid slag layer only and the thickness of the solidified slag layer can be calculated based on the thermal conductivity of the gasifier wall material and a measured temperature at some distance into the wall.

B.2 Model Description

The slag layer model is based upon standard transport equations for a fluid flowing down a wall. The model assumes a steady state condition in the gasifier with a constant mass flow of liquid slag, m in figure B.1. If the slag is in thermal equilibrium the indicated flux of heat to the slag from the gas, q_1, will be equal to the flux from the liquid slag into the solid slag, q_2. These two quantities are calculated as given in equations 1 and 2, where ε_{Slag} is the slag emissivity and k_{Slag} is the slag thermal conductivity. For this model the radiative transfer equation neglects the emissivity of the hot gases and convective transfer is ignored.

$$q_1 = \sigma . \varepsilon_{Slag} \left(T_g^4 - T_0^4 \right) \qquad \text{Equation (1)}$$

$$q_2 = \frac{k_{Slag}}{d} \left(T_0 - T_m \right) \qquad \text{Equation (2)}$$

The mass transfer in the fluid layer is calculated on the basis of the assumptions that the gasifier is cylindrical and temperature varies linearly with distance into the slag layer. In this case the velocity of slag flow at any distance into the slag layer is a function of the viscosity, which for a known slag is generally an exponential function

of temperature. The total mass flow of slag down the gasifier wall can then be calculated by integrating the slag velocity over the thickness of the slag layer, as given in equation 3, where μ_x refers to the viscosity at distance x into the slag.

$$m = \rho.g.d^3 \left[\frac{\left(\frac{2}{\mu_0} - \frac{2}{\mu_d} \right)}{\ln\left(\frac{\mu_d}{\mu_0} \right)} - \frac{1}{\mu_d \ln\left(\frac{\mu_d}{\mu_0} \right)} - \frac{2}{\mu_d \ln\left(\frac{\mu_d}{\mu_0} \right)^2} \right] \qquad \text{Equation (3)}$$

In the case of a steady state system q_1 will equal q_2, and therefore equations 1 and 2 can be equated and solved simultaneously with equation 3 to give T_0 and d. This solution is not easily obtained as the slag viscosity is a function of temperature when the slag surface temperature is unknown. The equations were solved for particular cases using the Microsoft Excel spreadsheet 'Solver' command to simultaneously find suitable slag thickness and surface temperatures.

B.3 Sensitivity Analysis

A set of base variable values was defined for a gasifier and a particular coal ash and the variables varied to show the sensitivity of the model to changes. The base values for these variables are given in table B.1, with the slag property data being sourced from Schoen (1993) and Mills and Rhine (1989). The slag viscosity, described by two terms in the table, is calculated using equation 4, where the subscript x refers to variable values at distance x into the slag layer.

$$\mu_x = A.\exp\left(\frac{E}{T_x} \right) \qquad \text{Equation (4)}$$

Additional gasifier data is based upon a large scale gasifier using 2000 tonne per day of 14% ash content coal. As assumed by Schoen (1993) all of the ash is taken to impact at the top of the gasifier and flows evenly down the gasifier. This assumption is unlikely but complex fluid dynamics modelling is required to predict the impact locations of the ash particles.

Table B.1: Base values used in sensitivity analysis of slag layer model.

Variable	Symbol	Value	Units
Slag Viscosity Pre-exponential	A	5.12×10^{-6}	Pa.s
Slag Viscosity Exponential Term	E	23180	K
Slag Density	ρ	2773	kg/m^3
Slag Thermal Conductivity	k_{Slag}	1.6	W/m/K
Slag Melting Temperature	T_m	1450	K
Slag Emissivity	ε_{Slag}	0.83	-
Slag Mass Flow Rate	m	2.645	kg/s
Gas Temperature	T_g	1800	K
Gasifier Diameter	D	3.0	m

The results of the sensitivity analysis are shown in figures B.2 and B.3 as the impact of changes on predicted values of slag fluid layer thickness and slag fluid layer surface temperatures respectively. Two variables are dominant in the sensitivity analysis, the slag melting temperature in determining the slag fluid layer thickness and the gas temperature in determining the slag surface temperature.

B.4 Estimation of Slag Layer Properties

The slag layer properties, that is thickness of fluid layer and surface temperature, can be predicted for a particular coal in a gasifier if the slag melting temperature is known accurately. Given the results of the sensitivity analysis of the model and the parameter values given in table B.1, excepting gas temperature, the slag layer properties calculated at varying gas temperatures by the model are shown in figure B.4. The predicted slag surface temperatures show a near linear relationship with the gas temperatures corresponding to the surface temperature being estimated as approximately 95% percent of the gas temperature. Slag fluid layer thickness is less readily correlated and, as previously indicated, is subject to error in the melting point used for the slag. The thickness of the fluid layer is also of little use in modelling as the solid slag thickness is not estimated by the model.

B.5 Discussion and Conclusions

The predicted slag surface temperature from the model can be used in other models as the wall temperature. This relies upon either experimental or assumed knowledge that a fluid slag layer coats the entire inner wall of the subject gasifier. This is relatively uncommon in atmospheric pressure experimental gasifiers due to low temperatures is some parts of the gasifiers. In high pressure gasifiers, particularly those using oxygen rather than air, temperatures may be uniformly high enough to maintain fluid slag throughout the gasifier. In these cases the accuracy of the model predictions then relies upon the assumptions relating to the deposition of slag on the walls. In the model all slag is assumed to be deposited at the top of the gasifier and flow down the entire length of the gasifier. This assumption appears simplistic but complex modelling of the fluid dynamics in the gasifiers is required to identify accurately the locations at which coal and ash particles impact with the gasifier walls. Due to these limitations the model was not used as part of the gasification model but may be suitable, with revision, in future gasifier models.

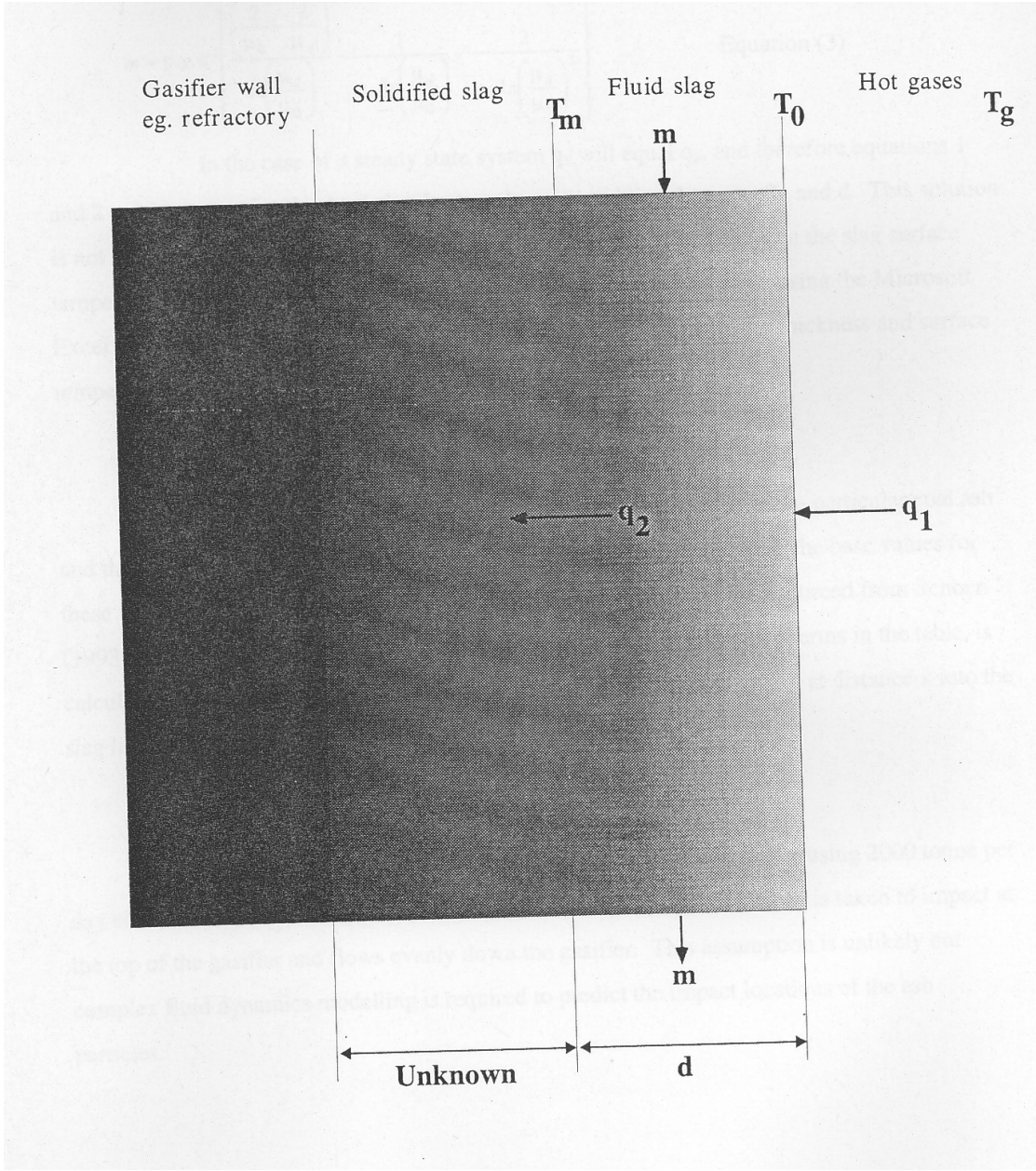

Figure B.1: Schematic of slag layer indicating dimensions, temperatures and mass flow

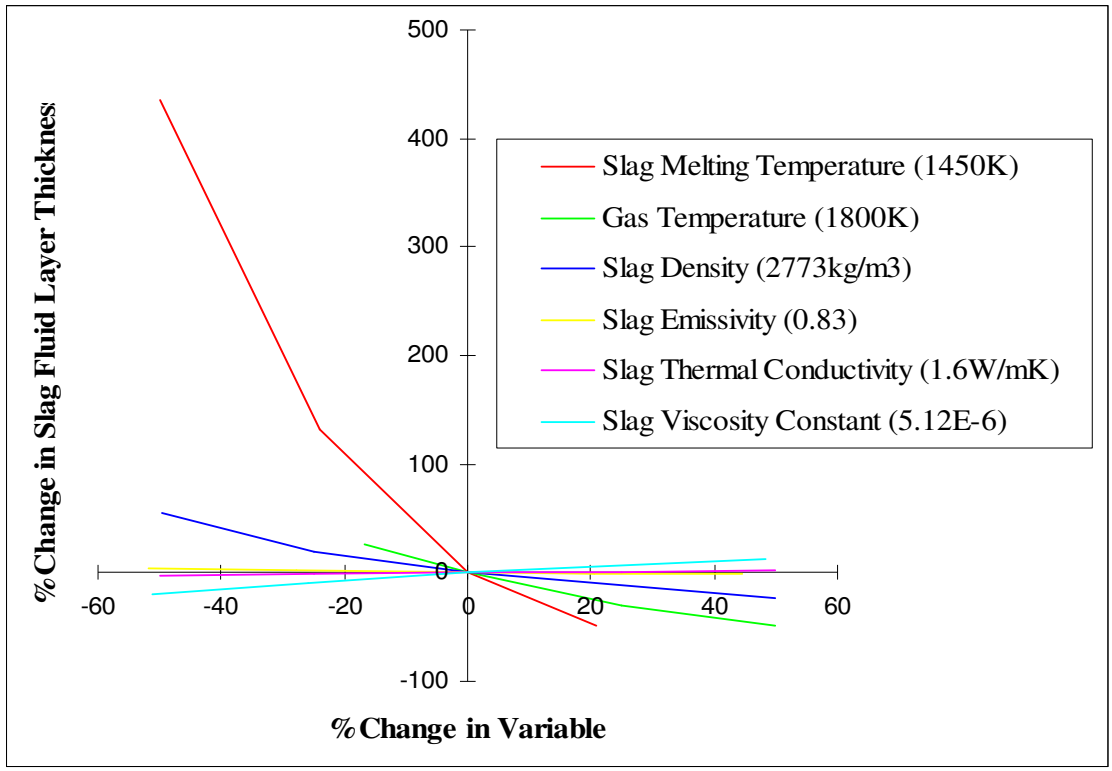

Figure B.2: Sensitivity of predicted slag fluid layer thickness to inputs

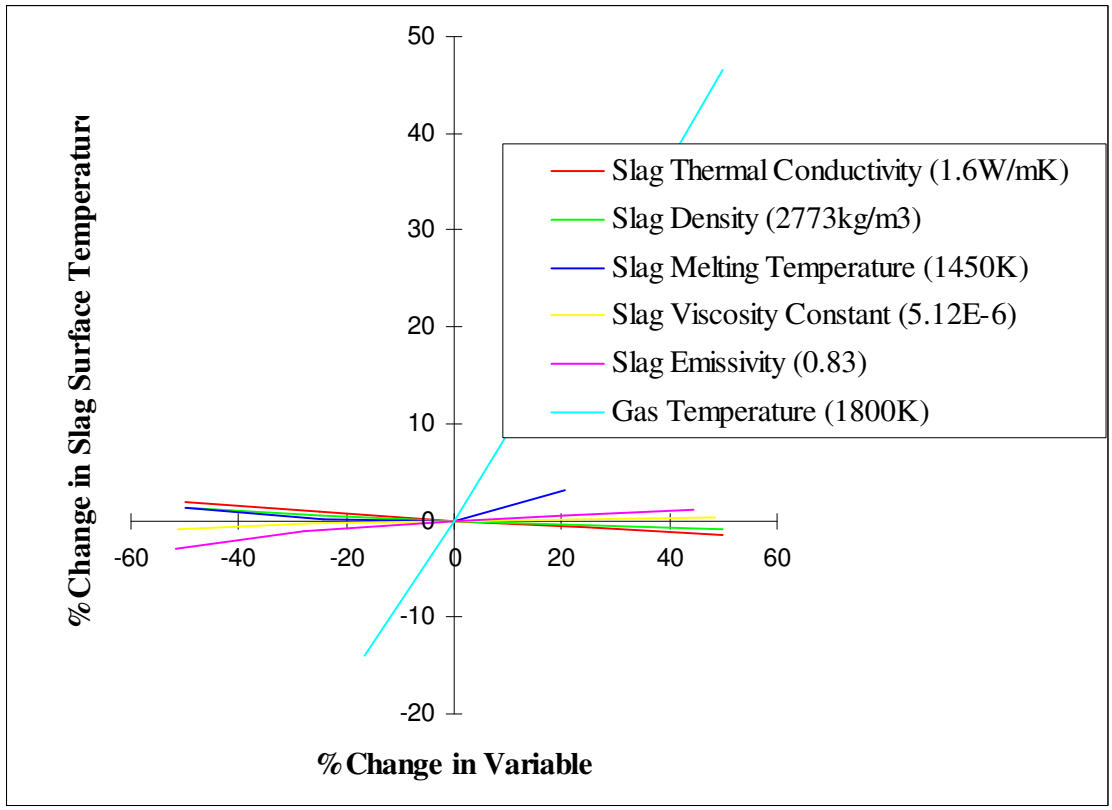

Figure B.3: Sensitivity of predicted slag fluid layer surface temperature to inputs

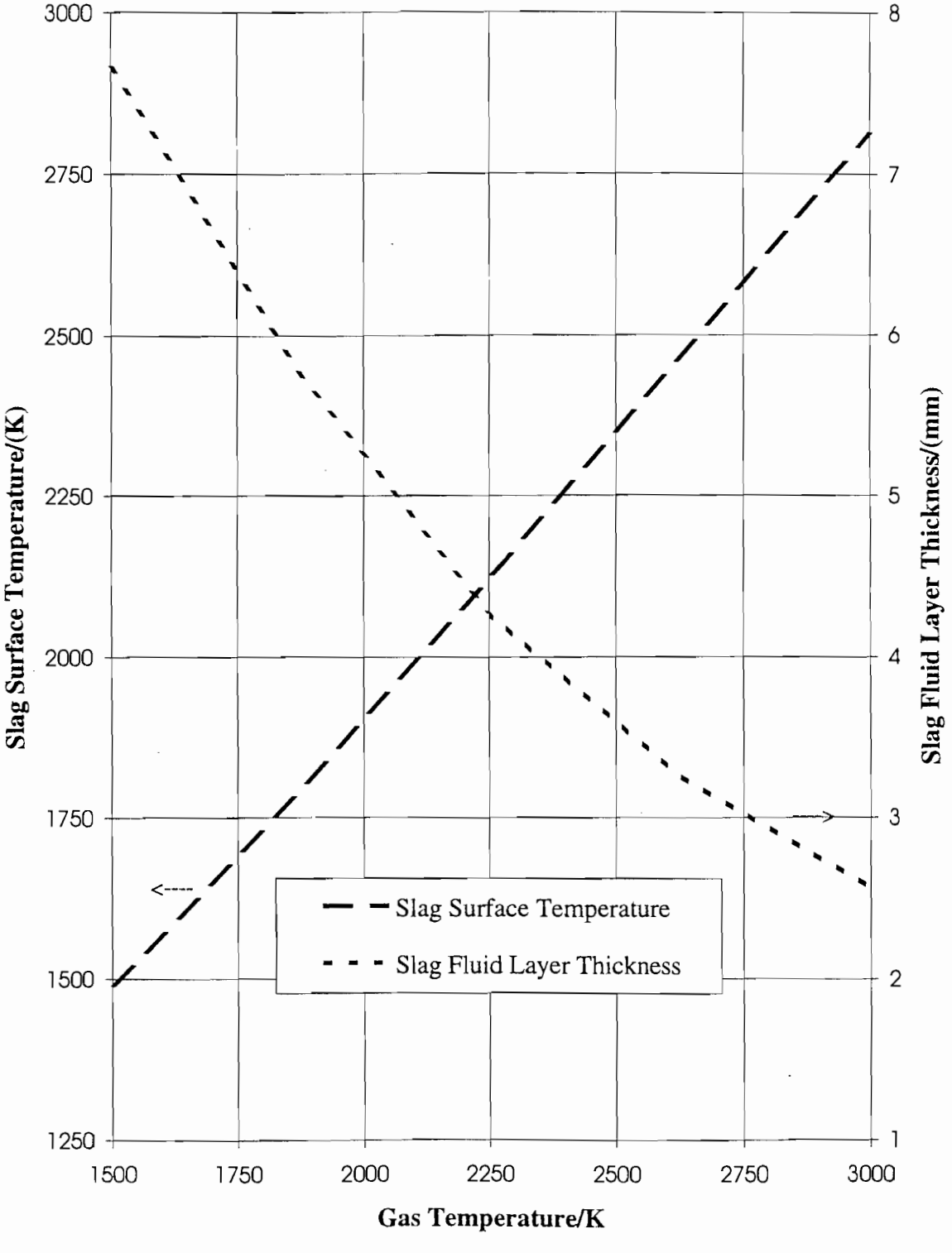

Figure B.4: Influence of gas temperature on predicted slag surface temperature and fluid layer thickness.